Identification of small molecules and genetic factors that alter cellular aging

Inaugural-Dissertation

zur

Erlangung des Doktorgrades

Dr. rer. nat.

der Fakultät für

Biologie

an der

Universität Duisburg-Essen

vorgelegt von

Jessica Stephan

aus Mönchengladbach

Dezember 2011

Die der vorliegenden Arbeit zugrunde liegenden Experimente wurden in der Abteilung für Genetik der Fakultät für Biologie an der Universität Duisburg-Essen sowie bei der Screening Unit des Leibniz-Instituts für Molekulare Pharmakologie (FMP) in Berlin durchgeführt.

1. Gutachter: Prof. Dr. Ann E. Ehrenhofer-Murray

2. Gutachter: Prof. Dr. George Iliakis

3. Gutachter: ---

Vorsitzender des Prüfungsausschusses: Prof. Dr. Hemmo Meyer

Tag der mündlichen Prüfung: 21. März 2012

Abstract

Aging is a multifaceted process that is regulated by several factors and pathways, among which the best known are the nutrient signalling pathways. As the amount of people suffering from age-related diseases increases, it is of special interest to identify compounds and genetic factors that delay aging, thereby displaying promising indications for the development of anti-aging therapeutics.

In this study, a novel high-throughput method was developed to screen for compounds that extend the CLS of the fission yeast *Schizosaccharomyces pombe*. Eight of the final 20 candidates that increased CLS were further characterized. We found that their life-extending effect was independent of caloric restriction as well as of the TOR signalling pathway. Furthermore, six compounds led to an increased resistance against oxidative stress. Individual analyses revealed that the CLS-extending effect of prostaglandin J_2 depended on the mitochondrial fission protein Dnm1 as well as on components of the Git3/PKA signalling pathway. In contrast, monensin and nigericin required V-ATPase activity to promote longevity. The molecular targets of the other compounds remain to be determined.

Additionally, we used our new CLS assay to screen an *S. pombe* deletion library for gene deletions that extend the CLS of fission yeast. However, in later experiments, we found that the observed increase of CLS was caused by an unknown factor in the strain background of the deletion library rather than by the indicated gene deletions.

In another approach, we used a new high-throughput method established within this study to screen approximately 19,000 compounds for their impact on the telomeric silencing of the budding yeast *Saccharomyces cerevisiae*, as this has been associated with RLS. We found that nicotine increased silencing at all heterochromatic loci in budding yeast, namely the telomeres, the rDNA locus, and the *HM* loci. *In vitro* experiments indicated that nicotine might act by activating Sir2. This hypothesis was supported by the finding that nicotine extended the CLS of *S. pombe* in a Sir2-dependent manner.

Zusammenfassung

Alterung ist ein komplexer Prozess, der durch viele Faktoren und Signalwege reguliert wird, wobei die bekanntesten die Nährstoff-Signalwege sind. Da die Anzahl an Menschen, welche an alterungsbedingten Krankheiten leiden, zunimmt, ist die Identifizierung von Substanzen und genetischen Faktoren, die das Altern verzögern und dadurch vielversprechende Ansätze für die Entwicklung von Anti-Aging-Mitteln darstellen, von besonderem Interesse.

In dieser Arbeit wurde eine neue High-Throughput-Methode entwickelt, um nach Substanzen zu suchen, welche die chronologische Lebensspanne (CLS) der Spalthefe *Schizosaccharomyces pombe* verlängern. Acht der finalen 20 lebensverlängernden Kandidaten wurden näher untersucht. Wir fanden heraus, dass ihr lebensverlängernder Effekt weder von der kalorischen Restriktion noch vom TOR-Signalweg abhängig war. Des Weiteren führten sechs Substanzen zu einer erhöhten Resistenz gegenüber oxidativem Stress. Einzelanalysen ergaben, dass der lebensverlängernde Effekt von Prostaglandin J_2 sowohl von dem an der mitochondrialen Spaltung beteiligten Protein Dnm1 als auch von Komponenten des Git3/PKA-Signalweges abhängig war. Im Gegensatz dazu benötigten Monensin und Nigericin die Aktivität der V-ATPase zur Lebensverlängerung. Allerdings sind die molekularen Ziele der anderen Substanzen weiterhin nicht bekannt.

Darüber hinaus haben wir den etablierten High-Throughput-Assay verwendet, um eine *S. pombe*-Deletionsbank nach lebensverlängernden Gendeletionen zu durchsuchen. Allerdings fanden wir in späteren Experimenten heraus, dass die beobachtete Verlängerung der CLS eher auf einem unbekannten Faktor im Stammhintergrund der Deletionsbank als auf die angegebenen Gendeletionen zurück zu führen war.

In einem weiteren Ansatz verwendeten wir eine neue High-Throughput-Methode, welche im Rahmen dieser Arbeit etabliert wurde, um ca. 19.000 Substanzen auf ihren Einfluss auf das telomerische Silencing der Bäckerhefe *Saccharomyces cerevisiae* hin zu testen, da dieses bereits mit der replikativen Alterung in Verbindung gebracht worden war. Wir fanden heraus, dass Nikotin das Silencing an allen drei heterochromatischen Bereichen in der Bäckerhefe, sprich den Telomeren, dem rDNA-Lokus und den *HM*-Loki, verbesserte. *In vitro*-Experimente deuteten darauf hin, dass Nikotin über die Aktivierung von Sir2 wirken könnte. Diese Hypothese wurde durch die Erkenntnis gestützt, dass Nikotin die CLS von *S. pombe* Sir2-abhängig verlängerte.

Table of contents

List of figures

List of tables

Abbreviations

15d-PGJ_2	15-deoxy-Δ-12, 14-prostaglandine J_2
5-FAA	5-fluoroanthranilic acid
5-FOA	5-fluoroorotic acid
6-AU	6-azauracil
αAA	α-amino adipic acid
aa	amino acid
Abf	ARS binding factor
AC	adenylate cyclase
AMP	adenosine monophosphate
AP	apurinic/apyrimidinic
AP-1	activator protein 1
ATP	adenosine-5'-triphosphate
bp	base pair
BER	base excision repair
CFU	colony forming units
CLS	chronological lifespan
CR	caloric restriction
CS	Cockyane syndrome
DHR123	dihydrorhodamine123
DIM	3,3’-diindolylmethane
DMSO	dimethylsulfoxid
DNA	deoxyribonucleic acid
DR	dietary restriction
Drp1	dynamin-related protein 1
DSB	double-strand break
EDTA	ethylenediaminetetraacetic acid
EGCG	epigallocatechin-3-gallate
EMM	Edinburgh minimal medium
ER	endoplasmic reticulum
ERCs	extrachromosomal ribosomal DNA circles
GGR	global genomic repair
GMP	guanosine monophosphate

H_2O	distilled water
H_2O_2	hydrogen peroxide
HAT	histone acetyltransferase
HDAC	histone deacetylase
HIF-1α	hypoxia inducible factor 1α
HM	homothallic mating
HML / HMR	*HM* loci on the left/right arm of chromosome III
HPLC-MS	high-performance liquid chromatography combined with mass spectrometry
HR	homologous recombination
IDL	insertion/deletion loop
IFNγ	interferon gamma
IGF-1	insulin-like growth factor 1
IMP	inosine monophosphate
IMPDH	IMP dehydrogenase
IPTG	isopropyl β-D-1-thiogalactopyranoside
kb(s)	kilobasepair(s)
LB	Luria-Bertani medium
MAT	mating type locus
MD	menadione (sodium bisulfite)
Mfn1/2	Mitofusin 1/2
MMR	mismatch repair
MMS	methyl methanesulfonate
MNNG	1-methyl-3-nitro-1-nitroguanidine
MPA	mycophenolic acid
MS	mass spectrometry
MSX	methionine sulfoxime
mTOR	mammalian TOR
NAD^+	nicotine adenine dinucleotide
NAM	nicotinamide
NER	nucleotide excision repair
NF-κB	nuclear factor kappa-light-chain-enhancer of activated B cells
NFR	nucleosome-free region
NHEJ	non-homologous end-joining

nt	nucleotide/s
NTA	nitrilotriacetic acid
OAADPR	2'-O-acetyl-ADP-ribose
$OD_{595/600}$	optical density at 595 nm or 600 nm
ORC	origin recognition complex
ORF	open reading frame
PCR	polymerase chain reaction
PEV	position-effect variegation
PGJ_2	prostaglandin J_2
PI3K	phosphatidylinositol 3-kinase
PKA	protein kinase A
PTM	post-translational modification
Rap	repressor activator protein
RENT	regulator of nucleolar silencing and telophase (complex)
RLS	replicative lifespan
RNA	ribonucleic acid
RNAi	RNA interference
rpm	rounds per minute
ROS	reactive oxygen species
RT	room temperature (20 - 22 °C)
S6K	S6 kinase
SAS	something about silencing
SDC	synthetic dextrose complete (medium)
SDS	sodium dodecyl sulfate
Sir	silent information regulator
Sod	superoxide dismutase
STAR	subtelomeric anti-silencing regions
TCR	transcription-coupled repair
TERT	telomerase reverse transcriptase
TOR	target of rapamycin
TPE	telomeric position effect
TSA	trichostatin A
UPR^{ER}	unfolded protein response at the ER
UVER	UV-damaged DNA endonuclease-dependent excision repair

V-ATPase	vacuolar adenosine triphosphatase
w/o	without
wt	wild-type
XMP	xanthosine monophosphate
XP	*Xeroderma pigmentosum*
YES	yeast extract with supplements (medium)
YM	yeast minimal (medium)
YPD	yeast peptone dextrose (medium)

Yeast genes are named according to the *Saccharomyces cerevisiae* genome database (SGD) and the *Schizosaccharomyces pombe* gene database (*S. pombe* Gene DB) gene nomenclature conventions:
http://www.yeastgenome.org/help/yeastGeneNomenclature.shtml
http://old.genedb.org/genedb/pombe/ .
For amino acids, the one letter code was used, for instance: K, Lysine; R, Arginine; Q, Glutamine.

1 Introduction

1.1 Lifespan and aging

Nowadays, there is an increase in the number and proportion of older people in the human society. In this aging population, the prevention and treatment of age-related diseases is becoming more and more important. Therefore, it is necessary to understand the mechanisms that lead to aging – starting on the molecular level.

In the general public as well as in the scientific community, confusion exists regarding the precise usage of the terms aging and lifespan (Lithgow, 2006). Lifespan is defined by the time a given population or species has been observed to survive between birth and death. Maximum lifespan describes the maximum time one or more members of a population live, whereas mean lifespan stands for the average of the lifespan of all members of a population. In contrast, aging refers to the sum of changes that occur during later stages of life (Tollefsbol, 2010). Characteristics associated with aging are reduced functional capacity, increased vulnerability to multiple diseases, and a reduction in the ability to respond to stress or injury (Sell, 2009). Nutrient restriction results in a delay of the aging process or, in other words, in an increased lifespan (see 1.3).

There are several pathways responding to environmental influences that are ultimately responsible for lifespan changes. Based on the timing of their response to environmental changes, these pathways were grouped into general categories. The first category contains pathways that rapidly respond to acute stress, toxicity, and damage. The pathways of the second category respond moderately to nutrient availability, for instance the growth hormone, the insulin-like growth factor (IGF-1) (Wright *et al.*, 1992), and the target of rapamycin (TOR) pathway (see 1.3). The third category comprises the slowly responding pathways that are critical for genome integrity and other basic functions like DNA damage repair (see 1.5). Mutations in genes encoding proteins that are involved in genomic maintenance result in reduced lifespan and rapid senescence phenotypes. One example is the Werner's syndrome, where a DNA helicase involved in DNA repair, DNA recombination, and telomere maintenance is mutated (Sell, 2009).

Budding and fission yeast are useful model organisms for aging studies. As unicellular eukaryotes, they are both cell and organism. Their relatively short lifespan in combination with the availability of straightforward genetic techniques, new high-

throughput technologies, and the finding that several pathways affecting aging are evolutionarily conserved, provide good conditions to understand the basic mechanisms that alter lifespan.

Currently, aging is in the spotlight of science. There are a multitude of studies about the way aging and lifespan are altered, but there are also many disagreements concerning the exact mechanism and the evaluation of the individual components. However, it seems that the complex process of aging is regulated by many complex pathways, which in addition seem to affect each other. To get a general overview, the most prominent factors affecting aging and lifespan are discussed in the next paragraphs (1.3 – 1.7).

1.2 Replicative versus chronological lifespan in yeast

Two different types of aging or lifespan can be distinguished. Replicative lifespan (RLS) means the number of mitotic divisions a cell can undergo and serves as a model for the aging of actively dividing cells like germ line cells and stem cells (Roux *et al.*, 2010; Steinkraus *et al.*, 2008). In contrast, chronological lifespan (CLS) has been linked to the aging of differentiated somatic cells, for example neurons. CLS refers to the time a non-dividing cell population can remain viable, as defined by their ability to re-enter the cell cycle after a longer period of time in stationary phase (Fabrizio & Longo, 2003; Roux *et al.*, 2010). Notably, in the wild, yeast organisms are likely to exit the stationary phase only during the rare periods when all the nutrients required for growth become available.

RLS is best studied in *Saccharomyces cerevisiae*. One characteristic of the budding yeast is its asymmetrical division. To measure RLS, aged mother cells are isolated by micromanipulation, and daughter cells are counted and removed after every division (Park *et al.*, 2002). The mean RLS of *S. cerevisiae* amounts to approximately 20 generations and to 50 or more divisions for the maximum RLS. In *Schizosaccharomyces pombe*, the measurement of RLS is also possible but technically more difficult. The first three divisions of a virgin mother cell are morphologically symmetrical. Starting with the fourth division, the divisions are asymmetrical. The mother cell becomes rounder and bigger and can be distinguished from its daughter cells (Barker & Walmsley, 1999). Furthermore, Erjavec and colleagues found fission scars on the mother cells, which allow separation from the

very first division (Erjavec *et al.*, 2008). In contrast to budding yeast, the maximum lifespan of *S. pombe* is approximately 20 divisions.

CLS can be measured via staining with fluorescent dyes, like phloxine B or FUN-1 that distinguish living from dead cells (Longo, 2010). However, the traditional method to determine the CLS of budding and fission yeast is to measure the ability of individual cells to form a colony, which is referred to as the colony forming unit (CFU) method (Figure 1). Most studies have been performed using haploid *S. cerevisiae* strains, which were monitored until 99.9 % of the population died. In budding yeast, this takes 15 - 20 days, while the CLS of *S. pombe* is shorter. It was found that after approximately 10 h of incubation, the glucose concentration in the medium reaches very low levels, and *S. cerevisiae* cells switch from fermentation- to respiration-based metabolism. Furthermore, incubating the yeast cells in water results in increased chronological survival. This procedure rules out the possibility that extended CLS is an artefact caused by regrowth in the liquid culture (Longo, 2010).

Until today, the relationship between RLS and CLS is unclear, but there are at least the nutrient-sensing pathways that affect both RLS and CLS.

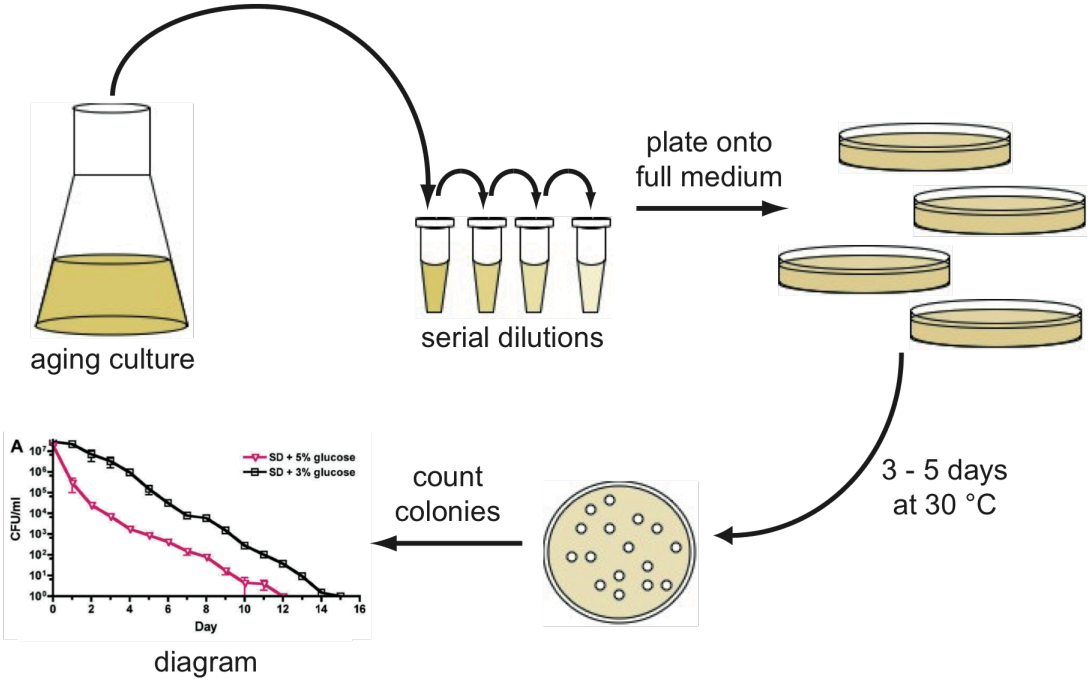

Figure 1 Schematic illustration of the traditional method used for measuring CLS
Aliquots of the aging cultures are taken at regular intervals and serially diluted. Multiple dilutions are plated on full medium plates and grown at 30 °C for 3 - 5 days. The forming colonies are then counted and used to calculate the number of colony forming units per ml culture (CFU/ml), which can be presented in a diagram. Diagram taken from (Chen & Runge, 2009).

1.3 Evolutionarily conserved nutrient-sensing pathways

Several evolutionarily conserved pathways and mechanisms are known to influence chronological and replicative lifespan in multiple organisms. The best studied regimen that extends lifespan from yeast to mammals is caloric restriction (CR) (Fontana *et al.*, 2010), which is defined by a moderate reduction in calorie intake. Due to the fact that lifespan can also be increased by changes of nutrition without altering the amount of calories, CR is often referred to as dietary restriction (DR). CR reduces the activity of various signal transduction pathways either directly, like the TOR pathway, or indirectly through reducing the levels of growth factors such as IGF-1 (worms, flies, mammals). A third pathway that affects lifespan in response to nutrients includes RAS, adenylate cyclase (AC), and protein kinase A (PKA) (Figure 2). Transcription factors like Msn2/4, DAF-16, and FOXO act downstream of these pathways to regulate the expression of enzymes and proteins involved in protective and metabolic activities that increase lifespan (Fontana *et al.*, 2010). In the presence of nutrients, the conserved biochemical signalling pathways are activated and the anti-aging transcription factors are kept in the cytoplasm in an inactive form. Notably, nutrition is not the only way to affect these pathways. Their life-extending effect can also be influenced by deleting or overexpressing one or more of the involved proteins as well as by treatment with compounds such as rapamycin, which inhibits TOR and therefore results in increased lifespan (Huang & Houghton, 2001; Huang *et al.*, 2003; Powers *et al.*, 2006). Compounds mimicking the beneficial effects of nutrient restriction are of special interest, because they are not only thought to delay aging but also to be potential therapeutic agents against age-related diseases and premature aging syndromes.

There are two major nutrient-sensing pathways in *S. cerevisae* (Figure 2). The first includes TOR and the serine-threonine kinase Sch9 (Fontana *et al.*, 2010). Deletion of *SCH9* promotes lifespan extension and resistance to both heat-shock and oxidative stress, as the inhibition or deletion of *TOR* does, probably by inactivating the downstream Sch9 (Kaeberlein *et al.*, 2005b). In the second pathway, the signal for glucose availability is transduced through the G-protein-coupled receptor Gpr1 and the Gα protein Gpa2. This results in the activation of the adenylate cyclase Cyr1. Upon stimulation by the Ras proteins Ras1 and Ras2, Cyr1 produces cAMP, which activates PKA (Dilova *et al.*, 2007).

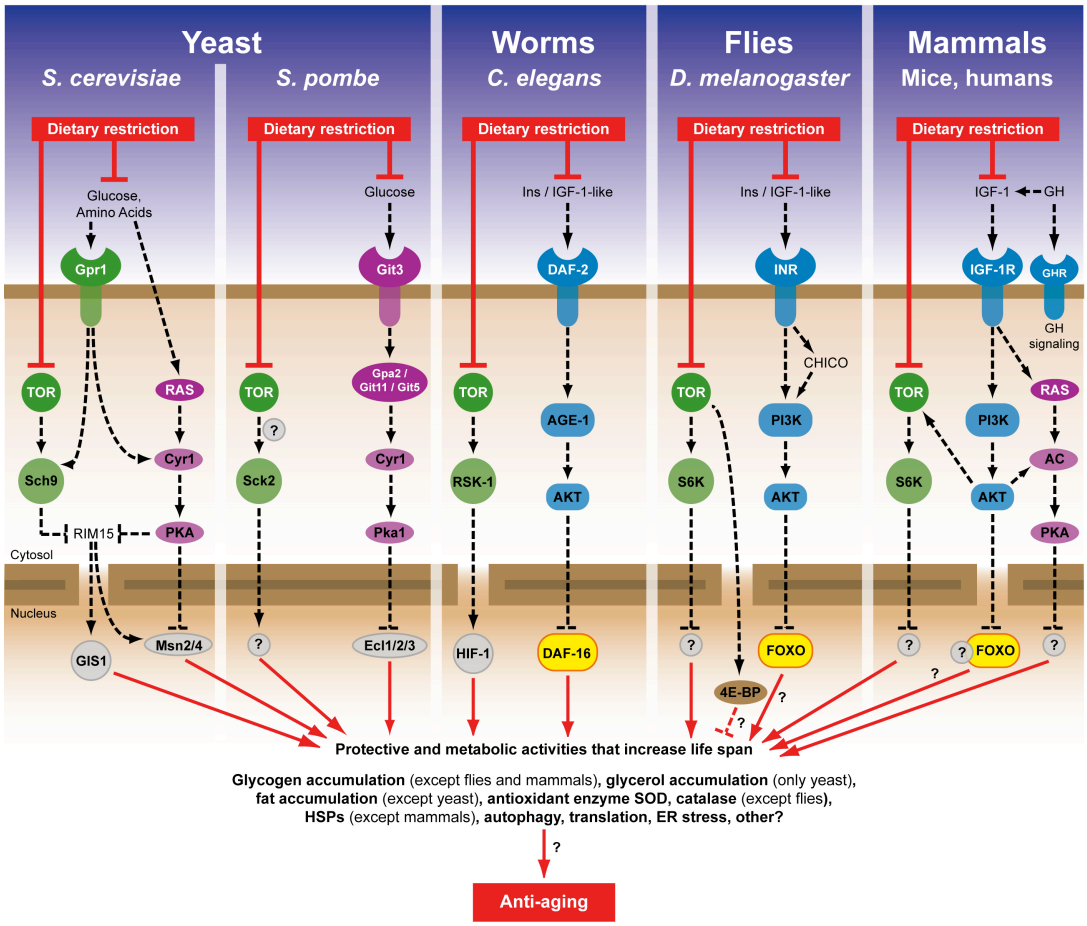

Figure 2 Schematic illustration of the conserved nutrient-sensing pathways regulating lifespan
The three evolutionarily conserved nutrient-sensing pathways that extend lifespan when inhibited by a restriction of nutrients (glucose, fat, proteins, amino acids) are the TOR signalling pathway (green), the RAS/AC/PKA pathway (purple), and the insulin/IGF-like signalling pathway (blue). Picture based on (Fontana et al., 2010) and (Roux et al., 2010).

In *S. pombe*, there are two known nutrient-sensing pathways that are affected by nutrient restriction, the Git3/protein kinase A (Pka1) signalling pathway and the TOR pathway including the serine-threonine kinase Sck2, which – like Sch9 in *S. cerevisiae* – shows similarity to the ribosomal protein S6 kinase (S6K) (Roux *et al.*, 2010) (Figure 2). Mutants that exhibit defects in one of these pathways like *pka1*Δ and *sck2*Δ display extended lifespan, but only *pka1*Δ (not *sck2*Δ) mutants are resistant to heat-shock and oxidative stress (Roux *et al.*, 2006). In general, lifespan changes are less well characterized in fission yeast than in budding yeast.

Although RLS and CLS are both influenced by the basic components of the nutrient-sensing pathways, there are also some differences that have been reported for *S. cerevisiae*. For instance, CLS is affected by TOR-controlled autophagy (Dilova *et al.*, 2007). Additionally, extension of CLS by CR requires mitochondrial respiration, which results in the formation of reactive oxygen species (ROS). This is contrary to

Harman's free-radical theory of aging, which states that free radicals lead to a reduced lifespan (Harman, 1956). However, recent studies showed that the increased formation of ROS within the mitochondria causes an adaptive reaction leading to an increased stress response via the transcription factors Msn2/4, Gis1, and the superoxide dismutase 2 (Sod2). This in turn results in a long-term reduction of oxidative stress. This kind of reverse effect of the response to ROS stress is called mitochondrial hormesis or mitohormesis and is thought to be the (or at least one) reason for the life-extending effect of glucose restriction (Dilova *et al.*, 2007; Fontana *et al.*, 2010; Ristow & Zarse, 2010; Ristow & Schmeisser, 2011). Extension of CLS by stress and the activation of stress responses has also been shown for *S. pombe* (Zuin *et al.*, 2010). On the other hand, replicative survival via decreasing PKA activity requires Sir2, which inhibits the formation of extrachromosomal rDNA circles (ERCs, see 1.7). Furthermore, TOR regulates ribosome biogenesis and the deletion of ribosomal proteins increases RLS (Dilova *et al.*, 2007; Mayer & Grummt, 2006). Although it is known that the TOR pathway controls many aspects of cell physiology, it still remains unclear precisely which aspect of TOR signalling contributes most significantly to aging and lifespan regulation.

Findings from model organisms such as yeasts, *Caenorhabditis elegans*, *Drosophila melanogaster* and mice are currently being tested in monkeys, human cell lines, and also in human volunteers (Fontana *et al.*, 2010). Multiple beneficial effects of reduced signalling are observed in mice. These include protection against cancer, diabetes, atherosclerosis, cardiomyopathy as well as protection against autoimmune, kidney, and respiratory diseases and reduced neurodegeneration (Fontana *et al.*, 2010). If these effects are confirmed in humans, drugs that block these pathways could be considered for the prevention of specific diseases.

1.4 Impact of epigenetics on aging

Epigenetic marks include chromatin modifications, DNA methylation, and histone variants that are inherited through cell divisions and alter chromatin status without changes in DNA or protein sequence (for details see 1.9). They are essential for normal development and for the maintenance of cellular functions in an adult organism (Allis *et al.*, 2007), and many epigenetic mechanisms are thought to have an impact in the aging process and age-related diseases.

Acetylation of histones is generally associated with increased transcriptional activity, while the effect of histone methylation depends on the residue. For instance, methylation of H3K4 (histone H3 lysine 4) is often found in active chromatin, but methylation of H3K9 usually leads to transcriptional repression (Kouzarides, 2007). During aging, changes in histone modifications occur (Tollefsbol, 2010). One example is the methylation of H4K20. H4K20me1 has been linked with transcriptional repression (Karachentsev *et al.*, 2005), while H4K20me2 plays an important role in the cellular response to DNA damage (Botuyan *et al.*, 2006; Schotta *et al.*, 2008). H4K20me3 is highly enriched at certain heterochromatic regions. Alterations in H4K20me3 levels correlate with important biological processes and increase with age (Sarg *et al.*, 2002). In line with this, premature aging syndrome cells show elevated H4K20me3 levels (Shumaker *et al.*, 2006). In contrast, reduced H4K20me3 correlates with cancer progression (Fraga *et al.*, 2005), perhaps due to reduced repression of repetitive elements and thus genomic instability (Howard *et al.*, 2008). Additionally, H4K20me3 might be involved in transcriptional regulation of genes (Donati *et al.*, 2008; Gurtner *et al.*, 2008). To date, it is not known whether loss of H4K20me3 is a cause or consequence for the carcinogenesis process.

DNA methylation controls the maintenance of gene expression programs. The DNA methylation status is balanced in mature cells, but with age this balance is strongly shifted in favour of loss of DNA methylation (Liu *et al.*, 2003). Therefore, DNA hypomethylation that occurs during normal aging appears to be a critical risk factor contributing to the development of chronic age-related human pathological states (Tollefsbol, 2010). In many eukaryotes, DNA methylation at the cytosine-5 position typically occurs in CpG dinucleotides. Hypermethylation is usually associated with transcriptional repression, while hypomethylation is generally linked to transcriptional activity. Nevertheless, there is also regional hypermethylation of specific genes whose promoters are rich in CpG islands (Liu *et al.*, 2003; Liu & Rando, 2011). This has been linked to the silencing of tumour suppressor genes (Liu & Rando, 2011). Changes in DNA methylation occur consistently near genes involved in metabolism and metabolic regulation and are implicated in the pathogenesis of age-related diseases (Thompson *et al.*, 2010). Notably, there is no DNA methylation in the yeasts *S. cerevisiae* and *S. pombe*.

Epigenetic mechanisms, especially changes in DNA methylation, appear not only to influence the fundamental aspects of aging, but also to contribute significantly to

premature aging syndromes and the pathogenesis of several major age-related human diseases including cancer, atherosclerosis, Alzheimer's disease, psychiatric disorders, and autoimmune pathologies (Tollefsbol, 2010). Therefore, compounds affecting these mechanisms can be considered potential therapeutics against these diseases. Notably, there is a possible link between nutrient restriction and epigenetic changes. For instance, epigallocatechin-3-gallate (EGCG), a component of green tea, is one of the natural products found to inhibit mTOR (Zhou *et al.*, 2010) and it seems to nutritionally modulate DNA methylation (Tollefsbol, 2010).

Altogether, the exact contribution of epigenetic dysregulation on aging and age-related diseases remains unclear (Thompson *et al.*, 2010). Additionally, some epigenetic modifications are secondary to DNA damage. For instance, phosphorylation of H2AX, a histone variant, is induced by double-strand breaks. There is also evidence that levels of acetylation of H3K56 and methylation of H3K79 increase after DNA damage (Liu & Rando, 2011) This leads to the question whether epigenetic changes may play a causal role in cellular aging or whether they are merely consequences of the aging process (Liu & Rando, 2011).

1.5 Defects in DNA repair as a cause of cancer and progeroid diseases

As mentioned in the previous paragraph, another factor that is associated with aging is DNA damage and DNA repair. DNA damage due to mismatches after DNA replication or caused by reactive chemicals, radiation or UV light are corrected by a variety of repair pathways to prevent the formation of mutations and thereby maintain the genetic information. Nevertheless, DNA damage accumulates in normal aging (Dolle *et al.*, 1997; Sedelnikova *et al.*, 2004). Defects in DNA repair result in premature aging and increased susceptibility to cancer, which are also linked to critically short telomeres in human chromosomal instability syndromes (Blasco, 2005) (see 1.6). For instance, Werner's syndrome is caused by a mutation of a helicase involved in DNA repair and telomere maintenance. Other DNA repair proteins with impact on telomere protection and telomere length regulation, such as proteins involved in the repair of mismatches and double-strand breaks (DSBs), are altered in various types of human tumour (Blasco, 2005).

DSBs, which can be caused by reactive oxygen species (ROS), are repaired by homologous recombination (HR) and non-homologous end-joining (NHEJ) (Sancar *et al.*, 2004). In the case of single-strand DNA damage, there are a number of excision repair pathways that remove the damaged nucleotide and replace it with an undamaged nucleotide complementary to that found in the undamaged DNA strand.

Mismatch repair (MMR)[1] corrects errors of DNA replication and recombination that result in mispaired, but undamaged nucleotides in a strand-specific manner (Li, 2008). Additionally, it repairs DNA changes that are caused by chemical agents such as alkylation. The majority of DNA mismatches and single base loops are recognized and bound by the MutSα heterodimer (hMsh2/hMsh6), while a second complex, MutSβ (hMsh2/hMsh3) recognizes insertion/deletion loops (IDLs). The MutS heterodimer forms a complex with the MutL heterodimer (hPms2/hMlh1), thus enhancing ATP hydrolysis-dependent translocation along the DNA (Buermeyer *et al.*, 1999; Marti *et al.*, 2002). As a result, the DNA mismatch is excised, but the exact mechanism is still unclear. There are different proteins that are known to be involved in excision and synthesis of the new DNA, for instance PCNA, exonuclease 1, and the endonuclease FEN1 (Marti *et al.*, 2002). There is the “futile DNA repair cycle” model suggesting that DNA lesions like ^{6Me}G in the template strand induce misincorporation, which triggers the strand-specific MMR reaction. Since MMR only targets the newly synthesised strand for repair, the offending lesion in the template strand cannot be removed, and will provoke a new cycle of MMR upon repair synthesis. Such a futile repair cycle persists and activates DNA damage signalling pathways to promote cell cycle arrest and/or apoptosis (Li, 2008; Stojic *et al.*, 2004). The importance of MMR was discovered in humans with defects in this repair pathway. For instance, *MLH1* is mutated in the germ line of families, in which members are predisposed to a type of colon cancer (Liu *et al.*, 1995). Epigenetic silencing of a non-mutated *MLH1* gene was found in patients with non-familial colon cancer. In cell culture, re-expression of this silenced *MLH1* gene produces reappearance of a functional protein that restores a considerable portion of the damage MMR (Herman *et al.*, 1998). Notably, defects in MMR seem to promote cellular proliferation in a telomerase-independent manner (Rizki & Lundblad, 2001).

[1] Unless indicated otherwise, the mentioned proteins represent the human homologs.

Nucleotide excision repair (NER)[1] is a DNA repair pathway that recognizes a variety of DNA damages, including bulky, helix-distorting lesions such as UV-induced pyrimidine dimers. It is divided into two subpathways designated “global genomic repair” (GGR), which scans the entire genome for strand-distorting lesions, and “transcription-coupled repair” (TCR) (Fukumoto *et al.*, 2002). The latter especially focuses on lesions that block elongating RNA polymerases. In GGR, which is specifically required for repair in germ cells (Lans *et al.*, 2010), DNA damage is recognized by the XPC/hHR23B complex, which is also involved in the assembly and disassembly of NER complexes. In TCR, the blocked DNA polymerase is removed by CSA and CSB. The next steps are common to both GGR and TCR. TFIIH, which includes the helicases XPB and XPD among others, opens the DNA helix in the region around the lesion. Two endonucleases, XPA and ERCC1/XPF, incise the 3’ and the 5’ end of the damaged DNA strand, respectively, resulting in the removal of a 25 - 30 nt DNA fragment containing the lesion. DNA polymerases fill the gap and DNA ligases seal the final nick (Schumacher *et al.*, 2008). Some of the proteins involved in NER contain XP in their name due to the fact that defects in GGR give rise to the cancer-prone syndrome *Xeroderma pigmentosum*. This disease is characterized by hypersensitivity to sunlight, elevated sun-induced skin cancer, and accelerated skin aging caused by non-repaired UV damages (de Boer & Hoeijmakers, 2000). In contrast, defects in TCR cause Cockyane syndrome (CS), a progressive neurodevelopmental disorder (Schumacher *et al.*, 2008).

Base excision repair (BER)[1] is primarily responsible for the genome-wide removal of single bases that are damaged by oxidation, alkylation, hydrolysis, or deamination (Wood, 1996). Damaged DNA bases are recognized and removed by lesion-specific DNA glycosylases resulting in the generation of apurinic/apyrimidinic (AP) sites that are bound by another enzyme, such as Nth1 in *S. pombe*, a DNA glycosylase associated with AP lyase activity (Kanamitsu & Ikeda, 2010). In combination with XRCC1, the DNA polymerase β (Polβ) fills the gap of one nucleotide. This mechanism is referred to as short-patch BER. In contrast, long-patch BER stands for the repair of single-stranded DNA breaks, where a fragment of 2 - 10 bases containing the lesion is incised by the FEN1 endonuclease. Different enzymes are involved in the synthesis of the new DNA and ligation, for instance Polβ, PCNA, and DNA ligase 1 (Sancar *et al.*, 2004). Notably, DNA damage usually recognized by BER is corrected by TCR, if it blocks gene transcription.

It is already known that factors that are part of NER, also interact with BER and MMR components (Bertrand *et al.*, 1998; Fleck *et al.*, 1999; Kanamitsu & Ikeda, 2010) and that these three DNA repair pathways exhibit partially overlapping functions (Fleck *et al.*, 1999; Kunz & Fleck, 2001; McCready *et al.*, 2000; Yonemasu *et al.*, 1997; Yoon *et al.*, 1999).

1.6 Relevance of telomere length and telomerase activity in aging and cancer

Telomeres are the protective ends of linear chromosomes with short, single-stranded DNA overhangs. They display a highly repetitive structure. The formation of subtelomeric heterochromatin prevents degradation, end-to-end fusions, and homologous recombination of the chromosome ends (see 1.10.2). The conventional DNA machinery is not able to fully synthesize the 3' end of linear DNA. This is called end replication problem and as a consequence, the telomeres shorten with each round of replication. This in turn leads to impaired telomere function resulting in chromosomal instability, loss of genetic information, and finally cell death (Gilson & Geli, 2007; Smogorzewska & de Lange, 2004). In general, telomere shortening has been linked to reduced lifespan and premature aging (Blasco, 2005). Therefore, telomere length can be used as an aging marker (Lai *et al.*, 2005).

An evolutionarily conserved ribonucleoprotein complex, the telomerase, maintains telomere length. In *S. cerevisiae*, this complex consists of three protein subunits, Est1 - 3, and a RNA moiety called TLC1. The telomerase is a reverse transcriptase that uses the telomerase RNA as a template and adds TG repeats onto the 3' end of the telomeric DNA during late S phase (Dionne & Wellinger, 1996; Wellinger *et al.*, 1993). Telomerase activity is coupled with conventional DNA replication to form double-stranded DNA by lagging strand synthesis (Diede & Gottschling, 1999; Grossi *et al.*, 2004). In addition to telomerase, there are several proteins that are also essential for telomere length, for instance by recruiting telomerase to the chromosome ends. The Ku heterodimer (Ku70/80) protects telomeres from degradation and determines the subnuclear localization of telomeres (Laroche *et al.*, 1998). In addition, Ku helps Rap1 to recruit the Sir complex to the telomeres (Martin *et al.*, 1999), thereby regulating telomeric silencing (Boulton & Jackson, 1996; Moretti *et al.*, 1994) (see 1.10.2). Rap1 in turn is a key component of a process that

"measures" the telomere length in *S. cerevisiae*. A high number of Rap1 molecules bound to the telomeres inhibits telomerase activity, whereas a low number of Rap1 molecules facilitates telomerase action (Marcand *et al.*, 1997).

In humans, germ line cells have high telomerase activity, resulting in the maintenance of telomere length. In contrast, somatic cells possess a low or no telomerase activity and their telomeres shorten with age (Blasco, 2005). Studies with human patients and tissues linked degenerative diseases, both inherited and acquired, and premature aging syndromes to aberrant telomerase expression (Lai *et al.*, 2005). For instance, Werner's syndrome fibroblasts show accelerated telomere attrition and undergo premature aging that can be rescued by enforced expression of the catalytic subunit of telomerase, the telomerase reverse transcriptase (TERT) (Wyllie *et al.*, 2000). Although the epigenetic control of the *TERT* gene is not yet fully resolved, it is clear that cellular modifications especially in DNA methylation and histone modifications affect the *TERT* promoter region, which lead in part to regulation of this important gene in cellular aging (Tollefsbol, 2010). Therefore, chemical or natural compounds that increase telomerase activity, for instance by affecting epigenetic modifications, are promising therapeutics against premature aging. However, telomere length, telomerase activity, and epigenetic mechanisms are not only essential for cellular aging. They also play an important role in cancer. In general, tumour cells have shorter telomeres than the surrounding tissue due to their faster proliferation. Early tumour cells lack telomerase activity and replicate fast, resulting in fast telomere shortening and increased apoptosis within the tumour (Blasco, 2005). In 90 % of all types of human tumour, telomerase is reactivated, potentially due to age-related changes in DNA methylation and histone modifications resulting in rescue of short telomeres and maintenance of cells with potential chromosomal instability (Blasco, 2005). The fact that cancer cells have generally shorter telomeres than normal cells, together with the fact that cancer growth seems to depend on telomerase reactivation, indicates that therapeutics inhibiting telomerase activity will preferentially kill tumour cells and have no toxicity in normal cells.

Importantly, telomere length and telomerase activity have a different effect on aging in *S. cerevisiae*. It has been shown that there is an inverse correlation between lifespan and telomere length in budding yeast (Austriaco & Guarente, 1997). Overexpression of truncated *TLC1* leads to a shorter steady-state telomere length

and RLS extension. In contrast, RLS is decreased in yeast strains with longer telomeres (Austriaco & Guarente, 1997). It appears that telomeres regulate lifespan by modulating genomic silencing. It has been suggested that shortening of telomeres results in less recruitment of the SIR silencing machinery to the telomeres and a concomitant redistribution of this machinery to non-telomeric sites, like subtelomeric regions and the rDNA locus, that causes a delay in aging (Austriaco & Guarente, 1997; Kozak *et al.*, 2010). Conversely, telomere lengthening decreases lifespan and this decrease is due, at least in part, to greater recruitment of the Sir complex by the long telomeres (Austriaco & Guarente, 1997). This assumption is supported by findings of Tgs1, a snRNA and snoRNA methyltransferase, which is responsible for the m_3G cap formation of the telomerase RNA moiety TLC1 in budding yeast. The absence of Tgs1 leads to elongated telomeres, enhanced telomeric silencing, and decreased RLS (Franke *et al.*, 2008). Notably, the three heterochromatic regions in *S. cerevisiae* compete for the limited amount of Sir proteins, especially Sir2. Increased telomeric and/or *HM* silencing results in reduced repression at the rDNA locus (Smith *et al.*, 1998), and derepression at this locus leads to the formation of ERCs whose accumulation in the mother cell correlates with aging (Sinclair & Guarente, 1997) (see 1.7).

1.7 Impact of sirtuins on aging

Sirtuins regulate various normal and abnormal cellular and metabolic processes, including tumorigenesis, neurodegeneration, and processes associated with type 2 diabetes and obesity. Several age-related diseases, such as Alzheimer's disease, and longevity have also been linked to the functions of sirtuins (Aljada *et al.*, 2010). Therefore, compounds affecting the activity of the sirtuins are potential therapeutics against these diseases.

The silent information regulator 2 (Sir2) is a NAD^+-dependent histone deacetylase (HDAC) in *S. cerevisiae* and it is the founding member of the family of sirtuins. It is the catalytic subunit of the SIR complex and is involved in several cellular functions such as formation of heterochromatin at the *HM* loci, the telomeres, and the rDNA locus (see 1.10). Sir2 also takes part in the maintenance of genome stability via the repair of double-strand DNA breaks (Tsukamoto *et al.*, 1997). This HDAC primarily affects replicative lifespan (RLS) not through telomeric repression or telomere length,

but through rDNA silencing (Kaeberlein *et al.*, 1999). Due to their repetitive nature, rDNA arrays tend to undergo unequal recombination, which is suppressed by Sir2 (Gottlieb & Esposito, 1989). In *S. cerevisiae*, deletion of *SIR2* results in shortened RLS due to the formation of extrachromosomal rDNA circles (ERCs) (Kaeberlein *et al.*, 1999; Steinkraus *et al.*, 2008), which segregate asymmetrically during cell division. Their accumulation in the mother cell correlates with senescence (Figure 3). In agreement with this finding, overexpression of *SIR2* increases RLS by suppressing rDNA recombination and decreasing ERC formation (Kaeberlein *et al.*, 1999; Steinkraus *et al.*, 2008). Notably, Sir2 abundance decreases with age (Dang *et al.*, 2009). Furthermore, there is some debate about the exact role of sirtuins in yeast caloric restriction (CR). Kaeberlein and colleagues reported that Sir2 and CR increase lifespan through independent pathways (Kaeberlein *et al.*, 2004). However, a recent study indicates that there is a correlation between Sir2 and TOR signalling, because inhibition of TOR signalling by treatment with rapamycin leads to enhanced association of Sir2 with rDNA, resulting in decreased formation of ERCs and thus in extended RLS in *S. cerevisiae* (Ha & Huh, 2011). On the other hand, it has been reported that improved RLS is caused by increased rDNA stability and not through reduced formation of ERCs (Ganley *et al.*, 2009; Unal *et al.*, 2011). In line with this, sirtuins have been shown to play a conserved anti-aging role in higher eukaryotes (Haigis & Sinclair, 2010) although the accumulation of excised rDNA rings has not been detected in other species. Nevertheless, there is a recent publication that stated that overexpression of *SIR2* homologs did not affect the lifespan of *C. elegans* and *D. melanogaster* and that previously described longevity might be effects of the genetic background (Burnett *et al.*, 2011).

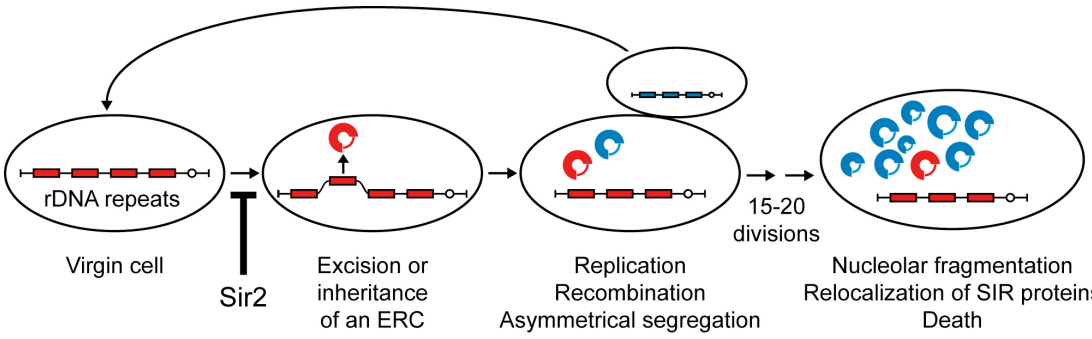

Figure 3 rDNA recombination results in cellular senescence
In *S. cerevisiae*, Sir2 represses the homologous recombination at the rDNA locus. Derepression results in the formation of extrachromosomal rDNA circles (ERCs), which segregate asymmetrically. Their accumulation in the mother cell finally leads to cell death. Picture based on (Grunstein & Gasser, 2007).

In mammals, there are seven sirtuins (SirT1 - 7), which are characterized by their highly conserved central NAD^+-binding and catalytic domain (Haigis & Sinclair, 2010). They are strongly inhibited by nicotinamide (NAM, Figure 4) (Bitterman *et al.*, 2002; Sauve & Schramm, 2003; Sauve *et al.*, 2006). The inhibition by NAM requires that NAM enters a highly conserved C-pocket, which is adjacent to the NAD^+-binding site, thereby blocking NAD^+ hydrolysis. In yeast, worms, and flies, NAM is recycled back to NAD^+ in four steps, among others by the nicotinamidase Pnc1, which produces nicotinic acid in the first step (Haigis & Sinclair, 2010).

The best studied mammalian sirtuin is SirT1. So far, most studies support the model that SirT1 mediates several beneficial effects of CR (Haigis & Sinclair, 2010), such as an increase in physical activity (Chen *et al.*, 2005). However, the exact mechanism is still unclear. SirT1-deficient mice have a shorter lifespan, and CR does not increase the lifespan of these animals (Li *et al.*, 2008). Therefore, SIRT1 may be required for lifespan extension by CR in mammals. However, upregulation of SirT1 expression by CR seems to be induced in a tissue-specific manner (Chen *et al.*, 2008; Cohen *et al.*, 2004). It is known that Sir2 is recruited to telomeres in yeast, and that the SIR complex spreads into subtelomeric regions via histone deacetylation, thereby forming heterochromatin. In contrast, potential functions of SirT1 at telomeres are less clear. A recent study showed that SirT1 is a positive regulator of telomere length *in vivo* and attenuates telomere shortening with aging, an effect that dependents on telomerase activity (Palacios *et al.*, 2010).

Sirtuins do not only modify histones, but also other substrates. For instance, mammalian SirT1 deacetylates among others the transcription factors FOXO and p53 in response to stress and DNA damage (Grunstein & Gasser, 2007; Haigis & Sinclair, 2010). This constitutes an additional possibility of SirT1-mediated lifespan extension, because acetylation of the tumour suppressor p53 promotes apoptosis (Luo *et al.*, 2001; Vaziri *et al.*, 2001). However, preventing apoptosis of cells with DNA damages may lead to cancer. Therefore, SirT1 is a possible cancer-related factor and compounds inhibiting SirT1, such as splitomicin (Figure 4), sirtinol, and EX-527, are potential anti-cancer therapeutics. Sirtuin activity can also be affected by modifications. SirT1 has at least 13 residues that are phosphorylated *in vivo*, and removal of these phosphates decreases its catalytic activity (Haigis & Sinclair, 2010). Additionally, the *SIRT1* gene is controlled by numerous transcription factors and microRNAs (Haigis & Sinclair, 2010).

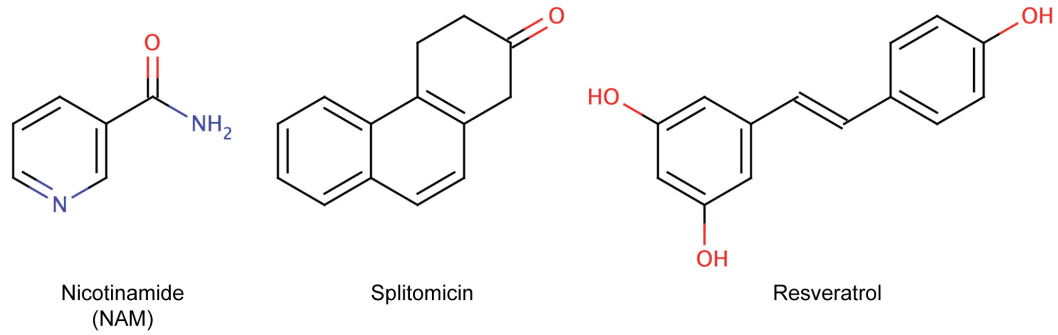

Nicotinamide (NAM) Splitomicin Resveratrol

Figure 4 Chemical structures of nicotinamide, splitomicin, and resveratrol
Nicotinamide and splitomicin are thought to inhibit sirtuin activity, while resveratrol is a potential sirtuin activator. The chemical structures were created by using the software MarvinSketch.

Work on sirtuins and the mechanisms of nutrient restriction have given hope to the synthesis of future drugs to increase human lifespan by simulating the effects of DR. There are already compounds that have been proposed to activate SirT1 including resveratrol (Figure 4), quercetin, butein, SRT1720, and SRT2183 (Haigis & Sinclair, 2010). They are thought to work by lowering the Michaelis constant for the substrate and for NAD^+ and, to a lesser extent, by increasing enzyme velocity (V_{max}) (Haigis & Sinclair, 2010). In contrast, analogues of NAM appear to activate sirtuins by occluding the C-pocket, thereby interfering with NAM inhibition (Sauve *et al.*, 2006). Among these potential sirtuin-activating compounds, the best known is resveratrol, a natural compound found in several plants including red grapes. It is thought to mimic some of the effects of CR in a wide variety of organisms from yeast to mice, possibly by the activation of Sir2/SirT1. A recent study concludes that SRT1720 and resveratrol are not direct activators of SirT1, but can only activate the HDAC activity of SirT1 *in vitro* using one particular substrate (Beher *et al.*, 2009). Another hypothesis is that resveratrol inhibits mTOR in mammals (Zhou *et al.*, 2010). However, it remains controversial whether resveratrol actually extends lifespan, since many laboratories have not been able to reproduce the original observation in yeast (Bass *et al.*, 2007; Howitz *et al.*, 2003; Kaeberlein *et al.*, 2005a; Wood *et al.*, 2004). Mice on a high-fat diet treated with resveratrol display reduced mortality or protection against morbidity, possibly by activating a set of genes affected by nutrient restriction (Baur *et al.*, 2006). However, mice and flies fed standard diet do not show increased survival (Fontana *et al.*, 2010; Pearson *et al.*, 2008). However, the resveratrol formulation SRT501 has already been tested on humans, but the clinical trial was suspended because several patients developed kidney failure.

1.8 Compounds known to extend lifespan

So far, several compounds have been identified that are thought to extend the lifespan of at least one model organism. In this paragraph the most prominent candidates and their potential mode of action are summarized.

Altering the nutrient signalling pathways displays the best known and so far the most effective way to extend lifespan (see 1.3). Apart from CR/DR, the deletion of components of these pathways or their inhibition by compounds also results in an increase in lifespan. For instance, rapamycin extends lifespan of *D. melanogster* (Bjedov *et al.*, 2010; Moskalev & Shaposhnikov, 2010) and mice (Harrison *et al.*, 2009) as well as CLS and RLS in yeast (Medvedik *et al.*, 2007; Wanke *et al.*, 2008) by inhibiting the TOR-containing complex TORC1. This in turn, leads to longevity-promoting effects, like enhanced stress resistance, which have also been reported for this compound (Medvedik *et al.*, 2007). Furthermore, methionine sulfoxime (MSX) is known to increase CLS in yeast by inhibiting the glutamine synthetase and reducing both intracellular glutamine level and TOR signalling (Crespo *et al.*, 2002). Additional compounds that have been reported to promote longevity by direct or indirect inhibition of the TOR signalling pathway, are caffeine (yeast, CLS) (Wanke *et al.*, 2008), metformin (*C. elegans* and mice) (Anisimov *et al.*, 2008; Onken & Driscoll, 2010), wortmannin (*D. melanogaster*) (Moskalev & Shaposhnikov, 2010), and curcumin (*D. melanogaster*, mammals) (Beevers *et al.*, 2009; Chen *et al.*, 2011; Yu *et al.*, 2008) as well as LY294002 and U0126 (human fibrosarcoma cells, RLS) (Demidenko *et al.*, 2009). In contrast, valproic acid may increase lifespan of *C. elegans* by promoting nuclear localization of DAF-16, thereby reducing the activity of the insulin/IGF-1 signalling pathway (Evason *et al.*, 2008).

Another mechanism that is thought to result in lifespan extension is the activation of Sir2 and SirT1. In this context, the most prominent compound is resveratrol. However, as mentioned above, the longevity-promoting effect of this polyphenol is controversial. Some labs report that resveratrol extends the lifespan for instance of S. *cerevisiae*, *C. elegans*, and *D. melanogaster* (Gruber *et al.*, 2007; Howitz *et al.*, 2003; Wood *et al.*, 2004), but other labs failed to reproduce these results (Bass *et al.*, 2007). Apparently, resveratrol increases the life of mice only if they were fed a high-calorie diet, but not a standard diet (Baur *et al.*, 2006; Pearson *et al.*, 2008). Actually, there are doubts whether resveratrol is a direct activator of SirT1 (Zarse *et al.*, 2010) or rather an inhibitor of TOR signalling (Zhou *et al.*, 2010). Other SirT1 activators that

are thought to increase lifespan are quercetin (Pietsch *et al.*, 2011) and fisetin (Chen *et al.*, 2011). Notably, resveratrol and quercetin have antioxidant properties (Cherniack, 2010) and according to Harman's free-radical theory of aging (Harman, 1956), antioxidants like lipoic acid may increase lifespan by detoxifying free radicals and/or enhancing resistance to age-related oxidative stress (Bauer *et al.*, 2004; Benedetti *et al.*, 2008).

Furthermore, compounds affecting the epigenetic state of the chromatin are thought to influence lifespan. For instance, it has been reported that lithium extends the lifespan of *C. elegans* by altering the transcription of genes involved in histone methylation, nucleosome composition, and chromatin structure, thereby modulating longevity-related processes (McColl *et al.*, 2008). HDAC inhibitors such as trichostatin A (TSA) and sodium butyrate promote longevity in *D. melanogaster* by hyperacetylation of the canonical histone H3 and increased expression of heat shock proteins (Zhao *et al.*, 2005). Another compound that has been shown to extend lifespan by affecting PTMs is spermidine. Treatment of aging yeast cells with this HAT inhibitor results in hypoacetylation of histone H3 as well as in reduced ROS levels and suppression of necrosis (Eisenberg *et al.*, 2009). Notably, the altered acetylation status of the chromatin led to significant upregulation of various autophagy-related transcripts, triggering autophagy in yeast, worms, flies, and human cells, where enhanced autophagy is crucial for polyamine-induced suppression of necrosis and improved longevity (Eisenberg *et al.*, 2009).

Compounds that promote longevity in model organisms and/or human cell lines are not only thought to extend human lifespan, but primarily to be potential therapeutics against premature aging syndromes and age-related diseases. One example is metformin, which is already used for the treatment of type 2 diabetes (Goldberg *et al.*, 2010). However, it is known that some compounds have side effects. For instance, rapamycin strongly suppresses the immune system. As a consequence, the life-extending effect of those compounds can not be studied in humans. Therefore, the identification of novel longevity-promoting compounds is of continued interest.

1.9 Eukaryotic chromatin and epigenetic marks

Since chromatin structure and epigenetic marks play an important role in aging (see 1.4, 1.6, 1.7), they are explained in more detail in this and the following paragraph.
The human genome consists of a total of about 3×10^9 base pairs (bp), which are organized into 23 chromosome pairs, and contains approximately 23,000 protein-coding genes, far fewer than had been expected before its sequencing (Consortium, 2004). In fact, only about 1.5 % of the genome codes for proteins, while the rest consists of non-coding RNA (ncRNA) genes, regulatory sequences, introns, and non-coding DNA (ncDNA) (Consortium, 2001).

In other organisms, the size and complexity of the genome differ as revealed by sequencing whole genomes of many eukaryotic organisms. The first eukaryotic organism whose genome was completely sequenced is the unicellular budding yeast *S. cerevisiae* (Goffeau *et al.*, 1996). This genome contains about 6,000 genes on 16 chromosomes and is more compact than the human genome meaning that the majority of the DNA sequence consists of open reading frames (ORFs) (Dujon, 1996).

For the development of higher eukaryotes, not only the nucleotide sequence or the number of genes are important, but also the precise control of gene expression. There are regulatory options that change gene transcription through modulation of chromatin without affecting the actual sequence of DNA nucleotides. Examples are replacement of canonical histones by histone variants, chromatin remodelling, posttranslational modifications (PTMs) of histone tails, and DNA methylation. These epigenetic marks appear to be inherited through all cell divisions, providing cellular "memory" that may extend the heritable information of the genetic (DNA) code. They are not only important for regulating gene expression, but also for genome replication and other cellular processes (Allis *et al.*, 2007; Bernstein *et al.*, 2007; Misteli, 2007).

In eukaryotic cells, DNA is packed into a nucleoprotein structure called chromatin that contains nucleosomes as the basic unit. The nucleosome consists of 147 bp DNA wrapped around one histone octamer, which is formed by two copies of each of the canonical histones – H2A, H2B, H3, and H4 (Kornberg, 1974; Luger *et al.*, 1997a; Luger *et al.*, 1997b). Several amino acids of the highly conserved histones have been found to be a target of PTMs – primarily at the N-terminal tails of histones, but also in the globular histone domains (Xu *et al.*, 2005). For instance, lysines can be acetylated (ac), methylated (me) or ubiquitinated (ub). These residues can not only

be (mono-) methylated but also di- and tri-methylated. Arginines can be methylated and serines or threonines can be phosphorylated (ph) (Figure 5). Additionally, there are isomerisation of prolines, SUMOylation, ADP-ribosylation, and deimination (Kouzarides, 2007). This diversity of modifications displays some kind of a “histone code” and increases the amount of information beyond the DNA sequence (Jenuwein & Allis, 2001).

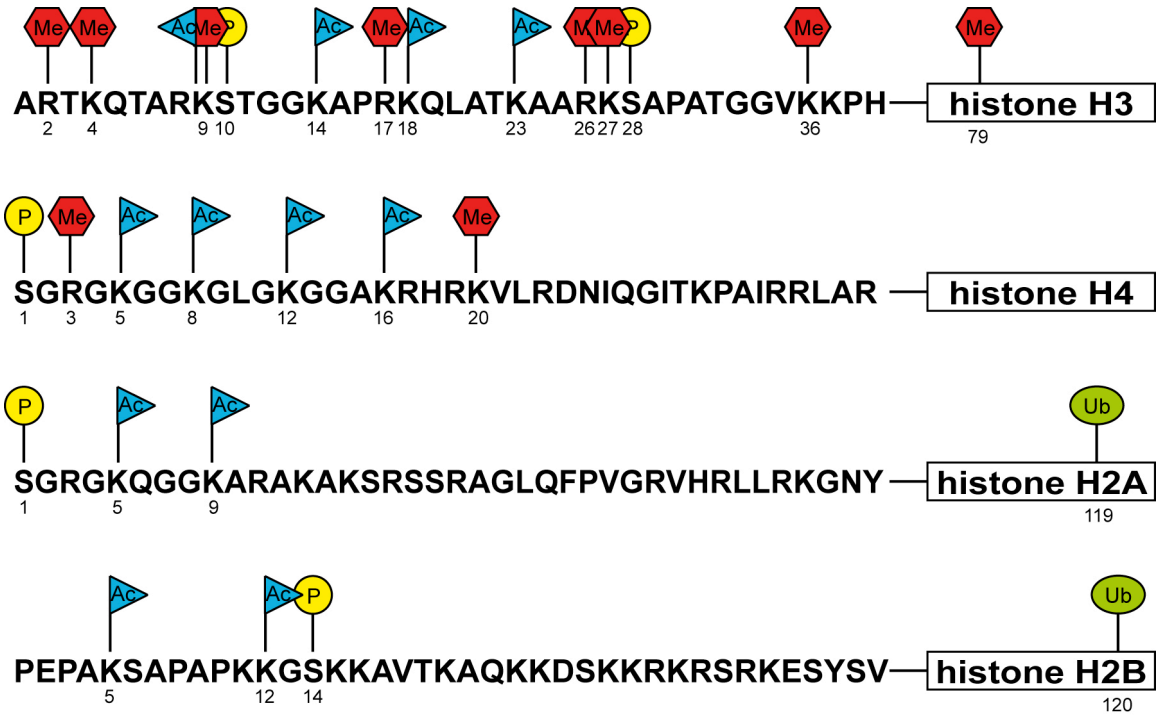

Figure 5 Sites of histone tail modifications
The majority of histone modifications are illustrated. They primarily occur at the N-terminal histone tails, which are given in the single amino acid code but also in the globular domain (boxed). The blue, red, yellow, and green flags represent acetyl, methyl, phosphate, and ubiquitine groups. Picture based on (Allis *et al.*, 2007).

Most modifications are dynamic and reversible (Kouzarides, 2007). For instance, the action of histone acetyltransferases (HATs), which acetylate specific lysine residues in histone substrates (Marmorstein & Roth, 2001), is reversed by histone deacetylases (HDACs) (Grozinger & Schreiber, 2002). The modifications do not occur in isolation but rather in combination (H3K9me and H3S10ph or H4S1ph, H4R3me and H4K4ac). In addition to this, they affect each other. For instance, the phosphorylation of H3S10 by Snf1 kinase promotes the acetylation of H3K14 by Gcn5 (Cheung *et al.*, 2000; Lo *et al.*, 2000).

An important effect of histone modifications is their impact on the chromatin status (Figure 6). The chromatin of eukaryotic cells is not uniform in structure but organized

in a highly condensed chromatin fiber known as heterochromatin and a less compacted type called euchromatin. The “open” euchromatin consists largely of coding sequences comprising the ubiquitously expressed housekeeping genes but also genes that are developmentally regulated or stress-induced in response to environmental cues. One epigenetic mark that is associated with euchromatin is the acetylation of lysine residues that neutralizes the positive charge of the amino acid, leading to reduced interaction with the negatively charged DNA. As a consequence, the chromatin structure is less condensed. Additionally, nucleosome-remodelling machines are recruited through the induction of the activating histone modifications and facilitate the engagement of the transcription machinery. So the euchromatin is transcriptionally active. This in turn alters the interaction of histones with regulatory proteins or other histones (Grant & Berger, 1999; Roth, 1995). Furthermore, the replacement of canonical histones by histone variants, is associated with active chromatin (Ahmad & Henikoff, 2002; Allis *et al.*, 2007).

In general, euchromatic genes that are not transcribed are transferred into more compact heterochromatin to protect the genes while they are not in use. Notably, inactivation of gene expression in heterochromatin is not restricted to specific genes but to their chromosomal location. Heterochromatin can spread and repress nearby genes. Thus, the expression status of a gene can be changed by its insertion adjacent to heterochromatic regions. This phenomenon is called position-effect variegation (PEV) (Muller, 1930). The time- and region-dependent regulation of gene expression by inactivating chromosomal domains is referred to as silencing (Rusche *et al.*, 2003) and leads to a chromatin state known as facultative heterochromatin. In contrast, constitutive heterochromatin describes chromatin that is silent in all cell types. It may by default be induced at non-coding and highly repetitive regions like the telomeres. Modifications resulting in repressed chromatin are deacetylation and the phosphorylation of certain histone residues. Notably, the effect of histone methylation depends on the localization. It is associated with active (H3K4, H3K36, H3K79) or silenced chromatin (H3K9, H3K27, H4K20) (Kouzarides, 2007).

However, not all sites are equally modified (Smith *et al.*, 2003). Many of the modifying enzymes are recruited to special promoters (e.g. HDAC Hst1) (Robert *et al.*, 2004), but there are also HDACs like Rpd3 and HATs that globally regulate transcription independently of sequence-specific transcription factors (Kurdistani *et al.*, 2002).

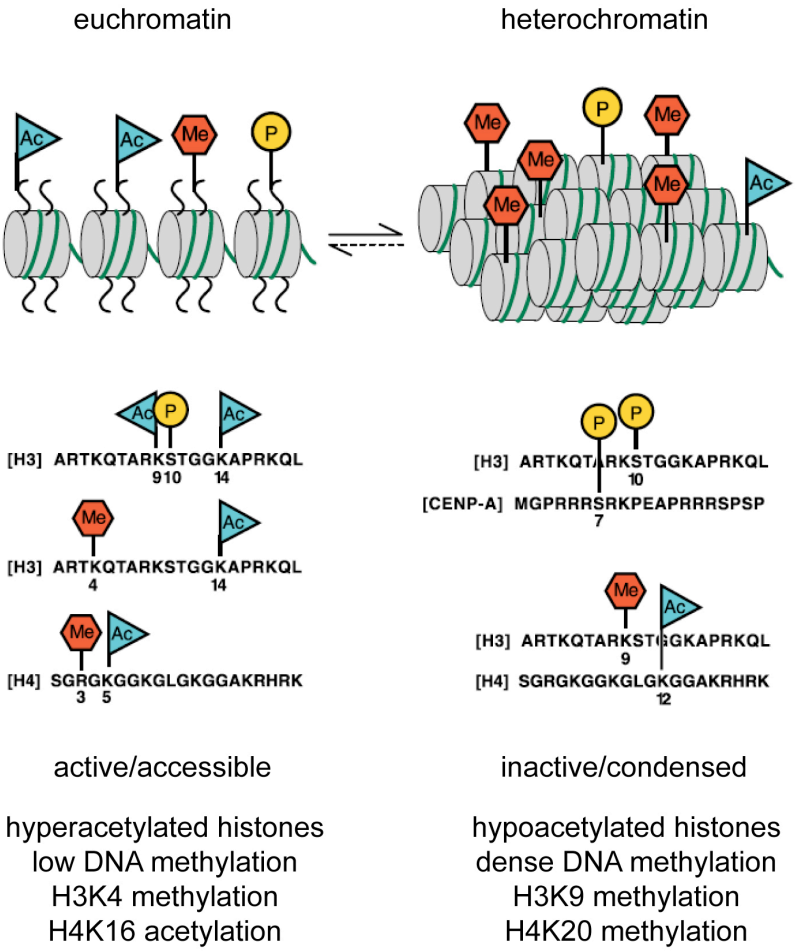

Figure 6 Schematic illustration of euchromatin and heterochromatin
In loosely packed euchromatin (left), transcription is active, whereas in tightly packed heterochromatin transcription is inactive (right). Green lines of DNA wrap around grey cylinders representing histone proteins. Black histone tails are modified where the blue, red, and yellow flags represent acetyl, methyl, and phosphate groups. Picture modified from (Jenuwein & Allis, 2001).

An additional recruiting factor for chromatin-modifying activities is DNA methylation. This epigenetic mark is linked to methylation of H3K9 and repression (Bird, 2002) (see Figure 6). Abnormalities in the DNA methylation imprint cause several diseases, e.g. Prader-Willi-syndrome in humans (Driscoll *et al.*, 1992) (see also 1.4). Furthermore, the RNA interference (RNAi) machinery has been linked to the formation of silent heterochromatic regions in *S. pombe* by inducing repressive histone marks (Hall *et al.*, 2002; Volpe *et al.*, 2002). Other examples for RNA-facilitated repression are non-coding RNAs (ncRNAs). They are involved in mammalian rDNA silencing (Mayer *et al.*, 2006) and dosage compensation. In female mammals, one of the two X-chromosomes is inactivated by the binding of the Xist RNA, resulting in heterochromatin formation along the entire chromosome, and

therefore the dosage of sex chromosome-linked gene expression is equalized between males and females (Avner & Heard, 2001). Notably, DNA methylation and RNAi do not occur in *S. cerevisiae*.

Heterochromatic regions are located at the nuclear periphery (Andrulis *et al.*, 1998; Oki & Kamakaka, 2002). However, until today it is not clear if this localisation is a cause or consequence of heterochromatin formation. Nevertheless, there appears to be a highly conserved pathway leading to a heterochromatic state. It involves recruitment of heterochromatin-associated proteins like heterochromatic protein 1 (HP1) and establishment of DNA methylation as well as repressive histone modifications like histone tail deacetylation and methylation of specific lysine residues (e.g. H3K9). Due to these epigenetic marks, silencing is inherited during DNA replication and multiple cell divisions (Ehrenhofer-Murray, 2004).

In summary, epigenetic marks like histone modifications, DNA methylation, and histone variants influence diverse biological processes. This includes the regulation of gene expression by providing binding sites for transcription factors and silencing by heterochromatin formation (Berger, 2002) as well as replication (Vogelauer *et al.*, 2002), DNA damage repair (Dinant *et al.*, 2008), and apoptosis (Ahn *et al.*, 2005).

1.10 Heterochromatic regions in *S. cerevisiae*

In *S. cerevisiae*, there are three distinct heterochromatic regions – the silent mating-type loci *HML* and *HMR*, the telomeres, and the rDNA locus (Stone & Pillus, 1998). The key component for silencing is Sir2, which belongs to the Class III of HDACs that are NAD^+-dependent (Fukuda *et al.*, 2006; Imai *et al.*, 2000a; Imai *et al.*, 2000b; Moazed, 2001) and is conserved from bacteria to humans. For instance, its homolog in *S. pombe* is also required for heterochromatin formation (Shankaranarayana *et al.*, 2003). Enzymes of the Sir2 family do not only modify histones, but also other substrates like the mammalian SirT1, which deacetylates the transcription factors FOXO and p53 in response to stress and DNA damage (Grunstein & Gasser, 2007) (see 1.7).

In *S. cerevisiae*, Sir2 is the only factor present at all three heterochromatic loci, indicating that there are different mechanisms of silencing, which are explained in the next paragraphs (1.10.1 - 1.10.3). Apart from this, spreading of heterochromatin into euchromatic regions is prevented by boundary mechanisms like hyperacetylation,

H3K79me (van Leeuwen *et al.*, 2002), the presence of the histone variant H2A.Z, Bdf1 (Meneghini *et al.*, 2003), and tethering of DNA to nuclear pores (Ishii *et al.*, 2002).

1.10.1 Silencing at the *HM* loci

The budding yeast *S. cerevisiae* exists in both a haploid and a diploid state. Haploid yeast cells can either be of **a** or α mating-type. The mating of two cells (**a** and α) with opposing mating types results in diploid cells, which in turn can undergo meiosis to form haploid cells. There are three mating-type loci determining the mating-type of haploid yeast cells. All of them are located on chromosome III. The mating type (*MAT*) locus is actively transcribed and determines mating type by either the expression of the *MAT***a**1 gene, resulting in the *MAT***a** mating type or the expression of the *MAT*α1 and *MAT*α2 genes, which give rise to α cells (Herskowitz *et al.*, 1977).

Yeast cells carry an additional copy of the **a** and α genes at the *HM* loci, which are permanently repressed. Derepression leads to a concomitant expression of **a** and α genes. Therefore, it results in pseudodiploid cells that display cell-type characteristics of diploid cells and thus are in a non-mating, sterile state (Perrod & Gasser, 2003). For that reason, silencing of the *HM* loci is essential for maintaining the mating potential of the cells. Repression is mediated by two silencer DNA elements, called E (for essential) and I (for important) that flank the silent genes (Loo & Rine, 1994). They provide binding sites for the repressor activator protein (Rap1), the ARS binding factor (Abf1), and the origin recognition complex (ORC). Additional proteins that are involved in *HM* silencing are the Sir proteins (Sir1 - 4).

Abf1, Rap1, and ORC act not only in *HM* silencing, but also in transcriptional regulation (Abf1 and Rap1) or replication initiation (ORC). They are recruiting factors for Sir proteins at the silencers (Lustig, 1998), where they function in a redundant manner. Rap1 recruits Sir4, Abf1 interacts with Sir3 and ORC has high affinity for Sir1. They all result in recruitment of Sir4 and in turn to binding of the SIR complex, which consists of Sir2/3/4 (Rusche *et al.*, 2003). The formation of heterochromatin occurs in a stepwise manner. First, ORC binds Sir1. Sir4 is then recruited via its interaction with Sir1 and Rap1, leading to the binding of Sir2 and Sir3 (Rusche *et al.*, 2003). Nearby nucleosomes are deacetylated by the HDAC Sir2, providing new binding sites for the SIR complex (Hecht *et al.*, 1995; Imai *et al.*, 2000a). The

resulting positive feedback loop leads to the formation of heterochromatin across the *HM* loci. Notably, Sir1 is involved primarily in the establishment rather than the maintenance of heterochromatic repression (Pillus & Rine, 1989) and does not spread with the SIR complex beyond the silencers (Rusche *et al.*, 2003).

In addition to the mating-type loci, genes important for growth are located on chromosome III. Therefore, it is critical to restrict the repression to the *HM* loci. This is ensured by several boundary factors that prevent the multidirectional spreading of heterochromatin. For instance, the SAS-I complex globally acetylates H4K16, thereby antagonizing Sir2 activity (Kimura *et al.*, 2002; Suka *et al.*, 2002). Additionally, the binding of Bdf1 is thought to protect H4K16ac against deacetylation by Sir2 (Ladurner *et al.*, 2003). The methylation of H3K79 by Dot1 also has boundary function (Ng *et al.*, 2002; van Leeuwen *et al.*, 2002) and heterochromatin spreading toward the telomere from *HMR* is prevented by a tRNA gene (Donze & Kamakaka, 2001).

1.10.2 Telomeric silencing

Telomeres represent the protective ends of linear chromosomes with short, single-stranded DNA overhangs. In *S. cerevisiae*, they consist of $C_{1-3}A/TG_{1-3}$ repeats with a total length of 300 - 350 bp. This nucleosome-free region (NFR) contains 16 - 20 Rap1 binding sites (Gilson *et al.*, 1993; Wright *et al.*, 1992). Telomeres shield the chromosome ends from degradation, end-to-end fusions or homologous recombination (Smogorzewska & de Lange, 2004). This is due to the formation of subtelomeric heterochromatin.

At the telomeres of *S. cerevisiae*, the SIR complex (Sir2/3/4), Rap1, and the Ku heterodimer consisting of yKu70 and yKu80 are involved in silencing. Ku helps Rap1 to recruit Sir4 (Martin *et al.*, 1999), leading to the binding of Sir2 and deacetylation of nucleosomes next to the NFR. This in turn provides new binding sites for the SIR complex. The spreading of heterochromatin from telomere ends towards the centromere into subtelomeric regions is restricted by boundary mechanisms. It is controlled, at least in part, by the opposing activities of Sir2 and Sas2 on H4K16 in some kind of competition zone (Kimura *et al.*, 2002; Suka *et al.*, 2002). The deletion of *SIR2* results in hyperacetylation at telomere-proximal regions as well as at the *HM* and rDNA loci (Robyr *et al.*, 2002). Sir2 is further discussed in lifespan extension as well as in the establishment of cancer (Blander & Guarente, 2004) (see 1.7).

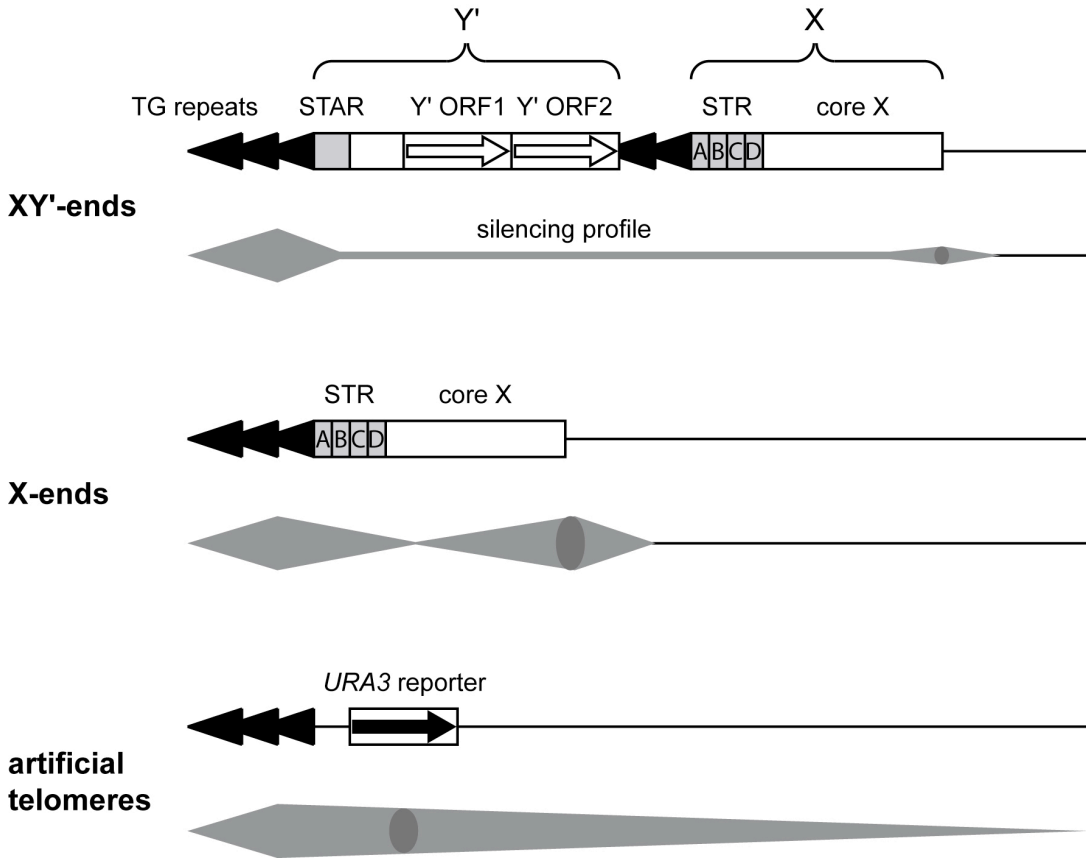

Figure 7 Organization and silencing patterns of *S. cerevisiae* telomeres
S. cerevisiae contains so called X and Y' elements in the subtelomeric region of native telomeres. The Y' element includes subtelomeric anti-silencing regions (STARs) with binding sites for transcriptional regulators that reduce the spreading of silent chromatin. In the X element, there are also binding sites for factors that have the opposing effect. This leads to a discontinuous silencing pattern. There is a gradient of repression at artificial telomeres, when a reporter gene is inserted instead of the X and Y' elements. Picture based on (Grunstein & Gasser, 2007).

In general, the silencing mechanism at the telomeres is similar to *HM* silencing – except for the absence of Sir1. However, native telomeres often contain an X element and mostly also an Y' element in their subtelomeric region (Figure 7), which make the situation more complex. Both elements include binding sites for the transcriptional regulators Tbf1 and Reb1, which reduce spreading of silent chromatin (Fourel *et al.*, 1999). X elements also contain binding sites for ORC and Abf1, which have the opposite effect. Consequently, subtelomeric repression is increased or decreased in a position-dependent manner (Pryde & Louis, 1999). This discontinuous silencing pattern cannot be observed at artificially truncated telomeres, where a reporter gene like *URA3* is inserted instead of the X and/or Y' element (Gottschling *et al.*, 1990) (Figure 7 bottom). In this case, there is a gradient of

repression due to the levels of Sir2 and Sir4, which decrease with increasing distance from the telomere (Strahl-Bolsinger *et al.*, 1997).

Based on a current model, chromosome ends stabilize subtelomeric silencing by forming a loop back to the X element (Pryde & Louis, 1999). Another model implies stabilization of silencing through localization of heterochromatic regions at the nuclear periphery (Andrulis *et al.*, 1998; Oki & Kamakaka, 2002), where they might interact with the nuclear pore complex (Galy *et al.*, 2000). Up to now, it is unclear whether silencing is a cause or a consequence for the localization.

1.10.3 rDNA silencing

The *S. cerevisiae* ribosomal DNA (rDNA) locus contains 100 - 200 repeats of a 9.1 kb DNA sequence that includes the gene encoding 35S rDNA, which is a precursor for 25S, 18S, and 5.8S rRNA (Petes & Botstein, 1977). Only approximately 50 % of the rDNA genes are transcribed at a given time, while the majority is silenced by the action of Sir2 (Smith & Boeke, 1997). Repression at the rDNA locus differs from *HM* and telomeric silencing, as it does not require Sir1 or Sir3 and Sir4 (Smith & Boeke, 1997) and Sir2 at the rDNA locus is part of the regulator of nucleolar silencing and telophase (RENT) complex (Straight *et al.*, 1999). It is known that heterochromatin formation at the rDNA locus prevents recombination and formation of ERCs (Sinclair & Guarente, 1997) (see 1.7), but the mechanistic aspects are still unclear.

1.11 Outline of this thesis

Several factors and pathways have been linked to the regulation of the complex aging process. So far, the best known and most effective way to extend lifespan is caloric restriction, in other words the alteration of the evolutionarily conserved nutrient signalling pathways. In addition, various compounds have been identified to promote longevity of at least one model organism. As some of these compounds display side effects, like suppression of the immune system, only a few are of potential use in humans. Therefore, it is of continued interest to identify novel longevity-promoting compounds. The aim of this study was to expand our knowledge of the molecular mechanisms of aging and to identify compounds that affect aging and lifespan.

To gain new insights into the process of chronological aging, a new high-throughput method that enables the CLS measurement of many *Schizosaccharomyces pombe* cultures in parallel was established. Using this assay, we screened a small compound library, and the compounds that showed the strongest effect in lifespan extension were further characterized. To determine the potential mode of action of these compounds and to identify their potential target/s, their impact on the stress response was investigated, and epistasis analyses were performed in order to relate their effect to known aging pathways.

In order to identify novel genetic factors that are involved in the regulation of aging and lifespan, we used the new CLS assay to screen a *S. pombe* deletion library for gene deletions that extend the CLS of fission yeast. However, in subsequent experiments, we found that the increase of CLS was caused by an unknown factor in the strain background of the deletion library rather than by the indicated gene deletions.

In another approach, we used telomeric silencing, which has been associated with RLS, to identify compounds that affect this type of aging in *Saccharomyces cerevisiae*. A high-throughput method was used to screen approximately 19,000 compounds for their impact on telomeric silencing of budding yeast. To identify the potential target/s of the compounds found to affect telomeric silencing, their effect on *HM* and rDNA silencing was also investigated and was put in the context of known silencing and aging pathways.

2 Material and Methods

2.1 *Escherichia coli* strains

TOP10	F$^-$ *mcr*A Δ(*mrr-hsd*RMS-*mcr*BC) φ80*lacZ*ΔM15 Δ*lac*X74 *rec*A1 *ara*Δ139Δ(*ara-leu*)7697 *gal*U *gal*K *rps*L (Str^R) *end*A1 *nup*G (Invitrogen)
DH5α	F$^-$ φ80d*lacZ*ΔM15 Δ(*lac*ZYA-*arg*F)U169 *rec*A1 *end*A1 *hsd*R17 (r_k^-, m_k^+) *pho*A *sup*E44 *thi*-1 *gyr*A96 *rel*A1 λ$^-$ (Invitrogen)
BL21 (DE3)	F$^-$ *ompT hsd*S_B(r_B^-, m_B^-) *dcm*$^+$ Tet^r *gal* λ(DE3) endA Hte [*argU ileY leuW* Cam^R]
Rosetta (DE3)	F$^-$ *ompT hsd*S_B(r_B^- m_B^-) *gal dcm* pRARE (Cam^R) (Merck)

2.2 Media and growth conditions

2.2.1 *E. coli* growth conditions

E. coli strains used for plasmid amplification were cultured according to standard procedures (Sambrook *et al.*, 1989) at 37 °C in Luria-Bertani (LB) medium (5 g/l yeast extract, 10 g/l tryptone, 5 g/l NaCl) supplemented with 100 µg/ml ampicillin, 50 µg/ml kanamycin or 34 µg/ml chloramphenicol.

2.2.2 *Saccharomyces cerevisiae* media and growth conditions

Media were as described previously (Sherman, 1991). Unless indicated otherwise, *S. cerevisiae* strains were grown on full medium (YPD: 10 g/l yeast extract, 20 g/l peptone, 2 g/l glucose). Marker selection was performed using selective minimal medium (YM: 6,7 g/l yeast nitrogen base w/o amino acids) supplemented with 2 % glucose and as required with 20 µg/ml for adenine, uracil, tryptophan, methionine, and histidine or 30 µg/ml leucine and lysine. YM + 5-FOA (5-fluoroorotic acid) medium contained 1 mg/ml 5-FOA, 20 µg/ml uracil and 2 % glucose. This medium was used to select against Ura3, since the *URA3* protein converts 5-FOA to 5-fluorouracil (5-FU), which is an inhibitor of DNA synthesis that causes cell death (Sherman, 1991). YM + αAA (α-amino-adipic acid) contained 2 g/l αAA and was used as *LYS2*-counterselective medium (Sherman, 1991). In contrast, YM medium containing 1 mg/ml 5-fluoroanthranilic acid (5-FAA) was used for counter selection of the tryptophan pathway represented by the expression of *TRP1* (Toyn *et al.*, 2000). For the analysis of *MET15* expression, lead indicator plates containing 1 mg/ml lead nitrate were used. All *S. cerevisiae* strains were grown at 30 °C.

2.2.3 *Schizosaccharomyces pombe* media and growth conditions

Media were as described previously (Moreno *et al.*, 1991). Unless indicated otherwise, *S. pombe* strains were grown on full medium (YES = yeast extract with supplements). Marker selection was performed using EMM (Edinburgh minimal medium) as selective minimal medium supplemented with 2 % glucose and as required with 225 mg/l for adenine, uracil, histidine, and leucine.

S. pombe strains were also grown in YM medium, which is usually used for *S. cerevisiae*. For *S. pombe*, this medium was supplemented with 3 % glucose and as required with 150 mg/l for adenine, uracil, histidine, and leucine. For overnutrition or dietary restriction 5 % and 1 % or 0.5 % glucose were used. Unless indicated otherwise, all *S. pombe* strains were grown at 30 °C.

2.3 *S. cerevisiae* strain construction

S. cerevisiae strains used in this study are listed in Table 1. They were generated by transformation with plasmids (Klebe *et al.*, 1983), direct gene disruption, genomic integration, genetic crosses or originated from the laboratory strain collection.

Table 1 *S. cerevisiae* strains used in this study

Strain[a]	Genotype	Source[b]
AEY1	*MATα ade2-1 his3-11,15 trp1-1 leu2-3,112 ura3-1 can1-100* (= W303-1B)	
AEY2	*MAT***a** *ade2-1 his3-11,15 trp1-1 leu2-3,112 ura3-1 can1-100* (= W303-1A)	
AEY3	AEY1, but *ADE2 lys2Δ*	
AEY4	AEY2, but *ADE2 lys2Δ*	
AEY12	AEY1 ss-ΔI *sir1Δ::URA3*	
AEY21	AEY3 *sir4Δ::LEU2*	
AEY160	*MATα his3Δ200 leu2Δ1 ura3-167 trp1Δ-6B3 met15Δ1 RDN::Ty1::MET15*	J. Boeke
AEY264	*MAT***a** *his4*	
AEY265	*MATα his4*	
AEY266	AEY2 *sas2Δ::TRP1*	
AEY269	AEY1 *sas2Δ::TRP1*	
AEY270	AEY1 + pRS316 (*URA3*)	
AEY303	JRY5078 = *MAT***a** *hmrΔ::URA3 ade2-1 his3-11 trp1-1 leu2-3,112 ura3-1*	
AEY325	*mat***a**Δp *hmlα*Δp *HMRssα trp1-1 ade2 leu2-3,112 ura3, his*$^-$	
AEY403	*MATα HMR***a**-e**	
AEY474	*MATα HMR***a**-e** *sas2Δ::TRP1*	
AEY565*	*MAT***a** *ura3-52 lys2-801 ade2-101 trp1-Δ1 his3-Δ200 leu2-Δ1 ppr1Δ::HIS3*	O. Aparicio / D. Gottschling
AEY567	*MAT***a** *ΔA hmr::TRP1 rap1-12* (*LEU2*)	
AEY581	*MATα ΔA hmr::TRP1*	
AEY630	AEY1 + pRS414 (*CEN-TRP1*)	
AEY743	*MAT***a** *ade2-1 ura3-1 his3-11,15 trp1-1 leu2-3,112 orc1Δ::TRP1 can1-100 ade2Δ::his4 HIS3::HMR-URADE2-E* + plasmid (*URA3*, *ORC1*)	S. Bell
AEY1017	AEY1 *TEL VII-L::URA3*	J. Berman

AEY1018	AEY2 *sir1*Δ::*HIS3 sir3*Δ::*TRP1 TEL VII-L::URA3*	
AEY1195	AEY160 *sas2*Δ*::TRP1*	
AEY1269	AEY1 *ppr1*Δ*::HIS3*	
AEY1499	AEY2 *hst1*Δ*::KanMX*	
AEY1676	*MAT*α *HMR::ADE2*	
AEY1778	*MAT*α *his3*Δ*200 leu2*Δ*1 ura3-167 RDN1::Ty1-mURA* (S2)	J. Boeke
AEY1779	*MAT*α *his3*Δ*200 leu2*Δ*1 ura3-167 RDN1::Ty1-mURA* (S6)	J. Boeke
AEY2156*	FEP 100-5 *TEL IX-L* position 1*::URA3*[c, d]	E. Louis
AEY2159*	FEP 100-10 *TEL XI-L* position 1*::URA3*[c, d]	E. Louis
AEY2162*	FEP 179 *TEL XII-R* position 2*::URA3*[c, d]	E. Louis
AEY2165*	FEP 180 *TEL XI-L* position 2*::URA3*[c, d]	E. Louis
AEY2741	AEY1 + StuI-cut pRS406	
AEY3087	*MAT***a** *his3*Δ*1 leu2*Δ*0 met15*Δ*0 ura3*Δ*0*	
AEY3590	*MAT***a** *rap1-12 TEL VII-L::ADE2::URA3*	
AEY3595	AEY1 *TEL VII-L::ADE2::URA3*	
AEY3903	AEY2 *rap1-17 HIS3 ura3 ADE2 – TEL VII-L*	D. Shore
AEY3908	AEY1 *adh4::URA3*-$(C_{1\text{-}3}\ A)_n$	L. Pillus
AEY3909	AEY1 *adh4::URA3-UAS*$_{Gal}$-$(C_{1\text{-}3}\ A)_n$	L. Pillus
AEY4017	AEY3909 *sir2::KanMX*	
AEY4019	AEY3909 *sir3::KanMX*	
AEY4064	AEY1 + pAE1232 (p*LEU2-SIR3*)	
AEY4162*	FEP100-5 *TEL IX-L* position 1*::URA3*[c]	E. Louis
AEY4163*	FEP100-10 *TEL XI-L* position 1*::URA3*[c]	E. Louis
AEY4164*	FEP179 *TEL XII-R* position 2*::URA3*[c]	E. Louis
AEY4165*	FEP180 *TEL XI-L* position 2*::URA3*[c]	E. Louis
AEY4166*	FEP184 *TEL XI-L* position 3*::URA3*[c]	E. Louis
AEY4167*	FEP230-32 *TEL XV-R* position 9*::URA3*[c]	E. Louis
AEY4168*	FEP239-7 *TEL IX-L* position 7*::URA3*[c]	E. Louis
AEY4185	AEY2 *hmr-ss::URA3* Δ*I*	
AEY4195	a *hmr-ss::3ARU*Δ*I* *sir2*Δ α *HMR-ss*Δ*I a* *SIR2*	
AEY4580	AEY4168, but *TEL IX-L* position 7*::LYS2*	
AEY4583	AEY4580 *sir2*Δ*::KanMX*	

[a] Strains were isogenic to W303 (AEY1, AEY2) except those marked with an asterisk.
[b] Unless indicated otherwise, strains were designed during this study or were from the laboratory strain collection.
[c] The exact genotypes of these strains are unknown. Positions of *URA3* gene are described in (Pryde & Louis, 1999).
[d] Notably, it turned out in later experiments that the indicated genotype of this strain is not correct, and thus, the precise site of *URA3* integration is not known.

2.3.1 Crossing, sporulation, and tetrad dissection of *S. cerevisiae* strains

Parental *S. cerevisiae* strains of opposite mating types were mixed in a drop of YPD medium and grown for 8 hours at 30 °C on a YPD plate. Cells were streaked YM plates supplemented with amino acids selecting for diploids.

To induce sporulation, diploids were plated on sporulation medium (19 g/l KAc, 0.675 mM ZnAc, 20 g/l agar) and incubated at 30 °C for at least three days. For asci digestion, a loop of sporulated cells was suspended in zymolyase buffer (1 M Sorbitol, 0.1 M NaCitrate, 60 mM EDTA pH 8.0, 5 mg/ml zymolyase) and incubated for 5 minutes at RT. The reaction was stopped by adding 100 µl H_2O. Subsequently, tetrads were dissected on YPD plates using a micromanipulator (Narishige) connected to a Zeiss Axioscope FS microscope. The ascospores were incubated for 2 - 3 days at 30 °C. Marker analysis was achieved by replicating the cells with the help of sterile velvet cloth on different selection plates.

2.3.2 DNA techniques in *S. cerevisiae*

Gene deletions with *KanMX* were performed as described (Wach *et al.*, 1994). Double mutants were generated by crosses, subsequent tetrad dissection and the analysis of marker segregation.

For the replacement of the telomeric *URA3* marker gene by *LYS2*, the *LYS2* gene (pAE896) was amplified by PCR, and the PCR products were integrated at different chromosomal locations in the appropriate *S. cerevisiae* strains by homologous recombination.

2.4 *S. pombe* strain construction

S. pombe strains used in this study are listed in Table 2. The majority of these strains originated from the *S. pombe* Haploid Deletion Mutant Set ver 1.0 (Bioneer). The corresponding auxotrophic wild-type strain is ED666 (AEP57). All gene deletions of strains from the deletion library that showed an effect in further experiments were verified by PCR. Double mutants were constructed by tetrad dissection using ED665 (AEP64) for changing the mating type.

The remaining strains were generated by transformation with plasmids (Moreno *et al.*, 1991), direct gene disruption, crossing of haploid h^+ and h^- cells, or they were derived from the laboratory strain collection.

Table 2 *S. pombe* strains used in this study

Strain	Genotype	Source[a]
AEP1	*h- leu1-32 ura4-D18 his3-D3*	
AEP14	*h- leu1-32 ade6-210 ura4-D18 mat1_m-cyhS, smt0, rpl42::cyh*^{R} (sP56Q)	N. Krogan
AEP55	*h- msh2::his3 his3-D1*	O. Fleck
AEP56	*h- msh6::arg3 arg3-D4*	O. Fleck
AEP57	ED666 = *h+ ade6-M210 leu1-32 ura4-D18*	Bioneer
AEP58	ED668 = *h+ ade6-M216 leu1-32 ura4-D18*	Bioneer
AEP59	*h- ade6-M216 ura4-D18 leu1-32 his7-366*	K. Runge

AEP60	AEP59 *sck1::LEU2*	K. Runge
AEP61	AEP59 *leu1::LEU2*	K. Runge
AEP62	AEP59 *sck2::LEU2*	K. Runge
AEP64	ED665 = *h- ade6-M210 leu1-32 ura4-D18*	Bioneer
AEP65	*h90 ura4-D18 swi10::ura4+*	H. Schmidt
AEP66	*h90 ura4-D18 swi9::ura4+*	H. Schmidt
AEP67	*h- ura4-C109T leu1-32*	K. Takegawa
AEP68	AEP67 *vma1::URA4*	K. Takegawa
AEP69	AEP67 *vma3::URA4*	K. Takegawa
AEP70	*msh6::KanMX mlh1::KanMX* #14	
AEP71	*msh6::KanMX mlh1::KanMX* #16	
AEP72	*msh6::KanMX rad2::KanMX* #4	
AEP73	*msh6::KanMX rad2::KanMX* #8	
AEP74	*rad2::KanMX mlh1::KanMX* #12	
AEP75	*rad2::KanMX mlh1::KanMX* #14	
AEP76	*rad2::KanMX rhp23::KanMX* #1	
AEP77	*rad2::KanMX rhp23::KanMX* #7	
AEP78	*rhp23::KanMX mlh1::KanMX* #5	
AEP79	*msh6::KanMX rhp23::KanMX* #2	
AEP80	*msh6::KanMX rhp23::KanMX* #4	
AEP81	AEP57 *rad2::NatMX* #4	
AEP82	AEP57 *rad2::NatMX* #5	
AEP83	AEP1 *rad2::NatMX* #10	
AEP84	AEP1 *rad2::NatMX* #11	
AEP85	AEP57 *rad13::NatMX* #12	
AEP86	AEP57 *rad13::NatMX* #37	
AEP87	AEP1 *rad13::NatMX* #6	
AEP88	AEP1 *rad13::NatMX* #13	
AEP89	AEP57 *msh6::NatMX* #8	
AEP90	AEP57 *msh6::NatMX* #9	
AEP91	AEP1 *msh6::NatMX* #15	
AEP92	AEP1 *msh6::NatMX* #16	
AEP93	AEP57 *ppk4::NatMX* #5	
AEP94	AEP57 *ppk4::NatMX* #9	
AEP95	AEP1 *ppk4::NatMX* #4	
AEP96	AEP1 *ppk4::NatMX* #12	

[a] Unless indicated otherwise, strains were designed during this study or were from the laboratory strain collection or the *S. pombe* Haploid Deletion Mutant Set ver 1.0 (Bioneer).

2.4.1 Crossing, sporulation, and tetrad dissection of *S. pombe* strains

Parental *S. pombe* strains of opposite mating types were mixed in a drop of YES medium and grown for 2 days at 23 °C on sporulation medium (SPAS). The mating cells will form transient diploids (zygotes) and then proceed directly into meiosis.

The sporulated cells were placed on YES plates, where zygotic asci were separated based on their characteristic zig-zag or banana shape using a micromanipulator (Narishige) connected to a Zeiss Axioscope FS microscope. After the fission yeast asci fell apart spontaneously (4 – 5 hours at 37 °C), the ascospores were separated and incubated for 2 - 3 days at 30 °C. Marker analysis was achieved by replicating the cells with the help of sterile velvet cloth on different selection plates. Double mutants arising from crosses were verified by PCR.

2.4.2 Gene disruption in *S. pombe*

For the gene knockouts in *S. pombe*, the PCR sewing technique, also called megaprime PCR, was used. With this technique, DNA sequences complementary to about 500 bp downstream or upstream the ORF of the target gene were generated in a first step. Next, the *NatMX* cassette was amplified by PCR. In a last step, all three PCR products were sewed together. All gene disruptions and sequence insertions were verified by PCR analysis.

2.5 Molecular cloning

Plasmids were generated according to standard cloning techniques (Sambrook *et al.*, 1989). Kits for plasmid isolation and gel elution were purchased from Qiagen. Enzymes and respective buffers were used from NEB and Promega. Plasmids and oligonucleotides used for molecular cloning, overexpression or gene knockouts are listed in Table 3 and Table 4.

Table 3 Plasmids used in this study

Plasmid[a]	Description	Source[b]
pAE192	pJR304 = JDB Sir2 = multicopy sir2	
pAE231	pRS315-*SIR2*	
pAE232	pRS315-*SIR3*	
pAE255	pRS306	(Sikorski & Hieter, 1989)
pAE264	pRS414	(Sikorski & Hieter, 1989)
pAE269	pRS425	(Sikorski & Hieter, 1989)
pAE478	pFA KanMX4	(Wach *et al.*, 1994)
pAE712	pRS305-*SIR2*	
pAE896	pRS317	
pAE916	pCT300	

pAE929	pFA6a – HIS3 MX6	(Wach *et al.*, 1994)
pAE1003	pAG25	(Wach *et al.*, 1994)
pAE1232	pRS425-*SIR3*	
pAE1325	pET15b	
pAE1373	2µ *URA3 HOP1/lacZ – URS1*^{H}	A. Vershon
pAE1394	pET24a(+) *Sir2-His6x*	
pAE1395	pAE1373 + *NDT80* (*-78*) *MSE*^{S}	A. Vershon
pAE1429	REP4X = as REP3X (ATG-less derivate of REP3 with LEU2 marker, nmt1 promoter and ars1), with ura4+ marker	

[a] Plasmids were generated according to standard cloning techniques.
[b] Unless indicated otherwise, plasmids were constructed during this study or originated from the laboratory plasmid collection.

Table 4 Oligonucleotides used for molecular cloning, knockout or replacement of telomeric *URA3* by *LYS2*

Oligonucleotide	Oligonucleotide sequence (in 5' to 3' direction)[a]
Integration LYS2 S1 (FOR)	ATG TCG AAA GCT ACA TAT AAG GAA CGT GCT GCT ACT CAT CCT AGT CCT GTt ggc tta act atg cgg cat cag agc
Integration LYS2 S2 (FOR)	TTA GTT TTG CTG GCC GCA TCT TCT CAA ATA TGC TTC CCA GCC TGC TTT TCt ctc ctt acg cat ctg tgc ggt at
Integration LYS2 S1 (REV)	TTA GTT TTG CTG GCC GCA TCT TCT CAA ATA TGC TTC CCA GCC TGC TTT TCt ggc tta act atg cgg cat cag agc
Integration LYS2 S2 (REV)	ATG TCG AAA GCT ACA TAT AAG GAA CGT GCT GCT ACT CAT CCT AGT CCT GTt ctc ctt acg cat ctg tgc ggt at
Sir2-S1	ATG ACC ATC CCA CAT ATG AAA TAC GCC GTA TCA AAG ACT AGC GAA AAT AAG GCG
Sir2-S2	TTA GAG GGT TTT GGG ATG TTC ATC TGA TGT AAC GAC ATA CAC GCC CTT ATC CAT
KanMX K2	GCC CCT GAG CTG CGC ACG TC
KanMX K3	CCC AGA TGC GAA GTT AAG TGC GC
Sir2_A1_500up	GAA AGA AAT GAT TAT TAG CAG
Sir2_A4_3200dwn	CAA ATG CCT TTC AAC CGT G
SIR2-A1	GGC ACC ACG AGC GGT TTA TTT GG
SIR2-A4	CCT ACT GAA CCG TTC TTC GG
NatMX K2	GTC CCC GGT GGC GGT GAC GCG G
NatMX K3	GGT CGC CCC GGA GCA CCG GG
CPN1	CGT CTG TGA GGG GAG CGT TT
Rad2_ctrl_Sp.fw	GCT AGT TTT GGA GAA AGC GTT GTT CGG G
Rad13_ctrl_Sp.fw	GGC TTG CTT TAA TCA CAT TTC TTC GTA TAA TAA TC
Ppk4_ctrl_Sp.fw	CTG TTT ACC TAC TAC CTA CTT CAA ATG TAT CGT C
Msh6_ctrl_Sp.fw	GCT CTC ATG TTA GCT TTG TTT ACT ATT AGA ATG C

Irc6_ctrl_Sp.fw	CCA CCA AAA ACT TGT TTA ATA TTC TAC AGA ACT G
Pms1_ctrl_Sp.fw	GTA CAT CAA GGT CCA AAA AAT TCG C
Nth1_ctrl_Sp.fw	GCG CTC ACC TGC GTT GTT TCT TGG
Spd1_ctrl_Sp.fw	CGT CAC AAA GCC GAG TAG CAA ACG C
Dss1_ctrl_Sp.fw	GTG TAA CTC AGT AGA CAT CGT TAC CAG TG
SPBC216.01c_ctrl_Sp.fw	CGT CTT CAC TTT TGA AAA TTT GGT GAC GAA CG
Rhp23_ctrl_Sp.fw	GCT ACC TTG ACA ATT ATT CTC TGA TGC AAC G
Msh1_ctrl_Sp.fw	GAC AAT GAT GCA TTC ATT GTC GCT TAT AGT AAC
Msh3_ctrl_Sp.fw	CCG CCT ATA TTC ATT TAG AAA CTA TAA ATG CG
Mlh1_ctrl_Sp.fw	CGG TAC TTG TAC ATT CTG CGC TAT G
KanB	CTG CAG CGA GGA GCC GTA AT
Rad27_ctrl_Sc.fw (A)	GCT GGT AAG TTA TGA TAG AAA GCC A
Rad2_ctrl_Sc.fw (A)	AAT ACC ACA TTT TGT TGC TGT TTT T
Ire1_ctrl_Sc.fw (A)	AAT AGG TTT TCG CTA TTT TAT TGC C
Rad2_NatMX_Sp.fw	GCG TTG TTC GGG ATC TCG TAA TAT ACA TAA ATA AGT ATA TTT GCT AAA CGA TGc cag ctg aag ctt cgt acg c
Rad2_NatMX_Sp.rev	GCT TTT TTT AAG TTT TTT TTT TAG ATT AAT AAC AAT TAC ATG ACT TCG TTT TCA gca tag gcc act agt gga tct g
Rad2_PCR1_Sp.fw	CGG TAA AGT TCC AAT GTA CTT TTC
Rad2_PCR1_Sp.rev	CTT ATT TAT GTA TAT TAC GAG ATC CCG
Rad2_PCR2_Sp.fw	GTC ATG TAA TTG TTA TTA ATC TAA AAA AAA AAC
Rad2_PCR2_Sp.rev	CCC TTC TTT CAA ACT GTG AAC
Rad13_NatMX_Sp.fw	CAA AAA TAA AGT CGT CTA CAA CGA AAC TTC TTG ACA TCG CAT ATA ATA TTT TGC AAT Gcc agc tga agc ttc gta cgc
Rad13_NatMX_Sp.rev	CTT TTA TAG GAA CAA CCA GTT AAG TAA ACA AAT AAA TAA ATA ATT TAT TAA ACT Tag cat agg cca cta gtg gat ctg
Rad13_PCR1_Sp.fw	GGG AGT GAA ATC CCA TGT TG
Rad13_PCR1_Sp.rev	GCG ATG TCA AGA AGT TTC GTT G
Rad13_PCR2_Sp.fw	ATT TGT TTA CTT AAC TGG TTG TTC C
Rad13_PCR2_Sp.rev	CCA TCA TAT TTT GCT CAA CTT ACG
Ppk4_NatMX_Sp.fw	TTA GTT AAG TTG CTC TTA AAA AAT ATT TTT GTT AAA AAC TTT TAC CAA TGc cag ctg aag ctt cgt acg c
Ppk4_NatMX_Sp.rev	GGA TTA AAT TAC ATA TAA AAT GAC TTT AAG AAT TTA GTA TGT AAA CGT CAg cat agg cca cta gtg gat ctg
Ppk4_PCR1_Sp.fw	GGT TAT GTC TTC TGA TAA TGC ATA C
Ppk4_PCR1_Sp.rev	GGT AAA AGT TTT TAA CAA AAA TAT TTT TTA AG
Ppk4_PCR2_Sp.fw	CAT ACT AAA TTC TTA AAG TCA TTT TAT ATG
Ppk4_PCR2_Sp.rev	CCT TCA GAC ATA ATT TTG AAT TAC
Msh6_NatMX_Sp.fw	GCT TTT TGT AAA TAA CTG AAC TTA GCC AAA ACC AAC ACT TGT TCC AGT ATG cca gct gaa gct tcg tac gc
Msh6_NatMX_Sp.rev	GAA AGA TAT TGC TTT GAA TAG TCA TAA AAC TGA TAG AGT GTT GAC AGT TAT Tag cat agg cca cta gtg gat ctg
Msh6_PCR1_Sp.fw	CCT AAA CTC TCC TTC TCT GAA GG

Msh6_PCR1_Sp.rev	GGT TTT GGC TAA GTT CAG TTA TTT AC
Msh6_PCR2_Sp.fw	GTC AAC ACT CTA TCA GTT TTA TG
Msh6_PCR2_Sp.rev	CCA TGT TGT TAG ACC AAG AAG
Rad13_ctrl_Sp.up	CGT CTC GTT CAC CAA TGG TGG G
Rad13_ctrl_Sp.down	GGG TCT TTA AAC TCG GGG AAG G
Rad2_ctrl_Sp.up	GAT CCG CAC GAA ATA CGT CGG
Rad2_ctrl_Sp.down	GAG GGC AAA GGT TTC AGG GG
Msh6_ctrl_Sp.up	GGC CAA CTT AGG GGA CAA CTT C
Msh6_ctrl_Sp.down	GGA ACG GGA TGT GTC ATC CAT G
Ppk4_ctrl_Sp.up	GCC TAT GGA TGA CTA TAC CCA AAG C
Ppk4_ctrl_Sp.down	CGA TCC CAC AAG CGG CTG G
Dnm1_ctrl_Sp.fw	GCATTCCCATAATCCAAATTGTGCGTGT
Git3_ctrl_Sp.fw	CGTTCTGATATTGCTTTTCTTGTTTTTTACTTTCTCACC
Pka1_ctrl_Sp.fw	GCCTCGACCTCTTTTAACCTTATTCTTGTTTTCGGG
Tim11_ctrl_Sp.fw	CGTTGCACTATTCGTGTTAAGTGTTTAGAGTTCG
Atp14_ctrl_Sp.fw	CAGCGATTGTTTATTTGGGCATTTAAAACTTTAGC

[a] Nucleotides complementary to the *URA3* marker gene (in case of replacement of by *LYS2*) or the *NatMX* cassette are shown in lower case letters.

2.6 Growth assays

Unless indicated otherwise, the growth assays were documented using the Molecular Imager GelDoc™ XR System (Bio-Rad) and the Quantity One® Software (Bio-Rad).

During this study, I spent time at the University of Applied Sciences (HTW) in Berlin in the lab of Prof. Dr. Jacqueline Franke to establish the automation of the high-throughput methods (2.6.1.1 and 2.6.3) by using the robotic workstation Freedom EVO® (Tecan) that is connected with the microplate reader Infinite® M200 (Tecan) and the Cytomat® Tower Shaker (Thermo Scientific).

2.6.1 Chronological lifespan assays

2.6.1.1 High-throughput method to measure chronological lifespan (CLS)

For each CLS assay, cells were inoculated from fresh single *S. pombe* colonies into YES medium for overnight cultures. 2 µl of these cultures (or of the *S. pombe* Haploid Deletion Mutant Set, Bioneer) were used to inoculate 150 µl medium per well in 96 well microplates (TPP). The medium for CLS assay was YM medium containing 3 % glucose with 150 mg/l of adenine, uracil, and histidine or leucine (Chen & Runge, 2009). For overnutrition or dietary restriction 5 % and 0.5 % or 1 % glucose were used. The microplates were coverd with SILVERseal™ films (Greiner Bio-One) to avoid mixing of the cultures while shaking with 900 rpm at 30 °C. Aliquots of the cultures were taken at regular intervals, spotted onto YES plates and grown for 2 days at 30 °C.

The effect of compounds on CLS was analyzed by adding the compounds to the medium immediately before the yeast cells were added (final concentration as indicated in the text and figure legends).

2.6.1.2 Colony forming unit (CFU) method

Overnight cultures (inoculated as described in 2.6.1.1) were used to inoculate 75 ml medium (see above) to an initial optical density at 600nm (OD_{600}) of 0.1. The OD_{600} of the aging culture was measured several times to ensure that the yeast cells reach stationary phase. Aliquots of the cultures were taken at regular intervals, serially diluted in sterile milliQ water and multiple dilutions were plated on YES plates and grown at 30 °C for 3 - 5 days. Colonies were then counted and used to calculate the number of colony forming units per ml culture (CFU/ml). For each strain or compound, at least 3 biological replicates were used.

For the compound prostaglandin J_2 and its controls, a modified approach was used. The aging cultures were inoculated as described above but in a smaller volume (3 - 5 ml medium). Aliquots taken at regular intervals were serially diluted in YES medium and spotted onto YES plates, which were incubated at 30 °C for 2 days.

2.6.2 Stress resistance

For testing stress resistance, *S. pombe* cells were cultured for 1 or 2 days at 30 °C in YM medium containing 3 % glucose, the required supplements and in some cases also compounds (final concentration as indicated in the text and figure legends). After washing with YM medium, the cell concentration was adjusted to OD_{600} of 0.5. Next, H_2O_2 (10 mM - 300 mM final concentration) or menadione sodium bisulfite (25 mM final concentration) were added and incubated at 30 °C. To analyze the resistance against DNA damage, MMS was added (0,2 % final concentration) and incubated for 15 - 60 minutes at 30 °C. For heat treatment, equal amounts of cells (OD_{600} of 0.5) were heat shocked for 45 - 90 minutes at 48 °C. Serial dilutions were spotted onto YES plates and incubated for 2 days at 30 °C.

In some cases, the addition of the compound slows down the growth rate of the cells. To avoid misinterpretations due to differences in stress response that depend on the time the cells are in stationary phase, cells treated with these compounds were compared with DMSO-treated cells that were cultured for only 1 day at 30 °C.

2.6.3 Telomeric silencing assay

S. cerevisiae strains, media, and positive controls used for the screens are listed in Table 5. Blank (DMSO) and positive control were always located on the same microplate with the samples.

The high-throughput screening (2.6.3.2) was performed at the Leibniz-Institute for Molecular Pharmacology (FMP) in Berlin.

Table 5 Strains, media, and positive controls used for telomeric silencing assay

Screen	*S. cerevisiae* strain	Medium	Positive control
Increased telomeric silencing	*TEL IX-L* pos 7*::URA3*	5-FOA[a]	+ p*LEU2-SIR3* (in 5-FOA -leu[c])
Decreased telomeric silencing	*TEL IX-L* pos 1*::URA3* + p*LEU2-SIR3*	YM -ura-leu[b]	10 µM splitomicin

[a] 5-FOA medium supplemented with adenine, histidine, lysine, tryptophan, and leucine.
[b] YM medium supplemented with adenine, histidine, lysine, and tryptophan, but lacking uracil and leucine.
[c] 5-FOA medium supplemented with adenine, histidine, lysine, and tryptophan, but lacking leucine.

2.6.3.1 Screening of small compound libraries for effects on telomeric silencing

S. cerevisiae strains were grown in YES medium over night at 30 °C. The medium used for the screen was inoculated with these cells to a final OD_{600} of 0.2 (5-FOA) or 0.05 (YM). Into each well of 96 well plates (TPP) or 384 well plates (Corning, #3701), 100 µl respectively 50 µl of this mixture were pipetted. DMSO or compounds from the Natural Products Library (Biomol; final concentration: 4 µg/ml or 20 µg/ml) or single compounds from Evonik were added (final concentration: 100 µg/ml). The microplates were incubated at 30 °C with constant shaking (300 rpm). At distinct time points, the microplates were removed from the incubator and the optical density at 595 nm (OD_{595}) was determined using the GENios Pro™ microplate reader (Tecan) and the XFluor4GENiosPro Software (Tecan).

Each primary candidate was validated several times.

2.6.3.2 High-throughput screening of large compound libraries for effects on telomeric silencing

Yeast cultures were inoculated as described above (see 2.6.3.1). 50 µl of the mixture were pipetted with the MicroFlo™ Select Dispenser (BioTek) into each well of 384 well plates (Corning, #3702) with sterile lids. For technical reasons, yeast cells and the corresponding medium used as control had to be manually added to the miroplates. The Sciclone ALH3000 Workstation (Caliper Life Science) was used to add 0.2 µl DMSO or 10 mM compounds from the ChemBioNet or the LOPAC compound library (final concentration: 40 µM). The microplates were incubated at 30 °C. At distinct time points, the microplates were removed from the incubator and the yeast cells were shaked for 5 minutes with 1500 rpm using the MixMate (Eppendorf). Subsequently, the optical density at 595 nm (OD_{595}) was determined using the Safire^{2TM} microplate reader (Tecan) and the Magellan Software (Tecan).

For validation, each primary candidate was tested 3 times in 3 concentrations (20 µM, 50 µM, 100 µM).

2.6.3.3 Analysis of high-throughput screening data

In both screens, the OD_{600} was first measured after the addition of the compounds. This blank value was subtracted from the following values to subtract out the absorption of the compounds.

The cut-off was set to the 1.5-fold of the blank (DMSO).

2.6.4 Spot filter assay of compounds for effects on telomeric silencing

S. cerevisiae cells (0.1 or 0.5 OD_{600}) were plated on YM or 5-FOA plates. Whatman paper was used to make small, sterile filters, which were placed on the prepared plates. To test telomeric silencing, 1.25 µl, 2.5 µl, and 10 µl of 10 mM resveratrol, 7.5 mM TSA, 10 mM splitomicin, or 623 mM nicotine were spotted onto these filters.

2.6.5 Spot filter assay for effects on *HM* silencing

To analyze the effect of compounds on *HM* silencing, 0.5 OD_{600} of *MAT***a** *his4* (AEY264) and *hml***a**Δp *mat***a**Δp *HMRss*α (AEY325) were mixed and plated onto YM plates without supplements. Small, sterile filters made out of Whatman paper were placed on the prepared YM plates. 1.25 µl, 2.5 µl, and 10 µl of 10 mM splitomicin (and DMSO) were spotted onto these filters to select for diploids by disturbing the *HMR* silencing.

In another approach, 0.5 OD_{600} of *MAT***a** *his4* (AEY264) and *MAT*α *HMR***a**-e** (AEY403) were mixed and plated onto YM plates without supplements. Different volumes of 623 mM nicotine were spotted onto small, sterile filters made of Whatman paper, which were placed on the YM plates.

2.6.6 Patch mating assay

HM silencing of *S. cerevisiae* was measured by determining the mating ability of a strain with a mating tester strain in a patch-mating assay. For this purpose, the candidate strains were streaked in 1 cm^2 patches on a YPD plate (master plate) and grown over night at 30 °C. Next, 2.5 OD_{600} of a tester strain, *MAT***a** *his4* (AEY264) or *MAT*α *his4* (AEY265), were plated on a YM plate. The master plate was then replicated onto the tester strain plate and incubated for 2 days at 30 °C.

2.7 Protein expression and purification in *E. coli*

For overproduction of His6x-tagged Sir2 protein, Rosetta cells harboring the plasmid pAE1394 were grown in LB medium supplemented with 50 µg/ml kanamycin and 34 µg/ml chloramphenicol. 1.5 l medium were inoculated with a fresh overnight culture and incubated at 37 °C until an OD_{600} of 0.5 was reached. Protein expression was then induced by adding isopropyl β-D-1-thiogalactopyranoside (IPTG) to a final concentration of 1 mM and the incubation was extended for additional 5 hours at 30 °C. To harvest the cells, they were centrifugated with 6000 rpm for 20 minutes at 4 °C. Next, they were resuspended in lysis buffer (50 mM NaH_2PO_4, 500 mM NaCl, 20 mM imidazole) with 1 mg/ml lysozyme. To lyse the cells, they were dipped into liquid nitrogen 3 times and stored on ice in between for 10 minutes. Subsequently, they were sonicated for 5 minutes with 10 second intervals of ultrasonic and rest and finally, they were drawn through needles (19 G and 23 G) several times. The cell extract was centrifugated with 10000 rpm for 20 minutes at 4 °C. The supernatant was mixed with Ni-NTA beads (Qiagen) for 1.5 hours at 4 °C and then applied onto a Ni-NTA sepharose column (Qiagen) equlibrated with lysis buffer. Chelate affinity chromatography was performed under native conditions according to the standard procedures recommended by the manufacturer (Qiagen).
Purification of the Sir2 protein was verified on SDS-PAGE by Coomassie Brilliant Blue R250 staining.

2.8 SDS-PAGE and Western Blotting

Purified proteins were separated by SDS-PAGE (10 %) in Tris-glycine buffer according to standard methods (Laemmli, 1970). Then, they were transferred to a nitrocellulose membrane (Amersham Hybond ECL, GE Healthcare) by blotting with the Bio-Rad Tank Transfer System with 5,5 mA x h/cm^2 in transfer buffer (25 mM Tris; 52 mM glycine; 10 % methanol). Subsequently, the nitrocellulose membrane was blocked in TBS-T + 5 % milk (50 mM Tris HCl pH 7.5; 150 mM NaCl; 0.1 % Tween20; 5 % milk powder) for 1 hour at RT. The blot was then incubated with the primary antibody (mouse α-His, Sigma, 1:3000) over night at 4 °C in TBS-T + 5 % milk and washed 2 times for 5 minutes with TBS-T. Next, the blot was incubated with the appropriate secondary antibody conjugated to horseradish peroxidase (sheep α-mouse, Sigma, 1:1000) in TBS-T + 5 % milk for 1 hour at RT. After washing 4 times for 5 minutes with TBS-T and TBS the Western blot signals were visualized on Amersham Hyperfilm^{TM} ECL chemiluminescence films (GE healthcare) by using the Amersham ECL^{TM} Western Blotting Analysis System (GE healthcare).

2.9 Fluorescence-based *in vitro* HDAC assay

To measure Sir2 deacetylase activity, a simple fluorescence-based assay (Heltweg *et al.*, 2003; Heltweg & Jung, 2003) was used. In two consecutive reactions, deacetylation of the substrate MAL generates a fluorophore that is excited at 360 nm. The emitted light at 460 nm was detected using the GENios Pro^{TM} microplate reader (Tecan). This experiment was performed by Gesine Hoffmann.

2.10 Telomeric restriction fragment (TRF) analysis

S. cerevisiae strains were grown over night in minimal medium. In some cases, 10 µM splitomicin or resveratrol were added. Genomic DNA was isolated and then digested with *Xho*I. After separation by agarose gel electrophoresis, DNA was transferred onto Zeta Probe GT Membranes (Bio-Rad) as described (Sambrook *et al.*, 1989). Next, Southern blotting was performed as described (Southern, 1975). The DNA was blotted onto a nitrocellulose membrane by capillary action. Afterwards, the membrane was baked at 80 °C for 1 - 2 hours. A $C_{1\text{-}3}A$ containing 280 bp *Eco*RI fragment of pCT300 (pAE916) labeled by random primer labeling with [α-^{32}P]dCTP was used as a probe for hybridization of the Southern blot (Wellinger *et al.*, 1993). Subsequently, the blot was exposed to a phosphorimager screen (Molecular Dynamics) for 12 hours.

2.11 Fluorescence staining

Fluorescence staining with phloxine B (Applichem), dihydrorhodamine123 (DHR123, Cayman) and FITC-VAD-fmk (CaspACE, Promega) was performed as described (Roux *et al.*, 2006) and analyzed under the Zeiss Axio Imager.M1 fluorescence microscope using the AxioVision Software (Zeiss). Stained cells were counted by using ImageJ 1.39.

Vacuolar membranes were stained using SynaptoRed (Merck), which is also called FM4-64, as previously described (Iwaki *et al.*, 2003). Based on the work of Liu and colleagues, staining of acidic compartments was performed using quinacrine

dihydrochloride (Sigma Aldrich) (Liu *et al.*, 1997). At variance with this protocol, quinacrine was dissolved in YES medium instead of YPD medium.

2.12 Measurement of the pH-value

The pH-value of yeast cultures was determined by spotting aliquots on pH indicator sticks (pH 2.0 - 9.0, Merck), which detect changes of the pH-value in 0.5 steps.

2.13 Compounds

The compound libraries used in this study are listed in Table 6. Secondary candidates were purchased from Biomol, Cayman, ChemDiv, ChromaDex, Enzo, Fluka, Latoxan, LKT, Roth, Sigma, and TimTec.

Table 6 Compound libraries used in this study

Library	Source[a]	Number of compounds	Concentration
Natural Products Library (v5.0)	Biomol	502	1 mg/ml in DMSO
Natural Products	Evonik	20	5 mg/ml in DMSO or H_2O
ChemBioNet	FMP (ChemDiv)	16,896	10 mM in DMSO
LOPAC	FMP (Sigma)	1,267	10 mM in DMSO

[a] FMP = Leibniz-Institute for Molecular Pharmacology, Screening Unit, Berlin

3 Results

3.1 Compounds and gene deletions affecting chronological aging of *S. pombe*

So far, the mechanisms that lead to chronological aging are less well characterized for *S. pombe* than for *S. cerevisiae*. CR, defined as reduced intake of glucose and amino acids, extends CLS of fission yeast by the downregulation of the two nutrient sensing pathways, namely the TOR signalling pathway, including Sck2, and the Git3/PKA pathway (Roux *et al.*, 2010). However, there are differences between these two pathways. A decrease in TOR signalling is proposed to increase mitochondrial activity, while a reduction of the Git3/PKA pathway is thought to additionally activate the Wis4/Wis1/Sty1 MAP kinase cascade thereby leading to enhanced stress resistance (Roux *et al.*, 2010). In contrast to *S. cerevisiae* (Burtner *et al.,* 2009), no study has reported an effect of ethanol and acetic acid on *S. pombe* lifespan so far.

3.1.1 Establishment of methods to measure the CLS of *S. pombe*

The chronological lifespan of *S. cerevisiae* and *S. pombe* is usually measured by plating serial dilutions of stationary phase aging cultures and determining the ability of individual yeast cells to form a colony. This so called CFU method is illustrated in Figure 1 (see 1.2). Since only a few yeast cultures can be analyzed in parallel by using this traditional method, it was necessary to develop a new high-throughput method that enables the CLS measurement of many yeast cultures simultaneously.

Different media can be used for *S. pombe* growth. Therefore in a first step, the yeast medium most suitable for measuring the CLS under our conditions had to be determined. To this end, *S. pombe* wild-type cells were grown in EMM and YM medium, each containing the standard glucose concentration (2 % for EMM, 3 % for YM), and the CLS was measured by using the CFU method. In both approaches, overnutrition was achieved by using a high glucose concentration of 5 %, while 0.5 % glucose modelled DR. In agreement with earlier results (Chen & Runge, 2009), lifespan was increased in YM medium containing a low glucose concentration of 0.5 % as compared to the standard concentration, and it was decreased by overnutrition (Figure 8A). In contrast, yeast cells grown in EMM medium containing 5 % glucose displayed a longer lifespan than cells grown under standard conditions

(Figure 8B), indicating that a higher glucose concentration in EMM medium had the opposite effect than in YM medium. This has already been observed and discussed by other groups (Chen & Runge, 2009; Roux *et al.*, 2010) and suggests that nutrients are limited in EMM medium to an extent that they cause lifespan shortening with 3 % glucose. Since lifespan-extension by CR and the shortening of CLS by overnutrition are evolutionarily conserved (see 1.3), we decided to use YM medium here for the analyses of chronological aging. Notably, the maximum lifespan is significantly shorter in standard YM medium compared to standard EMM medium (Figure 8) (Chen & Runge, 2009).

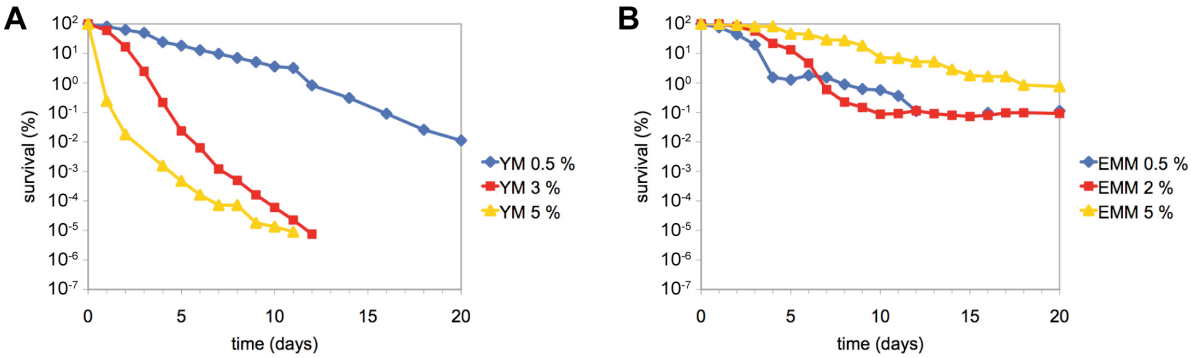

Figure 8 High glucose concentration shortened CLS of *S. pombe* in YM medium and extended lifespan in EMM medium
Wild-type cells (AEP57) were grown in 50 ml cultures at 30 °C. When reaching the stationary phase (day 0), samples were taken at the indicated time points, serially diluted in sterile water and then plated onto full medium plates. After incubating these plates at 30 °C for five days, the arising colonies were counted and the survival rate was calculated by defining the colony forming units (CFUs) per ml culture on day 0 as 100 %. Cells were grown under standard (2 % or 3 % glucose) as well as under CR (0.5 % glucose) and overnutrition conditions (5 % glucose) in either YM medium (A) or EMM medium (B).

Next, we sought to develop a high-throughput method to measure the CLS of many yeast cultures in parallel. For this purpose, small aging cultures were grown in 96 well microplates and spotted onto full medium plates at regular intervals to determine the viability of the culture. In the initial experiment, all wells were inoculated with the same wild-type strain, and six wells in a row contained medium with the same glucose concentration. In YM medium containing 5 % glucose, most yeast cells had lost viability on day five, whereas cells cultured in 3 % glucose were still viable (Figure 9). This indicated that this assay recapitulated the lifespan-shortening of high glucose concentrations. Similarly, lifespan was extended in YM medium containing 0.5 % glucose, thus modelling CR (Figure 9), showing that the assay reproduced the lifespan-shortening and -extending effects observed in Figure 8A, indicating that this method was a viable approach for large-scale studies.

Notably, both the CFU method and the new spotting method did only work using fission yeast, but not with budding yeast. As soon as the first *S. cerevisiae* cells died, re-growth of the remaining cells was observed (data not shown). This effect did not occur in *S. pombe* aging assays for unknown reasons.

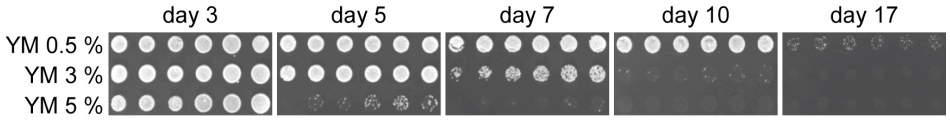

Figure 9 High-throughput method for the measurement of CLS of *S. pombe*
S. pombe wild-type cells (AEP57) were grown in 96 well microplates. Each row consisting of six wells contained YM medium with a different glucose concentration (top to bottom: 0.5 %, 3 %, 5 %). At the indicated time points, the aging cultures were spotted onto YES plates and incubated at 30 °C for two days. Each spot represents one well. Decreased growth implied a reduction in the ability to re-enter the cell cycle and therefore a shortening of the CLS.

3.1.2 Identification of lifespan-extending compounds

3.1.2.1 Screen for compounds that affect the CLS of *S. pombe*

After the establishment of a high-throughput measurement of CLS, it was used to analyze a small compound library (Biomol) consisting of 502 natural products for their effect on the CLS of wild-type *S. pombe* cells. Each compound was tested in a final concentration of 4 µg/ml as a biological duplicate in YM medium containing 3 % glucose, as first experiments using a final concentration of 20 µg/ml of some compounds led to increased rate of non-growing yeast cells (data not shown), indicating toxic effects. To determine the impact of the compounds on the lifespan and to correct for potential variations between individual microplates, each group of 6 x 8 wells contained as a control wild-type cells with the solvent DMSO and cultured in YM medium containing 0.5 %, 3 %, and 5 % glucose. An example of a screening plate is shown in Figure 10.

In this screen, we identified 48 primary candidates that showed an impact on the CLS of *S. pombe* (Table 7, Table 8) or delayed growth (Table 9). In the case of the latter, the yeast cells treated with these compounds reached stationary phase to a later time point than the control cells. Therefore, a potential lifespan-extension was hard to detect and thus, the corresponding compounds were analyzed a second time. For validation, all primary candidates were re-tested in two different concentrations (2 µg/ml and 4 µg/ml) in biological triplicates. In this experiment, 20 compounds extended lifespan (Table 10). Notably, rapamycin is also contained in the compound library, but did not show an effect at the tested concentrations of 2 µg/ml and 4 µg/ml,

which correspond to 2.19 µM and 4.38 µM for this compound (data not shown). However, there was a slight increase of CLS when 100 nM rapamycin was used (data not shown), indicating that the inability to identify rapamycin as a lifespan extending compound in our screen was due to the fact that the concentration tested here was too high.

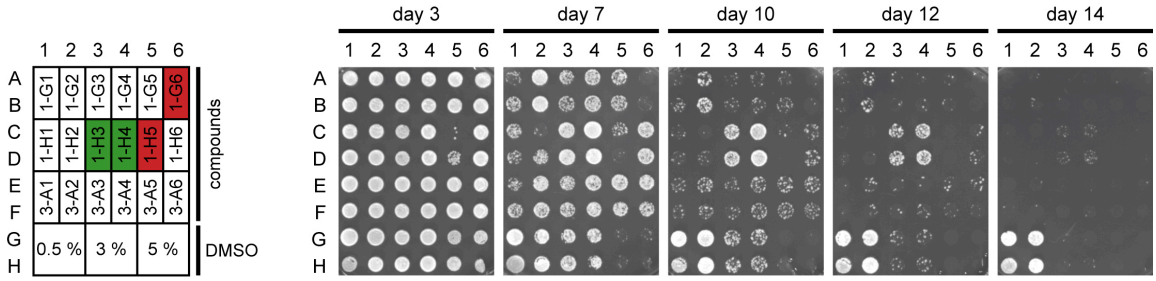

Figure 10 Example of the screen for compounds altering CLS
All wells of 96 well microplates were inoculated with a *S. pombe* wild-type strain (AEP57). The compounds indicated as their original position in the library (e.g. 1-H3 = microplate 1, row H, column 3) were tested in YM medium containing 3 % glucose. As controls, DMSO-treated cells were grown in standard YM medium (3 % glucose) as well as under CR and overnutrition conditions (0.5 % and 5 % glucose). At the indicated time points, the cells were spotted onto full medium plates and incubated at 30 °C for two days. Green: primary candidates that increased CLS, red: primary candidates that resulted in a shortened lifespan.

Table 7 Primary candidates of compounds that decreased CLS

CAS No.	compound	CAS No.	compound
42228-92-2	Acivicin[a]	13220-57-0	Tryptanthrin[b]
88495-63-0	Artesunate[a]	481-42-5	Plumbagin[a]
	C2 Phytoceramide[a]	596-85-0	Manool[a]
124753-97-5	C6 Ceramide[a]	126-19-2	Sarsasapogenin[a]
7059-24-7	Chromomycin A3[a]	512-64-1	Echinomycin[a]
59865-13-3	Cyclosporin A[a]	515-03-7	Sclareol[a]
76808-15-6	Ebelactone B[a]	51-56-9	Homatropine HBr[a]
116355-84-1	Fumonisin B2[a]	63968-64-9	Artemisinin[a]
83807-40-3	Geranylgeranoic Acid[a]	495-02-3	Auraptene[a]
500-64-1	Kavain (+/-)[a]	13190-97-1	Solanesol[a]
18378-89-7	Mithramycin A[a]	7184-60-3	Borrelidin[a]
35891-70-4	Myriocin[a]		Luffariellolide[c]
554-62-1	Phytosphingosine[b]		Phytosphingosine Nicotinic Acid[c]
13292-46-1	Rifampicin[b]		Salicyloyl-Phytosphingosine[c]

[a] final concentration of 4 µg/ml
[b] final concentration of 20 µg/ml
[c] final concentration of 100 µg/ml

Table 8 Primary candidates of compounds that increased CLS

CAS No.	compound
22373-78-0	Monensin Sodium[a]
24280-93-1	Mycophenolic Acid[a]
16561-29-8	Phorbol 12-myristate 13-acetate[b]
60203-57-8	Prostaglandin J_2[b]
83-79-4	Rotenone[a]
19545-26-7	Wortmannin[a]
54-11-5	(-)- Nicotine[a]
38970-49-9	Tschimganine[a]
77029-83-5	Hypocrellin A[a]
518-17-2	Evodiamine[a]
548-83-4	Galangine[a]
1968-05-4	3,3'-Diindolylmethane[a]

[a] final concentration of 4 µg/ml
[b] final concentration of 20 µg/ml

Table 9 Primary candidates of compounds that delayed growth

CAS No.	compound
52665-69-7	Antibiotic A-23187[a]
28380-24-7	Nigericin Sodium[a]
2001-95-8	Valinomycin[a]
19545-26-7	Wortmannin[b]
54-11-5	(-)- Nicotine[b]
481-42-5	Plumbagin[a]
484-12-8	Osthole[a]
1397-89-3	Amphotericin B[a]
	Mangosteen[c]
	Turmeric Oil[c]

[a] final concentration of 4 µg/ml
[b] final concentration of 20 µg/ml
[c] final concentration of 100 µg/ml

Notably, compounds that decreased lifespan in the validation experiment were not further evaluated, as cytotoxic effects could not be excluded.

Among the secondary candidates that extended lifespan, we identified nicotine and wortmannin (Table 10). The effect of nicotine on CLS was further investigated and is described in paragraph 3.2.4.6. Since wortmannin is an immunosuppressive drug that is already known to inhibit phosphatidylinositol 3-kinases (PI3Ks) and

mTOR (Feldman & Shokat, 2010) and thereby to promote longevity (Moskalev & Shaposhnikov, 2010), this compound was not further analyzed.

Table 10 Secondary candidates of compounds that improved CLS

CAS No.	compound	Strength of CLS extension[a]	
		2 µg/ml	4 µg/ml
42228-92-2	Acivicin[2]	+++	+++
83807-40-3	Geranylgeranoic Acid[2]	O	(+)
22373-78-0	Monensin Sodium	O	+
24280-93-1	Mycophenolic Acid	++	++
28380-24-7	Nigericin Sodium[2]	(+)	++
60203-57-8	Prostaglandin J_2	+++[b]	+++[c]
83-79-4	Rotenone	(+)	+
2001-95-8	Valinomycin	(+)	O
19545-26-7	Wortmannin	+++	+++
54-11-5	(-)- Nicotine	(+)	++
38970-49-9	Tschimganine	O	+
481-42-5	Plumbagin[2]	(+)	+
512-64-1	Echinomycin[2]	++	O
515-03-7	Sclareol[2]	O	(+)
495-02-3	Auraptene[2]	O	(+)
77029-83-5	Hypocrellin A	(+)	(+)
518-17-2	Evodiamine	(+)	(+)
548-83-4	Galangine	O	(+)
1968-05-4	3,3'-Diindolylmethane	(+)	+
	Mangosteen[2]	+++[d]	(+)[e]

[a] (+) slight increase, + moderate increase, ++ strong increase, +++ very strong increase of CLS, O no change
[b] final concentration of 10 µg/ml
[c] final concentration of 20 µg/ml
[d] final concentration of 50 µg/ml
[e] final concentration of 100 µg/ml

The secondary candidates that showed the strongest effects in the validation experiment were re-ordered from different companies for further analyses. Four different concentrations of the compounds originating from the library and of the

[2] The compound showed a different effect in the primary screen. However, the effect in the validation experiment was the reproducible result.

re-ordered compounds were tested in parallel to ensure that the observed lifespan-extension was truly caused by the indicated compound and was not due to degradation products or contaminations. Additionally, the effect of the re-ordered compounds on the CLS of another *S. pombe* wild-type strain (AEP1) was investigated to confirm that it did not depend on the background of the strain. As an example, the results of mycophenolic acid (MPA) are shown in Figure 11. This compound extended the CLS of both wild-type strains at a final concentration of 20 µg/ml.

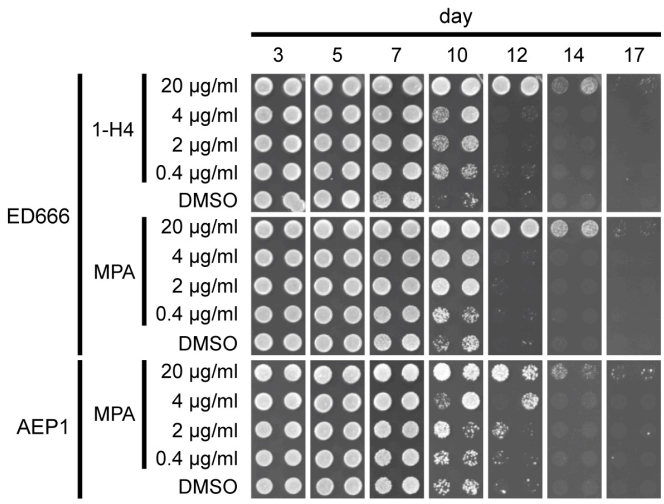

Figure 11 Example of a lifespan-extending compound
96 well microplates with YM medium containing 3 % glucose were inoculated with *S. pombe* wild-type cells (AEP57 and AEP1). The indicated concentrations of the compound originating from the library (here: well 1 -H4) and of the re-ordered compound (here: mycophenolic acid, MPA) were added (day 0). At the indicated time points, the aging cultures were spotted onto full medium plates that were incubated at 30 °C for two days. DMSO-treated cells served as control.

Finally, eight secondary candidates could be shown to promote longevity. In addition to MPA, the remaining candidates were acivicin, 3,3'-diindolylmethane (DIM), mangosteen, monensin, nigericin, prostaglandin J_2 (PGJ_2), and tschimganine (Figure 12). Based on these initial tests, the concentration of the compounds that led to the strongest effect was used for the following experiments.

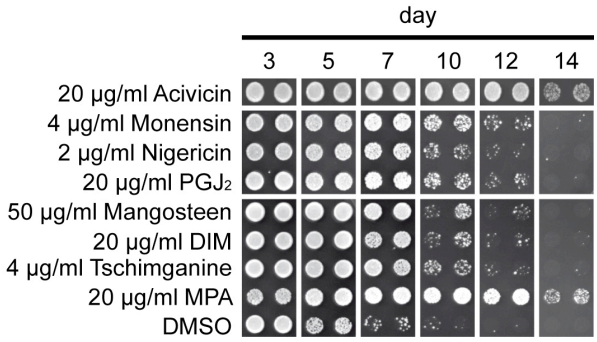

Figure 12 Final candidates of longevity-promoting compounds
S. pombe wild-type cells (AEP57) were grown in 96 well microplates in YM medium containing 3 % glucose and the indicated compounds. DMSO served as control.

In contrast to the other candidates, mangosteen is not a single compound but rather a compound mixture. The effect of its main constituents α-mangostin, β-mangostin, gartanin, and 8-desoxygartanin on CLS was also analyzed with the new method. However, none of the several tested concentrations extended lifespan of *S. pombe* wild-type cells (AEP57) (data not shown), indicating that it is probably the interplay of the single compounds or another unidentified component that leads to increased CLS.

So far, the effect of the compounds had only been measured by using the new microplate CLS method. To further verify their life-extending effect, seven of the eight secondary candidates were subsequently tested with the traditional CFU method. In the case of the eighth candidate, PGJ_2, for economic reasons only small amounts of the compound were at our disposal, which were not sufficient for the CFU method. For the CFU experiment, the concentration that led to the strongest lifespan-extension in the previous experiments was chosen. The analysis was performed at least twice to ensure the reproducibility and indeed, all results were similar to those shown in Figure 13, thereby confirming the impact of the compounds on CLS.

PGJ_2 was tested using a modified approach, in which cultures of wild-type cells (AEP57) were grown in test tubes in the presence of PGJ_2 or DMSO. At regular intervals, aliquots were taken, serially diluted and subsequently spotted on fullmedium plates. The viability of the cells treated with the compound was increased ten-fold compared to the control on day seven and also on day 12 (Figure 14), thereby verifying its lifespan-extending effect.

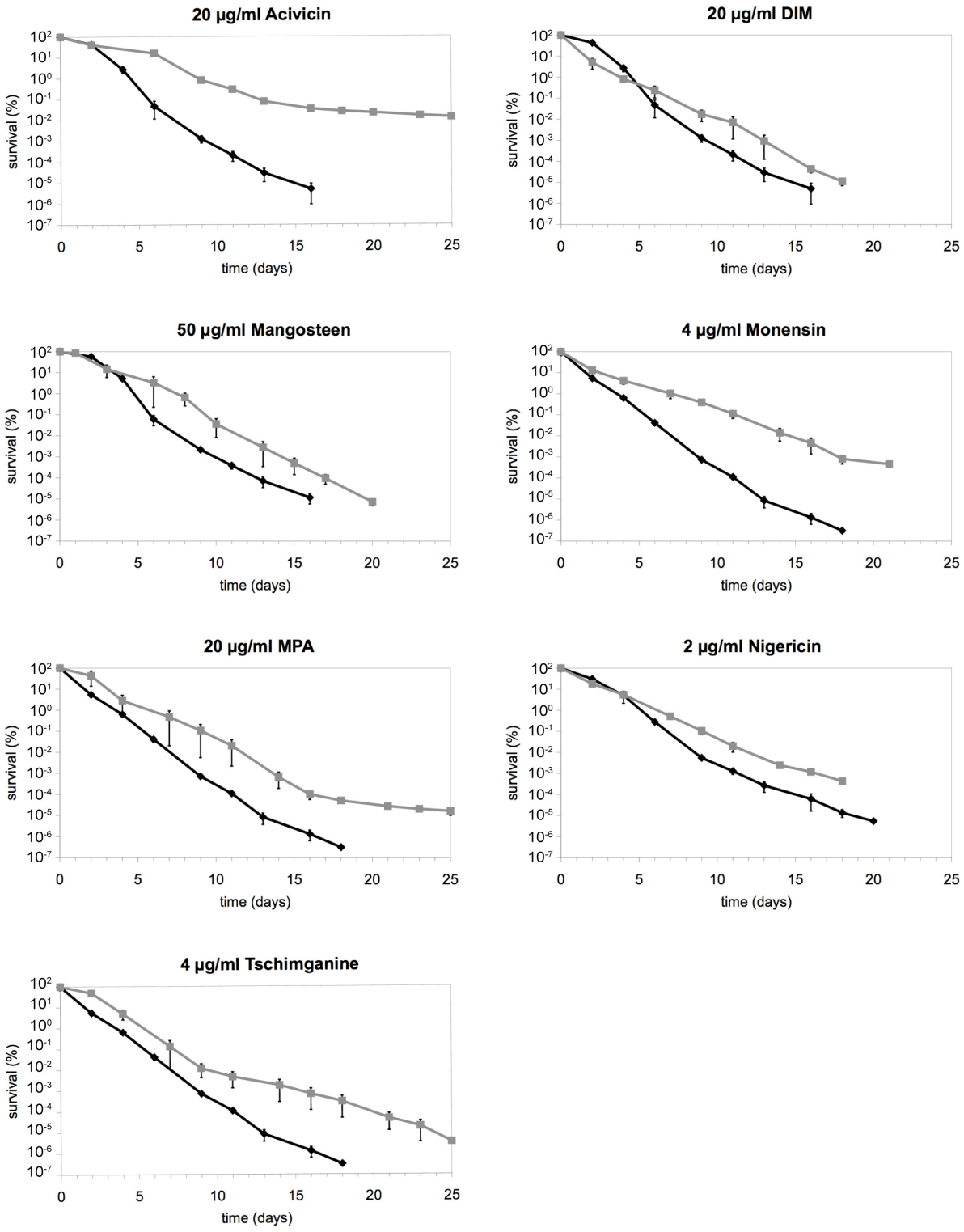

Figure 13 Lifespan-extension could be confirmed by using the CFU method
For this experiment, *S. pombe* wild-type cells (AEP57) were grown in YM medium containing 3 % glucose. The indicated compounds (grey) were tested at least one time in biological duplicate or triplicate and the corresponding averages are shown in the graphs. The black bars represent the standard deviation. DMSO-treated cells served as control (black).

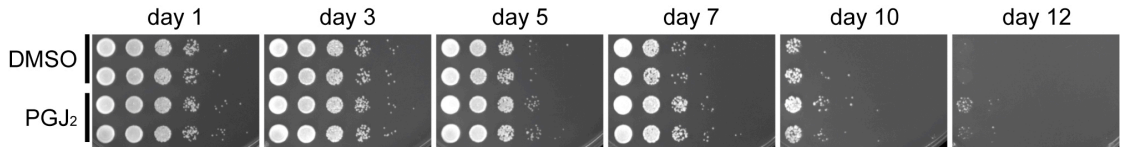

Figure 14 CLS of *S. pombe* was increased by PGJ_2
Cultures of *S. pombe* wild-type cells (AEP57) in YM medium containing 3 % glucose and 20 µg/ml prostaglandin J_2 (PGJ_2) were grown in test tubes. Aliquots taken at the indicated time points were ten-fold serially diluted in YES medium and spotted onto full medium plates that were incubated at 30 °C for two days. DMSO-treated cells served as control.

In another approach, the effect of the compounds on the viability of fission yeast was further verified by fluorescence staining. For this purpose, wild-type cells (AEP57) treated with the compounds were stained using FITC-VAD-fmk (CaspACE) or phloxine B to detect apoptotic and dead cells respectively. All stainings were performed with exponentially grown cells as well as with cells that were in stationary phase for approximately three days. To quantify the impact of the compounds, the amount of stained cells compared to the total cell number was calculated. Since apoptosis is the process of programmed cell death, staining apoptotic and dead cells is nearly the same. Therefore, it was not surprising that the results of these two experiments were similar (Figure 15, Figure 16). Four compounds, namely DIM, mangosteen, PGJ_2, and tschimganine, led to a reduction of apoptotic and dead cells in stationary phase compared to the control treated with DMSO (Figure 15, Figure 16), thereby confirming their longevity-promoting effect again. MPA treatment resulted only in a reduction of dead cells (Figure 16). In contrast, an increase of apoptotic and dead cells was observed in stationary phase of acivicin-, monensin-, and nigericin-treated cells (Figure 15, Figure 16). The reasons are unknown.

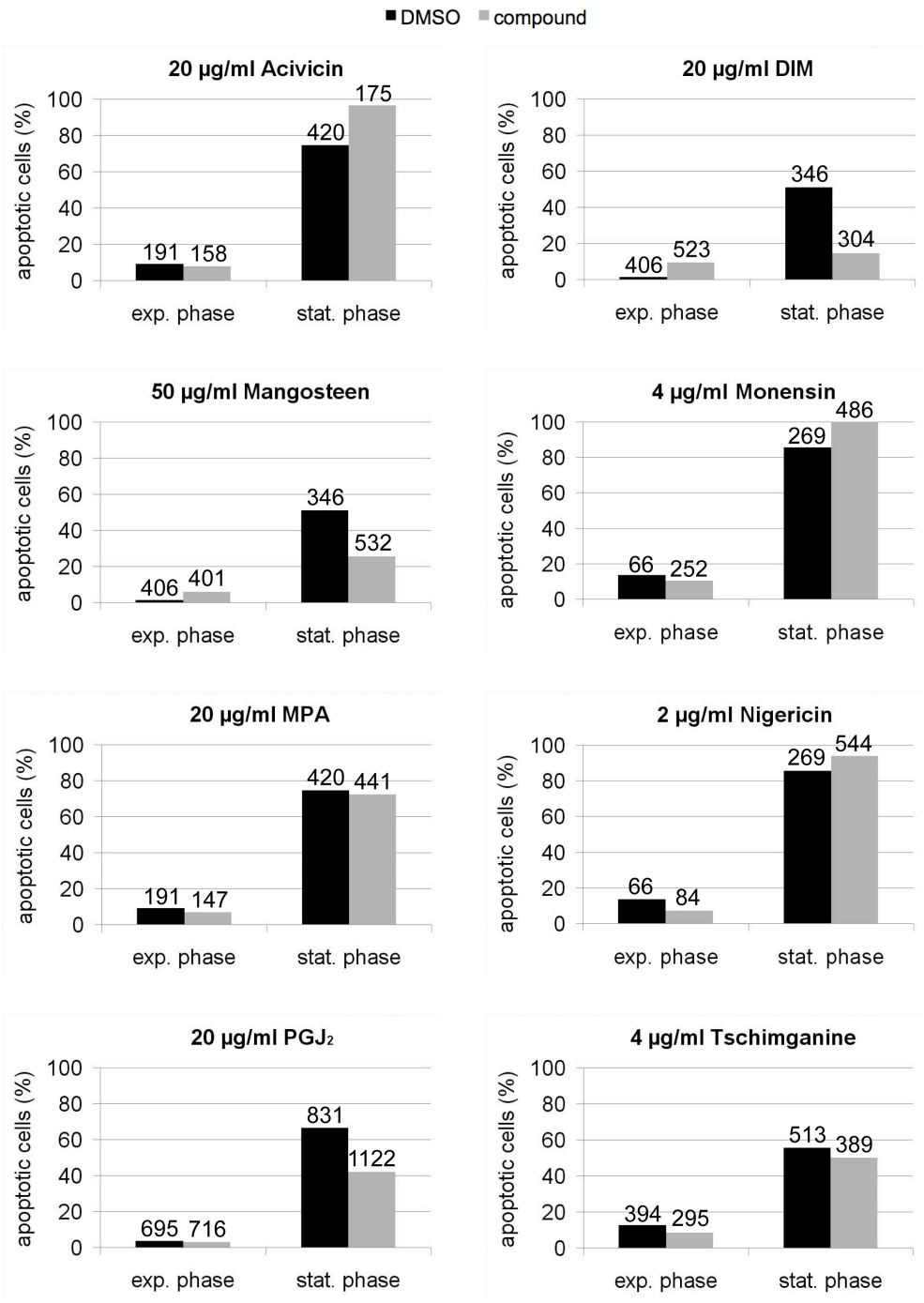

Figure 15 Fluorescence staining of apoptotic cells
S. pombe wild-type cells (AEP57) were grown in YM medium containing 3 % glucose and the indicated compounds (grey bars) or DMSO as control (black bars). During exponential (exp.) phase and stationary (stat.) phase, aliquots of the cultures were taken and stained with 10 µM FITC-VAD-fmk (CaspACE). Subsequently, the samples were analyzed using a fluorescence microscope. Stained cells were counted and their amount compared to the total cell number was calculated. Total numbers of counted cells are given above the bars.

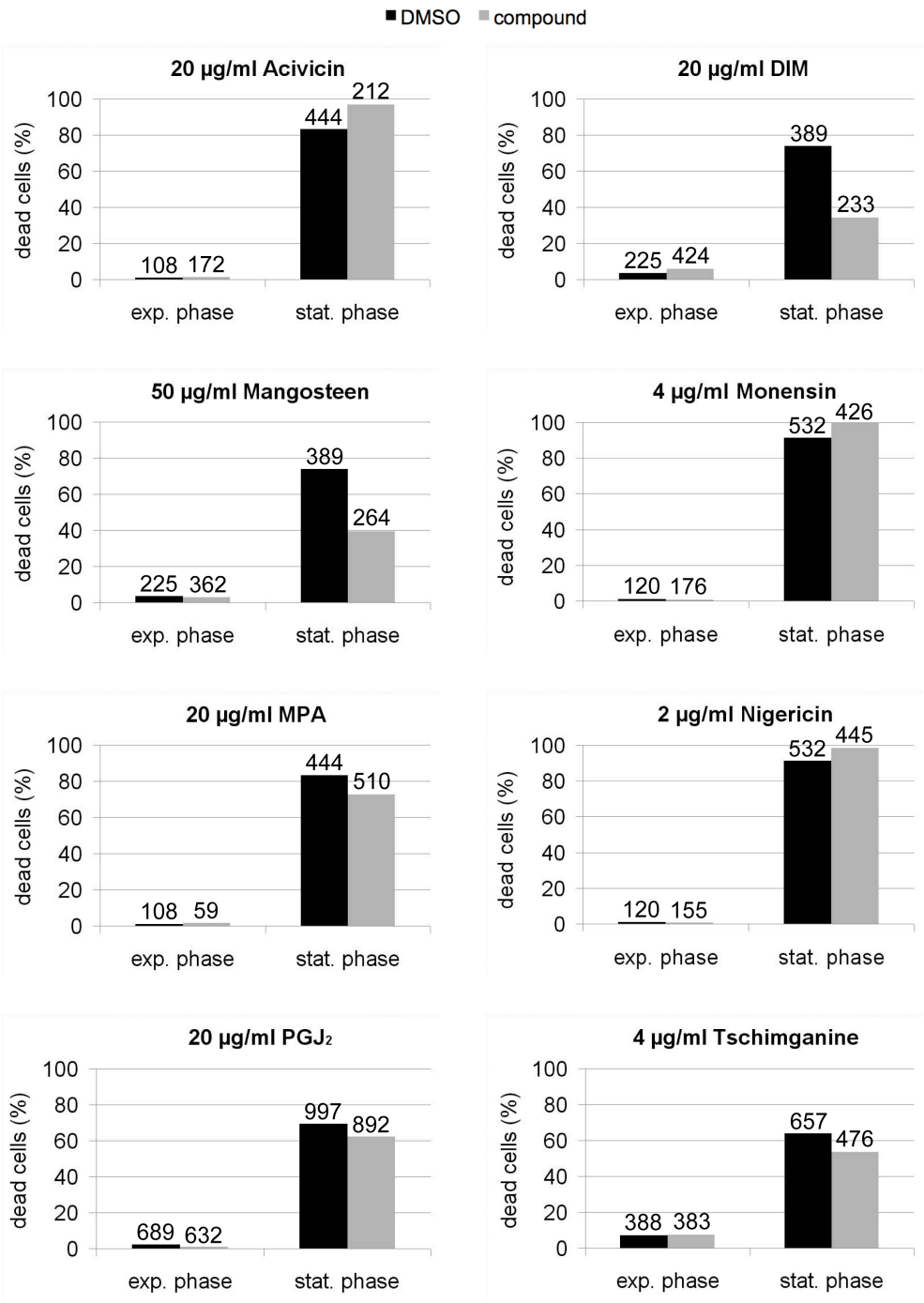

Figure 16 Fluorescence staining of dead cells
S. pombe wild-type cells (AEP57) were grown in YM medium containing 3 % glucose and the indicated compounds (grey bars) or DMSO as control (black bars). During exponential (exp.) phase and stationary (stat.) phase, aliquots of the cultures were taken and stained with 5 mg/ml phloxine B. Subsequently, the samples were analyzed using a fluorescence microscope. Stained cells were counted and their amount compared to the total cell number was calculated. Total numbers of counted cells are given above the bars.

3.1.2.2 Impact of CLS-extending compounds on stress response

In general, lifespan extension through CR has been linked to increased stress resistance. In *S. pombe*, this is true for *pka1*Δ cells, but not for *sck2*Δ cells (Roux *et al.*, 2006), indicating that there are differences between the two nutrient signalling pathways in fission yeast. Here, we therefore sought to determine whether the identified compounds might act by affecting the stress resistance of *S. pombe* wild-type cells (AEP57). For this purpose, the cells were grown in medium containing the compounds or DMSO as a control. Subsequently, they were exposed to heat or treated with the DNA-damaging agent methyl methanesulfonate (MMS) or with hydrogen peroxide (H_2O_2), which causes oxidative stress. Surprisingly, variations in the stress response could be observed for DMSO-treated cells as a function of the duration the cells spent in stationary phase before they were exposed to the different kinds of stress. Notably, stationary phase was reached after less than one day at 30 °C. Cells that were grown for two days were more sensitive to DNA damage (MMS) than cells that were grown for only one day. Conversely, they were significantly more resistant against oxidative stress (Figure 17). The reason for these differences is not known.

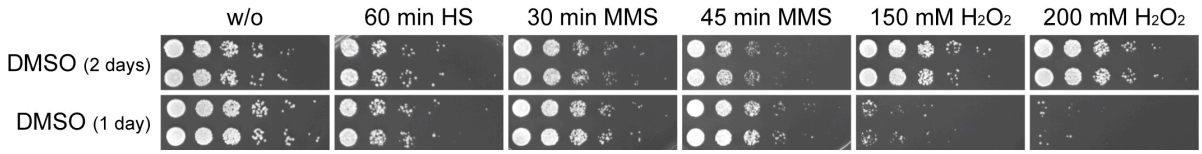

Figure 17 Stress resistance was altered by the duration in stationary phase
S. pombe wild-type cells (AEP57) were treated with DMSO and grown in YM medium containing 3 % glucose for one or two days. The cultures were adjusted to an OD_{600} of 0.5. Aliquots were treated with 150 mM or 200 mM hydrogen peroxide (H_2O_2) for one hour at 30°C or with 0.2 % methyl methanesulfonate (MMS) for 30 minutes or 45 minutes at 30 °C. Another sample was incubated for one hour at 48 °C (HS). Subsequently, the cells were six-fold serially diluted and spotted onto full medium plates that were incubated at 30 °C for two days.

This was an important observation, since some of the analyzed compounds slowed down the growth rate of cultures that were grown in test tubes and thereby led to a delay in reaching stationary phase. Therefore, three compounds that delayed growth were compared to DMSO-treated cells that were grown for two days (Figure 18A), while the remaining five compounds that did not delay growth were compared to control cells that were grown for one day (Figure 18B).

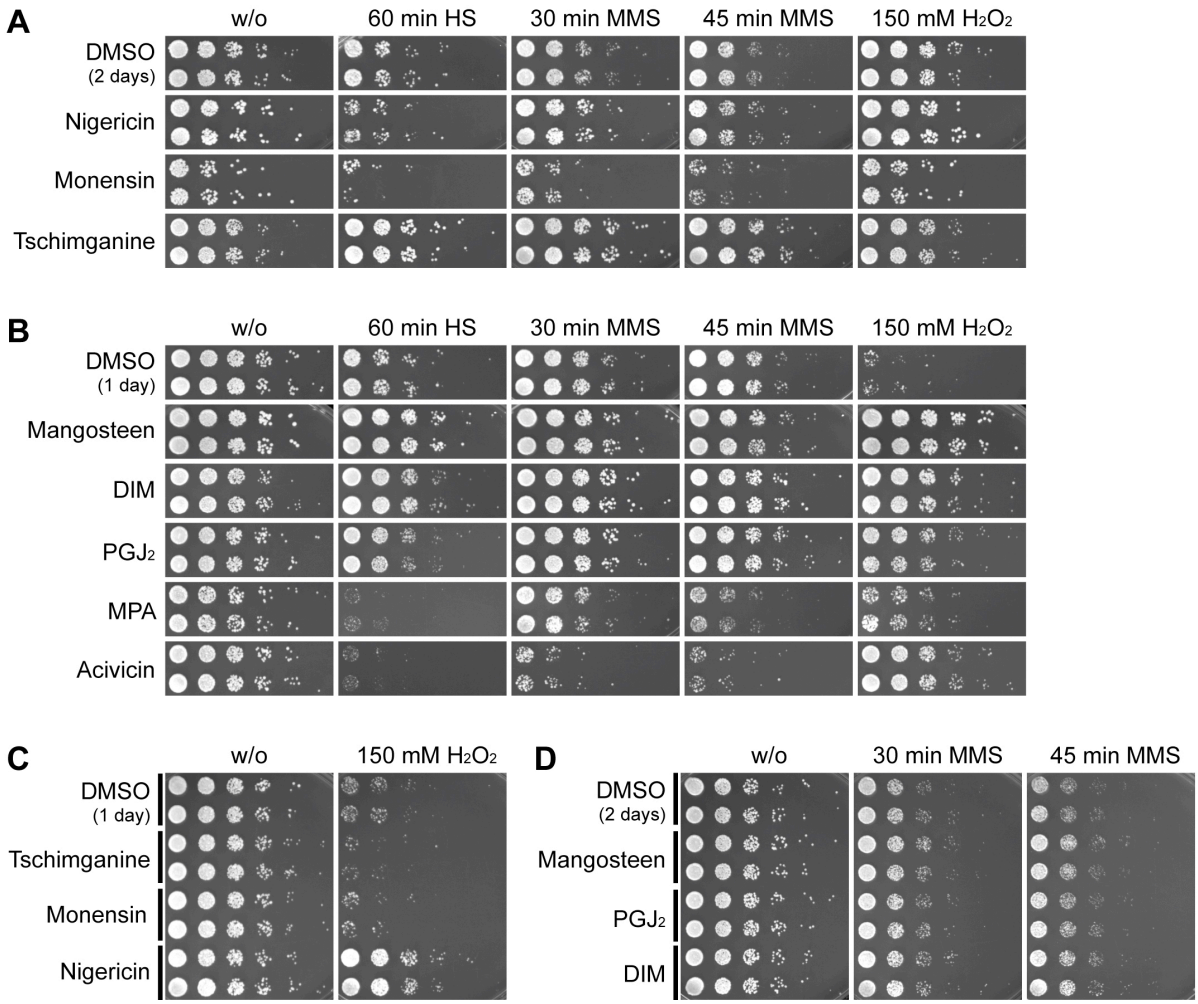

Figure 18 Impact of compounds on stress resistance
Analysis of stress resistance of *S. pombe* wild-type cells (AEP57) that were treated with compounds as described in Figure 17. DMSO-treated cells served as control.
(A) Stress response of cells that were treated with DMSO, 2 µg/ml nigericin, 4 µg/ml monensin or 4 µg/ml tschimganine for two days.
(B) Analysis of stress resistance cells that that were treated with 50 µg/ml mangosteen, 20 µg/ml 3,3'-diindolylmethane (DIM), 20 µg/ml prostaglandin J_2 (PGJ_2), 20 µg/ml mycophenolic acid (MPA) or 20 µg/ml acivicin after one day.
(C) Impact of two day-treatment with DMSO, 2 µg/ml nigericin, 4 µg/ml monensin or 4 µg/ml tschimganine on oxidative stress resistance.
(D) Stress response to MMS of cells that were treated with DMSO, 50 µg/ml mangosteen, 20 µg/ml PGJ_2 or 20 µg/ml DIM for one day.

Due to the fact that the control cells treated with H_2O_2 in Figure 18A and those treated with MMS in Figure 18B already showed maximal growth, it was not possible to measure a potential increase of the stress resistance by the compounds. However, increased concentrations or a longer incubation time did not change the result (data not shown). Therefore, we tested the response to these particular stresses under conditions where the control cells were more sensitive. As a result, the impact of tschimganine, monensin, and nigericin on oxidative stress resistance after one day was analyzed. Nigericin treatment led to increased resistance, while the cells treated

with tschimganine or monensin showed a slightly increased sensitivity against oxidative stress (Figure 18C). Additionally, we tested the resistance against MMS of mangosteen-, DIM-, and PGJ_2-treated cells after two days in stationary phase. The MMS resistance of the DMSO-treated cells was reduced under these conditions, and this was also the case for the compound-treated cells (Figure 18D), indicating that the compounds did not affect this particular stress response. All results concerning the impact of the compounds on stress resistance are summarized in Table 11.

Based on their impact on stress resistance (Table 11), first hypotheses about the potential mode of action of the compounds could be made. Only DIM and mangosteen caused increased resistance against both heat and oxidative stress as has been reported for *pka1*Δ cells (Roux *et al.*, 2006), indicating that these two compounds might affect the Git3/PKA pathway in *S. pombe*. In the case of acivicin, MPA, nigericin, and PGJ_2, the cells treated with these compounds showed improved resistance against oxidative stress, which could be a possible explanation for their life-extending effect. Tschimganine enhanced the resistance against heat and DNA damage, which might be a reason for increased CLS. Monensin was the only compound that did not improve any of the tested stress responses, thereby giving no indications as to its potential mode of action.

Table 11 Impact of compounds on stress resistance

compound	HS	MMS	H_2O_2
20 µg/ml Acivicin	—	—	+
20 µg/ml DIM	+	O	+
50 µg/ml Mangosteen	+	O	+
4 µg/ml Monensin	O	O	(—)
20 µg/ml MPA	—	—	+
2 µg/ml Nigericin	O	O	+
20 µg/ml PGJ_2	O	O	+
20 µg/ml Tschimganine	+	+	(—)

O unchanged, (—) slightly decreased, — decreased, + increased stress resistance
Abbrevations: HS = heat shock, MMS = methyl methanesulfonate,

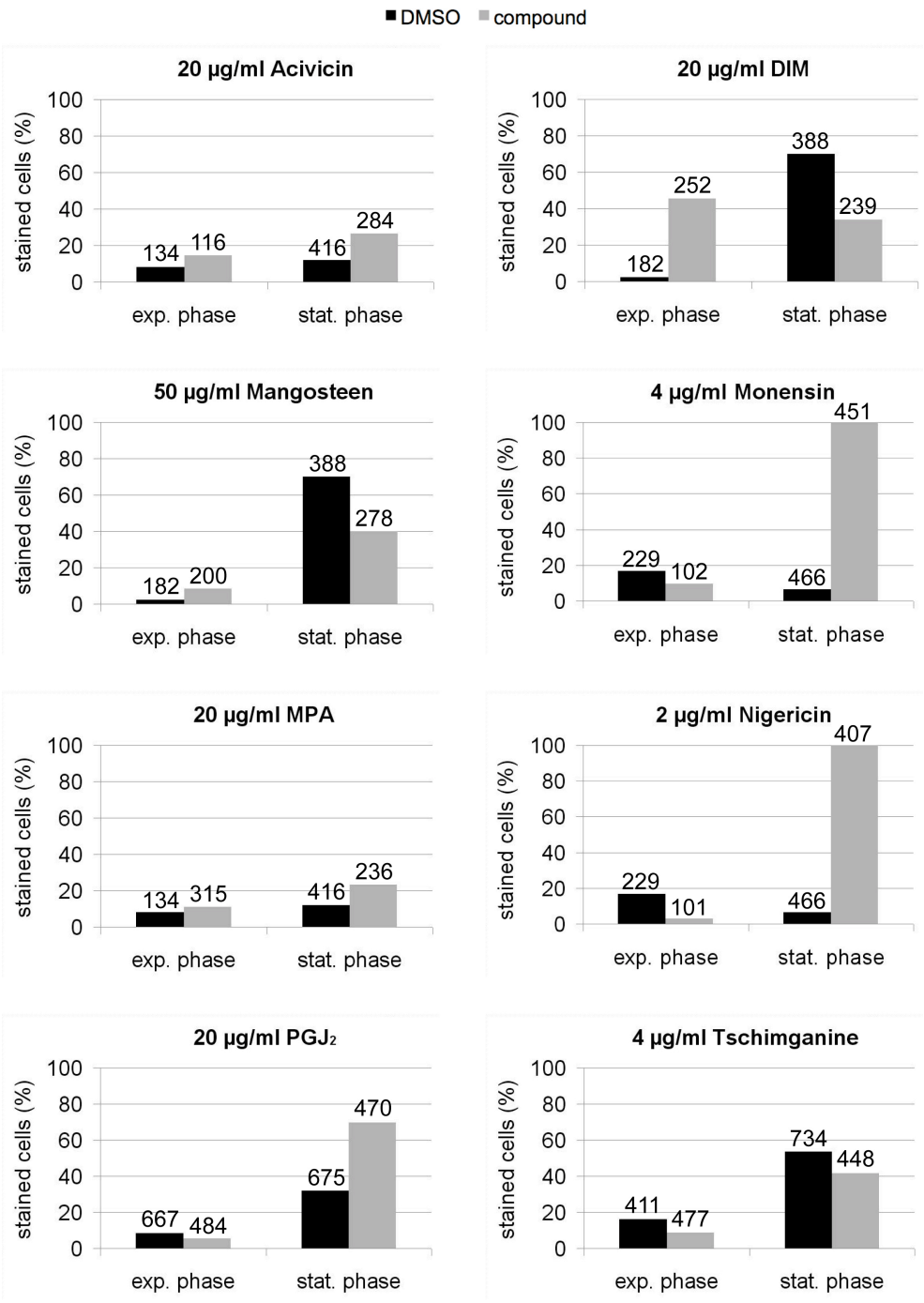

Figure 19 Fluorescence staining of ROS
S. pombe wild-type cells (AEP57) were grown in YM medium containing 3 % glucose and the indicated compounds (grey bars) or DMSO as control (black bars). During exponential (exp.) phase and stationary (stat.) phase, aliquots of the cultures were taken and stained with 30 µM dihydrorhodamine 123 (DHR123). Subsequently, the samples were analyzed using a fluorescence microscope. Stained cells were counted and their amount compared to the total cell number was calculated. Total numbers of counted cells are given above the bars.

In general, an increased resistance against oxidative stress is thought to be associated with decreased ROS levels. To test this, fluorescence staining was performed using wild-type cells (AEP57) treated with the compounds. Exponentially grown cells as well as cells that were in stationary phase for approximately three

days were stained for ROS by using dihydrorhodamine 123 (DHR123). To quantify the impact of the compounds, the amount of stained cells compared to the total cell number was calculated (Figure 19).

Contrary to our expectation, all compounds, except for tschimganine, showed increased amounts of ROS-labelled cells either during exponential growth or in stationary phase (Figure 19). In the case of acivicin, DIM, mangosteen, MPA, nigericin, and PGJ_2, the increased number of DHR123-stained cells could be a hint that these compounds caused the previously found enhanced resistance against oxidative stress (Figure 18, Table 11) by increased ROS levels resulting in the expression and activation of proteins involved in this kind of stress response.

3.1.2.3 General characterization of the CLS-extending compounds

In a next step, we wanted to determine whether the identified compounds might act through pathways that are already known to extend lifespan (CR, Sir2). For this purpose, their effect was analyzed under different conditions by using the microplate CLS method (see 3.1.1). First, wild-type cells (AEP57) were treated with the compounds and grown in YM medium containing different glucose concentrations, whereby 3 % glucose represented the standard condition and 1 % glucose was used to model DR, while 5 % glucose constituted overnutrition. Notably, *pka1*Δ cells showed a stronger effect under overnutrition conditions (data not shown) (Zuin *et al.*, 2010). Second, we sought to determine whether the compounds altered CLS by affecting one of the known life-extending pathways. Therefore, their effect on *sck2*Δ (AEP62) and *pka1*Δ cells was investigated. Since rapamycin and wortmannin have previously been shown to extend the CLS by inhibiting TOR signalling, wild-type cells (AEP57) were simultaneously treated with the compounds and 100 nM rapamycin or 2.5 µM wortmannin to test whether they might act synergistically. Furthermore, given that Sir2 is an important factor in regulating the lifespan of *S. cerevisiae* (see 1.7), *S. pombe* strains carrying deletions of the Sir2 homologs Sir2 and Hst2 were additionally tested for life-extending effects by the compounds. Except for the *pka1*Δ cells that were grown in YM medium containing 5 % glucose, the remaining deletion strains were grown under standard conditions. The results of these experiments, which were performed at least three times, are summarized in (Table 12).

Table 12 Summary of epistasis analyses

compound	glucose			*pka1*Δ[a]	*sck2*Δ	100 nM Rapa-mycin	2.5 µM Wort-mannin	*sir2*Δ	*hst2*Δ
	1 %	3 %	5 %						
20 µg/ml Acivicin	+	+	+	→	+	+	→	→	→
20 µg/ml DIM	+	+	+	+	(+)	(+)	O	+	+
50 µg/ml Mangosteen	+	+	+	+	+	+	O	→	+
4 µg/ml Monensin	+	+	+	O	(+)	+	O	O	O
20 µg/ml MPA	+	+	+	→	+	+	→	+	+
2 µg/ml Nigericin	+	+	(+)	+	(+)	+	+	(+)	—
20 µg/ml PGJ_2	+	+	+	O	+	+	(+)	(+)	+
20 µg/ml Tschimganine	+	+	+	+	+	+	O	+	(+)

[a] *pka1*Δ cells were grown in YM medium containing 5 % glucose.
O no change, → delayed growth, — decreased, (+) slightly increased or + increased CLS

Notably, the conditions where the compounds did not increase CLS were of special interest because this can be interpreted as epistasis, meaning that a compound acts in the same pathway as another gene or treatment. In general, the lifespan-extending effect of the compounds seemed to be independent of the glucose concentration of the medium, as all of them increased CLS compared to the DMSO control (Table 12). Notably, the lifespan of wild-type yeast cells could be even further extended compared to cells grown in medium containing 1 % glucose by lower glucose concentrations, for instance 0.5 % (data not shown), indicating that there is still a potential way to increase CLS by the same pathways. As a conclusion, the lifespan extension by the compounds in medium containing 1 % glucose was no irrefutable proof that they did not act through to the CR pathways. Nevertheless, it could be suggested that the tested compounds act independently from the TOR signalling pathway because the compounds promoted longevity of *sck2*Δ cells and rapamycin-treated wild-type cells (Table 12).

Strikingly, PGJ_2 extended lifespan with only one exception. It did not improve the CLS of *pka1*Δ cells (Figure 20C), suggesting that its effect might be linked to the Git3/PKA signalling pathway. Monensin failed to extend the CLS of *pka1*Δ, *sir2*Δ, and *hst2*Δ cells (Figure 20). This indicated that monensin might promote longevity through the Git3/PKA signalling pathway, and that its action required the Sir2 homologs or at least one of their targets. The latter might also be true for nigericin, since *hst2*Δ cells treated with this compound displayed a reduced lifespan (Figure 20B). On the other hand, MPA and acivicin delayed the growth of *pka1*Δ cells

(Figure 20C), which already have a slowed growth rate, and of wortmannin treated cells. Therefore, this could be an indication that MPA and acivicin affect a target that acts in a pathway parallel to the nutrient sensing pathways to extend lifespan. As acivicin also delayed the growth of *sir2*Δ and *hst2*Δ cells, this compound might additionally act parallel to these HDACs.

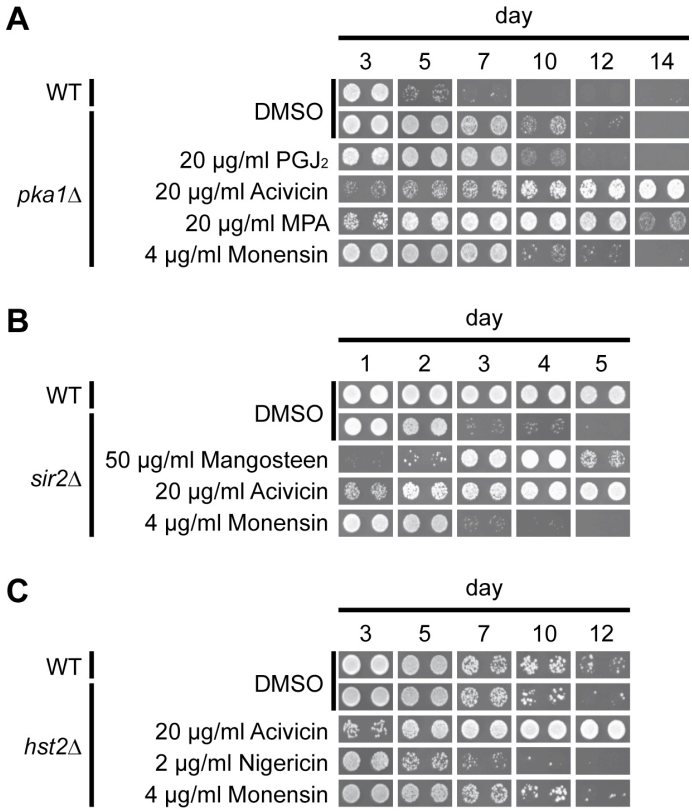

Figure 20 Examples of epistasis analysis
(A) *pka1*Δ, (B) *sir2*Δ, and (C) *hst1*Δ cells originating from the *S. pombe* deletion library (Bioneer) were grown in YM medium containing 5 % (B) or 3 % glucose (A, C) and the indicated compounds. DMSO-treated deletion cells as well as wild-type cells (AEP57) treated with DMSO served as controls. The aging cultures were spotted on YES plates at the indicated time points. All plates were incubated at 30 °C for two days.

However, DIM, mangosteen, tschimganine, and monensin did not further increase the lifespan of wild-type cells that were additionally treated with wortmannin although they improved CLS of *sck2*Δ cells and rapamycin-treated wild-type cells (Table 12). Since the results of the wortmannin-treated cells showed comparatively strong variability (data not shown), the absence of a lifespan-extending effect might be due to effects of wortmannin as a PI3K inhibitor other than inhibiting TOR signalling. As mangosteen delayed the growth of cells carrying a deletion of *SIR2* (Figure 20A), it might act in parallel to the HDAC coded by this gene.

3.1.2.4 Potential mechanisms of lifespan extension by the compounds

In order to gain insight into the mode of action of the identified compounds, we searched the literature for information known about them. Based on this, we hypothesized what could be the potential target of the individual compound. As far as practicable, these hypotheses were investigated, and the corresponding results are presented in the following paragraphs.

Notably, DIM, mangosteen, and tschimganine were tested in the experiments for monensin and nigericin, as we had no separate hypotheses how these three compounds may lead to increased lifespan.

3.1.2.4.1 PGJ_2 did not extend the CLS of *dnm1*Δ and *git3*Δ cells

The group of prostaglandins is divided into three main classes based on their mode of synthesis. For instance, class 2 prostaglandins, like PGJ_2, originate from arachidonic acid. To test whether the lifespan extension by PGJ_2 is a general effect of prostaglandins or not, those contained in the small compound library (Biomol), namely PGA_1, PGB_1, PGE_1, PGE_2, and $PGF_{2\alpha}$, were re-tested in our lifespan assay. Wild-type cells (AEP57) were treated with four different concentrations of each of those prostaglandins, but none of them altered CLS (Figure 21). Since the re-tested prostaglandins belong to class 1 as well as class 2, this led to the conclusion that increased lifespan is specific for PGJ_2 and not an effect of prostaglandins *per se* or members of a certain class of prostaglandins.

A derivative of PGJ_2 called 15-deoxy-Δ-12, 14-prostaglandine J_2 (15d-PGJ_2) has previously been shown to induce mitochondrial fusion by inactivating the dynamin-related protein 1 (Drp1) (Mishra *et al.*, 2010) whose homolog is called Dnm1 in fission yeast. In general, the activity of Drp1/Dnm1 leads to mitochondrial fission, while its counterpart, OPA1/Msp1, promotes the fusion of mitochondria. To test whether there is a relationship between the potential inactivation of Dnm1 and lifespan extension by PGJ_2, the CLS of *dnm1*Δ and *msp1*Δ cells originating from the *S. pombe* deletion library (Bioneer) was analyzed. Notably, the CLS of *dnm1*Δ cells was comparable to that of wild-type cells (AEP57), while *msp1*Δ cells displayed a slightly reduced lifespan (Figure 22, DMSO). Treatment with PGJ_2 resulted in increased lifespan of wild-type and *msp1*Δ cells, whereas the CLS of *dnm1*Δ cells was unchanged (Figure 22, PGJ_2). These results indicate that lifespan extension by

PGJ_2 requires Dnm1 and mitochondrial fission. However, as *dnm1*Δ cells did not display an increased CLS compared to wild-type cells, this might be not the (Fang *et al.*) reason for the lifespan-extending effect of this compound.

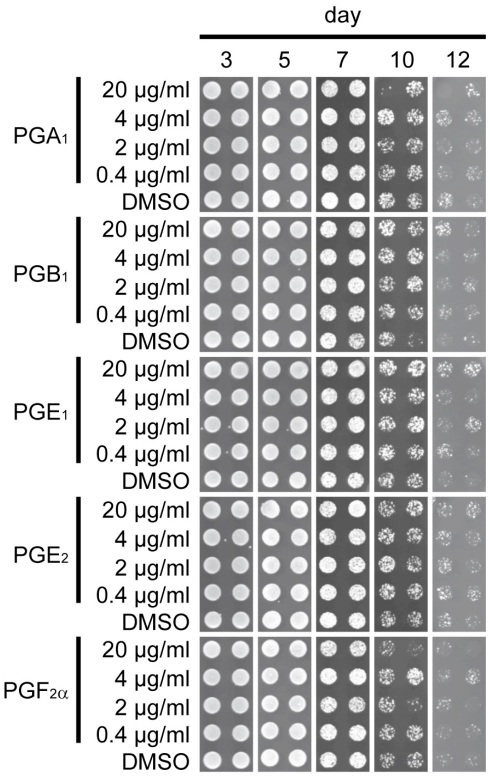

Figure 21 Other tested prostaglandins did not extend CLS
S. pombe wild-type cells (AEP57) were grown in YM medium containing 3 % glucose and 0.4/2/4/20 µg/ml of the indicated prostglandins. At regular intervals, the cultures were spotted on YES plates that were then incubated at 30 °C for two days.

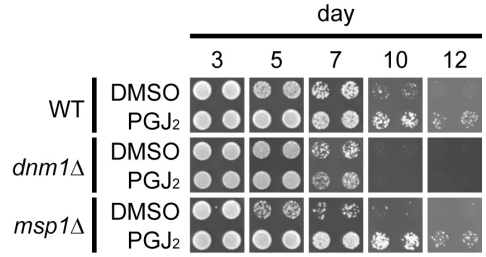

Figure 22 CLS of *dnm1*Δ cells was not increased by PGJ_2
*dnm1*Δ and *msp1*Δ cells originating from the *S. pombe* deletion library (Bioneer) as well as the corresponding wild-type cells (AEP57) were grown in YM medium containing 3 % glucose and 20 µg/ml prostaglandin J_2 (PGJ_2) or DMSO. These cultures were spotted on YES plates at the indicated time points. The plates were incubated for two days at 30 °C.

Furthermore, it was known that human prostaglandins inhibit G-protein coupled receptors (Narumiya *et al.*, 1999). Notably, the glucose receptor Git3, which is part of the nutrient sensing pathways in *S. pombe*, is such a transmembrane receptor. Therefore, we analyzed the CLS of strains carrying a deletion of G-protein coupled receptors or proteins involved in G-protein signalling. *git3*Δ cells were the only cells whose lifespan was increased compared to the wild-type cells (AEP57) (Figure 23, DMSO). On the other hand, these cells were also the only ones whose lifespan was not further improved by PGJ_2-treatment (Figure 23, PGJ_2). In summary these results suggest that PGJ_2 extended the CLS of fission yeast by inhibiting Git3 and thus mimicking CR.

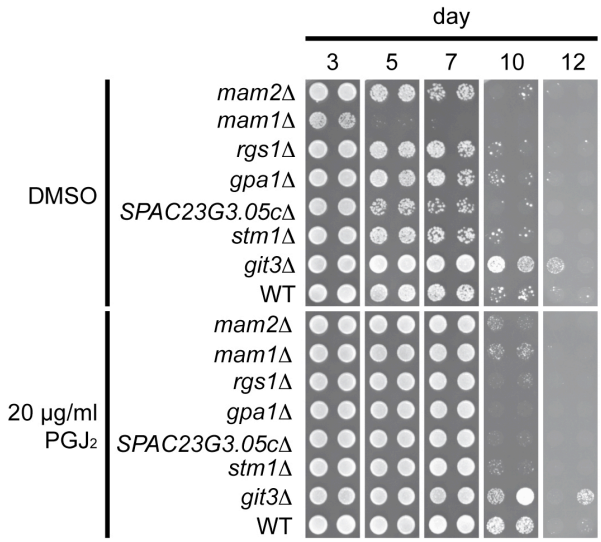

Figure 23 PGJ_2 did not enhance the CLS of *git3*Δ cells
The indicated strains originating from the *S. pombe* deletion library carry single deletions of genes encoding for G-protein coupled receptors and proteins involved in G-protein signalling. These cells as well as the corresponding wild-type cells (AEP57) were grown in YM medium containing 3 % glucose and 20 µg/ml prostaglandin J_2 (PGJ_2) or DMSO. At the indicated time points, all cultures were spotted on YES plats that were subsequently incubated at 30 °C for two days.

3.1.2.4.2 CLS of strains carrying deletions of V-ATPase subunits was not increased by monensin and nigericin

Monensin and nigericin are both naturally occurring polyethers that exhibit a similar structure (Figure 24A, B) and display a significant preference to form complexes with monovalent cations, for instance sodium. Furthermore, they have been described as Golgi-disturbing agents (Dinter & Berger, 1998). However, their precise mode of action at the level of Golgi membranes is still unknown. Nevertheless, if their impact on the Golgi apparatus leads to the lifespan extension, other Golgi-disturbing agents should have the same effect. To test this hypothesis, *S. pombe* wild-type cells

(AEP57) were treated with brefeldin A (Figure 24C), and the tested concentrations were identical to those used for monensin and nigericin. However, CLS was not affected by the brefeldin A-treatment (Figure 25), indicating that the life-extending effect of monensin and nigericin is probably not due to their Golgi-disturbing function.

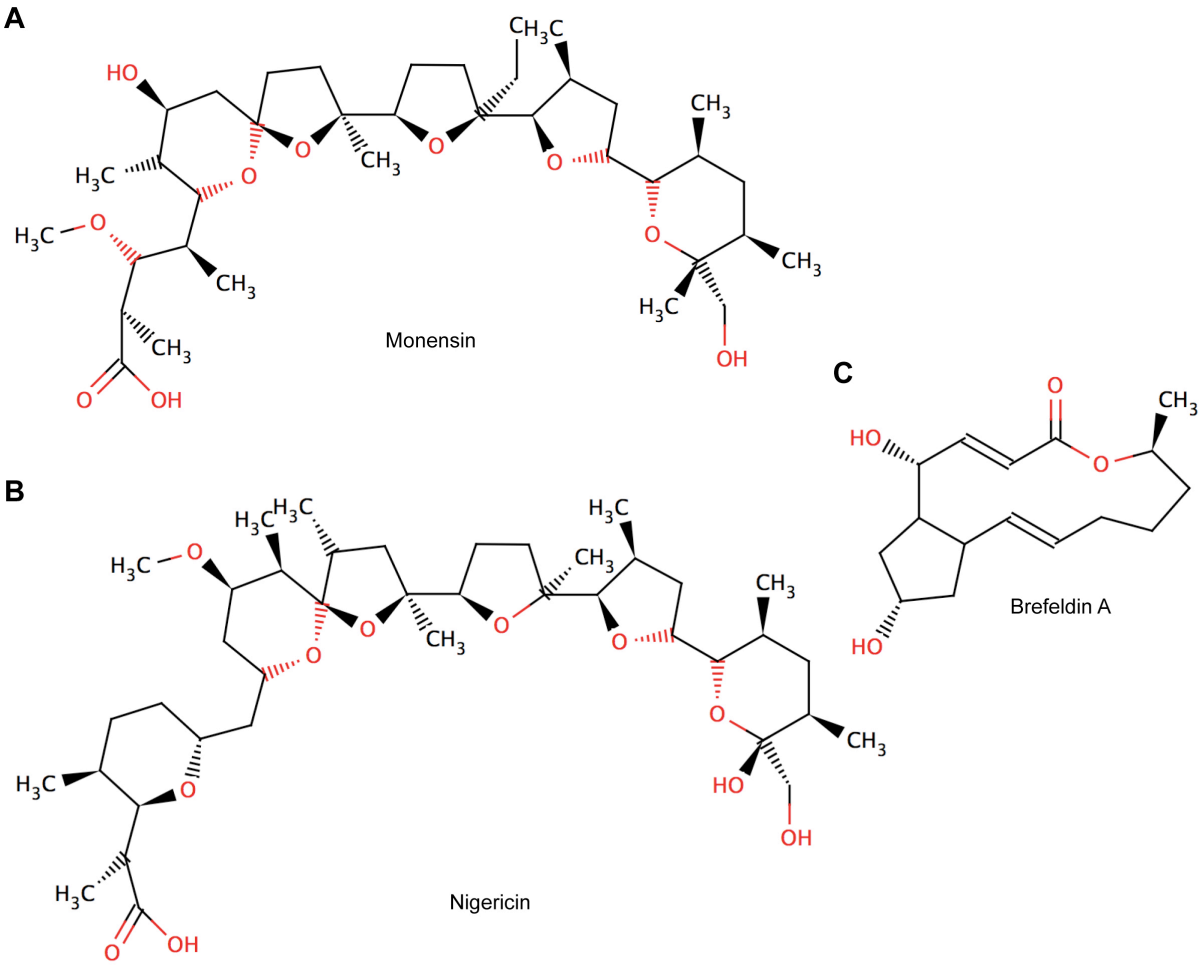

Figure 24 Chemical structures of monensin, nigericin, and brefeldin A
The chemical structures were created by using the software MarvinSketch.

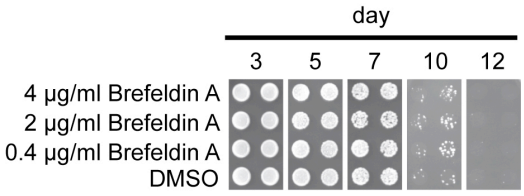

Figure 25 Brefeldin A had no impact on CLS
S. pombe wild-type cells (AEP57) were grown in YM medium containing 3 % glucose and the indicated concentrations of the Golgi-disturbing agent brefeldin A. DMSO served as control. At regular intervals, the cultures were spotted on YES plates that were subsequently incubated at 30 °C for two days.

It is known for *S. cerevisae* that this yeast produces acetic acid, which in turn has been reported to be the primary molecular factor limiting the lifespan of yeast cells under these standard conditions (Burtner *et al.*, 2009). Since monensin and nigericin are both ionophores that are incorporated into biological membranes (Liu, 1982), it was possible that this function of the compounds is the cause not only for their known antibiotic properties but also for their effect on CLS. To test this theory, wild-type cells (AEP57) were grown in the presence of these compounds, and the pH-value of the medium was subsequently determined at regular intervals. Simultaneously, the OD of the culture was measured, and the resulting values were used for normalization in order to exclude the possibility that differences of the pH-value are caused by altered maximal growth. As shown in Figure 26 (right), the extracellular pH-value was not changed by monensin and nigericin, suggesting that they did not act as ionophores in the plasma membrane. This has already been reported for *S. cerevisiae*, where they selectively act on the mitochondrial inner membrane (Kovac *et al.*, 1982).

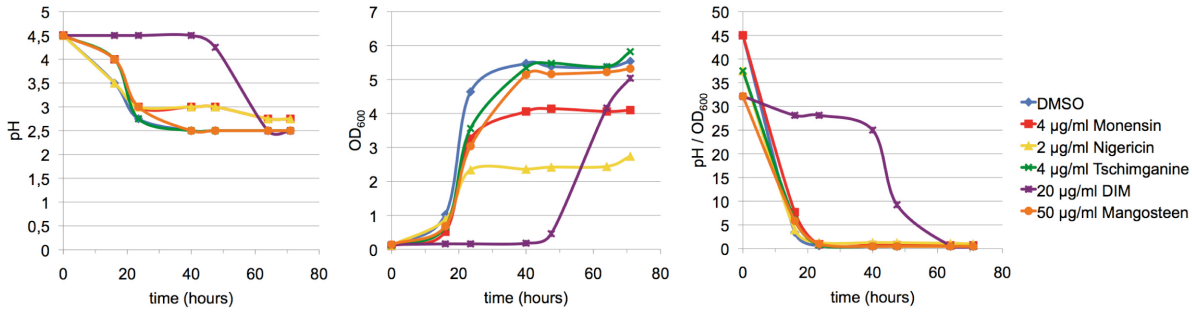

Figure 26 Compounds did not affect the extracellular pH-value
S. pombe wild-type cells (AEP57) were grown in YM medium containing 3 % glucose and the indicated compounds. At regular interval, the pH-value was determined by spotting aliquots on pH indicator sticks that detect changes of the pH-value in 0.5 steps (left). In parallel, the optical density at 600 nm (OD_{600}) was measured (middle). The resulting pH-values were normalized by using the corresponding OD_{600} value (right).

Significantly, while the pH-value of the medium dropped from 4.5 to 2.3 – 3 in the initial 20 hours for four of the five compounds, the pH-value of the medium of cells DIM-treated did not change during the initial 40 hours, but only decreased at a later time point (Figure 26 left). This was in line with the observation that the corresponding cells started growing after 40 hours (Figure 26 middle), confirming that the changes of the pH-value depend on the optical density of the culture. However, neither DIM nor mangosteen or tschimganine significantly slowed the acidification of the medium.

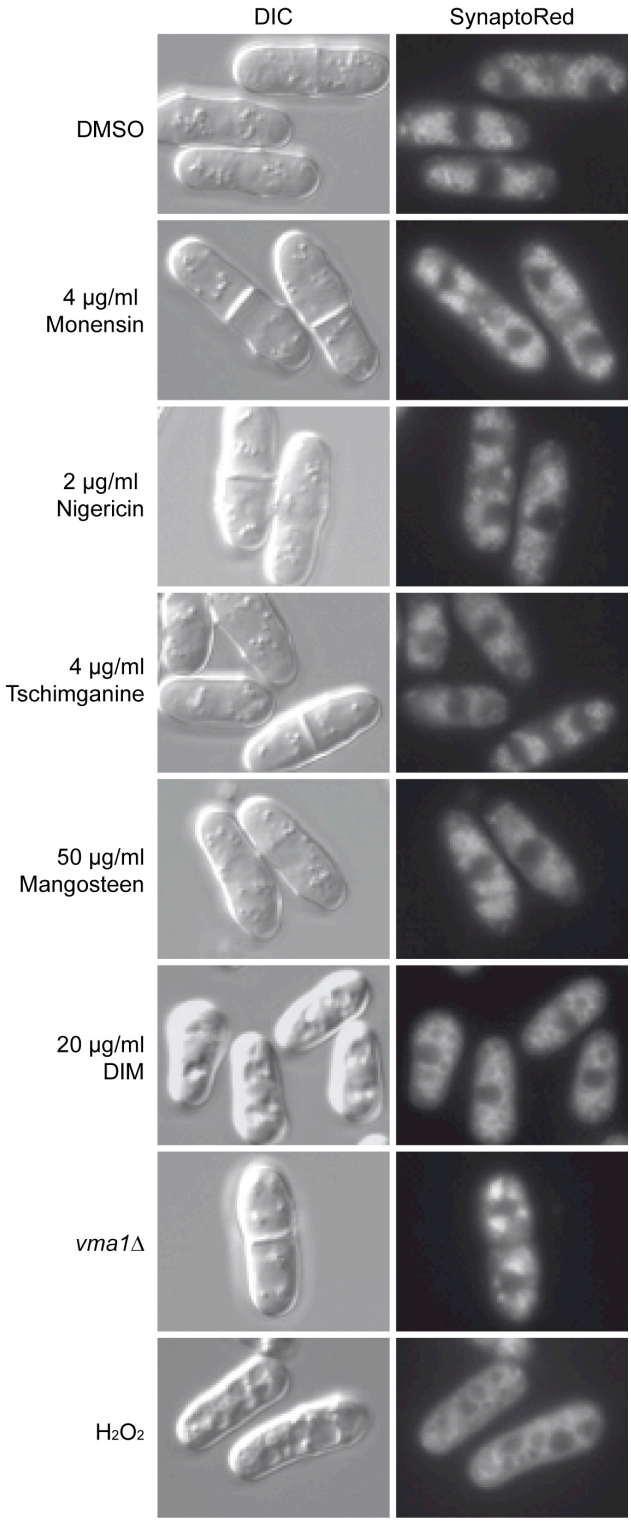

Figure 27 The analyzed compounds did not disrupt endocytosis
S. pombe wild-type cells (AEP57) were grown in YM medium containing 3 % glucose and the indicated compounds. The cells were harvested during exponential growth and stained with 80 µM SynaptoRed. Wild-type cells treated with 150 mM hydrogen peroxide (H_2O_2) for one hour after the staining or with DMSO as well as *vma1*Δ cells (AEP68) served as control. All samples were analyzed using a fluorescence microscope.

Monensin and nigericin are not only Ionophores, but also act as Na^+/H^+- respectively K^+/H^+-antiporters (Liu, 1982). As a consequence, they affect the

membrane potential and several processes that depend on the ionic gradient. One enzyme whose activity is linked to the ionic gradient is the vacuolar adenosine triphosphatase (V-ATPase), which consists of various subunits. The deletion of two of these subunits has previously been shown to affect the acidification of intracellular compartments and to disrupt endocytosis (Iwaki *et al.*, 2004). To determine whether monensin and nigericin led to a similar effect, the vacuolar membranes of *S. pombe* wild-type cells treated with these two compounds as well as with DIM, tschimganine, and mangosteen were stained with SynaptoRed, a dye that becomes fluorescent when incorporated into the plasma membrane. The DMSO-treated control cells were filled with several small vacuoles, and the nucleus was “visible” as a non-fluorescent structure in the middle of the cell (Figure 27). In contrast, *vma1*Δ cells (AEP68) displayed an accumulation of the fluorescent dye at structures that are supposed to be pre-vacuolar compartments (Iwaki *et al.*, 2004) (Figure 27). Notably, the cells treated with the compounds exhibited no defects in endocytosis as observed for *vma1*Δ cells but rather looked like the control cells (Figure 27). These results indicate that the compounds did affect lifespan by disrupting endocytosis.

Nevertheless, the vacuoles of the cells treated with DIM appeared to be slightly enlarged compared to those of the cells treated with the other compounds (Figure 27). Another result that was previously shown to be distinct for DIM-treated cells, was the significantly increased ROS level during exponential growth (Figure 19. Notably, it was already known that (osmotic) stress results in vacuolar fusion, thereby leading to less but enlarged vacuoles in *S. pombe* (Takegawa *et al.*, 2003). To determine whether there was a relationship between the slightly enlarged vacuoles and the increased ROS level, DMSO-treated cells were stained with SynaptoRed and subsequently treated with 150 mM H_2O_2 for one hour to induce the formation of ROS. As a result, the vacuoles of these cells were even more enlarged compared to those of DIM-treated cells (Figure 27 bottom), maybe due to higher amounts of ROS. This led to the suggestion that the increased ROS level during exponential growth by DIM treatment might be the cause for the slightly enlarged vacuoles of the DIM-treated cells. Furthermore, these results showed that treatment with the remaining compounds did not stress the cells.

As the deletion of Vma1 and Vma3 has previously been shown to affect the acidification (Iwaki *et al.*, 2004), the acidic compartments were analyzed in the next step. For this purpose, wild-type cells (AEP57) treated with the compounds were

harvested during the exponential growth phase and stained with quinacrine, which is a weakly basic dye that accumulates in acidic compartments in response to proton gradients. In general, acidic compartments display a special kind of vacuoles, the equivalent to mammalian lysosomes. At first glance, no reduction of the staining, like it was the case for *vma3*Δ, was observed (Figure 28A). In all samples, there are a few cells that were completely stained, probably representing dead cells.

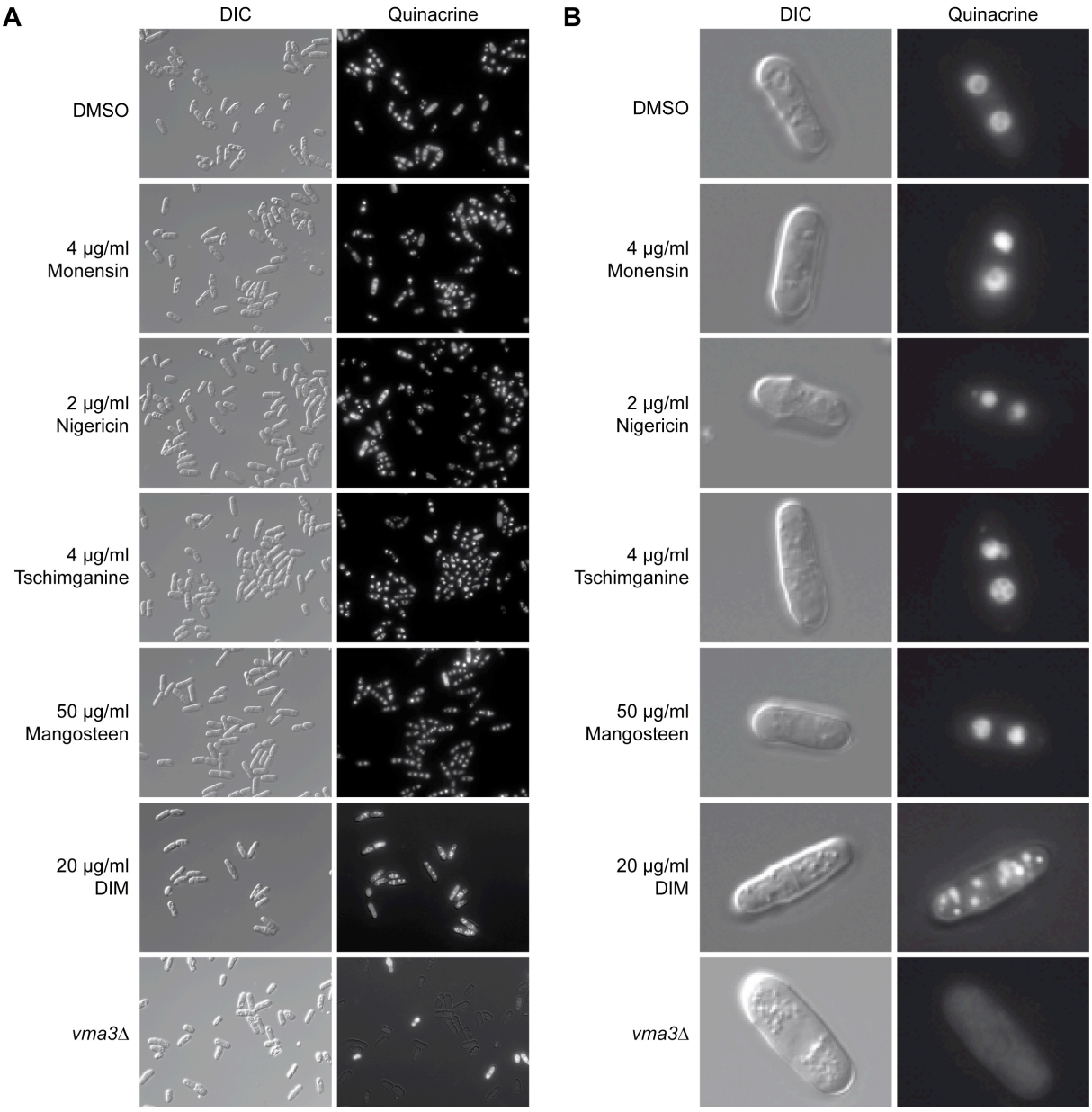

Figure 28 Impact on the acidification of intracellular compartments
S. pombe wild-type cells (AEP57) were grown in YM medium containing 3 % glucose and the indicated compounds. *vma3*Δ cells (AEP69) served as control. The cells were harvested during exponential growth and stained with 200 µM quinacrine. Subsequently, the samples were analyzed using a fluorescence microscope.

However, at higher magnification, it became obvious that cells treated with DIM differed from the other compound-treated cells. Instead of a few (mostly two) distinct compartments, several smaller compartments were visible (Figure 28B). To determine whether this effect was also a consequence of the increased ROS level in the exponential growth phase of DIM-treated cells, this experiment was repeated. This time, an aliquot of the DMSO-treated wild-type cells was incubated with 150 mM H_2O_2 for one hour before the staining. For unknown reasons, the DMSO- and DIM-treated cells look different in comparison with Figure 28, even if the general tendency meaning more and smaller compartments in the DIM-treated cells was similar (Figure 29). However, those cells that were additionally incubated with H_2O_2 were uniformly stained. As the treatment with H_2O_2 led to an enhanced effect compared to DIM in the endocytosis experiment (Figure 27), this might also be the case for the acidic compartments. As a consequence, the whole-cell-staining could be due to a strong fragmentation of the acidic compartments leading to tiny, undistinguishable structures. This could be tested by repeating this experiment with lower H_2O_2 concentrations that should lead to a weaker phenotype.

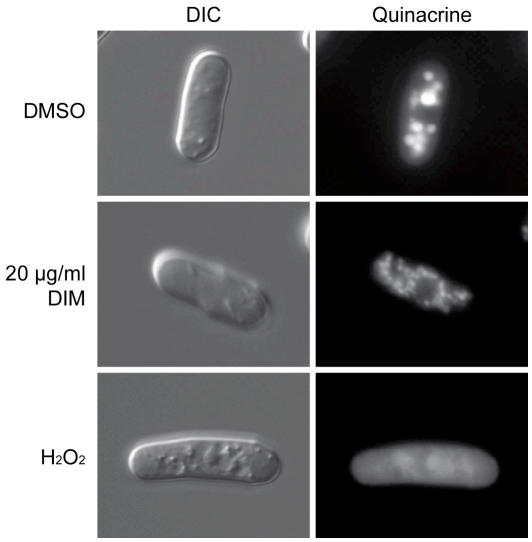

Figure 29 Effect of DIM on intracellular compartments did not depend on increased ROS levels
S. pombe wild-type cells (AEP57) were grown in YM medium containing 3 % glucose and 20 µg/ml DIM or DMSO The cells were harvested during exponential growth and stained with 200 µM quinacrine. An aliquot of the DMSO-treated cells was incubated for one hour at 30 °C with 150 mM hydrogen peroxide (H_2O_2) before the staining. Subsequently, the samples were analyzed using a fluorescence microscope

In summary, the results of the fluorescence stainings suggested that none of the tested compounds inhibited the V-ATPase. Furthermore, altered endocytosis by treatment with DIM seemed to be an effect of increased ROS levels while the reason

for the fragmentation of the acidic compartments in DIM-treated cells remained unclear. Notably, there seemed to be no direct relationship between the acidic compartments and the vacuoles as their size and number per size differed (Figure 27 - 29) (Iwaki *et al.*, 2004).

We next hypothesized that the potential disturbance of the ionic gradient by monensin and nigericin might activate the V-ATPase and right thereby lead to lifespan extension. Therefore, we analyzed the CLS of *vma1*Δ (AEP68) and *vma3*Δ cells (AEP69). When only treated with DMSO, these cells displayed a reduced lifespan (Figure 30). Furthermore, treatment with monensin or nigericin did not increase their lifespan (Figure 30), suggesting that monensin or nigericin might extend lifespan by an activation of the V-ATPase.

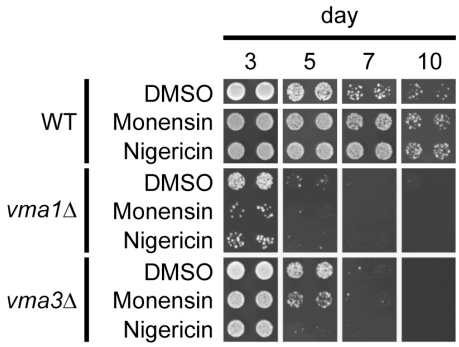

Figure 30 Deletion of V-ATPase subunits led to a reduced lifespan, which could not be extended by monensin or nigericin
S. pombe wild-type cells (AEP57) as well as *vma1*Δ (AEP68) and *vma3*Δ cells (AEP69) were grown in YM medium containing 3 % glucose and 4 µg/ml monensin or 2 µg/ml nigericin. DMSO served as control. At the indicated time points, the aging cultures were spotted on YES plates that were incubated at 30 °C for two days.

3.1.2.4.3 The lifespan-extending effect of mycophenolic acid and acivicin was not affected by guanine or glutamine

MPA and acivicin are known to inhibit the inosine monophosphate (IMP) dehydrogenase (Ransom, 1995) and the guanosine monophosphate (GMP) synthetase (Nakamura *et al.*, 1995) respectively, the two enzymes involved in the conversion of IMP to GMP and thereby in the *de novo* biosynthesis of guanine nucleotides. Based on this, we hypothesised that these two compounds extended CLS by depleting nucleotide levels. Notably, an agent that is known to inhibit the same enzyme as MPA is 6-azauracil (6-AU) (Exinger & Lacroute, 1992). Thus, 6-AU might be expected to increase lifespan. To test this, we used the same concentrations of 6-AU as for the initial experiments with MPA and acivicin

(0.4/2/4/20 µg/ml) as well as concentrations that were used in other studies (75/100/150 µg/ml). We analyzed its impact on normal wild-type cells (AEP57) and also on wild-type cells carrying an *ura4*$^+$-marked plasmid (AEP57 + pAE1429) in YM medium containing 1 %, 3 % or 5 % glucose. However, the CLS was not altered under any of the tested conditions (Figure 31, data not shown), suggesting that MPA and acivicin might act different from 6-AU to extend lifespan.

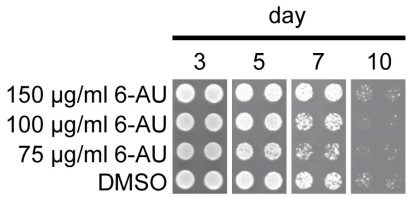

Figure 31 CLS was not altered by 6-AU
S. pombe wild-type cells (AEP57) were grown in YM medium containing 3 % glucose and the indicated concentrations of 6-azauracil (6-AU). DMSO served as control. At regular intervals the cultures were spotted on YES plates that were subsequently incubated at 30 °C for two days.

The next logical step would be to determine the CLS of cells where the IMP dehydrogenase is deleted. In fission yeast, this enzyme is predicted to be encoded by the gene *gua1*$^+$ whose deletion is lethal and therefore could not be analyzed here.

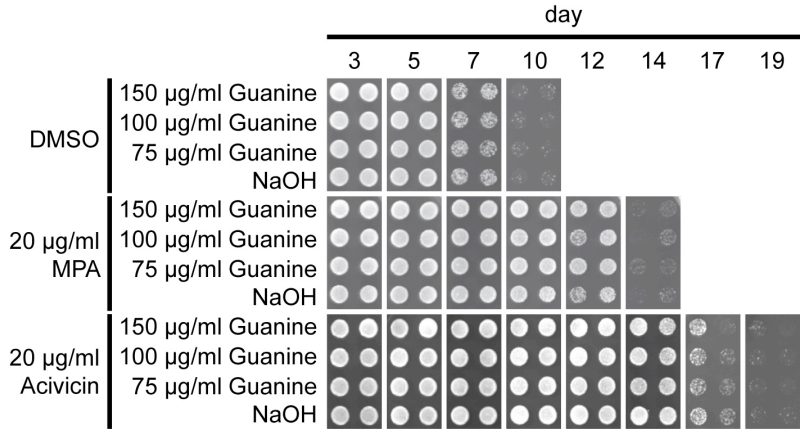

Figure 32 Guanine did not affect lifespan of *S. pombe*
The indicated concentrations of guanine were added to YM medium containing 3 % glucose and 20 µg/ml mycophenolic acid (MPA) or acivicin. As a solvent control for guanine, NaOH was added, while DMSO served as control for MPA and acivicin. All the resulting media were used for cultures of *S. pombe* wild-type cells (AEP57). At the indicated time points, these cultures were spotted onto YES plates that were incubated at 30 °C for two days.

According to our hypothesis, the addition of guanine to the growth medium should increase the guanidine level, and as this is the opposite effect of MPA and acivicin, it should result in reduced CLS and abolish the lifespan-extension caused by MPA or acivicin. To test this, the effect of six guanine concentrations ranging from 75 µg/ml

up to 300 µg/ml was analyzed. None of them changed the lifespan of wild-type cells (AEP57) treated either with DMSO (control), MPA or acivicin (Figure 32, data not shown). Both MPA and acivicin still increased lifespan under these circumstances.

The GMP synthetase, which is inhibited by acivicin, catalyzes the amination of the intermediate xanthosine monophosphate (XMP) to GMP. This ATP-dependent reaction also requires glutamine, which is converted to glutamate. This led to the suggestion that low amounts of glutamine should extend lifespan, while higher concentrations should have the opposite effect. Based on this hypothesis, *S. pombe* wild-type cells (AEP57) were grown in YM medium containing 3 % glucose and 3.75 g/l or 1 g/l glutamine. Notably, the lower concentration did not change the CLS compared to medium without glutamine, while the higher concentration increased lifespan (Figure 33). This result was not only contrary to our hypothesis above, but also to previous studies that reported that reduced levels of glutamine as an activator of the TOR signalling pathway extended both CLS and RLS in *S. cerevisiae* (Kaeberlein *et al.*, 2005b; Powers *et al.*, 2006). Nevertheless, MPA and acivicin increased lifespan compared to DMSO in medium containing no, low or high amounts of glutamine (Figure 33). In summary, these results indicate that the life-extending effect of MPA and acivicin was independent of the GMP biosynthesis.

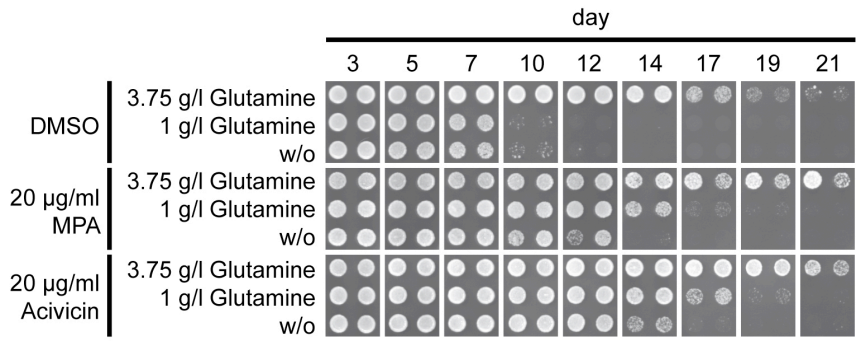

Figure 33 MPA and acivicin increased CLS independently of the glutamine concentration
S. pombe wild-type cells (AEP57) were grown in YM medium containing 3 % glucose, the indicated concentrations of glutamine and 20 µg/ml mycophenolic acid (MPA) or acivicin. DMSO served as control. At the indicated time points, the cultures were spotted onto YES plates that were incubated at 30 °C for two days.

3.1.3 Identification of genes that affect the lifespan of *S. pombe*

3.1.3.1 Screen for gene deletions that increase the CLS of *S. pombe*

The fission yeast genome contains about 5,000 protein-coding genes, which is the smallest number among the commonly used eukaryotic model organisms (Wood *et al.*, 2002). Comparative genomic analysis showed that around 500 fission yeast genes have no homologs in budding yeast, but are conserved in other eukaryotic species, including human, apparently due to lineage-specific gene losses that happened during the evolution of *S. cerevisiae* (Wood, 2006). However, compared to *S. cerevisiae,* less is known about the mechanisms that alter lifespan of *S. pombe*. Since it is known that lifespan is regulated by many evolutionarily conserved factors in a complex manner, the identification of novel genetic factors that affect the CLS of fission yeast might help as to understand lifespan regulation not only in fission yeast, but also in higher eukaryotes.

In this approach, we sought to identify novel genetic factors whose deletion extended the CLS of *S. pombe*. For this purpose, we screened a *S. pombe* deletion library (Bioneer) that contains 3,004 haploid strains carrying single deletions of non-essential genes by using the new microplate CLS method (see 3.1.1) for strains with increased CLS. This experiment was performed as previously described for the compounds in 3.1.2.1.

From this screen, we obtained 291 primary candidates that extended lifespan (Table 13).

Table 13 Primary candidates of gene deletions that increased CLS

Systematic Name	Systematic Name	Systematic Name	Systematic Name	Systematic Name
SPAC1002.05c	SPAC23G3.03	SPAC824.02	SPBC19F8.03c	SPBC947.08c
SPAC1002.07c	SPAC23G3.12c	SPAC869.11	SPBC19G7.17	SPBC947.15c
SPAC105.03c	SPAC23H3.15c	SPAC890.05	SPBC1A4.04	SPBP16F5.03c
SPAC1071.11	SPAC24B11.09	SPAC926.02	SPBC20F10.07	SPBP16F5.07
SPAC11D3.16c	SPAC24B11.12c	SPAC926.03	SPBC211.06	SPBP35G2.07
SPAC11E3.01c	SPAC24C9.12c	SPAC977.17	SPBC215.05	SPBP35G2.13c
SPAC11E3.05	SPAC25H1.07	SPAC9G1.02	SPBC215.06c	SPBP8B7.28c
SPAC11E3.08c	SPAC26A3.16	SPAC9G1.04	SPBC215.13	SPBPB2B2.11
SPAC12B10.13	SPAC26F1.05	SPACUNK4.16c	SPBC216.01c	SPBPB2B2.14c
SPAC12B10.16c	SPAC27D7.06	SPAP27G11.10c	SPBC21B10.03c	SPCC1020.11c
SPAC139.06	SPAC27F1.05c	SPAP7G5.04c	SPBC21B10.10	SPCC1235.09

SPAC13C5.04	SPAC29A4.19c	SPAPB1E7.02c	SPBC23E6.08	SPCC1235.11
SPAC144.06	SPAC29B12.03	SPAPB24D3.09c	SPBC24C6.05	SPCC1235.15
SPAC14C4.07	SPAC29B12.04	SPAPB2B4.07	SPBC25B2.03	SPCC1259.03
SPAC14C4.09	SPAC2E1P3.01	SPAPJ695.01c	SPBC25D12.06	SPCC1259.10
SPAC14C4.11	SPAC2F3.11	SPAPYUG7.03c	SPBC25H2.16c	SPCC126.08c
SPAC1556.04c	SPAC2F3.16	SPBC106.17c	SPBC27B12.11c	SPCC126.13c
SPAC1565.07c	SPAC2F7.17	SPBC1105.02c	SPBC29A3.07c	SPCC1322.16
SPAC15F9.01c	SPAC30D11.07	SPBC1105.13c	SPBC29A3.14c	SPCC1393.13
SPAC16.04	SPAC323.01c	SPBC119.05c	SPBC2D10.12	SPCC13B11.02c
SPAC1610.01	SPAC32A11.02c	SPBC1198.06c	SPBC2G2.05	SPCC1442.05c
SPAC167.01	SPAC343.16	SPBC1198.08	SPBC2G2.07c	SPCC162.01c
SPAC1687.23c	SPAC3A11.03	SPBC1198.12	SPBC2G2.08	SPCC1620.02
SPAC16C9.02c	SPAC3A11.03	SPBC11B10.07c	SPBC2G5.02c	SPCC1682.15
SPAC16E8.05c	SPAC3A12.13c	SPBC1271.10c	SPBC30D10.03c	SPCC1682.16
SPAC16E8.18	SPAC3C7.06c	SPBC1271.15c	SPBC30D10.04	SPCC16A11.07
SPAC1782.11	SPAC3F10.04	SPBC146.06c	SPBC32F12.02	SPCC16C4.04
SPAC1783.01	SPAC3G6.01	SPBC146.10	SPBC336.10c	SPCC16C4.10
SPAC1783.02c	SPAC3G6.02	SPBC14C8.15	SPBC342.01c	SPCC16C4.11
SPAC1783.07c	SPAC3G6.06c	SPBC14F5.07	SPBC359.06	SPCC1739.06c
SPAC17A5.16	SPAC3G9.07c	SPBC1539.06	SPBC365.16	SPCC1739.15
SPAC17C9.02c	SPAC3G9.08	SPBC15C4.01c	SPBC36B7.03	SPCC18.15
SPAC17G8.11c	SPAC3H8.08c	SPBC15C4.04c	SPBC3B8.03	SPCC1840.05c
SPAC17H9.04c	SPAC4A8.09c	SPBC15D4.02	SPBC3B8.04c	SPCC1884.02
SPAC17H9.06c	SPAC4F10.14c	SPBC1685.01	SPBC3B8.06	SPCC18B5.01c
SPAC17H9.08	SPAC4F10.18	SPBC1685.06	SPBC3E7.08c	SPCC24B10.08c
SPAC17H9.13c	SPAC4F10.20	SPBC1685.10	SPBC3E7.10	SPCC24B10.22
SPAC1851.03	SPAC4G8.10	SPBC1685.13	SPBC3E7.12c	SPCC285.16c
SPAC18B11.04	SPAC4G9.09c	SPBC16D10.08c	SPBC3H7.14	SPCC297.05
SPAC1952.17c	SPAC4G9.10	SPBC16G5.15c	SPBC409.07c	SPCC364.03
SPAC19A8.03	SPAC4G9.14	SPBC16H5.04	SPBC4C3.08	SPCC4F11.03c
SPAC19A8.11c	SPAC4H3.07c	SPBC1709.05	SPBC4F6.08c	SPCC4G3.04c
SPAC19G12.02c	SPAC513.03	SPBC1709.06	SPBC4F6.11c	SPCC553.01c
SPAC1A6.01c	SPAC589.02c	SPBC1711.03	SPBC557.05	SPCC622.08c
SPAC1B1.02c	SPAC5H10.06c	SPBC1711.15c	SPBC577.06c	SPCC622.12c
SPAC1B3.04c	SPAC631.02	SPBC1718.02	SPBC609.04	SPCC622.14
SPAC1B3.17	SPAC637.09	SPBC1718.07c	SPBC660.05	SPCC70.06
SPAC1D4.05c	SPAC644.08	SPBC1734.06	SPBC660.11	SPCC74.05
SPAC1F7.08	SPAC644.09	SPBC1773.01	SPBC725.01	SPCC74.06
SPAC20G8.02	SPAC664.03	SPBC1773.12	SPBC725.14	SPCC757.09c
SPAC20G8.04c	SPAC6B12.16	SPBC1778.02	SPBC776.11	SPCC777.07

SPAC21E11.03c	SPAC6C3.07	SPBC17A3.08	SPBC800.02	SPCC777.10c
SPAC21E11.05c	SPAC6F12.06	SPBC17D1.02	SPBC800.03	SPCC790.03
SPAC227.11c	SPAC6F12.10c	SPBC17D11.01	SPBC839.04	SPCC794.02
SPAC227.15	SPAC6F12.12	SPBC17D11.03c	SPBC887.04c	SPCC794.07
SPAC22A12.16	SPAC6F6.09	SPBC17G9.10	SPBC887.11	SPCC794.15
SPAC22E12.18	SPAC6G10.02c	SPBC18E5.10	SPBC887.15c	SPCC965.08c
SPAC22F3.09c	SPAC821.03c	SPBC19C7.01	SPBC902.04	SPCC970.05
SPAC23D3.13c				

For validation, the primary candidates were re-tested in biological triplicates. The screening results could be reproduced for 87 gene deletions. To obtain an overview about the processes that were affected by these deletions and thus might play a role in the regulation of CLS, the secondary candidates were grouped based on their potential function, and the resulting groups were sorted depending on the average strength of their effect in the validation experiment (Table 14).

Table 14 Secondary candidates of gene deletion strains that exhibited increased CLS grouped based on the potential function of the coded protein

group	systematic name	gene name	strength of effect[a]
nutrition	SPCC16C4.11	pef1	+
	SPBC106.10	pka1	+++
	SPAC4G9.09c	arg11	++++
	SPBC725.14	arg6	++++
	SPAC343.16	lys2	++++
	SPBC4F6.11c		++++
	SPCC622.12c	gdh1	++++
	SPAP7G5.04c	lys1	++++
	SPAC24C9.12c		+++
	SPBC1105.02c	lys4	++++
	SPAC4G9.10	arg3	++++
	SPAC17C9.02c	lys7	++++
	SPAC23G3.03	sib2	+++
ER, Golgi	SPAC3G6.02	dss1	+++
	SPBC14F5.07	ssm4	+++
	SPAC824.02		++++
	SPBC23E6.08	sat1	++++
	SPBC4C3.08	mug136	++
	SPAC4G8.10	gos1	++

	SPAC24B11.12c		++++
	SPBC11B10.07c	ivn1	+++
ER, Golgi	SPBC1198.06c		+++
	SPBC342.01c	alg6	+++
	SPCC126.08c		+++
	SPAC19A8.11c	irc1	+++
	SPCC285.16c	msh6	++
	SPAC19G12.02c	pms1	+++
DNA repair	SPBC3E7.08c	rad13	+++
	SPAC3G6.06c	rad2	+++
	SPAC30D11.07	nth1	++++
	SPBC216.01c		++
	SPAC167.01	ppk4 / ire1	++++
	SPAC25H1.07		+
UPR^{ER}	SPCC1020.11c		+
	SPBC1711.03		++
	SPBC15C4.01c	oca3	+++
	SPBC16D10.08c	hsp104	++++
apoptosis	SPBC20F10.07		+++
	SPBC660.05		++
	SPCC297.05		+++
	SPBC359.06	mug14	+++
	SPCC74.06	mak3	++
	SPAC977.17		+
	SPAP27G11.10c	nup184	+++
	SPBC3E7.12c	chr1	+
	SPCC553.01c		+++
	SPBC211.06	gfh1	+++
mixed, unkown	SPAC6F12.06		++
	SPBC609.04	caf5	++++
	SPAC18B11.04	ncs1	+++
	SPBPB2B2.14c		++
	SPBC1105.13c		+++
	SPAC6C3.07	mug68	++
	SPAC513.03	mfm2	+
	SPAC6B12.16	meu26	++
	SPAC644.08		+++

	SPAC1F7.08	fio1	+++
iron homeostasis	SPCC1884.02	nic1	++
	SPBC1718.07c	zfs1	++
	SPAC4G9.14		+++
	SPBC947.15c		++
mitochondria	SPAC17H9.08		++++
	SPCC794.07	lat1	+
	SPAC4F10.20	grx1	+
	SPAC6F6.09	eaf6	+
	SPBP16F5.03c	tra1	++
	SPAC139.06	hat1	+++
	SPAC3G9.07c	hos2	++
	SPCC622.08c	hta1	+
transcription	SPBC947.08c		++
	SPAC631.02		+++
	SPBC1773.12		+
	SPAC1A6.01c		+++
	SPBC25B2.03		++
	SPAC29B12.03	spd1	+++
	SPBC2G2.05	rpl1603	++
	SPBC21B10.10	rps402	+
ribosome	SPBC839.04	rpl803	+
	SPCC70.06		++
	SPBC660.11	tcg1	++++
vacuole	SPAC1783.02c	vps66	++
	SPAC144.06	apl5	++
	SPBC336.10c	tif512	+
	SPAC3A12.13c		+++
RNA, translation	SPBC21B10.03c		+
	SPBC1685.06	cid11	+++
	SPBC19C7.01		+

[a] + slight increase, ++ moderate increase, +++ strong increase, ++++ very strong increase of CLS

In agreement with previous work, we found 13 strains with deletions in genes altering nutrient uptake and sensing to extend lifespan (Table 14), which was consistent with the notion that these mutants impart some kind of CR upon the cells. Furthermore, several strains carrying deletions of genes that code for ribosomal proteins or proteins involved in transcription or translation also displayed an

increased lifespan. This might be a secondary effect, as these deletions probably affect the expression of various genes, which in turn could also have an impact on lifespan. Significantly, strains with deletions of genes encoding for proteins that are involved in the repair of single-stranded DNA damage also improved CLS (Table 14). These results were surprising, because one might expect that defects in DNA repair would result in premature aging rather than in lifespan extension. To uncover how these gene deletions promote longevity, we decided to further analyze the effects of this group. Notably, later experiments showed that the lifespan extension of the analyzed deletion strains is rather an effect of the strain background than of the gene deletions themselves (see 3.1.3.6). As a consequence, other groups of genes affecting CLS (Table 14) were not pursued.

However, we wanted to verify the improvement of CLS at first. For this purpose, the secondary candidates of the DNA repair group were tested several times by using the new method. Another gene deletion (*rhp23*Δ), which displayed a strong effect in the primary screen but failed to increase lifespan in the validation screen, was additionally analyzed. An example of these experiments is shown in Figure 34. Six gene deletion strains, namely *rad2*Δ, *nth1*Δ, *rad13*Δ, *rhp23*Δ, *msh6*Δ, and *pms1*Δ, showed a reproducible lifespan extension compared to the corresponding wild-type cells (AEP57).

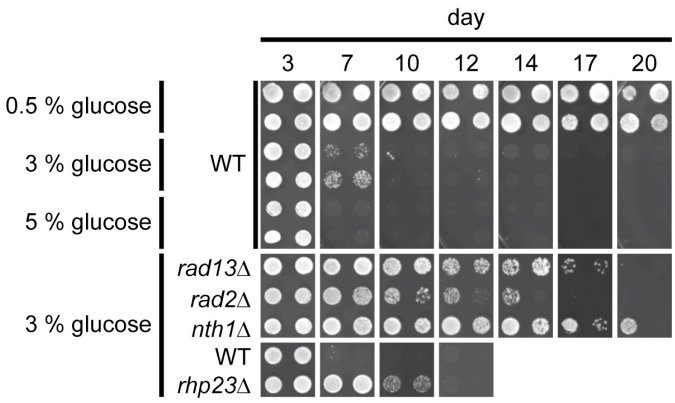

Figure 34 DNA repair mutants exhibited extended CLS
Deletion strains from the *S. pombe* deletion library (Bioneer) and the corresponding wild-type cells (AEP57) were grown in YM medium containing the indicated glucose concentrations and spotted onto YES plates at regular intervals. The plates were incubated for two days at 30 °C.

Furthermore, the CLS of four of these strains was investigated by using the traditional CFU method. To date, CR or the deletion of genes that encode for proteins involved in the nutrient sensing pathways are the most powerful tools known to promote longevity. In order to evaluate the potential lifespan-extending effect of the

candidates, *sck2*Δ cells (AEP62) and the corresponding wild-type cells (AEP61) were used for comparison because it was already published that this particular deletion strain had an increased CLS (Chen & Runge, 2009). All tested gene deletion strains extended lifespan at least as strong as the *sck2*Δ control (Figure 35), thereby verifying that they have a strong impact on the CLS of fission yeast.

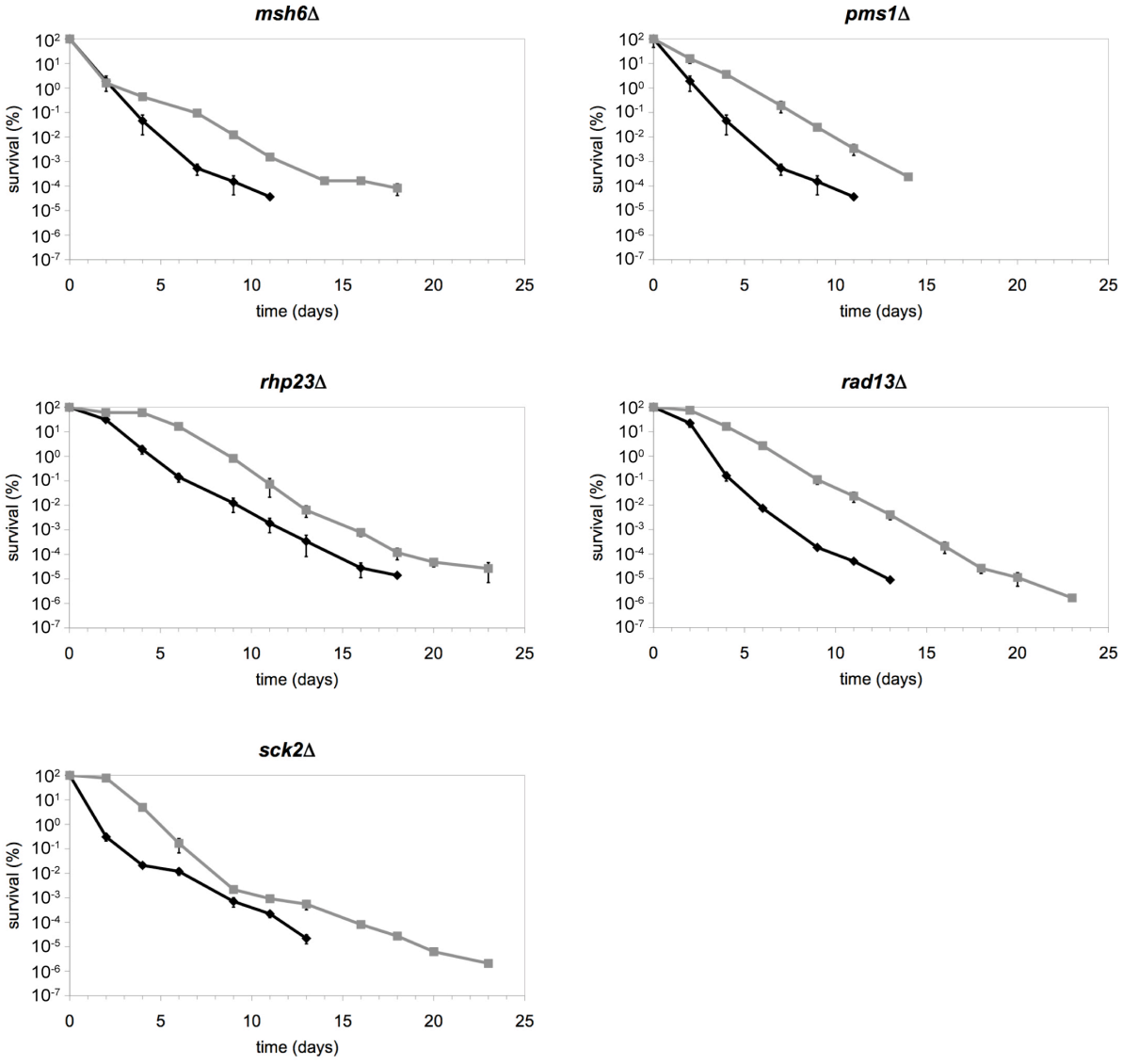

Figure 35 The tested gene deletion strains displayed an extended lifespan comparable to the *sck2*Δ cells

CLS of *S. pombe* strains from the deletion library (Bioneer) carrying single deletions of DNA repair genes (grey) and the corresponding wild-type cells (AEP57, black) were determined by using the CFU method. *sck2*Δ cells (AEP62, grey) and the corresponding wild-type strain (AEP61, black) served as positive control. All cells were tested at least one time in biological duplicate and the corresponding averages are shown in the graphs. The black bars represent the standard deviation.

3.1.3.2 General characterization of the CLS-extending DNA repair mutants

The DNA repair mutant strains found to increase lifespan in the screen affect different types of single-stranded DNA repair. Rad2 and Nth1 are part of base excision repair (BER), while Rad13 and Rhp23 belong to nucleotide excision repair (NER) (Kanamitsu & Ikeda, 2010; Wood, 1996). The third pair, Msh6 and Pms1, takes part in mismatch repair (MMR) (Marti *et al.*, 2002). Just like for the compounds, we sought to determine whether there is a correlation between the lifespan-extending effect of the identified strains and CR. Thereby, it would be interesting if there were any differences between the mutants of the three repair pathways.

We investigated the CLS of the respective strains compared to wild-type cells (AEP57) in YM medium containing the standard glucose concentration (3 %) as well as under CR and overnutrition conditions (0.5 % or 5 % glucose). Importantly, while lifespan was extended under CR conditions as expected, it was even further increased in the DNA repair deletion strains. Additionally, CLS was improved in medium containing higher glucose concentrations (5 %) in all six deletion strains (Table 15). These results suggested that the life-extending effect of the DNA repair mutant strains was independent of CR and that it was not mediated by the TOR or the Git3/PKA pathways.

Table 15 Summary of CLS improvement depending on glucose concentration

pathway	deletion	glucose concentration		
		0.5 %	3 %	5 %
BER	*rad2*Δ	+	++	(+)
	*nth1*Δ	++	+++	+
NER	*rad13*Δ	+++	+++	++
	*rhp23*Δ	++	++	++
MMR	*msh6*Δ	+++	+(+)	(+)
	*pms1*Δ	+	+++	(+)

(+) Minimal, + slight, +(+) moderate, ++ strong or +++ very strong increase of CLS

Next, we analyzed how the deletion of the DNA repair genes affected stress response. For this purpose, the resistance of these strains against heat, MMS-induced DNA damage and oxidative stress caused by menadione sodium bisulfite (MD) and H_2O_2 was tested at different concentrations (MD, H_2O_2) with diverse

incubation times (heat shock, MMS) and under changed conditions (one or two days in stationary phase). All results showed the same tendency in that the deletion strains are rather sensitive than resistant (Figure 36, data not shown). Especially *rhp23*Δ cells were highly sensitive to the analyzed stresses. *rad13*Δ, *rhp23*Δ, *rad2*Δ, and *nth1*Δ cells displayed improved sensitivity to MMS-induced DNA damage, indicating that MMS causes a type of DNA damage whose repair requires intact BER and NER pathways. In case of *nth1*Δ cells, it has already been shown that they are hypersensitive to MMS but not to H_2O_2 and menadione (Osman *et al.*, 2003).

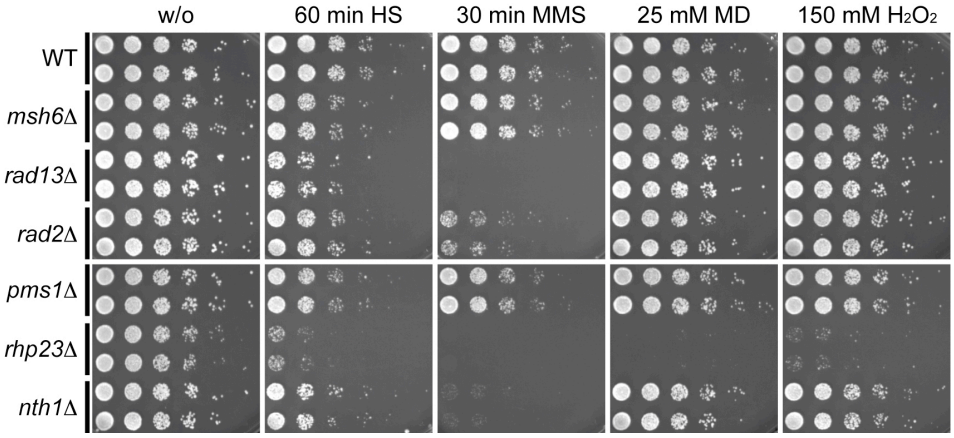

Figure 36 Analysis of stress resistance of DNA repair mutants
S. pombe wild-type cells (AEP57) and the indicated deletion strains were grown in YM medium containing 3 % glucose for one day. The cultures were adjusted to an OD_{600} of 0.5. Aliquots were treated with 25 mM menadione sodium bisulfite (MD) and 150 mM hydrogen peroxide (H_2O_2) for one hour at 30°C or with 0.2 % methyl methanesulfonate (MMS) for 30 minutes at 30 °C. Another sample was incubated for one hour at 48 °C (HS). Subsequently, the cells were six-fold serially diluted and spotted onto full medium plates that were incubated at 30 °C for two days.

3.1.3.3 Lifespan-extension was not due to altered auxotrophies or hormetic doses of DNA damage

Defects in DNA repair result in an elevated rate of spontaneous mutations (Fleck *et al.*, 1999; Li, 2008; Wood, 1996). It was therefore possible that the increased CLS of strains with deletions in DNA repair genes was due to mutations arising in genes involved in nutrient uptake and sensing. To test this hypothesis, we investigated 121 old yeast cells taken from the CFU experiments shown in Figure 35 for additional acquired auxotrophies. None of them exhibited altered auxotrophies (Figure 37), arguing that increased CLS was not due to secondary mutations in nutritional genes related to CR. This conclusion was supported by the fact that not all deletions causing increased mutation rates resulted in lifespan extension (see below).

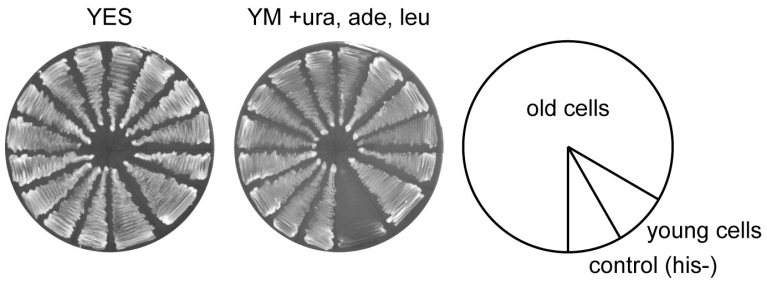

Figure 37 Auxotrophies were not altered in old DNA repair mutant cells
Old cells of the *S. pombe* strains carrying deletions of DNA repair genes were taken at the end of the CFU experiments (Figure 35) and streaked on YM plates supplemented with uracil, adenine, and leucine and on YES plates. The plates were incubated at 30 °C for two days.

In general, defects in DNA repair have been associated with premature aging (see 1.5). Therefore, finding DNA repair deletion strains to exhibit extended CLS seemed to be a paradox. However, one possible explanation is that lifespan extension in the absence of selected DNA repair proteins might be due to a hormetic effect. The term hormesis describes the phenomenon that low doses of harmful or toxic compounds may have a positive effect, whereas they inhibit at moderate and kill at high concentrations (Mattson, 2008; Schumacher *et al.*, 2008; Schumacher, 2009). It is assumed that low doses of toxins, or in this case low levels of DNA damage, might activate repair mechanisms and thus cause increased resistance. To test this, we used the DNA-alkylating agent MMS to determine whether lifespan was increased due to a hormetic effect. MMS causes a wide variety of DNA base damage whose repair o requires intact BER and NER pathways (see 3.1.3.2). We tested the influence of 14 different MMS concentrations between 0.0025 % and 0.00001 % on the CLS of wild-type cells (AEP57). Notably, these concentrations were only a fraction of the MMS concentration used for the analysis of the stress response (Figure 36). None of them altered lifespan (Figure 38) thus arguing that the increased CLS of the identified DNA repair deletion strains was not because of a hormetic effect of low level DNA damage.

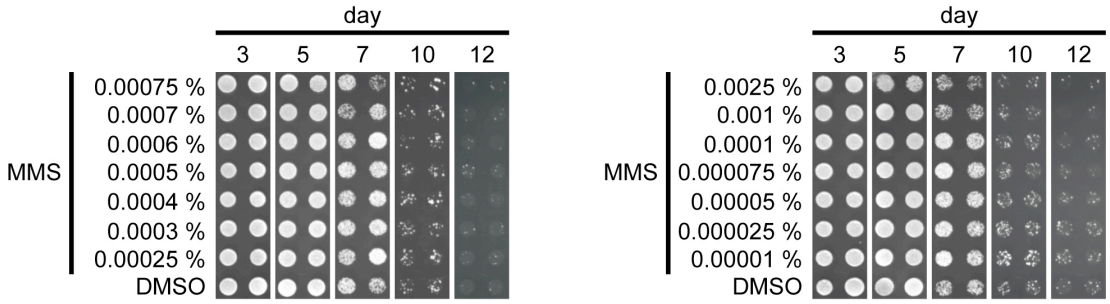

Figure 38 Hormetic doses of MMS did not alter CLS
S. pombe wild-type cells (AEP57) were cultured in YM medium containing 3 % glucose and different concentrations of the DNA damaging agent methyl methanesulfonate (MMS). At the indicated time points, the cells were spotted onto YES plates and incubated at 30 °C for two days to determine their viability.

3.1.3.4 Selected DNA repair mutants displayed extended CLS

The proteins encoded by the genes that were deleted in the CLS-extending strains identified here are not only involved in three different DNA repair pathways but also take part at diverse steps of DNA repair. The proteins affected by the identified deletions are involved in DNA damage recognition (Rhp23, Msh6, Pms1) (Buermeyer *et al.*, 1999; Fukumoto *et al.*, 2002; Marti *et al.*, 2002; Sugasawa *et al.*, 1998), damage excision (Rad2, Rad13) (Kanamitsu & Ikeda, 2010; Wood, 1996) or both (Nth1) (Kanamitsu & Ikeda, 2010). This raised the question whether there are more DNA repair deletion strains that might extend lifespan but failed to show an effect in the primary screen. To answer this question, we queried the deletion library for additional deletions that affect proteins involved in BER, NER or MMR and measured their CLS of the respective strains. An example is shown in Figure 39, and all results are summarized in Table 16.

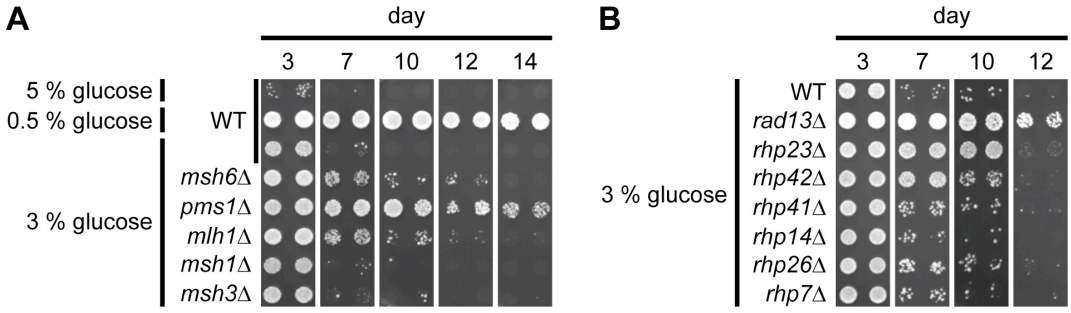

Figure 39 Not all DNA repair mutants showed increased lifespan
S. pombe strains from the deletion library (Bioneer) carrying single deletions of genes encoding for MMR (A) and NER (B) factors and the corresponding wild-type cells (AEP57) were grown in YM medium containing the indicated glucose concentrations. The aging cultures were spotted on YES plates that were incubated at 30 °C for two days.

Table 16 Summary of screening for DNA repair mutants with extended lifespan

pathway	deletion	*S. pombe* protein	human homolog	function	CLS[a]
BER/ UVER	*rad2*Δ	FEN-1 endonuclease	FEN-1	removal of 5' dRP end	++
	*nth1*Δ	DNA endonuclease III, DNA N-glycosylase, AP lyase	NTH1	binding, recognition, excision	+++
	*mag1*Δ	DNA-3-methyladenine glycosylase	AAG/MPG	binding, recognition, excision	—
	*mag2*Δ	DNA-3-methyladenine glycosylase	AAG/MPG	binding, recognition, excision	—
	*thp1*Δ	uracil DNA N-glycosylase		binding, recognition, excision	—
	*myh1*Δ	adenine DNA glycosylase		binding, recognition, excision	(+)
	*ung1*Δ	uracil DNA N-glycosylase	UNG1	binding, recognition, excision	(+)
	*apn1*Δ	AP endonuclease	HAP1/APE	excision	—
	*apn2*Δ	AP endonuclease	HAP1/APE	excision	—
	*uve1*Δ	endonuclease		excision	—
NER	*rad13*Δ	DNA endonuclease	XPG	excision	+++
	*rhp23*Δ		HR23B (GGR)	recognition	++
	*rhp14*Δ		XPA	damage verification	(+)
	*rhp26*Δ		CSB (TCR)	recognition	(+)
	*rhp7*Δ	homolog of Rad7 (*S.cerevisiae*)		binding of UV-damaged DNA	(+)
	*rhp41*Δ		XPC (TCR)	recognition	(+)
	*rhp42*Δ		XPC (GGR)	recognition	+(+)

	*msh6*Δ	MutS	hMsh6 (MutSα)	recognition	+(+)
	*msh2*Δ	MutS	hMsh2 (MutSα/β)	recognition	+++
	*pms1*Δ	MutL	hPms2 (MutL)	recognition	+++
MMR	*mlh1*Δ	MutL	hMlh1(MutL)	recognition	+(+)
	*msh1*Δ			mt MMR	—
	*msh3*Δ		hMsh3 (MutSβ)		—
	*exo1*Δ	exonuclease I		excision	(+)

[a] — No, (+) minimal, + slight, +(+) moderate, ++ strong or +++ very strong lifespan-extension compared to wild-type cells (AEP57).
Abbrevations: BER = base excision repair, UVER = UV-damaged DNA endonuclease-dependent excision repair, NER = nucleotided excision repair, MMR = mismatch repair, GGR = global genomic repair, TCR = transcription-coupled repair, mt = mitochondrial.

Importantly, our results did not disagree with previous publications reporting that defects in DNA repair result in premature aging in *S. cerevisiae* and in mice (de Boer *et al.*, 2002; Maclean *et al.*, 2003). The deletions analyzed in those studies have no or a functionally different homolog in *S. pombe* or did not show a significant life-extending effect in our assay. For instance, the homologs of Nth1 in budding yeast and mice, Ntg1/NTH1, act in both the nucleus and in mitochondria, while *S. pombe* Nth1 was not observed in mitochondria (Kanamitsu & Ikeda, 2010).

Mispaired but undamaged nucleotides are removed by the MMR pathway. In *S. pombe*, DNA mismatches are recognized by a complex, which is build by two heterodimers called MutS and MutL. So far, strains with deletions of *msh6*$^+$ and *pms1*$^+$ were shown here to exhibit an extended lifespan. The proteins encoded by these genes are each one part of the MutS and MutL heterodimer. Notably, the strains carrying single deletions of their counterparts (*msh2*$^+$ and *mlh1*$^+$) also displayed increased CLS. In fission yeast, there is only one MutS heterodimer consisting of Msh6 and Msh2 and one MutL heterodimer (Pms1/Mlh1), while other organisms have two MutS homologs, like MutSα and MutSβ in *S. cerevisiae*, and up to four MutL homologos that recognize different kinds of DNA mismatches (Marti *et al.*, 2002). One of these homologos that is involved in MMR in budding yeast and in humans is Msh3 (Marti *et al.*, 2002). However, the CLS of the tested *msh3*Δ cells was not affected in our assay (Table 16). The same was true for cells carrying a deletion of *msh1*$^+$, which codes for a protein that is part of the mitochondrial MMR. This result indicated that the life-extending effect was limited to the nuclear MMR.

NER recognizes bulky, helix-distorting lesions such as UV-induced pyrimidine dimers. There are two subpathways called TCR and GGR (Schumacher et al., 2008) (see 1.5). Rhp23 is involved in the GGR. There exist homologs of Rhp23 in budding yeast (Rad23) and humans (HR23A/HR23B), and they form a complex with Rad4 respectively XPC, which was found to be involved in DNA damage recognition as well as in the assembly and disassembly of NER complexes (Prakash & Prakash, 2000). One homolog of Rad4 in *S. pombe* is Rhp42, which is also termed Rhp4b (Fukumoto *et al.*, 2002). Strains carrying single deletions of both *rhp42*$^{+}$ and rhp*23*$^{+}$ exhibited a moderate to strong increase of CLS (Table 16). The DNA endonuclease Rad13 is the homolog of the human XPG protein and makes the 3' incision in NER (Wood, 1996), and the CLS of *rad3*Δ cells was also increased (Table 16). These results indicated an important role for the Rhp23-Rhp42 complex in affecting lifespan.

In the BER pathway, single bases that are damaged by oxidation, alkylation, hydrolysis, or deamination are recognized and removed by lesion-specific DNA glycosylases. Notably, we identified only one DNA glycosylase whose deletion extended CLS significantly (Table 16). This enzyme is called Nth1 and possesses also an apurinic/apyrimidinic (AP) lyase activity that removes oxidized bases in the early steps of the BER pathway. Additionally, a large portion of the AP sites generated by the action of the monofunctional DNA glycosylases is incised by Nth1 in short-patch BER (Kanamitsu & Ikeda, 2010). The second protein whose deletion increased lifespan is Rad2. In contrast to Nth1, the flap endonuclease Rad2 is involved in long-patch BER where it incises the flap DNA containing the lesion after DNA synthesis. Together with the UV endonuclease Uve1, Rad2 also acts in the alternative excision repair pathway (UVER) that is similar to the long-patch BER pathway, but excises UV damages normally repaired by NER (McCready *et al.*, 2000; Osman *et al.*, 2003). However, the CLS of *uve1*Δ cells was not extended, indicating that it is probably the Rad2 function in BER rather than its function in UVER that contributes to lifespan-extension.

3.1.3.5 Segregants from genetic crosses showed variability in CLS

Several studies have shown that proteins involved in NER interact with BER and MMR components (Bertrand *et al.*, 1998; Fleck *et al.*, 1999; Kanamitsu & Ikeda, 2010) and that these three DNA repair pathways display partially overlapping functions (Fleck *et al.*, 1999; Kunz & Fleck, 2001; McCready *et al.*, 2000; Yonemasu

et al., 1997; Yoon *et al.*, 1999). Therefore, we reasoned that the function of the repair pathway that is impaired by the deletion might be undertaken by one of the other (two) repair pathways. The resulting activation of additional DNA repair mechanisms might then lead to improved lifespan. To test this hypothesis, we planned to perform epistasis analysis and to determine the CLS of double mutants. Since our deletion strains originated from the *S. pombe* deletion library (Bioneer), all strains displayed the same mating type (h^+). To generate double mutants by genetic crosses, strains with the respective deletion but the opposite mating type had to be generated. For this initial experiment, a wild-type strain (AEP64) that was isogenic to the deletion library but had the opposite mating type (h^-) was used. The segregants that arose from these crosses were tested for their mating type and the presence of the deletion. Only those cells that were h^- and carried the deletion were used for further crosses.

Here, we made an unexpected observation regarding the lifespan of deletion mutants originating from genetic crosses. The original single deletion strains extended lifespan as expected. However, when measuring the CLS of the final double mutants, we observed a strong variability in the lifespan of the tested strains (Figure 40A, data not shown), although they displayed the same genotype as determined by PCR. To determine the potential cause for this variability, the lifespan of the deletion cells arising from the initial crosses was also analyzed. And again, there were great differences in their CLS (Figure 40B, data not shown) even if they were smaller compared to the previous experiment (Figure 40A), suggesting that their CLS was determined by factors other than the genotype. The only known difference between the *rad2*Δ segregants shown in Figure 40B and the presented strains was that they originated from a genetic cross. These results indicated that the CLS was some how influenced by genetic crosses *per se*. To test this hypothesis, two wild-type strains (AEP57, AEP64) were crossed. As shown in Figure 40C, the lifespan of all four spores arising from these tetrads varied slightly, suggesting that it was an unknown, non-Mendelian factor that affected the CLS of fission yeast. Possible explanations could be differences in mitochondrial DNA and/or epigenetic modifications, like PTMs on histones.

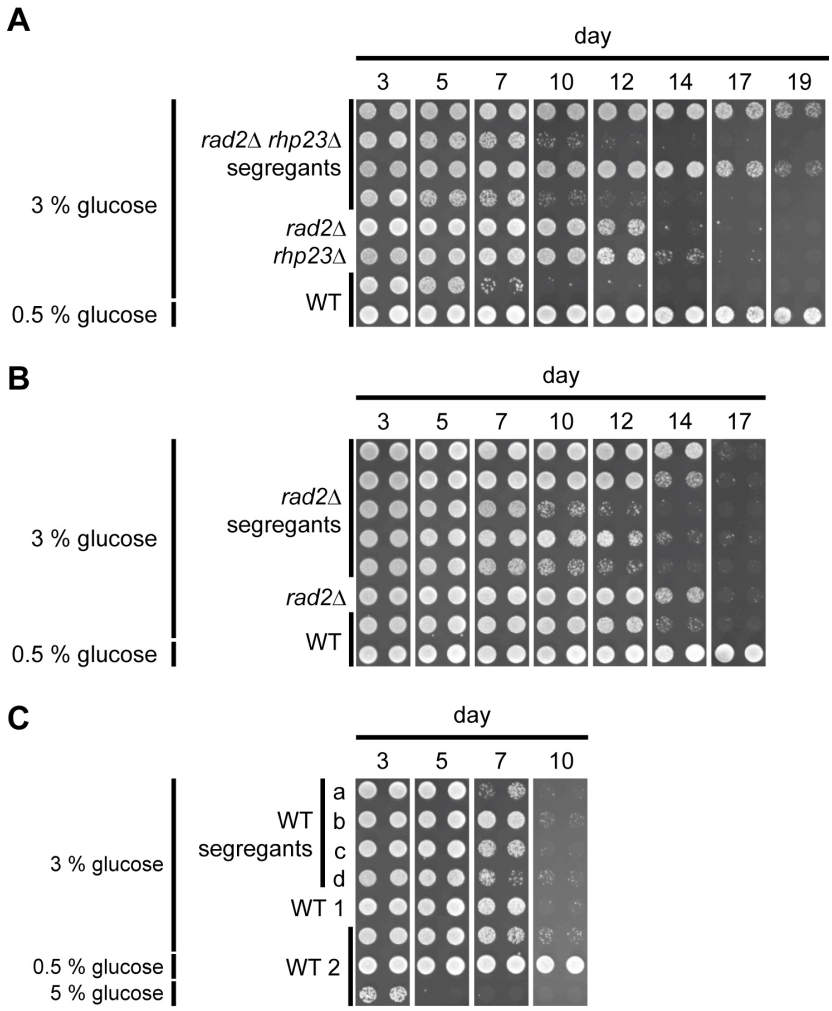

Figure 40 Varying CLS of yeast cells arising from crossings
(A) Measurement of the CLS of *rad2*Δ *rhp23*Δ double mutants arising from genetic crosses. *S. pombe* wild-type cells (AEP57) as well as *rad2*Δ and *rhp23*Δ cells originating from the deletion library (Bioneer) served as controls.
(B) Measurement of the CLS of *rad2*Δ segregants that arose from a genetic cross of wild-type cells (AEP64) and *rad2*Δ cells originating from the *S. pombe* deletion library (Bioneer). The initial mating partners served as control.
(C) Measurement of the CLS of four segragants (a-d) resulting from a single tetrad that arose from a genetic cross of two *S. pombe* wild-type strains (WT 1 = AEP64, WT 2 = AEP57). The initial mating partners served as control.
All gene deletions were confirmed by PCR.

3.1.3.6 Deletion of DNA repair genes did not extend CLS

The previous results raised the question whether the improvement of lifespan of the analyzed deletion strains was truly caused by their respective gene deletions or by other non-genetic factors. To address this question, three DNA repair genes (*rad2*$^+$, *rad13*$^+$, *msh6*$^+$) and one UPR^{ER} gene (*ppk4*$^+$) were deleted by replacing their open reading frame (ORF) with the *NatMX* cassette in two different *S. pombe* wild-type strains (AEP1 and AEP57). After confirming the deletion by PCR, the CLS was measured. Examples are shown in Figure 41. The deletion strains originating from

the *S. pombe* deletion library (Bioneer), which were used as controls, extended lifespan as expected (Figure 41, data not shown). However, the cells where the DNA repair genes were deleted with *NatMX* did not exhibit changes in lifespan (Figure 41, data not shown). The same was true for the deletion of the UPR^{ER} gene *ppk4*$^{+}$ (data not shown).

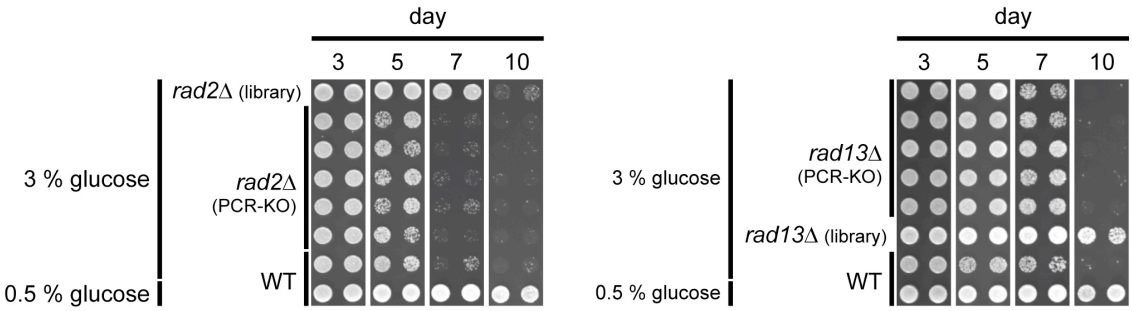

Figure 41 Deletion of DNA repair genes in wild-type cells did not extend CLS
rad2^{+} and *rad13*$^{+}$ were deleted in *S. pombe* wild-type cells (here: AEP57) by replacing their open reading frame with a *NatMX* cassette. After confirming the knockout (KO) by PCR, the CLS of these cells was analyzed in YM medium containing 3 % glucose. The original wild-type cells (AEP57) as well as the indicated deletion strains originating from the *S. pombe* deletion library (Bioneer) were used as controls.

In summary, these results indicated that the observed lifespan extension was probably not due to the indicated gene deletions. Since this was not only the case for the DNA repair genes but also for *ppk4*$^{+}$, secondary effects like additional mutations caused by defects in DNA repair could be excluded. This result posed a serious challenge to our previous observations concerning the lifespan-extending effect of individual gene deletions originating from the *S. pombe* deletion library (Bioneer). As a consequence, other groups of genes affecting CLS (Table 14) were not pursued.

3.2 Compounds altering telomeric silencing of *S. cerevisiae*

3.2.1 High-throughput *in vivo* screen for compounds affecting telomeric silencing

The regulation of telomere length is tightly linked to cellular aging and tumour growth. Shortening of telomeres is associated with premature aging in mammals, while activation of telomerase and telomere lengthening are linked to cancer. Intriguingly, there is an inverse correlation between lifespan and telomere length in *S. cerevisiae* (Austriaco & Guarente, 1997). Austriaco and Guarente suggested that telomeres regulate lifespan by modulating genomic silencing in budding yeast. According to their hypothesis, short telomeres recruit less of the SIR silencing machinery to the telomeres. As a result, this machinery is redistributed to non-telomeric sites, causing a delay in aging – probably by enhanced rDNA silencing. Conversely, telomere lengthening reduces lifespan. This decrease is due, at least in part, to greater recruitment of the SIR complex by the long telomeres and might lead to increased telomeric silencing (Austriaco & Guarente, 1997). Therefore, the measurement of telomeric silencing can be taken as an indicator of the potential lifespan of *S. cerevisiae*, with improved silencing implying a decrease in lifespan and reduced silencing representing lifespan extension. Since telomeric silencing is technically easier to measure than lifespan, an approach was taken here to identify compounds that affect telomeric silencing, hoping that they would also affect the lifespan of yeast.

3.2.2 Experimental set-up

3.2.2.1 Identification of potential positive controls

In a first step for setting up a high-throughput screen for compounds that affect telomeric silencing, an experimental strategy was required, in which increased or decreased telomeric silencing can be measured by a simple growth assay. To this end, different *S. cerevisiae* strains carrying an *URA3* reporter gene in the subtelomeric region were used. Spreading of telomeric heterochromatin into centromere-proximal regions causes repression of the integrated *URA3* gene, resulting in the ability to grow on *URA3*-counter-selective 5-FOA medium. Conversely, reduced silencing leads to *URA3* expression and the inability to grow on

5-FOA. An *SIR3* overexpression vector was constructed (pAE1232), as it was expected to improve the silencing at the telomeres by increased spreading of heterochromatin. Indeed, *TEL XI-L* position 2*::URA3* cells (AEY2165)[3] showed enhanced growth on 5-FOA plates when transformed with this plasmid compared to yeast cells carrying the empty vector (pAE269), indicating enhanced repression of the *URA3* gene (Figure 42).

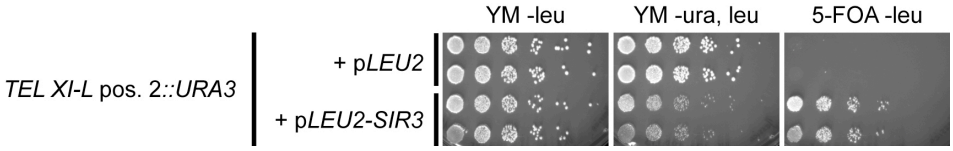

Figure 42 Telomeric silencing was improved by *SIR3* overexpression
The strain *TEL XI-L* position 2*::URA3* (AEY2165)[3] carries an *URA3* reporter gene at a (sub-) telomeric region. Six-fold serial dilution of these cells transformed with either a *SIR3* overexpression plasmid (pAE1232) or the corresponding empty vector (pAE269) were spotted on YM medium lacking uracil and *URA3*-counter-selective 5-FOA plates and subsequently incubated at 30 °C for two days to determine telomeric silencing.

Furthermore, the effect of resveratrol and splitomicin on telomeric silencing was tested. Resveratrol activated SirT1 in the fluorescence-based *in vitro* HDAC assay (unpublished data of Gesine Hoffmann) and may be an activator of sirtuins like yeast Sir2 (Haigis & Sinclair, 2010). Therefore, treatment with this compound should result in enhanced telomeric silencing in *S. cerevisiae*. However, resveratrol did not alter telomeric silencing, as the addition of this compound did not enhance the growth of *TEL XV-R* position 9*::URA3* (AEY4167) and *TEL IX-L* position 7*::URA3* (AEY4168) on 5-FOA (Figure 43A). Furthermore, the growth of *TEL XI-L* position 2*::URA3* (AEY2165)[3] on 5-FOA was not changed by either resveratrol or trichostatin A (TSA), a known inhibitor of Class I and II HDACs that does not affect sirtuins (Rusche *et al.*, 2003; Vanhaecke *et al.*, 2004) (Figure 43B). This led to the conclusion that resveratrol has no influence on telomeric silencing and does not activate Sir2, which is in line with observations of other groups that resveratrol does not affect aging in *S. cerevisiae* (Bass *et al.*, 2007; Howitz *et al.*, 2003; Kaeberlein *et al.*, 2005a; Wood *et al.*, 2004), and that its activation of sirtuins is highly dependent on the substrate (Beher *et al.*, 2009).

[3] Notably, it turned out in later experiments that the indicated genotype of this strain is not correct, and thus, the precise site of *URA3* integration is not known.

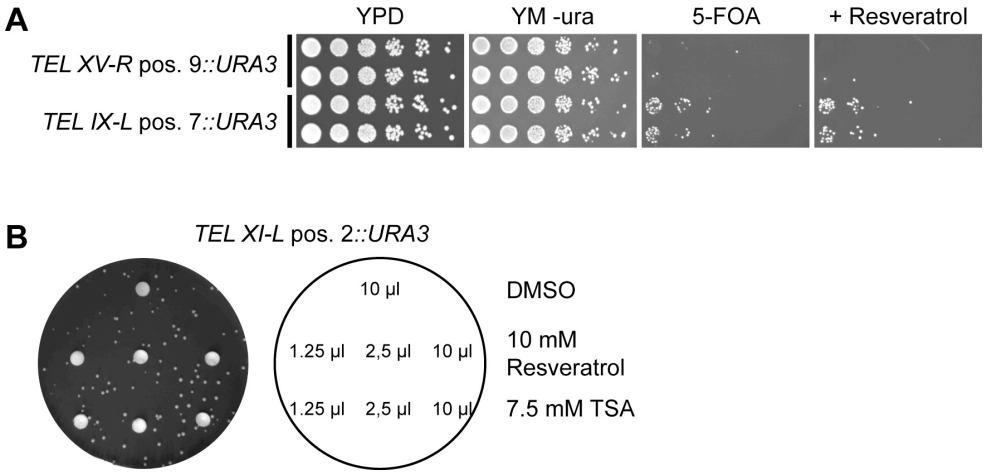

Figure 43 Resveratrol did not affect telomeric silencing
(A) The telomeric silencing of two strains carrying an *URA3* marker gene at distinct subtelomeric locations on different chromosome ends (AEY4167 and AEY4168) was analyzed. For this purpose, serial dilutions were spotted on 5-FOA plates with and without 10 µM resveratrol as well as on YM plates lacking uracil.
(B) 0.1 OD of *TEL XI-L* position 2*::URA3* (AEY2165)[3] were plated on a 5-FOA plate. The indicated volumes of DMSO, 10 mM resveratrol and 7.5 mM trichostatin A (TSA) were spotted on sterile filters made of Whatman paper.
All plates were incubated at 30 °C for two days.

On the other hand, splitomicin, a known Sir2 inhibitor (Bedalov *et al.*, 2001), inhibited Sir2 in the *in vitro* HDAC assay (Figure 44A) and was expected to disrupt at least the telomeric silencing *in vivo*. Indeed, splitomicin inhibited the growth of *TEL XI-L* position 2*::URA3* (AEY2165)[3] on 5-FOA (Figure 44B) as can be seen as a zone of growth inhibition around the filters, indicating reduced repression of the *URA3* marker gene. This concentration-dependent effect was not due to a general growth inhibition, since this compound increased the growth of *TEL IX-L* position 1*::URA3* cells (AEY4162) carrying the *SIR3* overexpression vector (pAE1232) on medium lacking uracil (Figure 44C). Together, these results indicated that splitomicin, as expected, disrupts telomeric silencing. However, as an inhibitor of Sir2, splitomicin was expected to affect all three types of silencing in *S. cerevisiae*. Therefore, its effect on *HM* silencing was additionally tested by a spot filter assay, where *MAT*a *his4* cells (AEY264) were mixed with *mat*aΔp *hml*$\alpha\Delta$p *HMRss*α cells (AEY325). These two yeast strains are only able to mate and form diploids if *HMR* silencing of the latter strain is disrupted. Indeed, the amount of diploid colonies around the filters increased with the concentration of splitomicin (Figure 44D), showing that this compound not only suppresses telomeric but also *HM* silencing – probably through the inhibition of Sir2.

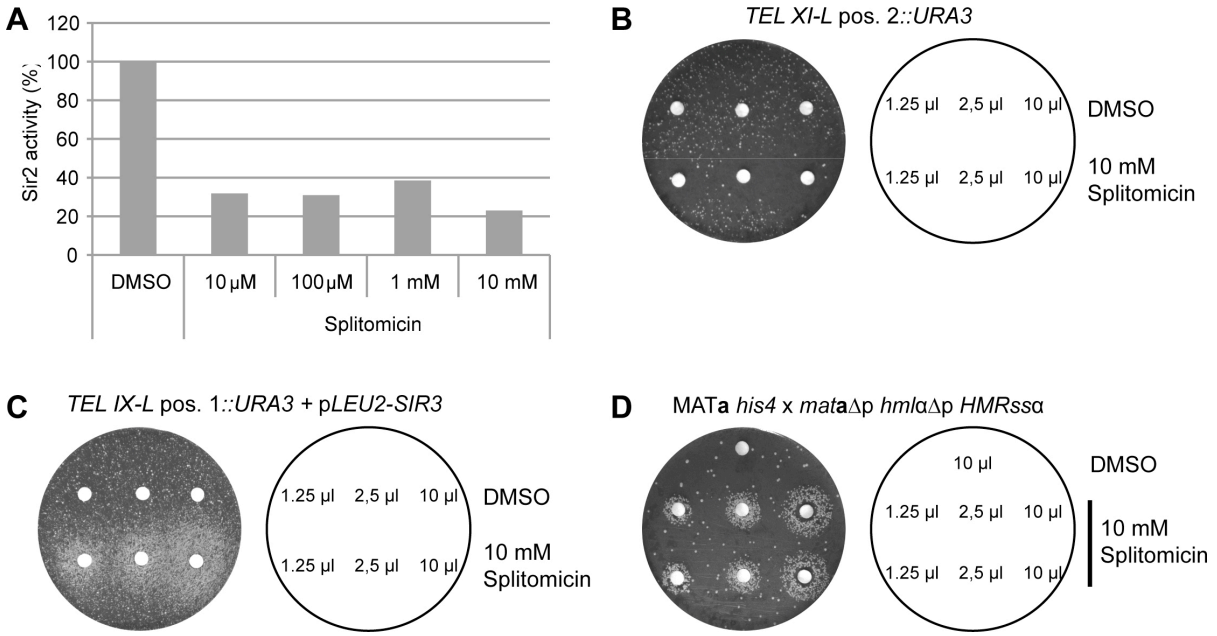

Figure 44 Splitomicin inhibited Sir2 activity *in vitro* and improved telomeric and *HM* silencing *in vivo*

(A) Sir2 deacetylase activity was measured by Gesine Hoffmann using a fluorescence-based assay. In two consecutive reactions, deacetylation of the substrate MAL generates a fluorophore that is excited at 360 nm and light at 460 nm was emitted. The blank (DMSO) was defined as 100 %.

(B) To determine telomeric silencing, 0.5 OD of the strain *TEL XI-L* position 2*::URA3* (AEY2165)[3] were plated on *URA3*-counter-selective 5-FOA plates.

(C) 0.1 OD of *TEL IX-L* position 1*::URA3* (AEY4162) carrying an SIR3 overexpression vector (pAE1232) were plated on a YM plate lacking uracil and leucine to analyze the repression of the sub telomeric *URA3* marker gene.

(D) To examine *HM* silencing, 0.5 OD of each MAT**a** *his4* (AEY264) and *mat***a**Δp *hml*αΔp *HMRss*α (AEY403) cells were mixed and plated on YM plates without supplements.

The indicated volumes of DMSO and 10 mM splitomicin were spotted on sterile filters made of Whatman paper. All plates were incubated at 30 °C for two days.

Based on the model of Austriaco and Guarente (Austriaco & Guarente, 1997) and the previous results, shortening of the telomeres was expected for *SIR3* overexpression, while splitomicin should lead to longer telomeres. Surprisingly, neither *SIR3* overexpression nor treatment with 10 µM splitomicin or 10 µM resveratrol affected telomere length of the analyzed yeast strains (Figure 45).

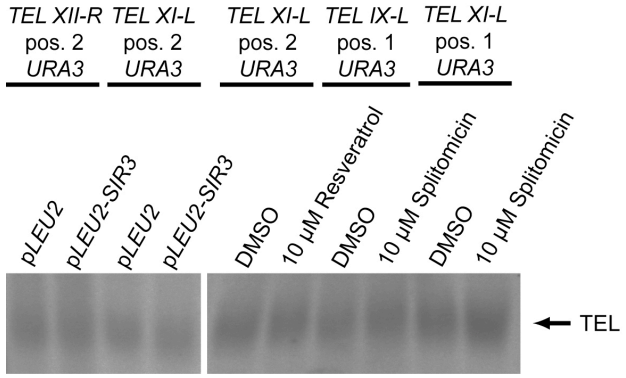

Figure 45 *SIR3* overexpression, resveratrol, and splitomicin did not affect telomere length
The telomere length of the indicated strains was determined by telomeric restriction fragment (TRF) analysis using a [α-^{32}P]dCTP-labelled probe for hybridization. Notably, it turned out in later experiments that the indicated genotype of these strains is not correct, and thus, the precise site of *URA3* integration is not known.

3.2.2.2 Yeast strains used in the *in vivo* screen for compounds affecting telomeric silencing

For *S. cerevisiae*, a discontinuous telomeric silencing pattern has been described at native telomeres. The repression of a subtelomeric (marker) gene is affected in a position-dependent manner (Pryde & Louis, 1999) (see 1.10.2). A yeast strain harbouring a subtelomeric *URA3* marker gene that is only slightly repressed could therefore be used to identify compounds that increase telomeric silencing. Therefore, such yeast cells are able to grow on minimal medium lacking uracil, but show only weak growth on the counter-selective 5-FOA medium. The addition of a compound that increases telomeric silencing should lead to *URA3* repression and to less synthesis of uracil. As a consequence, there should be more growth on 5-FOA, while the growth on YM medium lacking uracil should be reduced. The previous results suggested that *SIR3* overexpression represents an adequate positive control for this approach (see 3.2.1).

For the identification of compounds that decrease telomeric silencing, a yeast strain showing strong telomeric repression was needed. In contrast to the first approach, the addition of a compound that reduces telomeric silencing should lead to *URA3* expression resulting in less growth on 5-FOA and improved growth on minimal medium lacking uracil. The addition of 10 µM splitomicin was shown to mimick this effect (see 3.2.1). Therefore, it could be used as a positive control in the second approach.

In order to find suitable yeast strains for the screens that showed the telomeric silencing patterns described above, we obtained seven *S. cerevisiae* strains, each

carrying an *URA3* marker gene at a different subtelomeric region (Pryde & Louis, 1999). To analyze the telomeric silencing and the strength of the effect of the positive controls, these strains were transformed with the *SIR3* overexpression plasmid (pAE1232) and the corresponding empty vector (pAE269). Subsequently, serial dilutions were spotted on minimal medium lacking uracil and 5-FOA plates, each with and without 10 µM splitomicin (Figure 46). As a result, the strains could be clustered into two groups. The first group contains the strains with strong telomeric repression when carrying the *SIR3* overexpression plasmid, as indicated by reduced growth on YM lacking uracil compared to the empty vector (*TEL IX-L* position 1, *TEL XI-L* position 1, *TEL XI-L* position 2). This difference was reversible by disrupting telomeric silencing through the addition of 10 µM splitomicin (Figure 46, lines 1, 2, 4). The strains, whose growth on 5-FOA was increased by the presence of the *SIR3* overexpression plasmid (*TEL XII-R* position 2, *TEL XI-L* position 3, *TEL XV-R* position 9, *TEL IX-L* position 7) (Figure 46, lines 3, 5 - 7), were clustered in the second group. These strains displayed weak to moderate telomeric silencing, when carrying the empty vector.

Based on these results, *TEL IX-L* position 1*::URA3* (AEY4162) carrying the *SIR3* overexpression plasmid (pAE1232) was selected to screen for compounds that decrease telomeric silencing. This strain exhibited a strong telomeric silencing when *SIR3* was overexpressed (Figure 46, line 1). Compounds that disturb telomeric silencing cause an induction of cell growth on YM medium lacking uracil. Therefore, the addition of 10 µM splitomicin could be used as positive control. To identify compounds that increase telomeric silencing, *TEL IX-L* position 7*::URA3* (AEY4168) was chosen. This strain showed moderate silencing under normal conditions causing weak growth on counter-selective 5-FOA medium (Figure 46, line 7). The growth could be improved by a stronger repression of the reporter gene, here mimicked by the induction of a *SIR3* overexpression plasmid (pAE1232) that served as positive control in the screen. Importantly, both approaches exploit a positive growth selection that excludes the problem of achieving false-positive effects from compounds that are toxic to the cell and cause a decreased growth without affecting telomeric silencing.

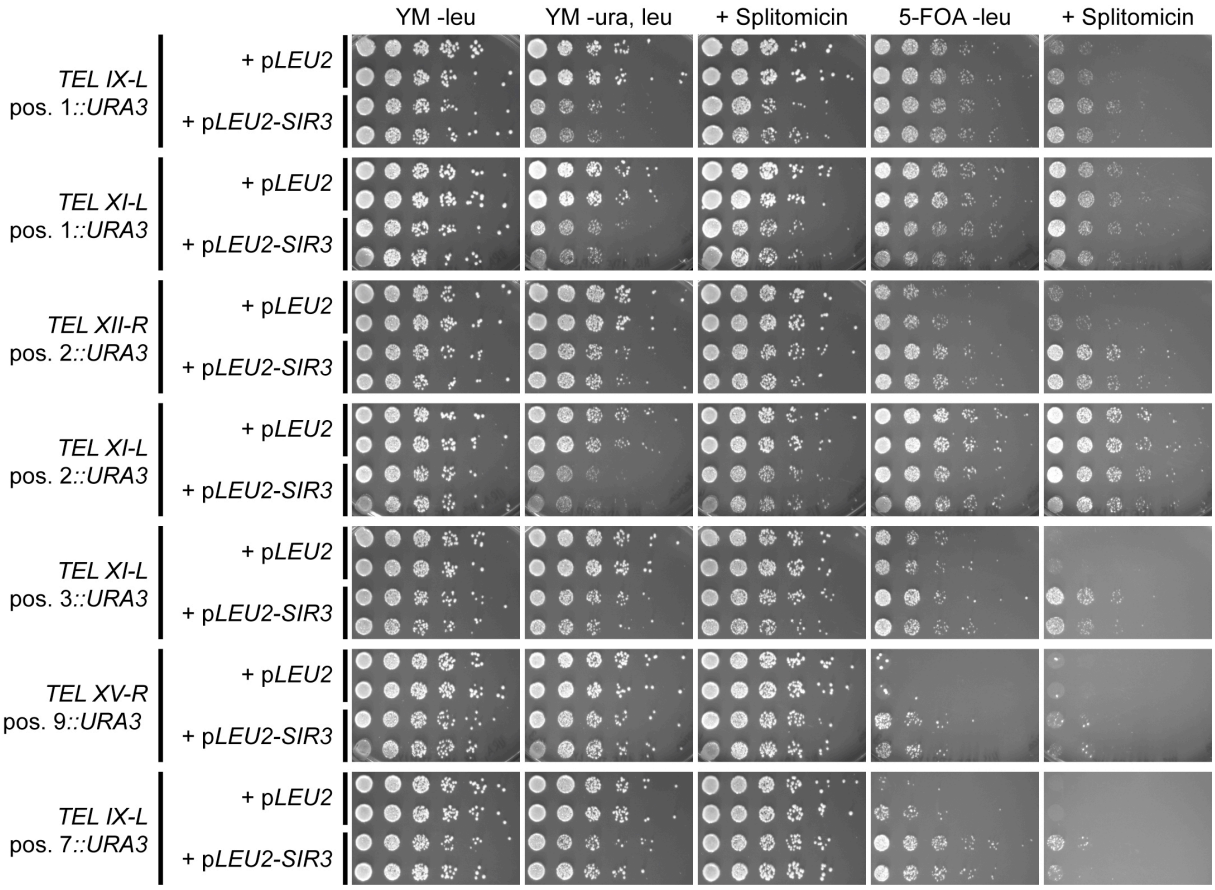

Figure 46 *SIR3* overexpression and splitomicin affected telomeric silencing of potential screening strains
Cells with an *URA3* marker gene inserted at distinct subtelomeric regions on different chromosome ends (top to bottom: AEY4162 - AEY4168; (Pryde & Louis, 1999) were transformed with a *SIR3* overexpression plasmid (pAE1232) and the corresponding empty vector (pAE269). To analyze their telomeric silencing, six-fold serial dilutions of the strains were spotted on YM plates lacking uracil and *URA3*-counter-selective 5-FOA plates, each with and without 10 µM splitomicin. All plates were incubated at 30 °C for two days.

3.2.3 Results of the high-throughput *in vivo* screen

To analyze the effect of several compounds on telomeric silencing at once, we established a novel high-throughput method. Small liquid cultures of the screening strains (see 3.2.2.2) were grown in 96-well or 384-well microtiter plates. Their growth was determined by measuring the optical density at distinct intervals using a microplate reader. Notably, the effects of the positive controls in liquid cultures were identical to those observed in the previous experiments where solid medium was used (see 3.2.2.2). Compounds that resulted in at least a 1.5 fold increase compared to DMSO-treated cells were scored as positive hits.

Using this method, we screened approximately 19,000 compounds for their impact on the telomeric silencing of *S. cerevisiae*. In the first step, a small compound library (Biomol) as well as a few single compounds (Evonik) were tested using two different

compound concentrations. Eight of these 522 compounds showed an effect in the screen for increased telomeric silencing (Table 17), while four compounds resulted in reduced silencing (Table 18). Next, we cooperated with the Screening Unit of the Leibniz-Institute for Molecular Pharmacology (FMP) in Berlin to analyze the ChemBioNet library containing approximately 17,000 compounds and the LOPAC library (1,280 compounds). In the screen for enhanced telomeric repression, 127 primary candidates were identified (Table 19). Additionally, 146 compounds were found in the screen for decreased telomeric silencing (Table 20). All primary candidates were re-tested as triplicates using at least three different compound concentrations. Finally, four compounds that increased telomeric silencing and two hits leading to reduced silencing could be validated (Table 21). Interestingly, these compounds showed only a weak or moderate effect in the initial screen (Tables 17 - 20, marked in dark grey).

Table 17 Primary candidates (Biomol and Evonik) that increased telomeric silencing

well	compound	fold change[a]	
		4 µg/ml	20 µg/ml
1-A9	Betulinic acid	3,48	1,51
1-B2	C6-Ceramide	7,29	2,86
1-G12	Mezerein	2,14	1,02
2-F8	Nicotine	4,46	0,57
2-H1	Oxytetracycline, a -apo-	1,82	1,04
3-D3	Chrysoeriol	2,06	1,24
6-B6	3,3-Diindolylmethane	0,49	1,71
6-E2	Phytosphingosine nicotinic acid (Evonik)	1,82[b]	---

[a] X-fold increase of optical density (OD_{600}) caused by 4 µg/ml or 20 µg/ml compound compared to the blank (DMSO)
[b] final concentration of 100 µg/ml
light grey = below cut-off (< 1.5); dark grey = secondary candidate

Table 18 Primary candidates (Biomol and Evonik) that decreased telomeric silencing

well	compound	fold change[a]	
		4 µg/ml	20 µg/ml
1-B2	C6-Ceramide	1,21	1,69
2-G2	Quercetin Dihydrat	0,98	1,60
3-G8	Tamarexitin	0,92	1,79
6-B4	Geraldol	0,85	1,70

[a] X-fold increase of optical density (OD_{600}) caused by 4 µg/ml or 20 µg/ml compound compared to the blank (DMSO)
light grey = below cut-off (< 1.5)

Table 19 Primary candidates (ChemBioNet and LOPAC) that increased telomeric silencing

Comp. ID[a]	fold change[b]	Comp. ID[a]	fold change[b]	Comp. ID[a]	fold change[b]	Comp. ID[a]	fold change[b]
39509	2,39	36556	1,73	37936	1,62	39104	1,55
36784	2,37	37253	1,73	38817	1,62	36976	1,55
35234	2,35	37904	1,72	29510	1,62	39681	1,55
37760	2,25	38480	1,72	32410	1,62	29862	1,55
38638	2,25	38977	1,72	34669	1,62	37169	1,55
26352	1,99	36206	1,71	37269	1,61	29511	1,55
39713	1,95	33932	1,71	39717	1,61	36558	1,55
37262	1,95	37585	1,71	37840	1,61	39745	1,55
36901	1,94	32173	1,70	38320	1,61	38240	1,54
36816	1,94	39873	1,70	27397	1,61	36550	1,54
34438	1,93	37257	1,70	37968	1,60	26004	1,54
31973	1,93	34438	1,93	37060	1,59	26689	1,54
34475	1,91	31981	1,70	39931	1,59	38593	1,54
39376	1,90	40064	1,69	27649	1,59	37267	1,53
37297	1,88	37278	1,69	36124	1,59	27585	1,53
38305	1,85	37256	1,69	41603	1,58	35840	1,53
40048	1,84	41762	1,68	37357	1,58	39771	1,53
31972	1,82	38672	1,68	35503	1,58	40080	1,53
37824	1,81	37255	1,67	39120	1,57	35232	1,53
38479	1,81	37664	1,67	39995	1,57	26069	1,53
37032	1,81	38945	1,67	36960	1,57	36900	1,53
37252	1,81	26317	1,67	37363	1,57	28405	1,53
36559	1,81	30211	1,66	39456	1,56	36096	1,53
36432	1,79	24889	1,66	37632	1,56	39728	1,52
30224	1,79	37263	1,66	38336	1,56	30918	1,52
37254	1,78	39729	1,66	27399	1,56	29163	1,52
38311	1,77	39714	1,65	38288	1,56	29509	1,52
36207	1,77	27393	1,65	39830	1,56	36479	1,51
39719	1,77	36961	1,65	36555	1,56	26229	1,51
31979	1,76	38128	1,65	27473	1,56	40909	1,51
39808	1,75	35449	1,64	35168	1,55	40160	1,51
35695	1,74	39601	1,64	27601	1,55		

[a] Compound IDs used at the Screening Unit of the Leibniz-Institute for Molecular Pharmacology (FMP) in Berlin.
[b] X-fold increase of optical density (OD_{595}) caused by 40 µM compound compared to the blank (DMSO).
dark grey = secondary candidates

Table 20 Primary candidates (ChemBioNet and LOPAC) that decreased telomeric silencing

Comp. ID[a]	fold change[b]	Comp. ID[a]	fold change[b]	Comp. ID[a]	fold change[b]	Comp. ID[a]	fold change[b]
100657	3,34	35637	1,88	30310	1,73	25185	1,63
38258	2,77	31412	1,88	27852	1,73	26322	1,63
38441	2,42	24020	1,87	31298	1,73	24580	1,62
33446	2,41	35441	1,87	32676	1,72	28388	1,62
28466	2,36	26226	1,86	41656	1,72	27012	1,61
36993	2,34	33424	1,85	24161	1,71	31651	1,60
24963	2,34	25271	1,85	27053	1,71	29908	1,60

100662	2,32	39625	1,85	27359	1,71	29618	1,60
35077	2,31	25107	1,85	29156	1,71	40080	1,59
100683	2,25	26673	1,84	31284	1,71	33064	1,59
40868	2,24	27715	1,82	28630	1,70	31229	1,59
28594	2,23	31588	1,81	25154	1,70	37980	1,59
33719	2,19	28147	1,81	24232	1,70	25825	1,58
27746	2,15	24883	1,81	26755	1,69	26882	1,58
26433	2,13	26372	1,81	29873	1,69	37810	1,58
39769	2,11	31379	1,80	27061	1,69	26397	1,57
39564	2,10	31601	1,80	31571	1,69	30272	1,57
27091	2,09	29857	1,80	28469	1,69	27697	1,57
33583	2,03	25652	1,80	29944	1,69	36036	1,56
35213	2,02	26497	1,79	30228	1,68	38579	1,56
26902	2,00	39928	1,79	29155	1,68	27157	1,56
39707	2,00	33164	1,78	25858	1,68	31474	1,55
24851	1,99	39684	1,78	25955	1,67	25202	1,55
27108	1,99	24244	1,78	32276	1,67	29842	1,54
100087	1,98	31299	1,77	30449	1,66	32332	1,54
29524	1,98	26347	1,77	28467	1,66	35183	1,53
41726	1,96	27090	1,77	25068	1,66	36053	1,53
26739	1,95	31364	1,76	37540	1,65	30135	1,53
24932	1,95	100403	1,76	27057	1,64	24582	1,53
36640	1,92	32721	1,75	27394	1,64	24916	1,52
27307	1,92	29860	1,75	32019	1,64	24835	1,52
32675	1,91	40086	1,75	28002	1,64	36004	1,52
38026	1,91	32212	1,75	36560	1,64	26620	1,52
25253	1,89	25637	1,75	27051	1,63	38468	1,51
30180	1,89	28516	1,75	31509	1,63	36788	1,50
27348	1,88	28454	1,74	26721	1,63	28403	1,50
28523	1,88	39708	1,73				

[a] Compound IDs used at the Screening Unit of the Leibniz-Institute for Molecular Pharmacology (FMP) in Berlin.
[b] X-fold increase of optical density (OD_{595}) caused by 40 µM compound compared to the blank (DMSO).
dark grey = secondary candidates

Table 21 Secondary candidates of compounds that alter telomeric silencing

Increased telomeric silencing		Decreased telomeric silencing	
Comp. ID[a]	**Compound[b]**	**Comp. ID[a]**	**Compound[b]**
—	nicotine	24835	8011-0384 (ChemDiv)
26004	8016-8224 (ChemDiv), ST4114419 (TimTec)	29944	C274-8454 (ChemDiv)
35168	K289-0473 (ChemDiv)		
35733	C593-0506 (ChemDiv)		

[a] Compound IDs used at the Screening Unit of the Leibniz-Institute for Molecular Pharmacology (FMP) in Berlin.
[b] Compound names of the companies from which the compounds were reordered.

To further verify the effect of the identified secondary candidates on telomeric silencing and to analyze their potential mode of action, they were reordered from Roth (nicotine), TimTec, and ChemDiv. However, the screening results for the compounds K289-0473, 8011-0384, and C274-8454 could not be reproduced, indicating that their effect might result from degradation products within the library or that their identity is mistaken at the ChemDiv library. Three compounds (C593-0506, ST4114419, nicotine) could be re-validated – all of them enhanced telomeric silencing (Figure 47). They were also tested in medium without yeast cells. Under these conditions, the addition of C593-0506 and ST4114419 resulted in increased optical density (data not shown). Additional observations indicated that this increase was rather caused by the precipitation of the compound, possibly due to a reaction with components of the medium, than by improved cell growth. Therefore, these compounds were not investigated further.

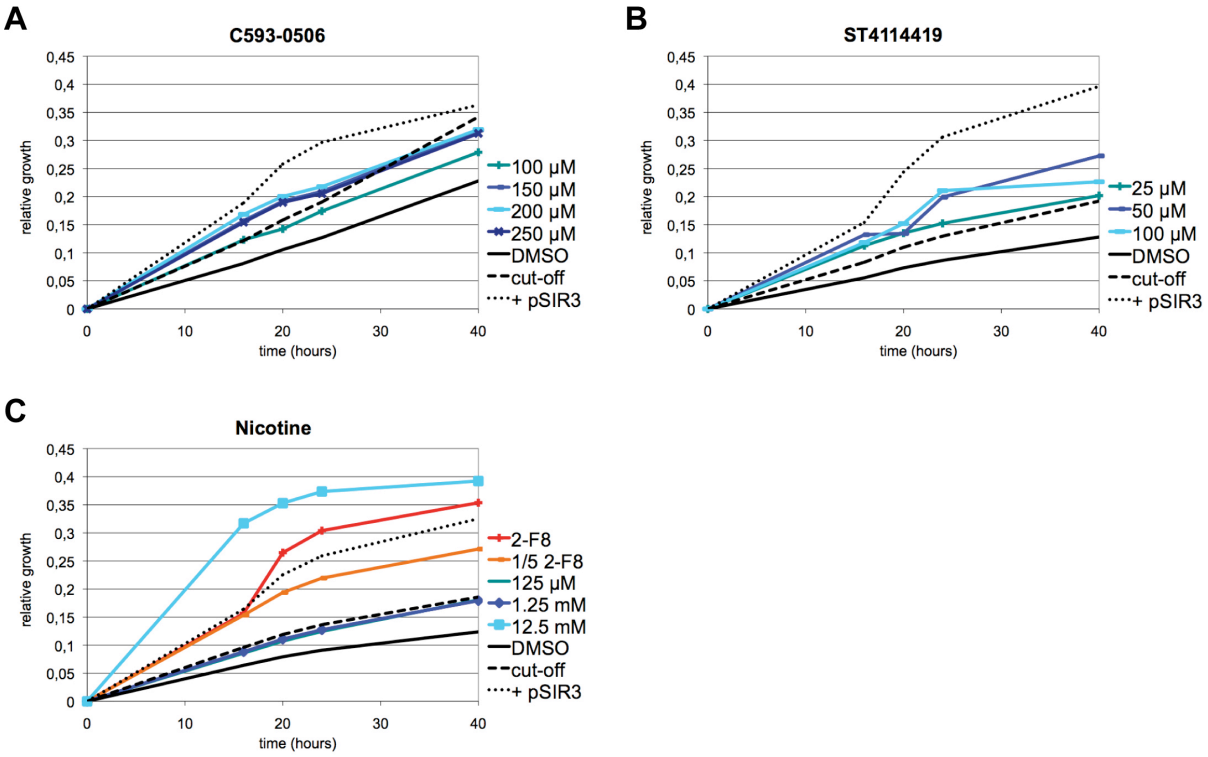

Figure 47 Three secondary candidates were re-validated for increased telomeric silencing
After the initial screens and the first validation, the effect of the identified compounds on telomeric silencing was analyzed by determining the growth of *TEL IX-L* position 7*::URA3* (AEY4168) in *URA3*-counter-selective 5-FOA medium in 96-well microplates. For this purpose, the optical density of the miniaturized liquid cultures was measured at the indicated time points after inoculation. The results of the three validated secondary compounds that increase telomeric silencing are shown ((A) C593-0506, (B) ST4114419, (C) nicotine). For each compound three different concentrations were tested as triplicates. 2-F8 represents the compound that originated from this well of the Natural Products Library (Biomol) that was indicated as 1 µg/µl nicotine.The *SIR3* overexpression strain (+ p*SIR3*) served as positive control and the dashed line shows the cut-off corresponding to the 1.5-fold of the blank (DMSO).

In the case of nicotine, there was some confusion regarding its real concentration in the library (well 2-F8), because 125 µM of nicotine reordered from Roth, which should approximately be the concentration of nicotine in the library, did not affect telomeric repression (Figure 47C). Even if the concentration was increased ten-fold (= 1.25 mM), there was no effect (Figure 47C). However, 12.5 mM nicotine enhanced telomeric silencing – even stronger than the compound from the library (Figure 47C). To confirm that this increase is caused by improved cell growth, 1 µl of the analyzed cultures was plated on YM plates. Indeed, the growth of cells carrying the *SIR3* overexpression plasmid (+ p*SIR3*) was enhanced compared to the blank (DMSO). In the case of 12.5 mM nicotine and the undiluted compound originating from well 2-F8 of the compound library, even more cells grew (data not shown) indicating that the increase in optical density was due to an increase in cell number and hence enhanced telomeric silencing. In summary, nicotine was the only secondary candidate that remained after these initial experiments.

3.2.4 Effect of nicotine on silencing and lifespan

3.2.4.1 The increase of telomeric silencing was caused by nicotine and was not due to degradation products

Based on the suggestion that the effect on telomeric silencing of some secondary candidates identified in the screen might be caused by degradation products (see 3.2.3), this had to be tested for nicotine. For this purpose, Werner Karow from the Faculty of Chemistry at the University of Duisburg-Essen performed mass spectrometry (MS) using the “original” nicotine from the Natural Products Library (Biomol) and the reordered compound (Roth). With this method, the mass-to-charge ratio of charged particles is measured (Sparkman, 2000) that can be used for determining the elemental composition of a sample. Additionally, high-performance liquid chromatography combined with mass spectrometry (HPLC-MS) was performed by Markus Kaiser at the Chemical Genomics Centre of the Max-Planck Society in Dortmund. By this means, the components of the sample are physically separated before being analyzed by MS. This technique is generally used for specific detection and potential identification of chemicals in the presence of other chemicals (in a complex mixture) (Gey, 2008). Both experiments showed that the majority of the analyzed sample consisted of nicotine. Furthermore, small quantities of oxidation

product nicotine-N-oxide were found (personal communication with Markus Kaiser, data not shown). To ensure that the effect on telomeric silencing was due to nicotine and not to nicotine-N-oxide, different concentrations of nicotine-N-oxide reaching from 10 nM to 100 µM were tested. None of them resulted in improved repression of the subtelomeric *URA3* marker gene (Figure 48), indicating that the effect observed in the previous experiments was indeed caused by nicotine.

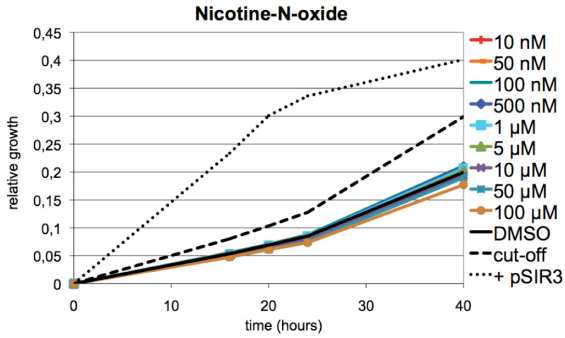

Figure 48 Nicotine-N-oxide did not alter telomeric silencing
The effect of several nicotine-N-oxide concentrations on telomeric silencing was analyzed by determining the growth of *TEL IX-L* position 7*::URA3* (AEY4168) in 5-FOA medium. Therefore, the optical density (OD_{600}) was measured at the indicated time points. The *SIR3* overexpression strain (+ p*SIR3*) served as positive control and the dashed line shows the cut-off corresponding to the 1.5-fold of the blank (DMSO).

So far, 12.5 mM was the only tested concentration of the reordered nicotine that affected telomeric silencing. In order to find a lower concentration with a comparable effect, 13 different concentrations between 1 mM and 12.5 mM were tested (Figure 49). Concentrations of at least 4 mM nicotine significantly increased telomeric silencing. This concentration-dependent effect was stronger than the effect of the positive control (+ p*SIR3*). The maximum enhancement of growth in 5-FOA medium, meaning maximal telomeric repression, was reached by the addition of 8 mM nicotine. Based on these results a nicotine concentration of 6 mM was chosen for further experiments.

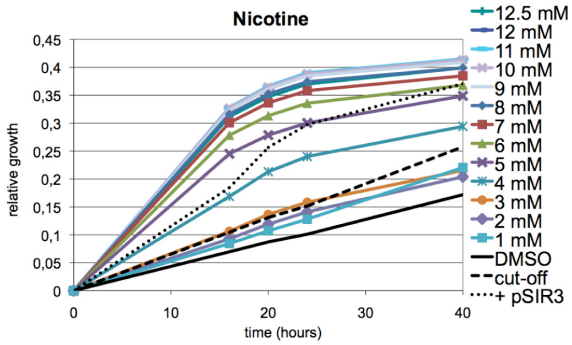

Figure 49 Nicotine increased telomeric silencing
To analyze the effect of several nicotine concentrations on telomeric silencing, the growth of *TEL IX-L* position 7*::URA3* (AEY4168) in 5-FOA medium was determined by measuring the optical density (OD_{600}) at the indicated time points. The *SIR3* overexpression strain (+ p*SIR3*) served as positive control and the dashed line shows the cut-off corresponding to the 1.5-fold of the blank (DMSO).

3.2.4.2 The effect of nicotine neither depended on the type of the medium nor on the telomeric position or the nature of the reporter gene

In the previous experiments, telomeric silencing was determined by measuring the optical density of small liquid cultures grown in 96-well or 384-well microplates, because it enabled the analysis of several cultures in parallel. In the following experiments, six-fold serial dilutions spotted on different plates were used to examine silencing in the following experiments.

To determine whether the enhancement of telomeric repression by nicotine depends on the position of the *URA3* marker gene within the telomere, the growth on 5-FOA of two strains carrying the *URA3* at distinct subtelomeric locations on different chromosome ends (AEY4167 and AEY4168) was analyzed. Under normal conditions both strains showed a weak to moderate silencing. The addition of 6 mM nicotine led to an increase of telomeric silencing, as measured by improved growth on 5-FOA (Figure 50A). This was confirmed in a spot filter assay, where growth on 5-FOA was increased around the filters with 0.5 µl and 1 µl undiluted nicotine, while 2.5 µl up to 10 µl inhibited growth in a concentration-dependent radius (data not shown). In another approach, the subtelomeric *URA3* gene was replaced by a *LYS2* reporter gene in the yeast strains *TEL XV-R* position 9*::URA3* (AEY4167) and *TEL IX-L* position 7*::URA3* (AEY4168). The resulting strains exhibited a moderate growth on *LYS2*-counter-selective α-amino adipic acid (αAA) medium. The cell growth was increased by the addition of 6 mM nicotine (Figure 50B, data not shown), indicating improved repression of the telomeric *LYS2*. This was confirmed by the wild-type

LYS2 strain (AEY1), whose growth on αAA was not affected by adding 6 mM nicotine (Figure 50B).

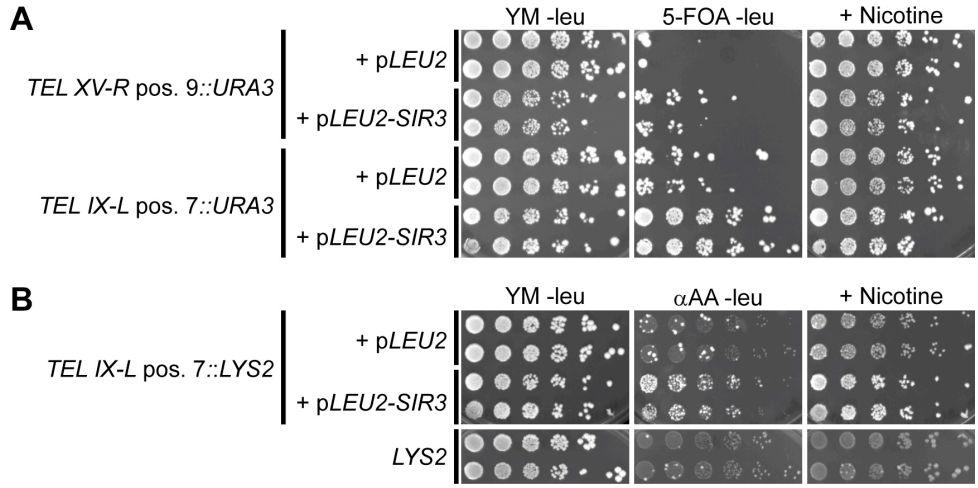

Figure 50 The effect of nicotine did not depend on the position within the telomere or the nature of the reporter gene
(A) The yeast strains *TEL XV-R* position 9*::URA3* (AEY4167) and *TEL IX-L* position 7*::URA3* (AEY4168) carry an *URA3* reporter gene at distinct subtelomeric locations on different chromosome ends. *URA3* repression was tested by spotting serial dilutions on counter-selective 5-FOA medium with and without 6 mM nicotine. All plates were incubated at 30 °C for two days.
(B) The subtelomeric *URA3* gene was replaced by a *LYS2* reporter gene in the yeast strain *TEL IX-L* position 7*::URA3* (AEY4168). Telomeric silencing of the resulting yeast strain (AEY4580) was analyzed like in (A) using αAA for *LYS2*-counter-selection.

To test whether the effect on nicotine did depend on 5-FOA, for instance by preventing the intake of 5-FOA, the telomeric silencing of *TEL XI-L* position 1*::URA3* cells (AEY4163) carrying the *SIR3* overexpression plasmid (pAE1232) or the corresponding empty vector (pAE269) was analyzed on YM medium. This strain displayed a weak silencing, as indicated by good growth on YM medium lacking uracil, which was only slightly reduced by the *SIR3* overexpression. When 6 mM nicotine was added, telomeric silencing was increased, causing impaired growth on this medium (Figure 51). This effect was not due to a general growth inhibition by nicotine, because the growth on YM plates containing uracil was not affected by the compound (Figure 51). Again, the growth on 5-FOA was improved by adding 6 mM nicotine (data not shown).

Together, these results suggested that the effect of nicotine neither depends on the type of the medium nor on the (sub-) telomeric position or the nature of the reporter gene.

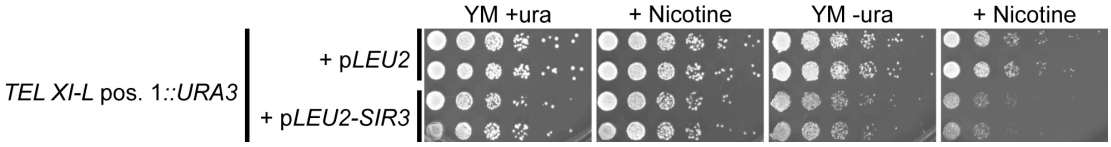

Figure 51 Nicotine enhanced telmeric silencing independently of 5-FOA
The strain *TEL XI-L* position 1*::URA3* (AEY4163) carries an *URA3* reporter gene at a subtelomeric region. Six-fold serial dilution of these cells transformed with either a *SIR3* overexpression plasmid (pAE1232) or the corresponding empty vector (pAE269) were spotted on YM plates with and without uracil, each with and without 6 mM nicotine, to determine telomeric silencing. The plates were subsequently incubated at 30 °C for two days.

3.2.4.3 Nicotine increased *HM* silencing *in vivo*, and its effect did not depend on Rap1

So far, only telomeric silencing was analyzed for an effect by nicotine. However, it is known that there are several components of the telomeric silencing machinery that also take part in *HM* silencing (see 1.10). Nevertheless, there are also some differences between these two types of silencing in *S. cerevisiae*. To obtain insight into the way nicotine might act and to limit the number of its potential targets, the effect of this compound on *HM* silencing was investigated. A spot filter assay using the yeast strains *MAT*a *his4* (AEY264) and *MAT*α *HMR*a-e** (AEY403) to test the impact of nicotine on *HM* silencing resulted in the same effects like in the telomeric spot filter assay (see 3.2.4.2). Increased growth could be observed around the filters with 0.5 µl and 1 µl undiluted nicotine, while higher volumes inhibited growth in a concentration-dependent manner (data not shown). In another approach, *hmr-ss::URA3* (AEY4185) cells were not able to grow on 5-FOA under normal conditions, but the strain showed maximal growth when 6 mM nicotine was added to the medium (Figure 52A), indicating that *HM* silencing was improved by nicotine. These results were confirmed using a yeast strain that carries an *ADE2* marker gene at the *HMR* locus (AEY1676), which was only slightly repressed under normal conditions (Figure 52B). Notably, *HMR::ADE2* silencing was increased by the addition of 6 mM nicotine, causing reduced growth on YM medium lacking adenine. Again, it could be excluded that this effect was due to a general growth inhibition by nicotine, because the growth on YM containing adenine was not affected by this compound (Figure 52B). These results are comparable to those observed for *hmr-URADE2-E* cells (AEY743), which harbour an *ADE2* marker gene under the control of an *URA3* promoter at the *HMR* locus. In this strain, *ADE2* is relatively strongly repressed, and the silencing was enhanced by nicotine (Figure 52B). The

effect of nicotine did not depend on the marker gene, because the growth of a strain with wild-type *ADE2* (AEY3) was not affected (Figure 52B).

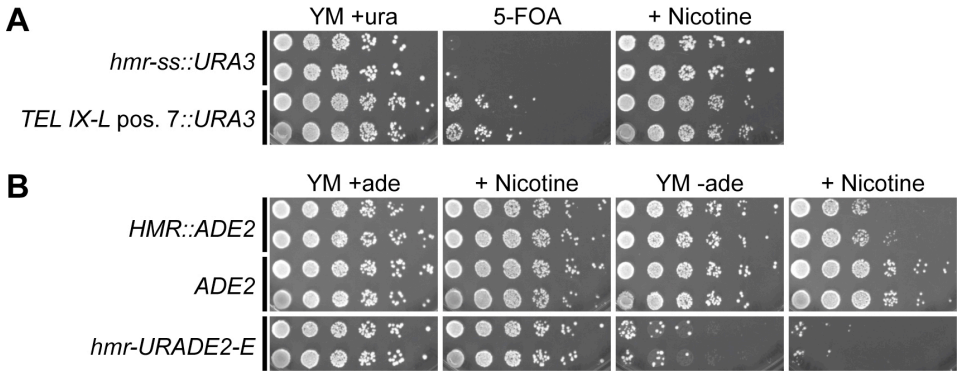

Figure 52 Nicotine increased *HM* silencing *in vivo*
(A) *HM* silencing of a strain that carries a synthetic silencer marked with an *URA3* gene at the *HMR* locus (AEY4185) was tested by spotting a six-fold serial dilution of the cells on the indicated plates. Growth on the counter-selective 5-FOA medium with and without 6 mM nicotine was used to determine the repression of *URA3*. The strain *TEL IX-L* position 7*::URA3* (AEY4168) served as positive control.
(B) In second approach, wild-type (AEY3) cells as well as a strain harbouring an *ADE2* gene at the *HMR* locus (AEY1676) were used. A third strain carries an *ADE2* marker gene under the control of an *URA3* promoter at the *HMR* locus (AEY743). The effect of 6 mM nicotine on the *HM* silencing of these three strains was analyzed by determining their ability to grow an YM plates with and without adenine. All plates were incubated at 30 °C for two days.

One of the components involved in telomeric and *HM* silencing is Rap1. This DNA-binding protein recruits Sir4, resulting in the binding of the SIR complex and subsequently to spreading of silencing (Rusche *et al.*, 2003). The observation that nicotine increased both telomeric and *HM* silencing suggested that Rap1 could be the target of this compound. This hypothesis was tested in the next step. The yeast strain *TEL VII-L::ADE2::URA3* (AEY3595) showed weak telomeric silencing, but mutation of *RAP1* enhanced silencing. The addition of 6 mM nicotine led to an increase in telomeric silencing in both strains as indicated by reduced growth on medium lacking uracil and an improved growth on 5-FOA (Figure 53A). Notably, nicotine did not cause a significant change of the cell colour on full medium (data not shown), although repression of the *ADE2* marker gene should result in red coloured cells. This was possibly due to the type of the medium. To determine whether the enhancement of *HM* silencing by nicotine was also Rap1-independent, *hmr::TRP1 rap1-12* cells (AEY567) were used. Since this strain carries a *TRP1* marker gene at the *HMR* locus, it also offered an additional possibility to test whether the potential effect of the compound did not depend on the nature of the marker gene. Due to the mutation of *RAP1*, there was almost no repression of the *TRP1* gene indicated by

maximum growth on YM medium lacking tryptophan and only minimal growth on plates containing 5-fluoroanthranilic acid (5-FAA), which is used for counter-selection of the tryptophan pathway (Figure 53B). However, the cells were able to grow on 5-FAA when 6 mM nicotine was added. On the other hand, the cell growth was reduced on YM medium lacking tryptophan. In general, these results are comparable to those of the corresponding wild-type (AEY581). These cells displayed a strong repression of the *TRP1* marker gene that was improved by the addition of nicotine (Figure 53B), indicating that Rap1 was not required for the enhancement of the *HM* silencing. In summary, the results indicated that nicotine increased not only telomeric but also *HM* silencing *in vivo*, and that this effect was independent of Rap1.

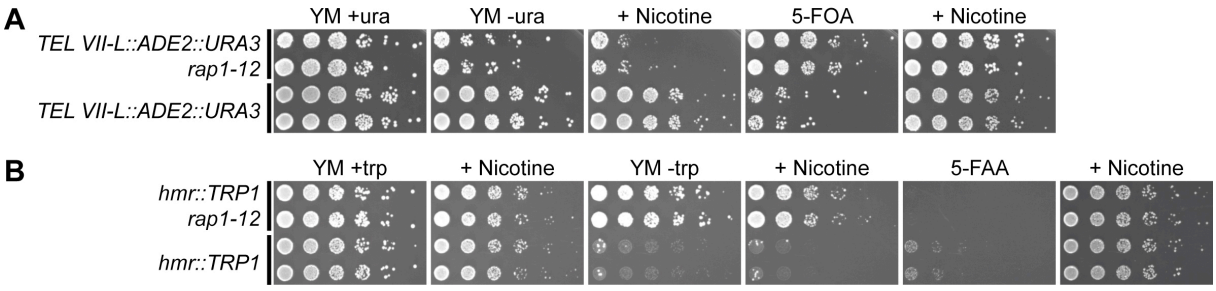

Figure 53 The effect of nicotine was independent of Rap1
(A) Telomeric silencing of a *rap1-12* strain (AEY3590) and its corresponding wild-type (AEY3595), each carrying an *ADE2* and *URA3* marker gene at *TEL VII-L*, was analyzed. Their ability to grow on YM medium lacking uracil and on *URA3*-counter-selective 5-FOA medium, each with and without 6 mM nicotine, was used to determine the strength of *URA3* repression. A six-fold serial dilution of the cells was spotted on the indicated plates and subsequently incubated at 30 °C for two days.
(B) In general, the same method like in (A) was used to determine the *HM* silencing of another *rap1-12* strain (AEY567) and its corresponding wild-type (AEY581), each harbouring a *TRP1* marker gene at the *HMR* locus. In this case, plates containing 5-FAA were used for counter-selection of *TRP1* expression.

3.2.4.4 Nicotine increased rDNA silencing *in vivo*

In *S. cerevisiae*, there are four sirtuins (Sir1 - 4). While Sir1 plays only a role in *HM* silencing, Sir2 - 4 are also involved in the formation of heterochromatin at the telomeres. Furthermore, the HDAC Sir2 is important for rDNA silencing. After excluding Rap1 as a potential target of nicotine (see 3.2.4.3), Sir2 - 4 were the next logical candidates to be analyzed. The potential target could be limited to Sir3 and Sir4, if only telomeric and *HM* silencing, but not rDNA silencing were altered. On the other hand, enhancement of all three types of silencing would point to Sir2 as the target of nicotine. For this reason, the effect of nicotine on rDNA silencing was tested using the yeast strain *RDN::Ty::MET15* (AEY160). These cells carry an *MET15* marker gene at the *RDN1* locus, which encodes the ribosomal DNA in *S. cerevisiae*.

Increased repression of *MET15* should change the colour of the cells from white to brown on lead indicator medium (Cost & Boeke, 1996), as it was already shown for *sas2*Δ cells (Meijsing & Ehrenhofer-Murray, 2001). Therefore, the strain was streaked on this medium with and without 6 mM nicotine using *RDN::Ty::MET15 sas2*Δ*::TRP1* cells (AEY1195) as positive control. However, there was no significant difference between the two strains or between the lead indicator plates with and without nicotine. All cells displayed a weak brown colour (data not shown). This was unexpected, because the "wild-type" cells should at least exhibit a white colour on the plate without the compound. Based on this result, the impact of nicotine on rDNA silencing could not be assessed. Therefore, two yeast strains carrying an *URA3* marker gene at the *RDN1* locus were used in a second approach. The growth of *RDN1::ty1-mURA3* (S2) (AEY1778) and *RDN1::ty1-mURA3* (S6) (AEY1779) cells on 5-FOA plates was equally good on medium lacking uracil indicating weak rDNA silencing (Figure 54, data not shown). The addition of 6 mM nicotine reduced the cell growth on both media, suggesting that the yeast strains were sensitive for this compound in general. However, in comparison to YM medium the growth was less reduced on 5-FOA indicating that the rDNA silencing may be increased by adding nicotine.

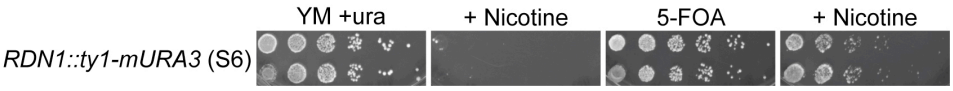

Figure 54 Nicotine increased rDNA silencing *in vivo*
rDNA silencing of the yeast strain *RDN1::ty1-mURA3* (S6) (AEY1779) was analyzed as the ability to grow on YM medium and on URA3-counter-selective 5-FOA medium each with and without 6 mM nicotine. A six-fold serial dilution of the cells was spotted on the indicated plates and subsequently incubated at 30 °C for two days.

3.2.4.5 Nicotine activated Sir2 at low concentrations *in vitro* and enhanced the loss of the marker gene in the absence of Sir2 and Sir3 *in vivo*

The previous experiments suggested that nicotine increased telomeric, *HM*, and rDNA silencing. The only factor that is known to take part in all three types of silencing in *S. cerevisiae* is the NAD^+-dependent HDAC Sir2. For this reason, Sir2 was evaluated as a target of nicotine. To test this hypothesis, a fluorescence-based *in vitro* HDAC assay was performed by Gesine Hoffmann using 6xHIS-tagged yeast Sir2 protein purified from *E. coli* and different concentrations of nicotine. Based on the observation that the Sir2 inhibitor splitomicin reduced telomeric silencing, nicotine

was suggested to activate Sir2. Indeed, final concentrations of 2.5 nM up to 0.5 µM led to a weak activation of Sir2 HDAC activity *in vitro*, while higher concentrations resulted in inhibition (Figure 55). However, these concentrations are much lower than those in the *in vivo* assays, calling into question whether the *in vivo* effects were truly reflected in this *in vitro* assay. Furthermore, the scientific literature is controversial concerning the *in vitro* stimulation of sirtuins (Beher *et al.*, 2009; Haigis & Sinclair, 2010). Therefore, this result must be interpreted with caution. Nevertheless, it is possible that only low amounts of the high concentration used in the *in vivo* experiments enter the cell.

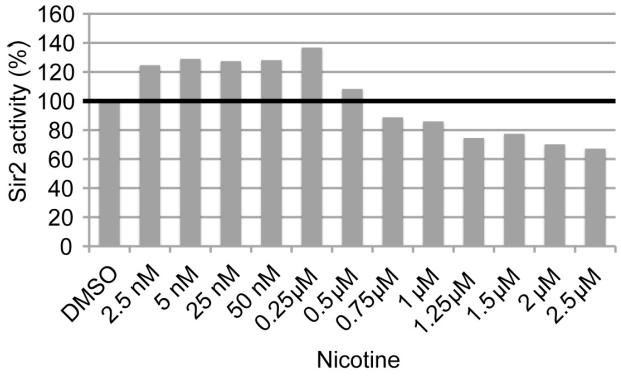

Figure 55 Low concentrations of nicotine activated Sir2 *in vitro*
Sir2 deacetylase activity was measured by Gesine Hoffmann using a fluorescence-based assay. In two consecutive reactions, deacetylation of the substrate MAL generates a fluorophore that is excited at 360 nm and light at 460 nm was emitted. The blank (DMSO) was defined as 100 %.

If nicotine truly increases silencing, then its effect is expected to be abrogated by the deletion of SIR components. Therefore, telomeric silencing of *TEL VII-L::gal4-URA3* cells (AEY3909) with deletions of *SIR2* (AEY4017) or *SIR3* (AEY4019) was investigated. Notably, Sir2 - 4 are essential for silencing, because formation of heterochromatin at the *HM* loci and at the telomeres requires the activity of the SIR complex (Rusche *et al.*, 2003). Accordingly, the analyzed *sir2*Δ and *sir3*Δ cells were not able to grow on 5-FOA, indicating a complete loss of telomeric silencing (Figure 56A). However, they showed maximal growth on 5-FOA when 6 mM nicotine was added. This was unexpected, because there was no Sir2 protein that could be activated by nicotine and therefore no telomeric silencing that could be improved. However, the same result was observed for a *sir1*Δ *sir3*Δ double mutant (AEY1018) that harbours a subtelomeric *URA3* marker gene (Figure 56B). In order to exclude the possibility that these effects depend on the *URA3* marker or the counter-selective 5-FOA medium, *SIR2* was deleted in *TEL IX-L* position 7*::LYS2* cells

(AEY4580). As expected, the *sir2*Δ cells (AEY4583) failed to grow on *LYS2*-counter-selective αAA medium (Figure 56C). Again, maximal growth was achieved by adding 6 mM nicotine, indicating that this was an effect independent of silencing. Notably, the theory that nicotine did not affect (telomeric) silencing, but only improved growth on counter-selective medium by inhibiting the intake of 5-FOA or αAA had seemingly disproved earlier, because it was shown that nicotine enhanced telomeric silencing independently of 5-FOA (see 3.2.4.2).

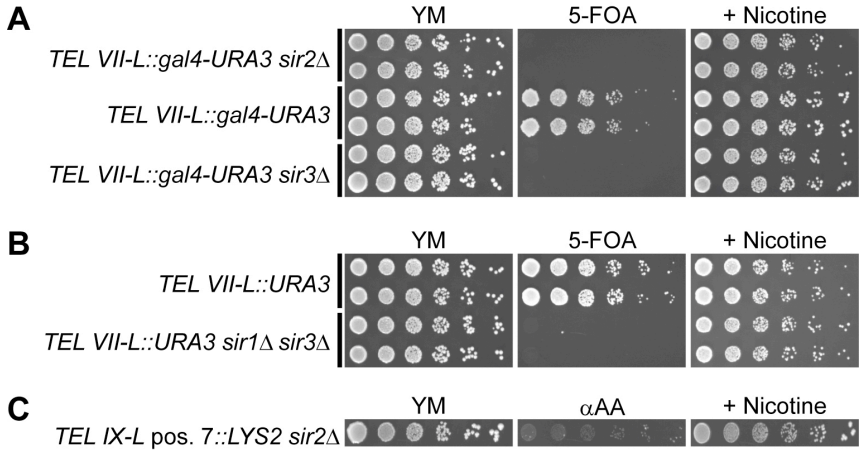

Figure 56 Nicotine improved growth on counter-selective medium even in the absence of Sir2 or Sir3
(A) Serial dilutions of *sir2*Δ (AEY4017) and *sir3*Δ (AEY4019) cells as well as of the corresponding wild-type (AEY3909) were spotted on 5-FOA plates with and without 6 mM nicotine to measure the repression of the (sub-) telomeric *URA3* marker gene.
(B) Telomeric silencing of *sir1*Δ *sir3*Δ double mutants (AEY1018) and the corresponding wild-type strain (AEY1017) was analyzed like described in (A).
(C) *TEL IX-L* position 7*::LYS2 sir2*Δ (AEY4583) cells were serially diluted and spotted on *LYS2*-counter-selective αAA plates with and without 6 mM nicotine to determine telomeric silencing.
All plates were incubated at 30 °C for two days.

Another possible explanation for the results shown in Figure 56 could be the loss of the *URA3*/*LYS2* marker gene/s upon nicotine treatment, which would lead to increased resistance against the counter-selective medium. To test this hypothesis, yeast strains shown in Figure 51 and Figure 56A were taken from 5-FOA plates containing 6 mM nicotine and were re-streaked on full medium and medium lacking uracil. The *TEL VII-L::gal4-URA3* strain (AEY3909) was able to grow on both media. 5-FOA-resistant *sir3*Δ derivates could only grow on full medium, but not on medium lacking uracil (Figure 57A), suggesting that they had lost their *URA3* marker gene. The *TEL XI-L* position 1*::URA3* (AEY4163) cells grew on both media, although growth on medium lacking uracil was slightly reduced (Figure 57B). As these results are in agreement to those shown in Figure 51, this indicated that the addition of

nicotine to counter-selective medium did not generally cause a loss of the marker gene, but only in the absence of Sir2 or Sir3. Since the formation of (sub-) telomeric heterochromatin by the SIR complex shields the chromosome ends for instance from homologous recombination (Smogorzewska & de Lange, 2004), nicotine might increase homologous recombination in the absence of Sir2 and Sir3, thereby leading to the loss of the marker gene.

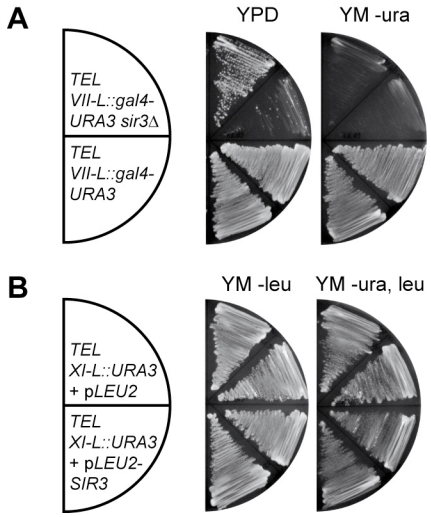

Figure 57 Nicotine enhanced the loss of marker genes in the absence of Sir2 or Sir3
(A) The potential loss of the *URA3* marker gene of the yeast strains shown in Figure 56A was analyzed by taking these cells from 5-FOA plates containing 6 mM nicotine and streaking them out on full medium and on YM medium lacking uracil.
(B) Yeast strains shown in Figure 51 were taken from 5-FOA plates containing 6 mM nicotine and streaked out on YM medium with and without uracil.
All plates were incubated at 30 °C for two days.

3.2.4.6 Nicotine-mediated extension of CLS was Sir2-dependent

As described previously, nicotine was not only found to increase telomeric silencing, but it was also a secondary candidate in the screen for compounds extending the CLS of *S. pombe* (see 3.1.2.1). Based on the observation that low concentrations of nicotine activated *S. cerevisiae* Sir2, while higher concentrations inhibited the enzyme *in vitro* (Figure 55), it was obvious to test whether there is a relationship between Sir2 activity and CLS. Sir2 is the *S. pombe* homolog that is most closely related to the *S. cerevisiae* Sir2 (Shankaranarayana *et al.*, 2003). As in budding yeast, it is reported to be a NAD^+-dependent HDAC that targets H3K9ac and H4K16ac *in vitro*. It is required for silencing at the heterochromatic regions and for the association of Swi6 with these loci *in vivo* (Freeman-Cook *et al.*, 2005; Shankaranarayana *et al.*, 2003), Interestingly, *sir2*Δ *S. pombe* cells treated with

DMSO displayed a reduced CLS compared to wild-type cells (AEP57) in our experiment (Figure 58). The addition of 6 mM nicotine increased the lifespan of wild-type cells but had no effect on the lifespan of *sir2*Δ cells (Figure 58), indicating that the observed lifespan extension by nicotine might be due to an activation of Sir2.

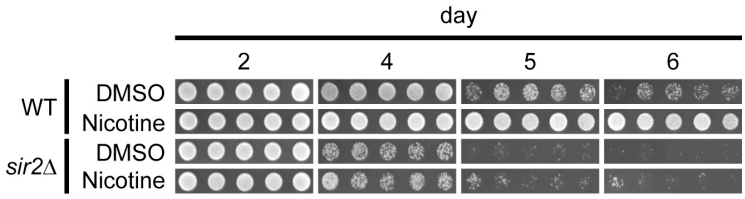

Figure 58 The reduced CLS of *sir2*Δ cells was not extended by the addition of nicotine
S. pombe wild-type (AEP57) and *sir2*Δ cells were grown in YM medium containing 3 % glucose and 6 mM nicotine, each in five adjacent wells of a 96 well microplate. Cells treated with DMSO served as control. At the indicated time points, the aging cultures were spotted onto YES plates that were subsequently incubated for two days at 30 °C.

As a consequence, this led to the question how increased Sir2 activity caused improved CLS. So far, the best-known way of Sir2 to promote longevity is by influencing rDNA recombination and thus ERC formation (Kaeberlein *et al.*, 1999; Steinkraus *et al.*, 2008) (see 1.7). Additionally, the carbonylation of proteins increases with age, and the asymmetric distribution of these oxidatively damaged proteins that are accumulated in the mother cell is Sir2-dependent and associated with accelerated aging in *S. cerevisiae* (Erjavec *et al.*, 2007). Nevertheless, this only affects RLS but not CLS. Furthermore, the age-related accumulation of excised rDNA circles has not been detected in organisms other than budding yeast. In general, it seemed as if Sir2 of *S. pombe* functions differently of that from *S. cerevisiae* because the deletion of *sir2*$^{+}$ shortened the CLS of fission yeast (Mutoh & Kitajima, 2007) (Figure 58), while Sir2 mutation does not reduce the CLS of budding yeast but even extends the lifespan of *sch9*Δ cells (Fabrizio *et al.*, 2005). In addition, it has been reported that Sir2 deficiency does not affect the cellular oxidation state of *S. pombe* as measured by the amount of carbonylated proteins during exponential growth and in stationary phase (Mutoh & Kitajima, 2007). Therefore, one remaining possible explanation for lifespan extension by increased Sir2 activity is improved (telomeric) silencing.

4 Discussion

The aim of this study was to gain new insights into the molecular mechanisms of the aging process by the identification of compounds and gene deletions that extend the CLS of *S. pombe* as well as of compounds that alter telomeric silencing in *S. cerevisiae*. To this end, novel high-throughput methods for the measurement of the CLS of fission yeast and the telomeric silencing in budding yeast were established. The former assay was used to screen a small compound library as well as a *S. pombe* deletion library. We obtained 20 compounds that extended lifespan, of which eight compounds were further analyzed to identify their potential molecular target/s. In the case of the deletion library, we found that it was an unknown factor in the strain background rather than the indicated gene deletions that affected lifespan. In the second approach, we identified nicotine to affect the telomeric silencing in *S. cerevisiae*. Further analyses showed that this compound also increased *HM* and rDNA silencing. Moreover, it was also identified to extend the CLS of *S. pombe*, and *in vitro* as well as *in vivo* experiments suggested that its effect on silencing and CLS is likely to be due to an activation of Sir2.

4.1 Anti-oxidative properties of DIM and mangosteen as the cause of their lifespan-extending effect

Two compounds that were identified in our screen to extend the CLS of *S. pombe* wild-type cells are 3,3'-diindolylmethane (DIM) and mangosteen (3.1.2.1).

DIM is the major acid condensation product of indole-3-carbinol, which is found in *Brassica* vegetables, like broccoli and cauliflower. The supposed healthy effects of these vegetables are attributed at least in part to the activity of DIM. Several studies were performed to analyze its effects, and various potential targets have been identified. In one of these studies, estrogenic as well as anti-androgenic properties of DIM were discovered (Bovee *et al.*, 2008). In addition, DIM was found to display an anti-inflammatory action by up-regulating the expression of interferon gamma (IFNγ) and IFNγ receptor (Riby *et al.*, 2006; Xue *et al.*, 2005) or reducing NF-κB signalling and/or AP-1 signalling (Cho *et al.*, 2008; Kim *et al.*, 2010; Kim *et al.*, 2009). Furthermore, DIM was shown to inhibit the hypoxia inducible factor 1α (HIF-1α) (Riby *et al.*, 2008). Notably, the HIF signalling cascade mediates the effects of hypoxia, the

state of low oxygen concentration, on the cell. Hypoxia promotes the formation of blood vessels and is important for the formation of a vascular system, for instance in cancer tumours. Therefore, DIM displays not only anti-angiogenesis but also anti-cancer activity. The latter is supported by the finding that DIM induces apoptosis in human cancer cells (Ge *et al.*, 1996) and that IFNγ signalling, which is up-regulated by DIM, contributes to the inhibition of primary and transplanted tumour development (Nastala *et al.*, 1994; Street *et al.*, 2001). Therefore, DIM represents a promising anti-tumour agent. Notably, HIF-1α, estrogenic/anti-androgenic activity as well as the inhibition of inflammatory pathways (NF-κB, AP-1) have already been linked to a delay of aging (Leiser & Kaeberlein, 2010; Rodier & Campisi, 2011; Vina *et al.*, 2008). Importantly, no direct homologs of these proteins have been described in yeast so far, indicating that a different mechanism is involved in the observed DIM-mediated extension of *S. pombe* CLS.

However, DIM has been reported to increase the production of ROS (Xue *et al.*, 2008) but also to protect against oxidative stress (Fan *et al.*, 2009). This seemed to be a contradiction, but both statements were in line with our results (3.1.2.2). One possible explanation could be that proteins involved in the oxidative stress response were expressed and/or activated as a result of a DIM-mediated formation of ROS, thereby leading to enhanced stress resistance and extended lifespan. This hypothesis was supported by our observation that cells treated with DIM displayed considerably increased ROS levels during exponential growth that were subsequently reduced in stationary phase (3.1.2.2). Furthermore, the increased ROS level seemed to be the cause at least of the slightly enlarged vacuoles of DIM-treated cells and possibly also of the fragmented acidic compartments (3.1.2.4.2), although the latter needs to be further investigated. Since increased stress resistance is also a result of CR, it was also possible that DIM promotes longevity in fission yeast by affecting the nutrient sensing pathways. This hypothesis was supported by the finding that DIM inhibits both mTOR and Akt in a prostate cancer cell line (Kong *et al.*, 2008). However, the lifespan of wild-type cells treated with rapamycin as well as of *pka1*Δ and *sck2*Δ cells was further extended by the addition of DIM in our experiments (3.1.2.3), indicating that it does not act through the inhibition one of the two known nutrient sensing pathways.

Mangosteen is not a single compound, but a compound mixture extracted from the exocarp the mangosteen fruit (*Garcinia mangostana*). According to present

knowledge, the mangosteen fruit contains the highest amount of naturally occurring xanthones. This type of flavonoids are broad-spectrum antioxidants that have been reported to be even more anti-oxidative than vitamin E, which in turn is one of the most effective antioxidants known so far (Yoshikawa *et al.*, 1994). Since various parts of the mangsteen fruit were used in the folk medicine, mostly in Southeast Asia (Obolskiy *et al.*, 2009), several studies were performed to analyze the containing xanthones in mangosteen. Several beneficial effects were reported: anti-inflammatory (Gopalakrishnan *et al.*, 1980), antimicrobial (Chen *et al.*, 1996; Sundaram *et al.*, 1983), antifungal (Jinsart *et al.*, 1992), antiviral (Chen *et al.*, 1996), anti-tumour (Peres *et al.*, 2000), and anti-allergic properties (Marona *et al.*, 2001). In our study, the four xanthones that are supposed to be the main constituents of the mangosteen fruit, namely α-mangostin, β-mangostin, gartanin, and 8-desoxygartanin did not alter the CLS of *S. pombe* wild-type cells (data not shown). Therefore, it could be assumed that it is probably the interplay of the single compounds or another unidentified component that leads to lifespan-extension. The results of mangosteen-treated cells concerning ROS levels, oxidative stress response, and nutrient sensing pathways were similar to those of DIM-treated cells (see above). As a consequence, the same conclusions could be drawn, namely that the anti-oxidative properties of mangosteen are the most likely explanation for the CLS-extending effect of this compound mixture.

4.2 Inhibition of Git3/PKA signalling and mitochondrial fission as a cause of PGJ_2-mediated CLS-extension

Prostaglandins are tissue hormones that are derived enzymatically from fatty acids and exert their effects by autocrine and paracrine mechanisms (Lupulescu, 1996). Importantly, prostaglandins are not produced by yeast cells, but in humans where they have been reported to inhibit G-protein coupled receptors (Narumiya *et al.*, 1999). Notably, the glucose receptor Git3, which is part of the nutrient sensing pathways in *S. pombe*, is such a transmembrane receptor. In our assay, PGJ_2 failed to extend the CLS of *git3*Δ cells while it increased the lifespan of wild-type cells as well as of all other tested strains carrying deletions of G-protein coupled receptors (3.1.2.1, 3.1.2.4.1). In combination with the observation that the CLS of *pka1*Δ was also not extended by PGJ_2 (3.1.2.3), this led to the suggestion that PGJ_2 promotes

longevity by inhibiting Git3. This hypothesis was confirmed by the enhanced resistance of PGJ_2-treated cells against oxidative stress (3.1.2.2), as a disruption of the Git3/PKA signalling pathway has been described to result in increased stress resistance (Roux *et al.*, 2006).

Importantly, PGJ_2 was the only tested prostaglandin that extended CLS in our assay (3.1.2.4.1), indicating that it might differ from the other prostaglandins, as it was already stated for its derivative 15d-PGJ_2 (Scher & Pillinger, 2005). 15d-PGJ_2 has been shown to inhibit NF-κB signalling (Scher & Pillinger, 2005) like DIM and mangosteen (4.1). Although the inhibition of inflammatory pathways, such as NF-κB, has already been associated with a delay of aging (Rodier & Campisi, 2011), this is probably not the reason for the life-extending effect of PGJ_2, as there are no such inflammatory pathways known in fission yeast.

Furthermore, 15d-PGJ_2 has been shown to induce mitochondrial elongation (Mishra *et al.*, 2010). Mitochondria are dynamic organelles that constantly fuse and divide. These processes are important for mitochondrial inheritance and for the maintenance of mitochondrial functions. The core components of the fusion and fission machineries are evolutionarily conserved. In mammals, the key molecules for mitochondrial fission are Fis1 and Drp1 (Scorrano, 2007). The reciprocal process, mitochondrial fusion, is controlled in mammalian cells by Mitofusin (Mfn) 1/2 and OPA1 (Scorrano, 2007), However, the functional mechanism by which these proteins cooperate to induce mitochondrial fission and fusion remains unidentified. The induction of mitochondrial fusion by 15d-PGJ_2 was a result of the inhibition of mitochondrial fission by modifying Drp1 (Mishra *et al.*, 2010). The homologs of Drp1 and OPA1 in fission yeast are called Dnm1 and Msp1. Notably, PGJ_2 increased the lifespan of *msp1*Δ cells comparable to wild-type cells, but failed to extend the CLS of *dnm1*Δ cells in our assay (3.1.2.4.1). This result indicated that Dnm1 is probably affected by PGJ_2, but since *dnm1*Δ cells displayed a normal CLS (3.1.2.4.1), this might be not the primary cause for the life-extending effect of PGJ_2. Nevertheless, this result was in line with a previous observation that the single deletion of the Dnm1 homolog DRP-1 in *C. elegans* did not affect lifespan (Yang *et al.*, 2011). However, loss of DRP-1 enhances the longevity phenotype of worms carrying mutations of the insulin/IGF-like signalling pathway (*age-1*Δ, *daf-2*Δ) in a DAF-16-dependent manner (Yang *et al.*, 2011). Notably, it has been previously suggested that cells harbouring elongated mitochondria caused by the inhibition of mitochondrial fission show

increased ROS levels (Lee *et al.*, 2007). This is in line with our hypothesis that PGJ_2 might inhibit the mitochondrial fission protein Dnm1, as wild-type cells treated with this compound displayed an increased ROS level in stationary phase (3.1.2.2).

In summary, our results confirmed previous suggestions that there is probably a relationship between at least one nutrient sensing pathway and mitochondrial dynamics and that they cooperate to modulate aging (Yang *et al.*, 2011). Furthermore, PGJ_2 seemed to extend the CLS of *S. pombe* by inhibiting these processes.

4.3 Monensin and Nigericin might promote longevity by affecting the V-ATPase

In this study, the two antibiotics monensin and nigericin isolated from *Streptomyces cinnamonensis* (Haney & Hoehn, 1967) and *Streptomyces hygroscopicus* (DeBoer & Dietz, 1976), respectively, were identified to extend the CLS of *S. pombe* wild-type cells (3.1.2.1). Both have been shown to inhibit androgen receptor signalling, thereby leading to apoptosis in prostate cancer cells (Ketola *et al.*, 2010; Mashima *et al.,* 2010). Since this type of signalling is not known in fission yeast, this is probably not the reason for their life-extending effect in yeast. Both compounds have been reported to be Golgi-disturbing agents (Dinter & Berger, 1998). However, this property might also not be the cause for the increased lifespan, as the CLS of wild-type cells was not altered by brefeldin A, another compound that has been found to inhibit the Golgi apparatus. Furthermore, monensin has previously been shown to increase the generation of intracellular ROS and to induce a transcriptional profile characteristic of an oxidative stress response (Ketola *et al.*, 2010). In line with this, monensin failed to extend the lifespan of *pka1*Δ cells (3.1.2.3), indicating that monensin might promote longevity through the Git3/PKA signalling pathway. However, this could not be confirmed by other experiments, as monensin did not lead to an increased stress resistance as reported for *pka1*Δ cells (Roux *et al.*, 2006), but to a slight sensitivity against oxidative stress in our test (3.1.2.2). In addition, the ROS level of the cells treated with monensin or nigericin was reduced during exponential growth, while it was highly increased in stationary phase (3.1.2.1). Another conclusion from the epistasis analyses is that monensin and nigericin seemed to affect Sir2 homologs in fission yeast (3.1.2.3), an observation that has to

be further investigated. Notably, it was already known that nigericin enhances the antifungal activity of rapamycin in an unknown manner (Fang et al., 2000). In line with this, we found that nigericin as well as the other seven compounds enhanced also the longevity-promoting effect of rapamycin (3.1.2.3), thereby indicating that they act parallel to the TOR signalling pathway.

Monensin is a Na^+/H^+-exchanger, while nigericin displays a higher affinity for potassium cations and acts as K^+/H^+-antiporter (Liu, 1982). Both compounds are polyether ionophores, which disrupt the membrane potential and affect the ionic gradient, which in turn is the motive force of many secondary active transports e.g. of metabolites. Both compounds did not change the extracellular pH-value (3.1.2.4.2), indicating that they do not act on the outer plasma membrane of *S. pombe*. This has already been shown for nigericin in *S. cerevisiae* (Kovac *et al.*, 1982). Furthermore, nigericin has been reported to act selectively on the mitochondrial inner membrane of budding yeast (Kovac *et al.*, 1982) and to induce the hydrolysis of ATP in mitochondria (Estrada *et al.*, 1967). One enzyme that localizes at the inner membrane of mitochondria and is linked to ATP is the F-ATPase, which is also called ATP synthase as it primarily uses the proton gradient to synthesize ATP from ADP. On the other hand, it can also create a proton gradient using the energy gained from the hydrolysis of ATP (Nakanishi-Matsui & Futai, 2008). Therefore, it was possible that nigericin (and monensin) affect the F-ATPase activity. Notably, their impact on this enzyme could not be assessed, as the deletion of F-ATPase subunits (Tim11, Atp14) in strains originating from the *S. pombe* deletion library could not be verified by PCR (data not shown). However, there is a second proton pump, the V-ATPase, which is similar in subunit structure and mechanism, but has different physiological functions (Nakanishi-Matsui *et al.*, 2010). This ATPase is found in the eukaryotic endomembrane system (vacuoles, Golgi apparatus, endosomes, lysosomes, clathrin-coated vesicles). V-ATPases hydrolyse ATP to drive a proton pump, thereby generating a proton gradient, but can not synthesize ATP (Nelson *et al.*, 2000). In general, V-ATPases are involved in a variety of cellular processes such as receptor-mediated endocytosis, protein trafficking, active transport of metabolites, acidification of several intracellular organelles and neurotransmitter release. However, monensin and nigericin did not inhibit the V-ATPase, as they affected neither endocytosis nor the acidification of intracellular compartments compared to cells carrying a deletion of V-ATPase subunits (Vma1/3) (3.1.2.4.2). However, the deletion of *vma1*$^+$ or *vma3*$^+$

led to a shortened lifespan (3.1.2.4.2). Furthermore, monensin and nigericin did not extend the CLS of these cells (3.1.2.4.2), suggesting that these compounds might promote longevity by activating the V-ATPase. One possible explanation could be as follows: The V-ATPase pumps protons into the lumen of e.g. acidic compartments (Figure 59 left). Based on diffusion, the ionophores monensin and nigericin transport protons into the cytoplasm (Figure 59 right). Thereby, they reduce the proton gradient generated by the V-ATPase and provide increased amounts of cytoplasmic protons that in turn could be actively transported across the intracellular membrane by the V-ATPase again.

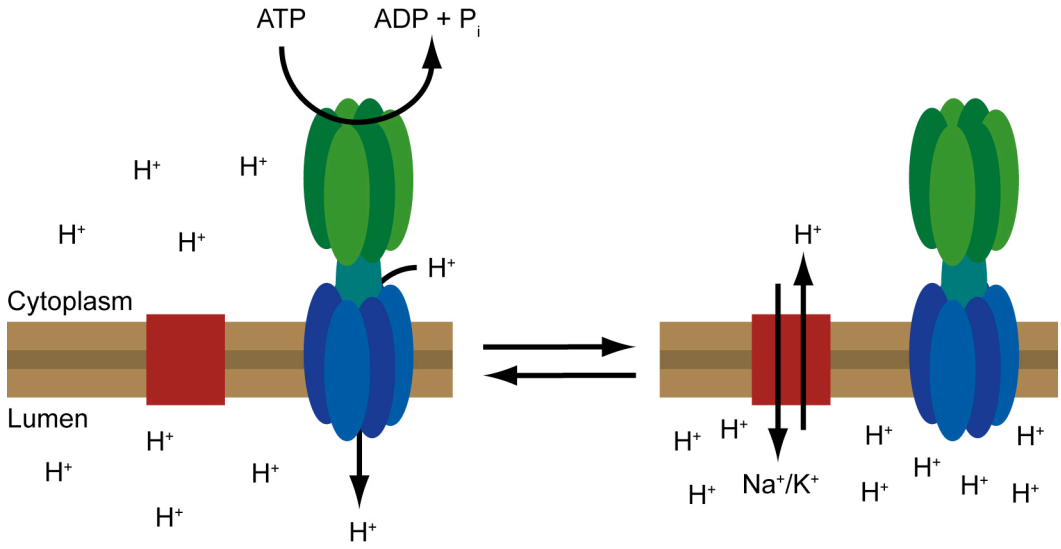

Figure 59 Simplified scheme of the potential interaction of monensin/nigericin and the V-ATPase
The V-ATPase (green/blue) transports protons across the membrane (brown) into the lumen of e.g. acidic compartments in an ATP-dependent manner, thereby generating a proton gradient. Based on diffusion the ionophores monensin and nigericin (red) tranport protons back into the cytoplasm and in return sodium or potassium are transported into the lumen. Thus, the proton gradient is reduced and increased amounts of protons are available in the cytoplasm, which in turn could be actively transported by the V-ATPase again.

4.4 Tschimganine might increase CLS through altering a novel pathway

Tschimganine, which is also called tschimganin or chimganin, was identified to increase the CLS of *S. pombe* wild-type cells (3.1.2.1). It was first isolated from the roots of *Ferula tschimganica*, a plant of the *Umbelliferae* family that is native to Central Asia (Kadyrov *et al.*, 1972). Except for an estrogenic activity (Nazrullaev *et al.*, 2008), little is known about this compound. Tschimgine and tschimganidine are two compounds isolated from plants of the genus *Ferula* whose chemical structure is

similar to tschimganine (Figure 60), and both have been shown to display estrogenic activity (Ikeda *et al.*, 2002; Nazrullaev *et al.*, 2008). Importantly, neither tschimganidine nor tschimgin affected CLS in our assay (data not shown), indicating that the structural differences between tschimganine and tschimganidine/tschimgine play a role in their ability to affect lifespan. Another designation of tschimganine is bornyl vanillate, since it consists of vanillate and a bornyl group (Trusheva *et al.*, 2010) (Figure 60A). In comparison, tschimgine lacks the methoxy group of the vanillate (Figure 60B), thereby forming *p*-hydroxybenzoate, which displays an increased pro-oxidative function compared to vanillate (Simic *et al.*, 2007). Since tschimgine did not increase CLS (data not shown), this indicates that the methoxy group is required for lifespan extension. However, tschimganidine contains this methoxy group (Figure 60C), but did not extend CLS (data not shown), suggesting that the bornyl group might also play a role in the longevity-promoting effect of tschimganine. Notably, the hydrophobic bornyl group of tschimganine might be required for entering the cells, as the hydrophobic effect is important for crossing the lipid bilayer of cell membranes. Since tschimganidine exhibits a more complex structure instead of the bornyl group (Figure 60C), one possible explanation for its missing effect on CLS could be that tschimganidine enters the cell to a lesser extent. Therefore, it could be useful to test higher concentrations of this compound.

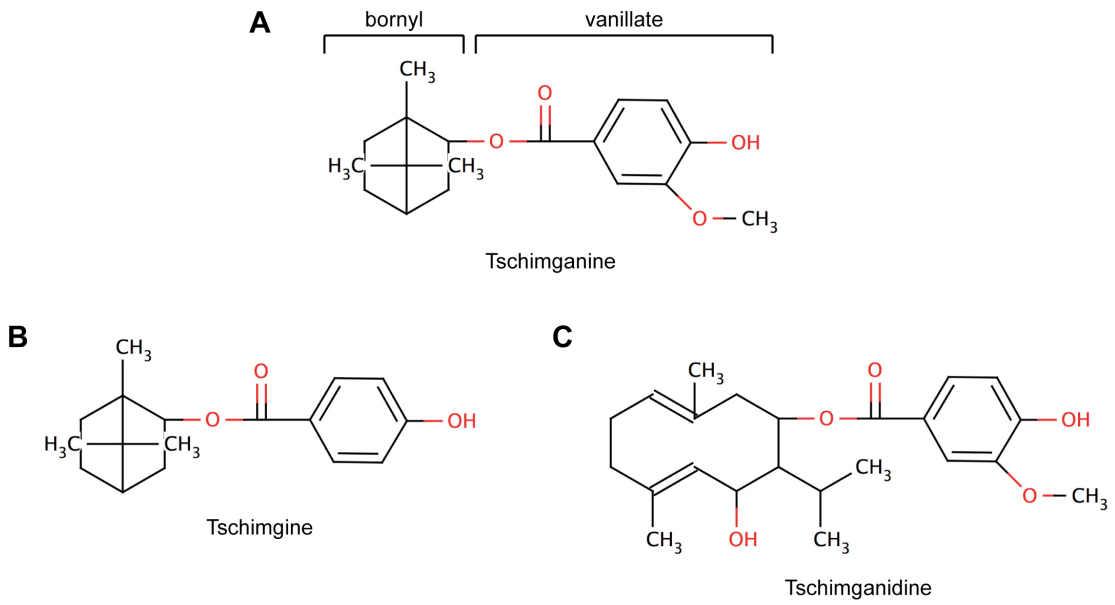

Figure 60 Chemical structures of tschimganine, tschimgine, and tschimganidine
The chemical structures were created by using the software MarvinSketch.

Interestingly, higher levels of estrogens in females have been shown to protect them against aging by up-regulating the expression of anti-oxidative, longevity-related genes and in turn lower ROS levels (Vina *et al.*, 2008). In line with this, tschimganine-treated cells displayed reduced ROS levels during exponential growth as well as in stationary phase (3.1.2.2). However, no direct homologs of estrogen receptors have been described for fission yeast, indicating that it is probably not an estrogenic effect that leads to lifespan extension of tschimganine. Furthermore, this compound increased the resistance against heat and DNA damage, while the resistance against oxidative stress was slightly decreased (3.1.2.2). As tschimganine seemed to extend lifespan parallel to the known nutrient sensing pathways and also independently of the sirtuins Sir2 and Hst2 (3.1.2.3), it might act through a novel pathway.

4.5 Inhibition of the *de novo* purine biosynthesis is not the cause for CLS extension by mycophenolic acid (MPA) and acivicin

Mycophenolic acid (MPA), a product of several *Penicillium* species (Frisvad *et al.*, 2004) that was initially discovered as an antibiotic against Bacillus anthracis (Bentley, 2000) is one of the compounds identified to extend the CLS of *S. pombe* wild-type cells in our screen (3.1.2.1). It has been reported to possess antiviral (Borroto-Esoda *et al.*, 2004; Diamond *et al.*, 2002), antifungal (Nicoletti *et al.*, 2004), antibacterial (Kavanagh, 1947; Torrenegra *et al.*, 2005), antitumor (Tressler *et al.*, 1994; Tsuchiya *et al.*, 2010), and antipsoriasis (Epinette *et al.*, 1987) activities. Most importantly, MPA is a potent and reversible, non-competitive inhibitor of IMP dehydrogenase (IMPDH) (Nakamura *et al.*, 1995), the enzyme that controls the rate of GMP in the *de novo* pathway of purine synthesis (Ransom, 1995) (Figure 61). Notably, B- and T-cells rely entirely on the IMPDH dependent *de novo* pathway for purine biosynthesis, while most other cell types express the IMPDH-independent salvage pathway, which allows purine production despite inhibition of IMPDH by MPA. Therefore, MPA is an immunsuppresive drug used to prevent organ rejection (Morris *et al.*, 1990), which is marketed under the brands CellCept (mycophenolate mofetil; Roche) and Myfortic (mycophenolate sodium; Novartis).

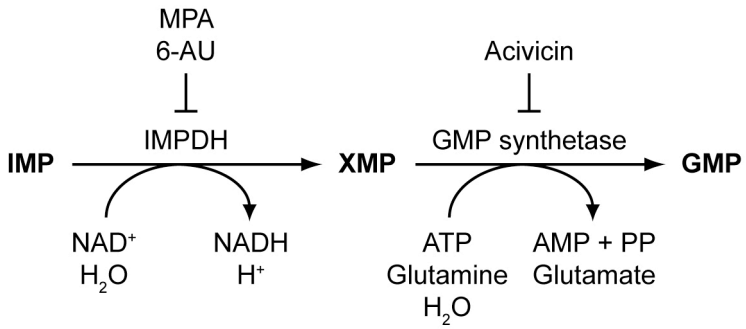

Figure 61 Inhibition of *de novo* GMP biosynthesis by MPA, 6-AU, and acivicin
In the pathway of *de novo* guanosine monophosphate (GMP) biosynthesis, inosine monophosphate (IMP), the basis of adenosine monophosphate (AMP) and GMP, is converted to xanthosine monophosphate (XMP) by the IMP dehydrogenase (IMPDH), which is inhibited by mycophenolic acid (MPA) and 6-azauracil (6-AU). In the next step, GMP is generated from XMP by the GMP synthetase, which is inhibited by acivicin.

Interestingly, there is a second compound identified to extend the CLS of *S. pombe* wild-type cells that also affects the *de novo* pathway for GMP biosynthesis. Acivicin was isolated from the actinobacterium *Streptomyces sviceus* (Martin *et al.*, 1973) and was first studied as an anti-cancer agent that inhibits various glutamine amidotransferases (Tso *et al.*, 1980). However, acivicin is a glutamine analog that selectively and irreversibly abolishes the glutaminase activity of the GMP synthetase by a covalent modification (Nakamura et al., 1995). Notably, there are only two enzymes involved in converting IMP to GMP, namely IMPDH, which catalyzes the oxidation of IMP to XMP and is inhibited by MPA, and the GMP synthetase, which catalyzes the amination of XMP to GMP and is inhibited by acivicin (Figure 61). Since 6-AU, another inhibitor of the IMPDH did not promote longevity (3.1.2.4.3), it is likely that the lifespan extension by MPA and acivicin is not due to an inhibition of the *de novo* purine biosynthesis. This was confirmed by an additional experiment using glutamine. Glutamine is required for the conversion of XMP to GMP by the GMP synthetase (Figure 61). Therefore, increased amounts of glutamine enhance purine synthesis. As this is the opposite effect of MPA and acivicin, it would be expected to reduce lifespan. Contrary to this notion, it led to an extension, which was even further extended by the addition of MPA and acivicin (3.1.2.4.3). This was not only contrary to our expectation, but also to previous studies that reported that reduced cellular glutamine levels increases both CLS and RLS of *S. cerevisiae* (Kaeberlein *et al.*, 2005b; Powers *et al.*, 2006).

In general, there is an additional way to produce purines besides the *de novo* biosynthesis. This so-called salvage pathway uses free guanine as a starting substrate to form GMP. However, as the addition of guanine did not affect the CLS

neither of the control nor the MPA- and acivicin-treated cells (3.1.2.4.3), it is probably not the GMP level that causes the lifespan extension by MPA and acivicin.

Apart from its impact on the GMP synthetase, acivicin is also a specific and the most active inhibitor of γ-glutamyl transpeptidase (Allen *et al.*, 1980), which is of central importance in the metabolism of glutathione (GSH), a pseudotripeptide consisting of glutamate, cysteine, and glycine (Tate, 1980). In this way, this compound inhibits the transmembrane GSH transport (Griffith & Meister, 1980) and thereby the release of the "bound" amino acids into the cytoplasm (Mehdi *et al.*, 2001). Therefore, acivicin might increase lifespan by depleting the level of these amino acids and thus exerting some degree of CR. In this context, it is notable that MPA has been shown to reduce Akt/mTOR signalling (He *et al.*, 2011), indicating that it might also extend CLS by affecting nutrient signalling. In line with this, MPA and acivicin enhanced the resistance against oxidative stress (3.1.2.2) although the ROS level in exponential and stationary phase was increased by treatment with these compounds (3.1.2.2). However, MPA as well as acivicin delayed the growth of *pka1*Δ cells (3.1.2.3). As these cells already displayed a slowed growth, this result suggested that MPA and acivicin might act parallel to the Git3/PKA signalling pathway. Both compounds seemed to increase lifespan independently of the TOR signalling pathway, since CLS of *sck2*Δ cells and of rapamycin-treated wild-type cells was further increased by MPA and acivicin (3.1.2.3). The latter compounds also delayed the growth of *sir2*Δ and *hst2*Δ cells, indicating that it might additionally act parallel to these sirtuins.

In summary, our results suggest that MPA and acivicin might not extend CLS by decreasing GMP levels. Nevertheless, they might lead to some kind of CR without affecting the known nutrient sensing pathways. Furthermore, acivicin seemed to act parallel to the sirtuins Sir2 and Hst2. The exact mechanisms of CLS extension by these compounds remained unclear.

4.6 An unknown factor altered the CLS of strains originating from the *S. pombe* deletion library

In this study, we established a novel high-throughput screen to measure the CLS of many *S. pombe* strains in parallel (3.1.1). Since this assay recapitulated lifespan analyses using the traditional CFU method (3.1.1), we used this new assay to screen

the *S. pombe* deletion library (Bioneer) for gene deletions that extend lifespan. After the primary screen and validation, we found several deletion strains that displayed an increased CLS compared to the control wild-type cells (3.1.3.1). Among these candidates, there were also 13 deletions in genes altering nutrient uptake and sensing. Notably, only lysine and arginine biosynthetic genes were affected (3.1.3.1). This implies that these strains of the deletion library, which are auxotrophic for uracil, adenine, and leucine, carried an additional auxotrophy. Our finding that these mutants exhibited an increased lifespan was consistent with the notion that the deletions impart some kind of CR upon the cells, which was already well established to extend lifespan (Fontana *et al.*, 2010; Roux *et al.*, 2010). We assumed this to be an indication that our new assay identified lifespan-affecting genes and did not further analyze these gene deletions, as similar effects of CR are already known.

We focused our further experiments on the group of strains carrying deletions of genes coding for proteins involved in DNA repair, since lifespan extension caused by defects in DNA repair has not been described so far. However, when mutants were generated by genetic crosses, we observed a strong variability in the CLS of segregants displaying the same genotype (3.1.3.5), indicating that there might be an unknown, non-Mendelian factor that affected the CLS of fission yeast. In line with this, a recent study has shown that there is also a great variance in the RLS of *S. cerevisiae* spores arising from the same tetrad (Unal *et al.*, 2011), although the reason for this variability remained unexplained in that study. Therefore, mixing the segregants with the same genotype might be a possibility to determine their average CLS. After careful analyses, we found that the CLS extension was not caused by the deletion of the DNA repair genes (3.1.3.6). This was also the case for cells where *ppk4*$^{+}$, a gene coding for an protein involved in UPR^{ER}, was deleted (3.1.3.6), indicating that it was not an effect specific for DNA repair mutants. This was unexpected, as it should make no difference whether a deletion is generated in a certain strain by genetic cross, PCR-mediated knock-out or the like.

In summary, our results suggest that there was something in the background of the deletion library that affects lifespan independently of the indicated gene deletions. Possible explanations could be differences in mitochondrial DNA and/or epigenetic modifications, like PTMs on histones. Nevertheless, the strains originating from the *S. pombe* deletion library could be used for a screen in the future to identify the potential molecular target of the compounds found to extend CLS (3.1.2.1). In this

case, the CLS of the deletion strain treated with the compound/s could be compared to that of the same strain treated with DMSO. If no lifespan extension is observed, one could conclude that the compound acts in the same pathway as the respective gene.

4.7 Nicotine increases silencing in *S. cerevisiae* and extends the CLS of *S. pombe*, possibly by activating Sir2

Nicotine is an anti-inflammatory alkaloid found in the nightshade family of plants (*Solanaceae*). Since it functions as an anti-herbivore chemical with particular specificity to insects, it was widely used as an insecticide in the past (Rodgman & Perfetti, 2009). Today, it is best known as a component of cigarettes, where it is responsible for the potential addiction to cigarette smoking, as it binds to nicotinic acetylcholine receptors, thereby increasing the levels of several neurotransmitters. Nicotine has been shown to delay the onset of Parkinson's disease in studies involving monkeys and humans (Quik *et al.*, 2006; Quik *et al.*, 2007). Furthermore, recent studies have reported a protective effect of nicotine itself on neurons due to activation of nicotinic acetylcholine receptors and the PI3K/Akt pathway, thereby reducing inflammation and cell death (Lakhan & Kirchgessner, 2011; Yu *et al.*, 2011). The latter results in decreased degradation of cells containing damaged DNA that may eventually become cancerous. Nevertheless, nicotine on its own does not promote the development of cancer in healthy tissue and to have no mutagenic properties (Doolittle *et al.*, 1995).

However, reduced apoptosis/cell death might also be an explanation for our observation that nicotine increased the CLS of *S. pombe* (3.1.2.1). Our results suggest that this lifespan extension is Sir2-dependent, as nicotine did not affect the CLS of *sir*2Δ cells (3.2.4.6) and low concentrations of this compound activated Sir2 in the *in vitro* fluorescence assay (3.2.4.5). Notably, these concentrations are much lower than those used in the *in vivo* assays. Therefore, this result must be interpreted with caution, especially because the *in vitro* stimulation of sirtuins is controversially discussed (Beher *et al.*, 2009; Haigis & Sinclair, 2010). Nevertheless, it is possible that only low amounts of the high nicotine concentration used in the *in vivo* experiments enter the cell, and that the effective intracellular concentration is thus in the range of Sir2 activation.

Also, increased Sir2 activity can explain our results concerning the impact of nicotine on the silencing of *S. cerevisisae*. Initially, nicotine was found in our high-throughput screen to increase telomeric silencing (3.2.3). The silencing effect was not caused by nicotine-N-oxide, a degradation product of nicotine (3.2.4.1), indicating that it was an effect of nicotine itself and not of a degradation product. Further experiments showed that nicotine also enhanced *HM* silencing, and that this effect was independent of Rap1 (3.2.4.3). Additionally, rDNA silencing was increased by nicotine (3.2.4.4). Since Sir2 is the only factor present at all three heterochromatic loci in *S. cerevisiae* (Rusche *et al.*, 2003), this HDAC was discussed as a potential target of nicotine.

Notably, Sir2 is an NAD^+-dependent HDAC that releases nicotinamide (NAM), 2'-O-acetyl-ADP-ribose (OAADPR), and the deacetylated substrate (Haigis & Sinclair, 2010). It is known that sirtuins are inhibited by NAM, which could be converted to NAD^+ by Pnc1 (Haigis & Sinclair, 2010). Based on the structural similarity between NAM and nicotine (Figure 62), one could argue that nicotine might act by replacing NAM. Although this would be in line with the inhibition of Sir2 by higher nicotine concentrations *in vitro* (3.2.4.5), NAM itself as well as nicotinic acid did not increase the telomeric silencing of *S. cerevisiae* in our assay (10 µM – 12 mM, data not shown), indicating that nicotine might act differently from NAM. In agreement with this, other studies have reported no increase, but a reduction of silencing by 5 mM NAM (Anderson *et al.*, 2003; Gallo *et al.*, 2004).

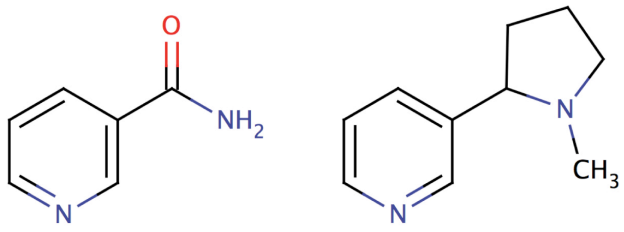

Figure 62 Chemical structures of NAM and nicotine
The chemical structures were created by using the software MarvinSketch.

However, it was remarkable that nicotine improved growth of all *S. cerevisiae* strains, including *sir2*Δ cells, on different types of counter-selective medium (5-FOA, αAA, FAA), regardless of how poorly the cells grew on this medium without nicotine (3.2.4.2 – 3.2.4.5). Importantly, there were also several experiments, where the

increased silencing by nicotine was confirmed independently of counter-selective medium. In these experiments, nicotine reduced the growth on YM medium lacking the supplement corresponding to the marker gene of the analyzed yeast strain (3.2.4.2 - 3.2.4.3), thereby excluding a general improvement of growth. However, cells where *SIR2* is deleted display no silencing, as Sir2 is essential for this process, and they are not able to grow on counter-selective medium. As a consequence, nicotine should have no effect and not improve their growth on this medium. Nevertheless, their growth on counter-selective medium was enabled by the addition of nicotine (3.2.4.5). In contrast to the other tested strains, this was caused by the loss of the marker gene (3.2.4.5), which could be explained by the lack of heterochromatin formation in the absence of Sir2. As a consequence, the repetitive sequences at the telomeres were not protected against homologous recombination, which might be increased by nicotine under these conditions in an unknown manner.

So far, deletion of *SIR2* has primarily been known to reduce the RLS of *S. cerevisiae* by the lack of rDNA silencing leading to the formation of ERCs. However, there were also some hints that link Sir2 and CLS. In this context, *SIR2* deletion in *S. cerevisiae* did not alter the CLS of wild type cells, but extends lifespan of long-lived mutants, like *sch9*Δ (Fabrizio *et al.*, 2005), indicating that there are opposite effects of Sir2 on CLS and RLS. Furthermore, there are differences between *S. cerevisiae* and *S. pombe*, as the deletion of *sir2*+ shortened the CLS of fission yeast (3.2.4.6). In contrast to *S. pombe* wild-type cells, nicotine did not extend the CLS of *sir2*Δ cells (3.2.4.6), suggesting that its longevity-promoting effect in fission yeast is Sir2-dependent.

In summary, our results indicate that nicotine enhanced Sir2 activity, thereby leading to increased silencing at all three heterochromatic loci in *S. cerevisiae* and extended CLS of *S. pombe*. Notably, CLS extension by increased Sir2 activity would confirm that there is another function of Sir2 apart from inhibiting the formation of ERCs that affects yeast lifespan.

4.8 Summary and outlook

In this study, we identified 20 compounds that increased the CLS of *S. pombe*. Eight of them were further investigated. Based on our analyses, we have a concrete hypothesis concerning the molecular targets responsible for the life-extending effect of three of them. To identify the potential targets of the remaining compounds, for instance tschimganine, a haploinsufficiency assay (Giaever *et al.*, 1999) or microarray analysis could be performed using yeast cells treated with the corresponding compound/s. Furthermore, the *S. pombe* deletion library could be screened for potential targets as long as the CLS of the deletion strains treated with the compound/s is only compared to the one of DMSO-treated deletion cells. Notably, for these experiments, high amounts of the compound/s are required. However, the identification of the molecular targets of the longevity-promoting compounds will allow new insights into the mechanisms that regulate the aging process.

We found that PGJ_2 extended the CLS of *S. pombe* wild-type cells but not of *pka1*Δ, *git3*Δ, and *dnm1*Δ cells (3.1.2.3, 3.1.2.4.1). Therefore, we hypothesized that PGJ_2 promoted longevity by inhibiting the Git3/PKA signalling pathway as well as the mitochondrial fission protein Dnm1. To confirm the relationship of nutrient sensing pathways and mitochondrial dynamics in lifespan-extension, the CLS of double mutants carrying deletions of Dnm1 and components of the Git3/PKA signalling pathway could be measured. Notably, it is known that the loss of DRP-1, the worm homolog of Dnm1, increases the CLS of *C. elegans* in a DAF-16 dependent manner (Yang *et al.*, 2011). Since DAF-16 is a stress resistance transcription factor, whose exact homolog in fission yeast is unknown, it could be useful to delete components of the Wis4/Wis1/Sty1 MAP kinase cascade, which is thought to mediate stress resistance, in *dnm1*Δ *S. pombe* cells and to determine the lifespan of these cells.

Two other compounds identified to extend the CLS of *S. pombe* were the ionophores monensin and nigericin. Based on the observation that strains carrying a deletion of genes coding for V-ATPase subunits displayed a shortened lifespan that was not increased by these compounds (3.1.2.4.2), we suggested that monensin and nigericin might extend CLS through activating the V-ATPase. To verify this hypothesis, the CLS of a *S. pombe* strain overexpressing $vma1^+$ or $vma3^+$ could be measured, the expectation being an increased lifespan upon overexpression.

Interestingly, nicotine was not only found in the screen for compounds that extend the CLS of *S. pombe*, but also in the screen for compounds increasing telomeric silencing in *S. cerevisiae* (3.1.2.1, 3.2.3). Further analyses showed that it enhanced the silencing at all three heterochromatic loci in budding yeast (telomeres, *HM* loci, and rDNA locus) (3.2.4.1, 3.2.4.3, 3.2.4.4). Since Sir2 is the only factor involved in all three types of silencing, it was obvious to test whether nicotine affected the activity of this HDAC. The results of the *in vitro* fluorescence assay showed that low concentrations of this compound activated Sir2 (3.2.4.5). The hypothesis that nicotine might act through an activation of Sir2 was supported by the finding that *sir2*Δ *S. pombe* cells displayed a shortened CLS that was not extended by the addition of nicotine (3.2.4.6). However, to ensure the relationship of increased (telomeric) silencing and extended lifespan by a suggested activation of Sir2 through nicotine-treatment, it would be useful to analyze the effect of nicotine on the CLS and/or RLS of *sir2*Δ *S. cerevisiae* cells. Increased telomeric silencing could be a hint for longer telomeres, which in turn are linked to extended lifespan in large eukaryotes. In contrast, there is an inverse correlation between lifespan and telomere length in budding yeast, meaning that cells with longer telomeres displayed a reduced RLS (Austriaco & Guarente, 1997). Therefore, it could be useful to determine the telomere length of *S. pombe* and *S. cerevisiae* cells treated with nicotine. Furthermore, the impact of nicotine on the (telomeric) silencing in *S. pombe* could be examined, as Sir2 is also essential for full transcriptional silencing at the telomeres of fission yeast (Freeman-Cook *et al.*, 2005). To verify that the life-extending effect of nicotine is due to improved Sir2 activity, the CLS of *sir2*$^{+}$ overexpressing *S. pombe* cells could be analyzed, where one expects an increased lifespan.

Importantly, the factors and pathways that affect aging, like the nutrient signalling pathways, are highly conserved throughout evolution (Fontana *et al.*, 2010). Therefore, it is likely that the life-extending effect of the identified compounds is conserved in higher eukaryotes. To test this, their impact on the lifespan of other organisms, like *C. elegans* and/or *D. melanogaster*, could be analyzed. Notably, it would make no sense to use human cell lines, since they are already immortalized.

Finally, the *S. pombe* deletion library should be investigated to identify the unknown factor/s that affect CLS independently of the indicated gene deletions. After doing so, the data obtained from the CLS screen of the deletion library could be re-

evaluated, to eventually identify novel factors that are involved in the regulation of (chronological) lifespan.

5 References

Ahmad, K. & Henikoff, S. (2002). The histone variant H3.3 marks active chromatin by replication-independent nucleosome assembly. *Mol Cell* **9**, 1191-1200.

Ahn, S. H., Cheung, W. L., Hsu, J. Y., Diaz, R. L., Smith, M. M. & Allis, C. D. (2005). Sterile 20 kinase phosphorylates histone H2B at serine 10 during hydrogen peroxide-induced apoptosis in S. cerevisiae. *Cell* **120**, 25-36.

Aljada, A., Dong, L. & Mousa, S. A. (2010). Sirtuin-targeting drugs: Mechanisms of action and potential therapeutic applications. *Curr Opin Investig Drugs* **11**, 1158-1168.

Allen, L., Meck, R. & Yunis, A. (1980). The inhibition of gamma-glutamyl transpeptidase from human pancreatic carcinoma cells by (alpha S,5S)-alpha-amino-3-chloro-4,5-dihydro-5-isoxazoleacetic acid (AT-125; NSC-163501). *Res Commun Chem Pathol Pharmacol* **27**, 175-182.

Allis, C. D., Jenuwein, T. & Reinberg, D. (2007). Overview and Concepts. In *Epigenetics*. Edited by C. D. Allis, T. Jenuwein & D. Reinberg. Cold Spring Harbor: Cold Spring Harbor Laboratory Press.

Anderson, R. M., Bitterman, K. J., Wood, J. G., Medvedik, O. & Sinclair, D. A. (2003). Nicotinamide and PNC1 govern lifespan extension by calorie restriction in Saccharomyces cerevisiae. *Nature* **423**, 181-185.

Andrulis, E. D., Neiman, A. M., Zappulla, D. C. & Sternglanz, R. (1998). Perinuclear localization of chromatin facilitates transcriptional silencing. *Nature* **394**, 592-595.

Anisimov, V. N., Berstein, L. M., Egormin, P. A. & other authors (2008). Metformin slows down aging and extends life span of female SHR mice. *Cell Cycle* **7**, 2769-2773.

Austriaco, N. R., Jr. & Guarente, L. P. (1997). Changes of telomere length cause reciprocal changes in the lifespan of mother cells in Saccharomyces cerevisiae. *Proc Natl Acad Sci U S A* **94**, 9768-9772.

Avner, P. & Heard, E. (2001). X-chromosome inactivation: counting, choice and initiation. *Nat Rev Genet* **2**, 59-67.

Barker, M. G. & Walmsley, R. M. (1999). Replicative ageing in the fission yeast Schizosaccharomyces pombe. *Yeast* **15**, 1511-1518.

Bass, T. M., Weinkove, D., Houthoofd, K., Gems, D. & Partridge, L. (2007). Effects of resveratrol on lifespan in Drosophila melanogaster and Caenorhabditis elegans. *Mech Ageing Dev* **128**, 546-552.

Bauer, J. H., Goupil, S., Garber, G. B. & Helfand, S. L. (2004). An accelerated assay for the identification of lifespan-extending interventions in Drosophila melanogaster. *Proc Natl Acad Sci U S A* **101**, 12980-12985.

Baur, J. A., Pearson, K. J., Price, N. L. & other authors (2006). Resveratrol improves health and survival of mice on a high-calorie diet. *Nature* **444**, 337-342.

Bedalov, A., Gatbonton, T., Irvine, W. P., Gottschling, D. E. & Simon, J. A. (2001). Identification of a small molecule inhibitor of Sir2p. *Proc Natl Acad Sci U S A* **98**, 15113-15118.

Beevers, C. S., Chen, L., Liu, L., Luo, Y., Webster, N. J. & Huang, S. (2009). Curcumin disrupts the Mammalian target of rapamycin-raptor complex. *Cancer Res* **69**, 1000-1008.

Beher, D., Wu, J., Cumine, S., Kim, K. W., Lu, S. C., Atangan, L. & Wang, M. (2009). Resveratrol is not a direct activator of SIRT1 enzyme activity. *Chem Biol Drug Des* **74**, 619-624.

Benedetti, M. G., Foster, A. L., Vantipalli, M. C., White, M. P., Sampayo, J. N., Gill, M. S., Olsen, A. & Lithgow, G. J. (2008). Compounds that confer thermal stress resistance and extended lifespan. *Exp Gerontol* **43**, 882-891.

Bentley, R. (2000). Mycophenolic Acid: a one hundred year odyssey from antibiotic to immunosuppressant. *Chem Rev* **100**, 3801-3826.

Berger, S. L. (2002). Histone modifications in transcriptional regulation. *Curr Opin Genet Dev* **12**, 142-148.

Bernstein, B. E., Meissner, A. & Lander, E. S. (2007). The mammalian epigenome. *Cell* **128**, 669-681.

Bertrand, P., Tishkoff, D. X., Filosi, N., Dasgupta, R. & Kolodner, R. D. (1998). Physical interaction between components of DNA mismatch repair and nucleotide excision repair. *Proc Natl Acad Sci U S A* **95**, 14278-14283.

Bird, A. (2002). DNA methylation patterns and epigenetic memory. *Genes Dev* **16**, 6-21.

Bitterman, K. J., Anderson, R. M., Cohen, H. Y., Latorre-Esteves, M. & Sinclair, D. A. (2002). Inhibition of silencing and accelerated aging by nicotinamide, a putative negative regulator of yeast sir2 and human SIRT1. *J Biol Chem* **277**, 45099-45107.

Bjedov, I., Toivonen, J. M., Kerr, F., Slack, C., Jacobson, J., Foley, A. & Partridge, L. (2010). Mechanisms of life span extension by rapamycin in the fruit fly Drosophila melanogaster. *Cell Metab* **11**, 35-46.

Blander, G. & Guarente, L. (2004). The Sir2 family of protein deacetylases. *Annu Rev Biochem* **73**, 417-435.

Blasco, M. A. (2005). Telomeres and human disease: ageing, cancer and beyond. *Nat Rev Genet* **6**, 611-622.

Borroto-Esoda, K., Myrick, F., Feng, J., Jeffrey, J. & Furman, P. (2004). In vitro combination of amdoxovir and the inosine monophosphate dehydrogenase inhibitors mycophenolic acid and ribavirin demonstrates potent activity against wild-type and drug-resistant variants of human immunodeficiency virus type 1. *Antimicrob Agents Chemother* **48**, 4387-4394.

Botuyan, M. V., Lee, J., Ward, I. M., Kim, J. E., Thompson, J. R., Chen, J. & Mer, G. (2006). Structural basis for the methylation state-specific recognition of histone H4-K20 by 53BP1 and Crb2 in DNA repair. *Cell* **127**, 1361-1373.

Boulton, S. J. & Jackson, S. P. (1996). Identification of a Saccharomyces cerevisiae Ku80 homologue: roles in DNA double strand break rejoining and in telomeric maintenance. *Nucleic Acids Res* **24**, 4639-4648.

Bovee, T. F., Schoonen, W. G., Hamers, A. R., Bento, M. J. & Peijnenburg, A. A. (2008). Screening of synthetic and plant-derived compounds for (anti)estrogenic and (anti)androgenic activities. *Anal Bioanal Chem* **390**, 1111-1119.

Buermeyer, A. B., Deschenes, S. M., Baker, S. M. & Liskay, R. M. (1999). Mammalian DNA mismatch repair. *Annu Rev Genet* **33**, 533-564.

Burnett, C., Valentini, S., Cabreiro, F. & other authors (2011). Absence of effects of Sir2 overexpression on lifespan in C. elegans and Drosophila. *Nature* **477**, 482-485.

Burtner, C. R., Murakami, C. J., Kennedy, B. K. & Kaeberlein, M. (2009). A molecular mechanism of chronological aging in yeast. *Cell Cycle* **8**, 1256-1270.

Chen, B. R. & Runge, K. W. (2009). A new Schizosaccharomyces pombe chronological lifespan assay reveals that caloric restriction promotes efficient cell cycle exit and extends longevity. *Exp Gerontol* **44**, 493-502.

Chen, D., Steele, A. D., Lindquist, S. & Guarente, L. (2005). Increase in activity during calorie restriction requires Sirt1. *Science* **310**, 1641.

Chen, D., Bruno, J., Easlon, E., Lin, S. J., Cheng, H. L., Alt, F. W. & Guarente, L. (2008). Tissue-specific regulation of SIRT1 by calorie restriction. *Genes Dev* **22**, 1753-1757.

Chen, S. X., Wan, M. & Loh, B. N. (1996). Active constituents against HIV-1 protease from Garcinia mangostana. *Planta Med* **62**, 381-382.

Chen, T., Shen, L., Yu, J., Wan, H., Guo, A., Chen, J., Long, Y., Zhao, J. & Pei, G. (2011). Rapamycin and other longevity-promoting compounds enhance the generation of mouse induced pluripotent stem cells. *Aging Cell*.

Cherniack, E. P. (2010). The potential influence of plant polyphenols on the aging process. *Forsch Komplementmed* **17**, 181-187.

Cheung, P., Tanner, K. G., Cheung, W. L., Sassone-Corsi, P., Denu, J. M. & Allis, C. D. (2000). Synergistic coupling of histone H3 phosphorylation and acetylation in response to epidermal growth factor stimulation. *Mol Cell* **5**, 905-915.

Cho, H. J., Seon, M. R., Lee, Y. M., Kim, J., Kim, J. K., Kim, S. G. & Park, J. H. (2008). 3,3'-Diindolylmethane suppresses the inflammatory response to lipopolysaccharide in murine macrophages. *J Nutr* **138**, 17-23.

Cohen, H. Y., Miller, C., Bitterman, K. J. & other authors (2004). Calorie restriction promotes mammalian cell survival by inducing the SIRT1 deacetylase. *Science* **305**, 390-392.

Consortium, I. H. G. S. (2001). Initial sequencing and analysis of the human genome. In *Nature*, pp. 860-921.

Consortium, I. H. G. S. (2004). Finishing the euchromatic sequence of the human genome. *Nature* **431**, 931-945.

Cost, G. J. & Boeke, J. D. (1996). A useful colony colour phenotype associated with the yeast selectable/counter-selectable marker MET15. *Yeast* **12**, 939-941.

Crespo, J. L., Powers, T., Fowler, B. & Hall, M. N. (2002). The TOR-controlled transcription activators GLN3, RTG1, and RTG3 are regulated in response to intracellular levels of glutamine. *Proc Natl Acad Sci U S A* **99**, 6784-6789.

Dang, W., Steffen, K. K., Perry, R., Dorsey, J. A., Johnson, F. B., Shilatifard, A., Kaeberlein, M., Kennedy, B. K. & Berger, S. L. (2009). Histone H4 lysine 16 acetylation regulates cellular lifespan. *Nature* **459**, 802-807.

de Boer, J. & Hoeijmakers, J. H. (2000). Nucleotide excision repair and human syndromes. *Carcinogenesis* **21**, 453-460.

de Boer, J., Andressoo, J. O., de Wit, J. & other authors (2002). Premature aging in mice deficient in DNA repair and transcription. *Science* **296**, 1276-1279.

DeBoer, C. & Dietz, A. (1976). The description and antibiotic production of Streptomyces hygroscopicus var. Geldanus. *J Antibiot (Tokyo)* **29**, 1182-1188.

Demidenko, Z. N., Shtutman, M. & Blagosklonny, M. V. (2009). Pharmacologic inhibition of MEK and PI-3K converges on the mTOR/S6 pathway to decelerate cellular senescence. *Cell Cycle* **8**, 1896-1900.

Diamond, M. S., Zachariah, M. & Harris, E. (2002). Mycophenolic acid inhibits dengue virus infection by preventing replication of viral RNA. *Virology* **304**, 211-221.

Diede, S. J. & Gottschling, D. E. (1999). Telomerase-mediated telomere addition in vivo requires DNA primase and DNA polymerases alpha and delta. *Cell* **99**, 723-733.

Dilova, I., Easlon, E. & Lin, S. J. (2007). Calorie restriction and the nutrient sensing signaling pathways. *Cell Mol Life Sci* **64**, 752-767.

Dinant, C., Houtsmuller, A. B. & Vermeulen, W. (2008). Chromatin structure and DNA damage repair. *Epigenetics Chromatin* **1**, 9.

Dinter, A. & Berger, E. G. (1998). Golgi-disturbing agents. *Histochem Cell Biol* **109**, 571-590.

Dionne, I. & Wellinger, R. J. (1996). Cell cycle-regulated generation of single-stranded G-rich DNA in the absence of telomerase. *Proc Natl Acad Sci U S A* **93**, 13902-13907.

Dolle, M. E., Giese, H., Hopkins, C. L., Martus, H. J., Hausdorff, J. M. & Vijg, J. (1997). Rapid accumulation of genome rearrangements in liver but not in brain of old mice. *Nat Genet* **17**, 431-434.

Donati, G., Gatta, R., Dolfini, D., Fossati, A., Ceribelli, M. & Mantovani, R. (2008). An NF-Y-dependent switch of positive and negative histone methyl marks on CCAAT promoters. *PLoS One* **3**, e2066.

Donze, D. & Kamakaka, R. T. (2001). RNA polymerase III and RNA polymerase II promoter complexes are heterochromatin barriers in Saccharomyces cerevisiae. *EMBO J* **20**, 520-531.

Doolittle, D. J., Winegar, R., Lee, C. K., Caldwell, W. S., Hayes, A. W. & de Bethizy, J. D. (1995). The genotoxic potential of nicotine and its major metabolites. *Mutat Res* **344**, 95-102.

Driscoll, D. J., Waters, M. F., Williams, C. A., Zori, R. T., Glenn, C. C., Avidano, K. M. & Nicholls, R. D. (1992). A DNA methylation imprint, determined by the sex of the parent, distinguishes the Angelman and Prader-Willi syndromes. *Genomics* **13**, 917-924.

Dujon, B. (1996). The yeast genome project: what did we learn? *Trends Genet* **12**, 263-270.

Ehrenhofer-Murray, A. E. (2004). Chromatin dynamics at DNA replication, transcription and repair. *Eur J Biochem* **271**, 2335-2349.

Eisenberg, T., Knauer, H., Schauer, A. & other authors (2009). Induction of autophagy by spermidine promotes longevity. *Nat Cell Biol* **11**, 1305-1314.

Epinette, W. W., Parker, C. M., Jones, E. L. & Greist, M. C. (1987). Mycophenolic acid for psoriasis. A review of pharmacology, long-term efficacy, and safety. *J Am Acad Dermatol* **17**, 962-971.

Erjavec, N., Larsson, L., Grantham, J. & Nystrom, T. (2007). Accelerated aging and failure to segregate damaged proteins in Sir2 mutants can be suppressed by overproducing the protein aggregation-remodeling factor Hsp104p. *Genes Dev* **21**, 2410-2421.

Erjavec, N., Cvijovic, M., Klipp, E. & Nystrom, T. (2008). Selective benefits of damage partitioning in unicellular systems and its effects on aging. *Proc Natl Acad Sci U S A* **105**, 18764-18769.

Estrada, O. S., Graven, S. N. & Lardy, H. A. (1967). Potassium Ion-dependent hydrolysis of adenosine triphosphate induced by nigericin in mitochondria. *J Biol Chem* **242**, 2925-2932.

Evason, K., Collins, J. J., Huang, C., Hughes, S. & Kornfeld, K. (2008). Valproic acid extends Caenorhabditis elegans lifespan. *Aging Cell* **7**, 305-317.

Exinger, F. & Lacroute, F. (1992). 6-Azauracil inhibition of GTP biosynthesis in Saccharomyces cerevisiae. *Curr Genet* **22**, 9-11.

Fabrizio, P. & Longo, V. D. (2003). The chronological life span of Saccharomyces cerevisiae. *Aging Cell* **2**, 73-81.

Fabrizio, P., Gattazzo, C., Battistella, L., Wei, M., Cheng, C., McGrew, K. & Longo, V. D. (2005). Sir2 blocks extreme life-span extension. *Cell* **123**, 655-667.

Fan, S., Meng, Q., Saha, T., Sarkar, F. H. & Rosen, E. M. (2009). Low concentrations of diindolylmethane, a metabolite of indole-3-carbinol, protect against oxidative stress in a BRCA1-dependent manner. *Cancer Res* **69**, 6083-6091.

Fang, A., Wong, G. K. & Demain, A. L. (2000). Enhancement of the antifungal activity of rapamycin by the coproduced elaiophylin and nigericin. *J Antibiot (Tokyo)* **53**, 158-162.

Feldman, M. E. & Shokat, K. M. (2010). New inhibitors of the PI3K-Akt-mTOR pathway: insights into mTOR signaling from a new generation of Tor Kinase Domain Inhibitors (TORKinibs). *Curr Top Microbiol Immunol* **347**, 241-262.

Fleck, O., Lehmann, E., Schar, P. & Kohli, J. (1999). Involvement of nucleotide-excision repair in msh2 pms1-independent mismatch repair. *Nat Genet* **21**, 314-317.

Fontana, L., Partridge, L. & Longo, V. D. (2010). Extending healthy life span--from yeast to humans. *Science* **328**, 321-326.

Fourel, G., Revardel, E., Koering, C. E. & Gilson, E. (1999). Cohabitation of insulators and silencing elements in yeast subtelomeric regions. *EMBO J* **18**, 2522-2537.

Fraga, M. F., Ballestar, E., Villar-Garea, A. & other authors (2005). Loss of acetylation at Lys16 and trimethylation at Lys20 of histone H4 is a common hallmark of human cancer. *Nat Genet* **37**, 391-400.

Franke, J., Gehlen, J. & Ehrenhofer-Murray, A. E. (2008). Hypermethylation of yeast telomerase RNA by the snRNA and snoRNA methyltransferase Tgs1. *J Cell Sci* **121**, 3553-3560.

Freeman-Cook, L. L., Gomez, E. B., Spedale, E. J., Marlett, J., Forsburg, S. L., Pillus, L. & Laurenson, P. (2005). Conserved locus-specific silencing functions of Schizosaccharomyces pombe sir2+. *Genetics* **169**, 1243-1260.

Frisvad, J. C., Smedsgaard, J., Larsen, T. O. & Samson, R. A. (2004). Mycotoxins, drugs and other extrolites produced by species in *Penicillium* subgenus *Penicillium Studies in Mycology* **49**, 201-241.

Fukuda, H., Sano, N., Muto, S. & Horikoshi, M. (2006). Simple histone acetylation plays a complex role in the regulation of gene expression. *Brief Funct Genomic Proteomic* **5**, 190-208.

Fukumoto, Y., Hiyama, H., Yokoi, M., Nakaseko, Y., Yanagida, M. & Hanaoka, F. (2002). Two budding yeast RAD4 homologs in fission yeast play different roles in the repair of UV-induced DNA damage. *DNA Repair (Amst)* **1**, 833-845.

Gallo, C. M., Smith, D. L., Jr. & Smith, J. S. (2004). Nicotinamide clearance by Pnc1 directly regulates Sir2-mediated silencing and longevity. *Mol Cell Biol* **24**, 1301-1312.

Galy, V., Olivo-Marin, J. C., Scherthan, H., Doye, V., Rascalou, N. & Nehrbass, U. (2000). Nuclear pore complexes in the organization of silent telomeric chromatin. *Nature* **403**, 108-112.

Ganley, A. R., Ide, S., Saka, K. & Kobayashi, T. (2009). The effect of replication initiation on gene amplification in the rDNA and its relationship to aging. *Mol Cell* **35**, 683-693.

Ge, X., Yannai, S., Rennert, G., Gruener, N. & Fares, F. A. (1996). 3,3'-Diindolylmethane induces apoptosis in human cancer cells. *Biochem Biophys Res Commun* **228**, 153-158.

Gey, M. H. (2008). *Instrumentelle Analytik und Bioanalytik*, 2nd edn. Berlin: Springer Verlag.

Giaever, G., Shoemaker, D. D., Jones, T. W., Liang, H., Winzeler, E. A., Astromoff, A. & Davis, R. W. (1999). Genomic profiling of drug sensitivities via induced haploinsufficiency. *Nat Genet* **21**, 278-283.

Gilson, E., Laroche, T. & Gasser, S. M. (1993). Telomeres and the functional architecture of the nucleus. *Trends Cell Biol* **3**, 128-134.

Gilson, E. & Geli, V. (2007). How telomeres are replicated. *Nat Rev Mol Cell Biol* **8**, 825-838.

Goffeau, A., Barrell, B. G., Bussey, H. & other authors (1996). Life with 6000 genes. *Science* **274**, 546, 563-547.

Goldberg, A. A., Richard, V. R., Kyryakov, P. & other authors (2010). Chemical genetic screen identifies lithocholic acid as an anti-aging compound that extends yeast chronological life span in a TOR-independent manner, by modulating housekeeping longevity assurance processes. *Aging (Albany NY)* **2**, 393-414.

Gopalakrishnan, C., Shankaranarayanan, D., Kameswaran, L. & Nazimudeen, S. K. (1980). Effect of mangostin, a xanthone from Garcinia mangostana Linn. in immunopathological & inflammatory reactions. *Indian J Exp Biol* **18**, 843-846.

Gottlieb, S. & Esposito, R. E. (1989). A new role for a yeast transcriptional silencer gene, SIR2, in regulation of recombination in ribosomal DNA. *Cell* **56**, 771-776.

Gottschling, D. E., Aparicio, O. M., Billington, B. L. & Zakian, V. A. (1990). Position effect at S. cerevisiae telomeres: reversible repression of Pol II transcription. *Cell* **63**, 751-762.

Grant, P. A. & Berger, S. L. (1999). Histone acetyltransferase complexes. *Semin Cell Dev Biol* **10**, 169-177.

Griffith, O. W. & Meister, A. (1980). Excretion of cysteine and gamma-glutamylcysteine moieties in human and experimental animal gamma-glutamyl transpeptidase deficiency. *Proc Natl Acad Sci U S A* **77**, 3384-3387.

Grossi, S., Puglisi, A., Dmitriev, P. V., Lopes, M. & Shore, D. (2004). Pol12, the B subunit of DNA polymerase alpha, functions in both telomere capping and length regulation. *Genes Dev* **18**, 992-1006.

Grozinger, C. M. & Schreiber, S. L. (2002). Deacetylase enzymes: biological functions and the use of small-molecule inhibitors. *Chem Biol* **9**, 3-16.

Gruber, J., Tang, S. Y. & Halliwell, B. (2007). Evidence for a trade-off between survival and fitness caused by resveratrol treatment of Caenorhabditis elegans. *Ann N Y Acad Sci* **1100**, 530-542.

Grunstein, M. & Gasser, S. M. (2007). Epigenetics in *Saccharomyces cerevisiae*. In *Epigenetics*. Edited by C. D. Allis, T. Jenuwein & D. Reinberg. Cold Spring Harbor: Cold Spring Harbor Laboratory Press.

Gurtner, A., Fuschi, P., Magi, F., Colussi, C., Gaetano, C., Dobbelstein, M., Sacchi, A. & Piaggio, G. (2008). NF-Y dependent epigenetic modifications discriminate between proliferating and postmitotic tissue. *PLoS One* **3**, e2047.

Ha, C. W. & Huh, W. K. (2011). Rapamycin increases rDNA stability by enhancing association of Sir2 with rDNA in Saccharomyces cerevisiae. *Nucleic Acids Res* **39**, 1336-1350.

Haigis, M. C. & Sinclair, D. A. (2010). Mammalian sirtuins: biological insights and disease relevance. *Annu Rev Pathol* **5**, 253-295.

Hall, I. M., Shankaranarayana, G. D., Noma, K., Ayoub, N., Cohen, A. & Grewal, S. I. (2002). Establishment and maintenance of a heterochromatin domain. *Science* **297**, 2232-2237.

Haney, M. E., Jr. & Hoehn, M. M. (1967). Monensin, a new biologically active compound. I. Discovery and isolation. *Antimicrob Agents Chemother (Bethesda)* **7**, 349-352.

Harman, D. (1956). Aging: a theory based on free radical and radiation chemistry. *J Gerontol* **11**, 298-300.

Harrison, D. E., Strong, R., Sharp, Z. D. & other authors (2009). Rapamycin fed late in life extends lifespan in genetically heterogeneous mice. *Nature* **460**, 392-395.

He, X., Smeets, R. L., Koenen, H. J., Vink, P. M., Wagenaars, J., Boots, A. M. & Joosten, I. (2011). Mycophenolic acid-mediated suppression of human CD4+ T cells: more than mere guanine nucleotide deprivation. *Am J Transplant* **11**, 439-449.

Hecht, A., Laroche, T., Strahl-Bolsinger, S., Gasser, S. M. & Grunstein, M. (1995). Histone H3 and H4 N-termini interact with SIR3 and SIR4 proteins: a molecular model for the formation of heterochromatin in yeast. *Cell* **80**, 583-592.

Heltweg, B., Dequiedt, F., Verdin, E. & Jung, M. (2003). Nonisotopic substrate for assaying both human zinc and NAD+-dependent histone deacetylases. *Anal Biochem* **319**, 42-48.

Heltweg, B. & Jung, M. (2003). A homogeneous nonisotopic histone deacetylase activity assay. *J Biomol Screen* **8**, 89-95.

Herman, J. G., Umar, A., Polyak, K. & other authors (1998). Incidence and functional consequences of hMLH1 promoter hypermethylation in colorectal carcinoma. *Proc Natl Acad Sci U S A* **95**, 6870-6875.

Herskowitz, I., Hicks, J. B. & Rine, J. (1977). *Mating type interconversion in yeast and its relationship to development in higher eukaryotes*. New York: Academic Press.

Howard, G., Eiges, R., Gaudet, F., Jaenisch, R. & Eden, A. (2008). Activation and transposition of endogenous retroviral elements in hypomethylation induced tumors in mice. *Oncogene* **27**, 404-408.

Howitz, K. T., Bitterman, K. J., Cohen, H. Y. & other authors (2003). Small molecule activators of sirtuins extend Saccharomyces cerevisiae lifespan. *Nature* **425**, 191-196.

Huang, S. & Houghton, P. J. (2001). Mechanisms of resistance to rapamycins. *Drug Resist Updat* **4**, 378-391.

Huang, S., Bjornsti, M. A. & Houghton, P. J. (2003). Rapamycins: mechanism of action and cellular resistance. *Cancer Biol Ther* **2**, 222-232.

Ikeda, K., Arao, Y., Otsuka, H., Nomoto, S., Horiguchi, H., Kato, S. & Kayama, F. (2002). Terpenoids found in the umbelliferae family act as agonists/antagonists for ER(alpha) and ERbeta: differential transcription activity between ferutinine-liganded ER(alpha) and ERbeta. *Biochem Biophys Res Commun* **291**, 354-360.

Imai, S., Armstrong, C. M., Kaeberlein, M. & Guarente, L. (2000a). Transcriptional silencing and longevity protein Sir2 is an NAD-dependent histone deacetylase. *Nature* **403**, 795-800.

Imai, S., Johnson, F. B., Marciniak, R. A., McVey, M., Park, P. U. & Guarente, L. (2000b). Sir2: an NAD-dependent histone deacetylase that connects chromatin silencing, metabolism, and aging. *Cold Spring Harb Symp Quant Biol* **65**, 297-302.

Ishii, K., Arib, G., Lin, C., Van Houwe, G. & Laemmli, U. K. (2002). Chromatin boundaries in budding yeast: the nuclear pore connection. *Cell* **109**, 551-562.

Iwaki, T., Osawa, F., Onishi, M., Koga, T., Fujita, Y., Hosomi, A., Tanaka, N., Fukui, Y. & Takegawa, K. (2003). Characterization of vps33+, a gene required for vacuolar biogenesis and protein sorting in Schizosaccharomyces pombe. *Yeast* **20**, 845-855.

Iwaki, T., Goa, T., Tanaka, N. & Takegawa, K. (2004). Characterization of Schizosaccharomyces pombe mutants defective in vacuolar acidification and protein sorting. *Mol Genet Genomics* **271**, 197-207.

Jenuwein, T. & Allis, C. D. (2001). Translating the histone code. *Science* **293**, 1074-1080.

Jinsart, W., Ternai, B., Buddhasukh, D. & Polya, G. M. (1992). Inhibition of wheat embryo calcium-dependent protein kinase and other kinases by mangostin and gamma-mangostin. *Phytochemistry* **31**, 3711-3713.

Kadyrov, A. S., Khasanov, T. K., Saidkhodzhaev, A. I. & Nikonov, G. K. (1972). New Phenolic Compounds of the Roots of Ferula tschimganica. *Chemistry of Natural Compounds* **8**, 796-797.

Kaeberlein, M., McVey, M. & Guarente, L. (1999). The SIR2/3/4 complex and SIR2 alone promote longevity in Saccharomyces cerevisiae by two different mechanisms. *Genes Dev* **13**, 2570-2580.

Kaeberlein, M., Kirkland, K. T., Fields, S. & Kennedy, B. K. (2004). Sir2-independent life span extension by calorie restriction in yeast. *PLoS Biol* **2**, E296.

Kaeberlein, M., McDonagh, T., Heltweg, B. & other authors (2005a). Substrate-specific activation of sirtuins by resveratrol. *J Biol Chem* **280**, 17038-17045.

Kaeberlein, M., Powers, R. W., 3rd, Steffen, K. K. & other authors (2005b). Regulation of yeast replicative life span by TOR and Sch9 in response to nutrients. *Science* **310**, 1193-1196.

Kanamitsu, K. & Ikeda, S. (2010). Early Steps in the DNA Base Excision Repair Pathway of a Fission Yeast Schizosaccharomyces pombe. *J Nucleic Acids* **2010**.

Karachentsev, D., Sarma, K., Reinberg, D. & Steward, R. (2005). PR-Set7-dependent methylation of histone H4 Lys 20 functions in repression of gene expression and is essential for mitosis. *Genes Dev* **19**, 431-435.

Kavanagh, F. (1947). Activities of Twenty-two Antibacterial Substances against Nine Species of Bacteria. *J Bacteriol* **54**, 761-766.

Ketola, K., Vainio, P., Fey, V., Kallioniemi, O. & Iljin, K. (2010). Monensin is a potent inducer of oxidative stress and inhibitor of androgen signaling leading to apoptosis in prostate cancer cells. *Mol Cancer Ther* **9**, 3175-3185.

Kim, E. J., Park, H., Kim, J. & Park, J. H. (2010). 3,3'-diindolylmethane suppresses 12-O-tetradecanoylphorbol-13-acetate-induced inflammation and tumor promotion in mouse skin via the downregulation of inflammatory mediators. *Mol Carcinog* **49**, 672-683.

Kim, Y. H., Kwon, H. S., Kim, D. H., Shin, E. K., Kang, Y. H., Park, J. H., Shin, H. K. & Kim, J. K. (2009). 3,3'-diindolylmethane attenuates colonic inflammation and tumorigenesis in mice. *Inflamm Bowel Dis* **15**, 1164-1173.

Kimura, A., Umehara, T. & Horikoshi, M. (2002). Chromosomal gradient of histone acetylation established by Sas2p and Sir2p functions as a shield against gene silencing. *Nat Genet* **32**, 370-377.

Klebe, R. J., Harriss, J. V., Sharp, Z. D. & Douglas, M. G. (1983). A general method for polyethylene-glycol-induced genetic transformation of bacteria and yeast. *Gene* **25**, 333-341.

Kong, D., Banerjee, S., Huang, W., Li, Y., Wang, Z., Kim, H. R. & Sarkar, F. H. (2008). Mammalian target of rapamycin repression by 3,3'-diindolylmethane inhibits invasion and angiogenesis in platelet-derived growth factor-D-overexpressing PC3 cells. *Cancer Res* **68**, 1927-1934.

Kornberg, R. D. (1974). Chromatin structure: a repeating unit of histones and DNA. *Science* **184**, 868-871.

Kouzarides, T. (2007). Chromatin modifications and their function. *Cell* **128**, 693-705.

Kovac, L., Bohmerova, E. & Butko, P. (1982). Ionophores and intact cells. I. Valinomycin and nigericin act preferentially on mitochondria and not on the plasma membrane of Saccharomyces cerevisiae. *Biochim Biophys Acta* **721**, 341-348.

Kozak, M. L., Chavez, A., Dang, W., Berger, S. L., Ashok, A., Guo, X. & Johnson, F. B. (2010). Inactivation of the Sas2 histone acetyltransferase delays senescence driven by telomere dysfunction. *EMBO J* **29**, 158-170.

Kunz, C. & Fleck, O. (2001). Role of the DNA repair nucleases Rad13, Rad2 and Uve1 of Schizosaccharomyces pombe in mismatch correction. *J Mol Biol* **313**, 241-253.

Kurdistani, S. K., Robyr, D., Tavazoie, S. & Grunstein, M. (2002). Genome-wide binding map of the histone deacetylase Rpd3 in yeast. *Nat Genet* **31**, 248-254.

Ladurner, A. G., Inouye, C., Jain, R. & Tjian, R. (2003). Bromodomains mediate an acetyl-histone encoded antisilencing function at heterochromatin boundaries. *Mol Cell* **11**, 365-376.

Laemmli, U. K. (1970). Cleavage of structural proteins during the assembly of the head of bacteriophage T4. *Nature* **227**, 680-685.

Lai, S. R., Phipps, S. M., Liu, L., Andrews, L. G. & Tollefsbol, T. O. (2005). Epigenetic control of telomerase and modes of telomere maintenance in aging and abnormal systems. *Front Biosci* **10**, 1779-1796.

Lakhan, S. E. & Kirchgessner, A. (2011). Anti-inflammatory effects of nicotine in obesity and ulcerative colitis. *J Transl Med* **9**, 129.

Lans, H., Marteijn, J. A., Schumacher, B., Hoeijmakers, J. H., Jansen, G. & Vermeulen, W. (2010). Involvement of global genome repair, transcription coupled repair, and chromatin remodeling in UV DNA damage response changes during development. *PLoS Genet* **6**, e1000941.

Laroche, T., Martin, S. G., Gotta, M., Gorham, H. C., Pryde, F. E., Louis, E. J. & Gasser, S. M. (1998). Mutation of yeast Ku genes disrupts the subnuclear organization of telomeres. *Curr Biol* **8**, 653-656.

Lee, S., Jeong, S. Y., Lim, W. C., Kim, S., Park, Y. Y., Sun, X., Youle, R. J. & Cho, H. (2007). Mitochondrial fission and fusion mediators, hFis1 and OPA1, modulate cellular senescence. *J Biol Chem* **282**, 22977-22983.

Leiser, S. F. & Kaeberlein, M. (2010). The hypoxia-inducible factor HIF-1 functions as both a positive and negative modulator of aging. *Biol Chem* **391**, 1131-1137.

Li, G. M. (2008). Mechanisms and functions of DNA mismatch repair. *Cell Res* **18**, 85-98.

Li, Y., Xu, W., McBurney, M. W. & Longo, V. D. (2008). SirT1 inhibition reduces IGF-I/IRS-2/Ras/ERK1/2 signaling and protects neurons. *Cell Metab* **8**, 38-48.

Lithgow, G. J. (2006). Why aging isn't regulated: a lamentation on the use of language in aging literature. *Exp Gerontol* **41**, 890-893.

Liu, B., Nicolaides, N. C., Markowitz, S. & other authors (1995). Mismatch repair gene defects in sporadic colorectal cancers with microsatellite instability. *Nat Genet* **9**, 48-55.

Liu, C.-M. (1982). Microbial aspects of polyether antibiotics: activity, production and biosynthesis. In *Polyether Antibiotics: Naturally Occurring Acid Ionophores*, pp. 43-102. Edited by J. W. Westley. New York and Basel: Marcel Dekker, Inc.

Liu, L., Wylie, R. C., Andrews, L. G. & Tollefsbol, T. O. (2003). Aging, cancer and nutrition: the DNA methylation connection. *Mech Ageing Dev* **124**, 989-998.

Liu, L. & Rando, T. A. (2011). Manifestations and mechanisms of stem cell aging. *J Cell Biol* **193**, 257-266.

Liu, Q., Leng, X. H., Newman, P. R., Vasilyeva, E., Kane, P. M. & Forgac, M. (1997). Site-directed mutagenesis of the yeast V-ATPase A subunit. *J Biol Chem* **272**, 11750-11756.

Lo, W. S., Trievel, R. C., Rojas, J. R., Duggan, L., Hsu, J. Y., Allis, C. D., Marmorstein, R. & Berger, S. L. (2000). Phosphorylation of serine 10 in histone H3 is functionally linked in vitro and in vivo to Gcn5-mediated acetylation at lysine 14. *Mol Cell* **5**, 917-926.

Longo, V. D. (2010). Reprogramming Cell Survival and Longevity: The Role of Tor, Sch9, Ras, and Sir2. In *Life-Span Extension: Single-Cell Organisms to Man*. Edited by C. Sell, A. Lorenzini & H. M. Brown-Borg. New York: Humana Press.

Loo, S. & Rine, J. (1994). Silencers and domains of generalized repression. *Science* **264**, 1768-1771.

Luger, K., Mader, A. W., Richmond, R. K., Sargent, D. F. & Richmond, T. J. (1997a). Crystal structure of the nucleosome core particle at 2.8 A resolution. *Nature* **389**, 251-260.

Luger, K., Rechsteiner, T. J., Flaus, A. J., Waye, M. M. & Richmond, T. J. (1997b). Characterization of nucleosome core particles containing histone proteins made in bacteria. *J Mol Biol* **272**, 301-311.

Luo, J., Nikolaev, A. Y., Imai, S., Chen, D., Su, F., Shiloh, A., Guarente, L. & Gu, W. (2001). Negative control of p53 by Sir2alpha promotes cell survival under stress. *Cell* **107**, 137-148.

Lupulescu, A. (1996). Prostaglandins, their inhibitors and cancer. *Prostaglandins Leukot Essent Fatty Acids* **54**, 83-94.

Lustig, A. J. (1998). Mechanisms of silencing in Saccharomyces cerevisiae. *Curr Opin Genet Dev* **8**, 233-239.

Maclean, M. J., Aamodt, R., Harris, N., Alseth, I., Seeberg, E., Bjoras, M. & Piper, P. W. (2003). Base excision repair activities required for yeast to attain a full chronological life span. *Aging Cell* **2**, 93-104.

Maeshima, K., Hihara, S. & Eltsov, M. (2010). Chromatin structure: does the 30-nm fibre exist in vivo? *Curr Opin Cell Biol* **22**, 291-297.

Marcand, S., Gilson, E. & Shore, D. (1997). A protein-counting mechanism for telomere length regulation in yeast. *Science* **275**, 986-990.

Marmorstein, R. & Roth, S. Y. (2001). Histone acetyltransferases: function, structure, and catalysis. *Curr Opin Genet Dev* **11**, 155-161.

Marona, H., Pekala, E., Filipek, B., Maciag, D. & Szneler, E. (2001). Pharmacological properties of some aminoalkanolic derivatives of xanthone. *Pharmazie* **56**, 567-572.

Marti, T. M., Kunz, C. & Fleck, O. (2002). DNA mismatch repair and mutation avoidance pathways. *J Cell Physiol* **191**, 28-41.

Martin, D. G., Duchamp, D. J. & Chidester, C. G. (1973). The isolation, structure and absolute configuration of U.42,126, a novel antitumor antibiotic. *Tetrahedron Lett* **27**, 2549-2552.

Martin, S. G., Laroche, T., Suka, N., Grunstein, M. & Gasser, S. M. (1999). Relocalization of telomeric Ku and SIR proteins in response to DNA strand breaks in yeast. *Cell* **97**, 621-633.

Mashima, T., Okabe, S. & Seimiya, H. (2010). Pharmacological targeting of constitutively active truncated androgen receptor by nigericin and suppression of hormone-refractory prostate cancer cell growth. *Mol Pharmacol* **78**, 846-854.

Mattson, M. P. (2008). Hormesis defined. *Ageing Res Rev* **7**, 1-7.

Mayer, C. & Grummt, I. (2006). Ribosome biogenesis and cell growth: mTOR coordinates transcription by all three classes of nuclear RNA polymerases. *Oncogene* **25**, 6384-6391.

Mayer, C., Schmitz, K. M., Li, J., Grummt, I. & Santoro, R. (2006). Intergenic transcripts regulate the epigenetic state of rRNA genes. *Mol Cell* **22**, 351-361.

McColl, G., Killilea, D. W., Hubbard, A. E., Vantipalli, M. C., Melov, S. & Lithgow, G. J. (2008). Pharmacogenetic analysis of lithium-induced delayed aging in Caenorhabditis elegans. *J Biol Chem* **283**, 350-357.

McCready, S. J., Osman, F. & Yasui, A. (2000). Repair of UV damage in the fission yeast Schizosaccharomyces pombe. *Mutat Res* **451**, 197-210.

Medvedik, O., Lamming, D. W., Kim, K. D. & Sinclair, D. A. (2007). MSN2 and MSN4 link calorie restriction and TOR to sirtuin-mediated lifespan extension in Saccharomyces cerevisiae. *PLoS Biol* **5**, e261.

Mehdi, K., Thierie, J. & Penninckx, M. J. (2001). gamma-Glutamyl transpeptidase in the yeast Saccharomyces cerevisiae and its role in the vacuolar transport and metabolism of glutathione. *Biochem J* **359**, 631-637.

Meijsing, S. H. & Ehrenhofer-Murray, A. E. (2001). The silencing complex SAS-I links histone acetylation to the assembly of repressed chromatin by CAF-I and Asf1 in Saccharomyces cerevisiae. *Genes Dev* **15**, 3169-3182.

Meneghini, M. D., Wu, M. & Madhani, H. D. (2003). Conserved histone variant H2A.Z protects euchromatin from the ectopic spread of silent heterochromatin. *Cell* **112**, 725-736.

Mishra, N., Kar, R., Singha, P. K., Venkatachalam, M. A., McEwen, D. G. & Saikumar, P. (2010). Inhibition of mitochondrial division through covalent modification of Drp1 protein by 15 deoxy-Delta(12,14)-prostaglandin J2. *Biochem Biophys Res Commun* **395**, 17-24.

Misteli, T. (2007). Beyond the sequence: cellular organization of genome function. *Cell* **128**, 787-800.

Moazed, D. (2001). Enzymatic activities of Sir2 and chromatin silencing. *Curr Opin Cell Biol* **13**, 232-238.

Moreno, S., Klar, A. & Nurse, P. (1991). Molecular genetic analysis of fission yeast Schizosaccharomyces pombe. *Methods Enzymol* **194**, 795-823.

Moretti, P., Freeman, K., Coodly, L. & Shore, D. (1994). Evidence that a complex of SIR proteins interacts with the silencer and telomere-binding protein RAP1. *Genes Dev* **8**, 2257-2269.

Morris, R. E., Hoyt, E. G., Murphy, M. P., Eugui, E. M. & Allison, A. C. (1990). Mycophenolic acid morpholinoethylester (RS-61443) is a new immunosuppressant that prevents and halts heart allograft rejection by selective inhibition of T- and B-cell purine synthesis. *Transplant Proc* **22**, 1659-1662.

Moskalev, A. A. & Shaposhnikov, M. V. (2010). Pharmacological inhibition of phosphoinositide 3 and TOR kinases improves survival of Drosophila melanogaster. *Rejuvenation Res* **13**, 246-247.

Muller, H. J. (1930). Types of visible variations induced by X-rays in *Drosophila*. *Journal of Genetics* **22**, 299-335.

Mutoh, N. & Kitajima, S. (2007). Accelerated chronological aging of a mutant fission yeast deficient in both glutathione and superoxide dismutase having cu and zn as cofactors and its enhancement by sir2 deficiency. *Biosci Biotechnol Biochem* **71**, 2841-2844.

Nakamura, J., Straub, K., Wu, J. & Lou, L. (1995). The glutamine hydrolysis function of human GMP synthetase. Identification of an essential active site cysteine. *J Biol Chem* **270**, 23450-23455.

Narumiya, S., Sugimoto, Y. & Ushikubi, F. (1999). Prostanoid receptors: structures, properties, and functions. *Physiol Rev* **79**, 1193-1226.

Nastala, C. L., Edington, H. D., McKinney, T. G. & other authors (1994). Recombinant IL-12 administration induces tumor regression in association with IFN-gamma production. *J Immunol* **153**, 1697-1706.

Nazrullaev, S. S., Saidkhodzhaev, A. I., Akhmedkhodzhaeva, K. S., Syrov, V. N., Rasulev, B. F. & Khushbaktova, Z. A. (2008). Estrogen activity of terpenoids from plants of the genus Ferula. *Chemistry of Natural Compounds* **44**, 572-577.

Nelson, N., Perzov, N., Cohen, A., Hagai, K., Padler, V. & Nelson, H. (2000). The cellular biology of proton-motive force generation by V-ATPases. *J Exp Biol* **203**, 89-95.

Ng, H. H., Feng, Q., Wang, H., Erdjument-Bromage, H., Tempst, P., Zhang, Y. & Struhl, K. (2002). Lysine methylation within the globular domain of histone H3 by Dot1 is important for telomeric silencing and Sir protein association. *Genes Dev* **16**, 1518-1527.

Nicoletti, R., De Stefano, M., De Stefano, S., Trincone, A. & Marziano, F. (2004). Antagonism against Rhizoctonia solani and fungitoxic metabolite production by some Penicillium isolates. *Mycopathologia* **158**, 465-474.

Obolskiy, D., Pischel, I., Siriwatanametanon, N. & Heinrich, M. (2009). Garcinia mangostana L.: a phytochemical and pharmacological review. *Phytother Res* **23**, 1047-1065.

Oki, M. & Kamakaka, R. T. (2002). Blockers and barriers to transcription: competing activities? *Curr Opin Cell Biol* **14**, 299-304.

Onken, B. & Driscoll, M. (2010). Metformin induces a dietary restriction-like state and the oxidative stress response to extend C. elegans Healthspan via AMPK, LKB1, and SKN-1. *PLoS One* **5**, e8758.

Osman, F., Bjoras, M., Alseth, I., Morland, I., McCready, S., Seeberg, E. & Tsaneva, I. (2003). A new Schizosaccharomyces pombe base excision repair mutant, nth1, reveals overlapping pathways for repair of DNA base damage. *Mol Microbiol* **48**, 465-480.

Palacios, J. A., Herranz, D., De Bonis, M. L., Velasco, S., Serrano, M. & Blasco, M. A. (2010). SIRT1 contributes to telomere maintenance and augments global homologous recombination. *J Cell Biol* **191**, 1299-1313.

Park, P. U., McVey, M. & Guarente, L. (2002). Separation of mother and daughter cells. *Methods Enzymol* **351**, 468-477.

Pearson, K. J., Baur, J. A., Lewis, K. N. & other authors (2008). Resveratrol delays age-related deterioration and mimics transcriptional aspects of dietary restriction without extending life span. *Cell Metab* **8**, 157-168.

Peres, V., Nagem, T. J. & de Oliveira, F. F. (2000). Tetraoxygenated naturally occurring xanthones. *Phytochemistry* **55**, 683-710.

Perrod, S. & Gasser, S. M. (2003). Long-range silencing and position effects at telomeres and centromeres: parallels and differences. *Cell Mol Life Sci* **60**, 2303-2318.

Petes, T. D. & Botstein, D. (1977). Simple Mendelian inheritance of the reiterated ribosomal DNA of yeast. *Proc Natl Acad Sci U S A* **74**, 5091-5095.

Pietsch, K., Saul, N., Chakrabarti, S., Sturzenbaum, S. R., Menzel, R. & Steinberg, C. E. (2011). Hormetins, antioxidants and prooxidants: defining quercetin-, caffeic acid- and rosmarinic acid-mediated life extension in C. elegans. *Biogerontology* **12**, 329-347.

Pillus, L. & Rine, J. (1989). Epigenetic inheritance of transcriptional states in S. cerevisiae. *Cell* **59**, 637-647.

Powers, R. W., 3rd, Kaeberlein, M., Caldwell, S. D., Kennedy, B. K. & Fields, S. (2006). Extension of chronological life span in yeast by decreased TOR pathway signaling. *Genes Dev* **20**, 174-184.

Prakash, S. & Prakash, L. (2000). Nucleotide excision repair in yeast. *Mutat Res* **451**, 13-24.

Pryde, F. E. & Louis, E. J. (1999). Limitations of silencing at native yeast telomeres. *EMBO J* **18**, 2538-2550.

Quik, M., Parameswaran, N., McCallum, S. E. & other authors (2006). Chronic oral nicotine treatment protects against striatal degeneration in MPTP-treated primates. *J Neurochem* **98**, 1866-1875.

Quik, M., Cox, H., Parameswaran, N., O'Leary, K., Langston, J. W. & Di Monte, D. (2007). Nicotine reduces levodopa-induced dyskinesias in lesioned monkeys. *Ann Neurol* **62**, 588-596.

Ransom, J. T. (1995). Mechanism of action of mycophenolate mofetil. *Ther Drug Monit* **17**, 681-684.

Riby, J. E., Xue, L., Chatterji, U., Bjeldanes, E. L., Firestone, G. L. & Bjeldanes, L. F. (2006). Activation and potentiation of interferon-gamma signaling by 3,3'-diindolylmethane in MCF-7 breast cancer cells. *Mol Pharmacol* **69**, 430-439.

Riby, J. E., Firestone, G. L. & Bjeldanes, L. F. (2008). 3,3'-diindolylmethane reduces levels of HIF-1alpha and HIF-1 activity in hypoxic cultured human cancer cells. *Biochem Pharmacol* **75**, 1858-1867.

Ristow, M. & Zarse, K. (2010). How increased oxidative stress promotes longevity and metabolic health: The concept of mitochondrial hormesis (mitohormesis). *Exp Gerontol* **45**, 410-418.

Ristow, M. & Schmeisser, S. (2011). Extending life span by increasing oxidative stress. *Free Radic Biol Med* **51**, 327-336.

Rizki, A. & Lundblad, V. (2001). Defects in mismatch repair promote telomerase-independent proliferation. *Nature* **411**, 713-716.

Robert, F., Pokholok, D. K., Hannett, N. M., Rinaldi, N. J., Chandy, M., Rolfe, A., Workman, J. L., Gifford, D. K. & Young, R. A. (2004). Global position and recruitment of HATs and HDACs in the yeast genome. *Mol Cell* **16**, 199-209.

Robyr, D., Suka, Y., Xenarios, I., Kurdistani, S. K., Wang, A., Suka, N. & Grunstein, M. (2002). Microarray deacetylation maps determine genome-wide functions for yeast histone deacetylases. *Cell* **109**, 437-446.

Rodgman, A. & Perfetti, T. A. (2009). *The chemical components of tobacco and tobacco smoke*. Boca Raton: CRC Press.

Rodier, F. & Campisi, J. (2011). Four faces of cellular senescence. *J Cell Biol* **192**, 547-556.

Roth, S. Y. (1995). Chromatin-mediated transcriptional repression in yeast. *Curr Opin Genet Dev* **5**, 168-173.

Roux, A. E., Quissac, A., Chartrand, P., Ferbeyre, G. & Rokeach, L. A. (2006). Regulation of chronological aging in Schizosaccharomyces pombe by the protein kinases Pka1 and Sck2. *Aging Cell* **5**, 345-357.

Roux, A. E., Chartrand, P., Ferbeyre, G. & Rokeach, L. A. (2010). Fission yeast and other yeasts as emergent models to unravel cellular aging in eukaryotes. *J Gerontol A Biol Sci Med Sci* **65**, 1-8.

Rusche, L. N., Kirchmaier, A. L. & Rine, J. (2003). The establishment, inheritance, and function of silenced chromatin in Saccharomyces cerevisiae. *Annu Rev Biochem* **72**, 481-516.

Sambrook, J., Fritsch, E. F. & Maniatis, T. (1989). *Molecular Cloning: A Laboratory Manual*: Cold Spring Harbor, NY: Cold Spring Harbor Laboratory.

Sancar, A., Lindsey-Boltz, L. A., Unsal-Kacmaz, K. & Linn, S. (2004). Molecular mechanisms of mammalian DNA repair and the DNA damage checkpoints. *Annu Rev Biochem* **73**, 39-85.

Sarg, B., Koutzamani, E., Helliger, W., Rundquist, I. & Lindner, H. H. (2002). Postsynthetic trimethylation of histone H4 at lysine 20 in mammalian tissues is associated with aging. *J Biol Chem* **277**, 39195-39201.

Sauve, A. A. & Schramm, V. L. (2003). Sir2 regulation by nicotinamide results from switching between base exchange and deacetylation chemistry. *Biochemistry* **42**, 9249-9256.

Sauve, A. A., Wolberger, C., Schramm, V. L. & Boeke, J. D. (2006). The biochemistry of sirtuins. *Annu Rev Biochem* **75**, 435-465.

Scher, J. U. & Pillinger, M. H. (2005). 15d-PGJ2: the anti-inflammatory prostaglandin? *Clin Immunol* **114**, 100-109.

Schotta, G., Sengupta, R., Kubicek, S. & other authors (2008). A chromatin-wide transition to H4K20 monomethylation impairs genome integrity and programmed DNA rearrangements in the mouse. *Genes Dev* **22**, 2048-2061.

Schumacher, B., Garinis, G. A. & Hoeijmakers, J. H. (2008). Age to survive: DNA damage and aging. *Trends Genet* **24**, 77-85.

Schumacher, B. (2009). Transcription-blocking DNA damage in aging: a mechanism for hormesis. *Bioessays* **31**, 1347-1356.

Scorrano, L. (2007). Multiple functions of mitochondria-shaping proteins. *Novartis Found Symp* **287**, 47-55; discussion 55-49.

Sedelnikova, O. A., Horikawa, I., Zimonjic, D. B., Popescu, N. C., Bonner, W. M. & Barrett, J. C. (2004). Senescing human cells and ageing mice accumulate DNA lesions with unrepairable double-strand breaks. *Nat Cell Biol* **6**, 168-170.

Sell, C. (2009). Introduction. In *Life-Span Extension: Single-Cell Organisms to Man*. Edited by C. Sell, A. Lorenzini & H. M. Brown-Borg. New York: Humana Press.

Shankaranarayana, G. D., Motamedi, M. R., Moazed, D. & Grewal, S. I. (2003). Sir2 regulates histone H3 lysine 9 methylation and heterochromatin assembly in fission yeast. *Curr Biol* **13**, 1240-1246.

Sherman, F. (1991). Getting started with yeast. *Methods Enzymol* **194**, 3-21.

Shumaker, D. K., Dechat, T., Kohlmaier, A. & other authors (2006). Mutant nuclear lamin A leads to progressive alterations of epigenetic control in premature aging. *Proc Natl Acad Sci U S A* **103**, 8703-8708.

Sikorski, R. S. & Hieter, P. (1989). A system of shuttle vectors and yeast host strains designed for efficient manipulation of DNA in Saccharomyces cerevisiae. *Genetics* **122**, 19-27.

Simic, A., Manojlovic, D., Segan, D. & Todorovic, M. (2007). Electrochemical behavior and antioxidant and prooxidant activity of natural phenolics. *Molecules* **12**, 2327-2340.

Sinclair, D. A. & Guarente, L. (1997). Extrachromosomal rDNA circles--a cause of aging in yeast. *Cell* **91**, 1033-1042.

Smith, C. M., Gafken, P. R., Zhang, Z., Gottschling, D. E., Smith, J. B. & Smith, D. L. (2003). Mass spectrometric quantification of acetylation at specific lysines within the amino-terminal tail of histone H4. *Anal Biochem* **316**, 23-33.

Smith, J. S. & Boeke, J. D. (1997). An unusual form of transcriptional silencing in yeast ribosomal DNA. *Genes Dev* **11**, 241-254.

Smith, J. S., Brachmann, C. B., Pillus, L. & Boeke, J. D. (1998). Distribution of a limited Sir2 protein pool regulates the strength of yeast rDNA silencing and is modulated by Sir4p. *Genetics* **149**, 1205-1219.
Smogorzewska, A. & de Lange, T. (2004). Regulation of telomerase by telomeric proteins. *Annu Rev Biochem* **73**, 177-208.

Southern, E. M. (1975). Detection of specific sequences among DNA fragments separated by gel electrophoresis. *J Mol Biol* **98**, 503-517.

Sparkman, O. D. (2000). Review of the 48th ASMS conference on mass spectrometry and allied topics held in Long Beach, California June 11-15, 2000. *J Am Soc Mass Spectrom* **11**, 921.

Steinkraus, K. A., Kaeberlein, M. & Kennedy, B. K. (2008). Replicative aging in yeast: the means to the end. *Annu Rev Cell Dev Biol* **24**, 29-54.

Stojic, L., Brun, R. & Jiricny, J. (2004). Mismatch repair and DNA damage signalling. *DNA Repair (Amst)* **3**, 1091-1101.

Stone, E. M. & Pillus, L. (1998). Silent chromatin in yeast: an orchestrated medley featuring Sir3p [corrected]. *Bioessays* **20**, 30-40.

Strahl-Bolsinger, S., Hecht, A., Luo, K. & Grunstein, M. (1997). SIR2 and SIR4 interactions differ in core and extended telomeric heterochromatin in yeast. *Genes Dev* **11**, 83-93.

Straight, A. F., Shou, W., Dowd, G. J., Turck, C. W., Deshaies, R. J., Johnson, A. D. & Moazed, D. (1999). Net1, a Sir2-associated nucleolar protein required for rDNA silencing and nucleolar integrity. *Cell* **97**, 245-256.

Street, S. E., Cretney, E. & Smyth, M. J. (2001). Perforin and interferon-gamma activities independently control tumor initiation, growth, and metastasis. *Blood* **97**, 192-197.

Sugasawa, K., Ng, J. M., Masutani, C., Iwai, S., van der Spek, P. J., Eker, A. P., Hanaoka, F., Bootsma, D. & Hoeijmakers, J. H. (1998). Xeroderma pigmentosum group C protein complex is the initiator of global genome nucleotide excision repair. *Mol Cell* **2**, 223-232.

Suka, N., Luo, K. & Grunstein, M. (2002). Sir2p and Sas2p opposingly regulate acetylation of yeast histone H4 lysine16 and spreading of heterochromatin. *Nat Genet* **32**, 378-383.

Sundaram, B. M., Gopalakrishnan, C., Subramanian, S., Shankaranarayanan, D. & Kameswaran, L. (1983). Antimicrobial Activities of Garcinia mangostana. *Planta Med* **48**, 59-60.

Takegawa, K., Iwaki, T., Fujita, Y., Morita, T., Hosomi, A. & Tanaka, N. (2003). Vesicle-mediated protein transport pathways to the vacuole in Schizosaccharomyces pombe. *Cell Struct Funct* **28**, 399-417.

Tate, S. S. (1980). *Enzymatic basis of detoxification*. New York: Academic Press.

Thompson, R. F., Atzmon, G., Gheorghe, C., Liang, H. Q., Lowes, C., Greally, J. M. & Barzilai, N. (2010). Tissue-specific dysregulation of DNA methylation in aging. *Aging Cell* **9**, 506-518.

Tollefsbol, T. O. (2010). Epigenetics and the Aging Process. In *Epigenetics of Aging*. Edited by T. O. Tollefsbol. New York: Springer

Torrenegra, R. D., Baquero, J. E. & Calderon, J. S. (2005). Antibacterial activity and complete 1H and 13C NMR assignment of mycophenolic acid isolated from *Penicillium verrucosum*. *Rev Lat Am Quim* **33**, 76-81.

Toyn, J. H., Gunyuzlu, P. L., White, W. H., Thompson, L. A. & Hollis, G. F. (2000). A counterselection for the tryptophan pathway in yeast: 5-fluoroanthranilic acid resistance. *Yeast* **16**, 553-560.

Tressler, R. J., Garvin, L. J. & Slate, D. L. (1994). Anti-tumor activity of mycophenolate mofetil against human and mouse tumors in vivo. *Int J Cancer* **57**, 568-573.

Trusheva, B., Todorov, I., Ninova, M., Najdenski, H., Daneshmand, A. & Bankova, V. (2010). Antibacterial mono- and sesquiterpene esters of benzoic acids from Iranian propolis. *Chem Cent J* **4**, 8.

Tso, J. Y., Bower, S. G. & Zalkin, H. (1980). Mechanism of inactivation of glutamine amidotransferases by the antitumor drug L-(alpha S, 5S)-alpha-amino-3-chloro-4,5-dihydro-5-isoxazoleacetic acid (AT-125). *J Biol Chem* **255**, 6734-6738.

Tsuchiya, E., Yukawa, M., Ueno, M., Kimura, K. & Takahashi, H. (2010). A novel method of screening cell-cycle blockers as candidates for anti-tumor reagents using yeast as a screening tool. *Biosci Biotechnol Biochem* **74**, 411-414.

Tsukamoto, Y., Kato, J. & Ikeda, H. (1997). Silencing factors participate in DNA repair and recombination in Saccharomyces cerevisiae. *Nature* **388**, 900-903.

Unal, E., Kinde, B. & Amon, A. (2011). Gametogenesis eliminates age-induced cellular damage and resets life span in yeast. *Science* **332**, 1554-1557.

van Leeuwen, F., Gafken, P. R. & Gottschling, D. E. (2002). Dot1p modulates silencing in yeast by methylation of the nucleosome core. *Cell* **109**, 745-756.

Vanhaecke, T., Papeleu, P., Elaut, G. & Rogiers, V. (2004). Trichostatin A-like hydroxamate histone deacetylase inhibitors as therapeutic agents: toxicological point of view. *Curr Med Chem* **11**, 1629-1643.

Vaziri, H., Dessain, S. K., Ng Eaton, E., Imai, S. I., Frye, R. A., Pandita, T. K., Guarente, L. & Weinberg, R. A. (2001). hSIR2(SIRT1) functions as an NAD-dependent p53 deacetylase. *Cell* **107**, 149-159.

Vina, J., Sastre, J., Pallardo, F. V., Gambini, J. & Borras, C. (2008). Modulation of longevity-associated genes by estrogens or phytoestrogens. *Biol Chem* **389**, 273-277.

Vogelauer, M., Rubbi, L., Lucas, I., Brewer, B. J. & Grunstein, M. (2002). Histone acetylation regulates the time of replication origin firing. *Mol Cell* **10**, 1223-1233.

Volpe, T. A., Kidner, C., Hall, I. M., Teng, G., Grewal, S. I. & Martienssen, R. A. (2002). Regulation of heterochromatic silencing and histone H3 lysine-9 methylation by RNAi. *Science* **297**, 1833-1837.

Wach, A., Brachat, A., Pohlmann, R. & Philippsen, P. (1994). New heterologous modules for classical or PCR-based gene disruptions in Saccharomyces cerevisiae. *Yeast* **10**, 1793-1808.

Wanke, V., Cameroni, E., Uotila, A., Piccolis, M., Urban, J., Loewith, R. & De Virgilio, C. (2008). Caffeine extends yeast lifespan by targeting TORC1. *Mol Microbiol* **69**, 277-285.

Wellinger, R. J., Wolf, A. J. & Zakian, V. A. (1993). Saccharomyces telomeres acquire single-strand TG1-3 tails late in S phase. *Cell* **72**, 51-60.

Wood, J. G., Rogina, B., Lavu, S., Howitz, K., Helfand, S. L., Tatar, M. & Sinclair, D. (2004). Sirtuin activators mimic caloric restriction and delay ageing in metazoans. *Nature* **430**, 686-689.

Wood, R. D. (1996). DNA repair in eukaryotes. *Annu Rev Biochem* **65**, 135-167.

Wood, V., Gwilliam, R., Rajandream, M. A. & other authors (2002). The genome sequence of Schizosaccharomyces pombe. *Nature* **415**, 871-880.

Wood, V. (2006). Schizosaccharomyces pombe comparative genomics: from sequence to systems. In *Comparative Genomics: Using Fungi as Models*, pp. 233–285. Edited by P. J. Sunnerhagen P: Springer.

Wright, J. H., Gottschling, D. E. & Zakian, V. A. (1992). Saccharomyces telomeres assume a non-nucleosomal chromatin structure. *Genes Dev* **6**, 197-210.

Wyllie, F. S., Jones, C. J., Skinner, J. W., Haughton, M. F., Wallis, C., Wynford-Thomas, D., Faragher, R. G. & Kipling, D. (2000). Telomerase prevents the accelerated cell ageing of Werner syndrome fibroblasts. *Nat Genet* **24**, 16-17.

Xu, F., Zhang, K. & Grunstein, M. (2005). Acetylation in histone H3 globular domain regulates gene expression in yeast. *Cell* **121**, 375-385.

Xue, L., Firestone, G. L. & Bjeldanes, L. F. (2005). DIM stimulates IFNgamma gene expression in human breast cancer cells via the specific activation of JNK and p38 pathways. *Oncogene* **24**, 2343-2353.

Xue, L., Pestka, J. J., Li, M., Firestone, G. L. & Bjeldanes, L. F. (2008). 3,3'-Diindolylmethane stimulates murine immune function in vitro and in vivo. *J Nutr Biochem* **19**, 336-344.

Yang, C. C., Chen, D., Lee, S. S. & Walter, L. (2011). The dynamin-related protein DRP-1 and the insulin signaling pathway cooperate to modulate Caenorhabditis elegans longevity. *Aging Cell*.

Yonemasu, R., McCready, S. J., Murray, J. M., Osman, F., Takao, M., Yamamoto, K., Lehmann, A. R. & Yasui, A. (1997). Characterization of the alternative excision repair pathway of UV-damaged DNA in Schizosaccharomyces pombe. *Nucleic Acids Res* **25**, 1553-1558.

Yoon, J. H., Swiderski, P. M., Kaplan, B. E., Takao, M., Yasui, A., Shen, B. & Pfeifer, G. P. (1999). Processing of UV damage in vitro by FEN-1 proteins as part of an alternative DNA excision repair pathway. *Biochemistry* **38**, 4809-4817.

Yoshikawa, M., Harada, E., Miki, A., Tsukamoto, K., Liang, S., Yamahara, N. & Murakami, N. (1994). Antioxidant constituents from the fruit hulls of Mangosteen (Garcinia mangostana L.). *Yakugaku Zasshi*, 129-133.

Yu, S., Shen, G., Khor, T. O., Kim, J. H. & Kong, A. N. (2008). Curcumin inhibits Akt/mammalian target of rapamycin signaling through protein phosphatase-dependent mechanism. *Mol Cancer Ther* **7**, 2609-2620.

Yu, W., Mechawar, N., Krantic, S. & Quirion, R. (2011). alpha7 Nicotinic receptor activation reduces beta-amyloid-induced apoptosis by inhibiting caspase-independent death through phosphatidylinositol 3-kinase signaling. *J Neurochem* **119**, 848-858.

Zarse, K., Schmeisser, S., Birringer, M., Falk, E., Schmoll, D. & Ristow, M. (2010). Differential effects of resveratrol and SRT1720 on lifespan of adult Caenorhabditis elegans. *Horm Metab Res* **42**, 837-839.

Zhao, Y., Sun, H., Lu, J., Li, X., Chen, X., Tao, D., Huang, W. & Huang, B. (2005). Lifespan extension and elevated hsp gene expression in Drosophila caused by histone deacetylase inhibitors. *J Exp Biol* **208**, 697-705.

Zhou, H., Luo, Y. & Huang, S. (2010). Updates of mTOR inhibitors. *Anticancer Agents Med Chem* **10**, 571-581.

Zuin, A., Castellano-Esteve, D., Ayte, J. & Hidalgo, E. (2010). Living on the edge: stress and activation of stress responses promote lifespan extension. *Aging (Albany NY)* **2**, 231-237.

6 Danksagung

Mein großer Dank gilt Frau Prof. Dr. Ann Ehrenhofer-Murray, die mich in ihre Arbeitsgruppe aufgenommen und hervorragend betreut hat. Ihre fachliche Beratung und Unterstützung in allen Phasen des Projektes war entscheidend für das Gelingen dieser Arbeit.

Ich danke Frau Prof. Dr. Jacqueline Franke für die dreijährige, gute Betreuung, die Möglichkeiten, die sie mir gegeben hat und ihre Unterstützung während meiner Forschungsaufenthalte in Berlin.

Der Jürgen Manchot-Stiftung sowie der Deutschen Forschungsgemeinschaft (DfG) und der Fakultät für Biologie der Universität Duisburg-Essen danke ich für die Finanzierung dieser Forschungsarbeit.

Mein herzlicher Dank gilt den Mitarbeitern des FMP für ihre Unterstützung und Hilfsbereitschaft während meiner Substanzscreens in Berlin, insbesondere Carola und Chris. Ich danke Gesine für das Durchführen des *in vitro* Fluoreszenz-Versuches sowie Werner Karow und Markus Kaiser für die MS-Analysen. Ed Louis, Oliver Fleck, Kurt Runge, Henning Schmidt und Kaoru Takegawa danke ich für das Bereitstellen von Hefestämmen.

Allen aktuellen und ehemaligen Mitarbeitern der Arbeitsgruppe danke ich für ihre Hilfsbereitschaft und die angenehme Arbeitsatmosphäre. Besonders bedanken möchte ich mich bei Stefan und Maria dafür, dass sie sich immer die Zeit genommen haben, meine zahlreichen Fragen zu beantworten. Des Weiteren danke ich Rita, Christiane V. und Karolin, die das Organisatorische regeln und dadurch alles am Laufen halten. Ich danke Jessica W. für Körbe voller YES-Platten und Christiane H. für die vielen aufmunternden Gespräche.

Ich danke meiner Familie und Freunden, die immer an mich geglaubt, mich unterstützt und es mir ermöglicht haben, stets meine Ziele zu verfolgen.

Von ganzem Herzen danke ich Jonathan für seine immerwährende Unterstützung vor allem in stressigen Zeiten und seine scheinbar unendliche Geduld.

7 Lebenslauf

Der Lebenslauf ist in der Online-Version aus Gründen des Datenschutzes nicht enthalten.

8 Erklärungen

Erklärung:

Hiermit erkläre ich, gem. § 6 Abs. (2) f) der Promotionsordnung der Fakultäten für Biologie, Chemie und Mathematik zur Erlangung des Dr. rer. nat., dass ich das Arbeitgebiet, dem das Thema „Identification of small molecules and genetic factors that alter cellular aging" zuzuordnen ist, in Forschung und Lehre vertrete und den Antrag von Jessica Stephan befürworte und die Betreuung auch im Falle eines Weggangs, wenn nicht wichtige Gründe dem entgegenstehen, weiterführen werde.

Essen, den _____ _____
Prof. Dr. Ann Ehrenhofer-Murray

Erklärung:

Hiermit erkläre ich, gem. § 7 Abs. (2) c) + e) der Promotionsordnung Fakultäten für Biologie, Chemie und Mathematik zur Erlangung des Dr. rer. nat., dass ich die vorliegende Dissertation selbständig verfasst und mich keiner anderen als der angegebenen Hilfsmittel bedient habe.

Essen, den _____ _____
Jessica Stephan

Erklärung:

Hiermit erkläre ich, gem. § 7 Abs. (2) d) + f) der Promotionsordnung der Fakultäten für Biologie, Chemie und Mathematik zur Erlangung des Dr. rer. nat., dass ich keine anderen Promotionen bzw. Promotionsversuche in der Vergangenheit durchgeführt habe und dass diese Arbeit von keiner anderen Fakultät/Fachbereich abgelehnt worden ist.

Essen, den _____ _____
Jessica Stephan